No. 3

A/AC 105/492

SEMINARS

of the United Nations Programme on Space Applications

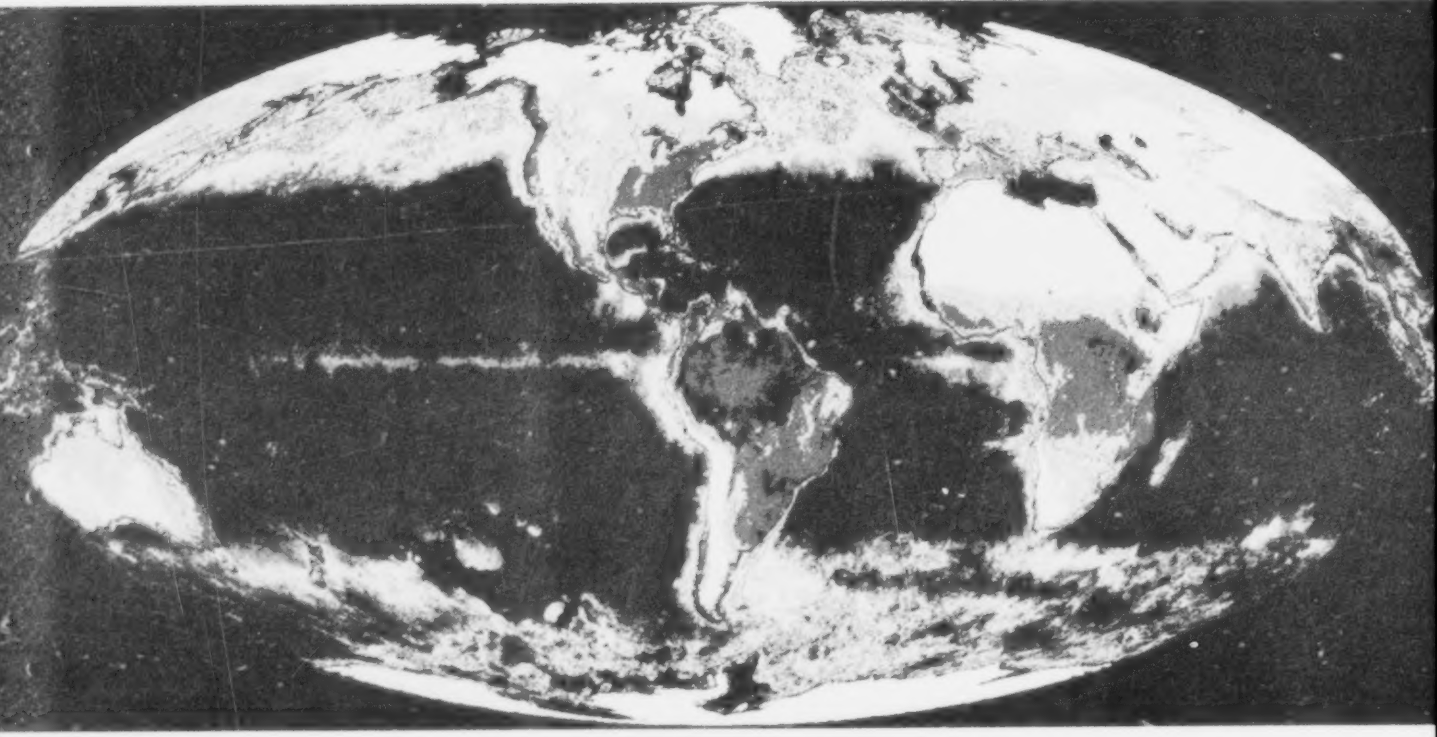

Selected Papers on Remote Sensing,
Satellite Communications and Space Science
1992

United Nations

A/AC.105/492

SEMINARS

of the
United Nations Programme on Space Applications

Selected Papers on Remote Sensing,
Satellite Communications and Space Science
1992

United Nations
1992

Foreword

Since 1972, the United Nations Outer Space Affairs Division, as part of its Programme on Space Applications, has organized and co-sponsored meetings, seminars, training courses and workshops on the applications of space technology in order to assist developing countries in establishing indigenous technological infrastructure and in developing and implementing local programmes. The United Nations carries out these activities in cooperation with other international and regional organizations and national institutions in accordance with the mandate of the Programme, relevant United Nations General Assembly resolutions, and the recommendations of the Second United nations Conference on the Exploration and Peaceful uses of Outer Space (UNISPACE 82). UNISPACE 82 had re-affirmed the importance of establishing and strengthening national and regional mechanisms to promote co-operation in the use of space technology for the benefit of developing countries. The Programme on Space Applications conducts a number of activities that are devoted to various fields of space technology. In 1991, it organized activities dedicated particularly to (a) improving information systems in agricultural, geological, oceanographic and coastal resources through remote sensing techniques, (b) satellite communications to combat natural disasters, (c) development of indigenous capability at the local level particularly through educational systems, and for the first time, basic space sciences. This publication comprises selected papers presented at the 1991 activities of the Programme.

The scope of the publication extends from a general overview of the use of remote sensing technology for development to specific areas of application, including the assessment of natural vegetation and agricultural systems, the determination and forecast of precipitation, the monitoring of ecological conditions in the coastal environment, and the development and implementation of educational curricula and database systems for educators, managers and researchers. In examining the technology available for monitoring the environment and for observing physical and biological processes, a number of papers focused on remote sensing instrumentation for aerial photography, current and future radar systems on Earth observation satellites, multispectral scanner systems on board the United States Landsat, the Japanese MOS-1, and the French SPOT satellites, and sensor systems on board meteorological satellites including the United States National Oceanic and Atmospheric Administration (NOAA) series, the European Space Agency (ESA) Meteosat series, the Soviet Union Meteor series, the Japanese series, Geostationary Meteorological Satellite (GMS) and the Indian INSAT series. This publication also includes various satellite-assisted technologies that can provide services and information that are essential for the social and economic development of a country. In particular, a review is presented of the new and evolving hardware and software technologies in the communications and computer fields that can assist rural education and health programmes as well as disaster relief efforts. Because the papers are selected from workshops, training courses and seminars held in various parts of the world, they addressed remote sensing and satellite communications issues that correspond to the particular needs of the regions concerned.

This publication is the third in the series of annual United Nations publications initiated in 1989 and dedicated to different fields of space technology applications. These publications aim to promote further international exchange of information and experience as well as disseminate information on United Nations activities in assisting developing countries to utilize space technologies for their social and economic development. They also constitute a contribution of the United Nations toward ensuring that the peaceful use of outer space is carried out for the benefit and in the interest of all countries.

V. Safronchuk

Vasiliy S. Safronchuk
Under-Secretary-General for
Political and Security Council Affairs

CONTENTS

Page

Foreword ... iii

Selected papers

Surveying and Mapping in Africa
Conventional Methods to Space Techniques
O.L. Adekoya ... 1

Oceanographic Applications of Microwave Radar Data
M. Cantón-Garbín ... 29

Theory of SAR
R.K. Raney ... 47

NDVI-Crop Monitoring and Early Yield Assessment
of Burkina Faso
S.M.E. Groten ... 69

Remote Sensing for Rural Water Supply in India
M.G. Chandrasekhar, A.K. Gupta, J. Krishnamurthy
and P.P.N. Rao ... 93

The Great Impact of the Educational Satellite
System in China
F. Gao ... 109

Operational Environmental Satellite
Remote Sensing for Food Security and
Locust Control by FAO
J.U. Hielkema ... 117

Remote Sensing Applications in Water Resources
with Case Studies in Sahel Areas, West Africa
A. Antoninetti, P.A. Brivio, M.A. Gomarasca
and Z. Zilioli ... 137

CONTENTS (continued)

Page

Selected papers

Remote Sensing Applications in Tropical Africa: Environmental Geology, Soils and Vegetation Coverage
M. Punkari.. 151

Advance Warning and Evaluation of Damage Caused by Cyclone, Flood and other Meteorological Phenomena in Bangladesh
Md. A. Rahman and S. Begum.............................. 169

Drought Preparedness Monitoring and Mapping for Peninsular Malaysia
M.K. Baharuddin and N. Hashim........................... 187

The Role of Space-Based Observations in Astrophysical Research
J. Grygar... 199

SURVEYING AND MAPPING IN AFRICA--CONVENTIONAL METHODS TO SPACE TECHNIQUES*

Mrs. Olayinka Lasebikan Adekoya
Deputy Surveyor-General of the Federal Republic of Nigeria

INTRODUCTION

Africa, a vast continent, indeed, the second largest continent of the world, extends over an area of 30 million square kilometres. It occupies one fifth of the Earth's land surface and has an estimated population of about half a billion people and an annual growth rate of 2.8 according to the 1980 statistics. It is compact and devoid of peninsulas and major inlets. Most of Africa existed as a rigid block of basement complex in Pre-Cambrian times. In Wegener's theory of continental drift, Africa was part of the Gondwanaland before the drift of South America, Antarctica, India and Australia. This explains why the coastline is relatively free of indentations. The continent, the most tropical of all the continents of the world, stretches between 35° North and South of the equator and longitudes 20° West and 50° East of the Greenwich meridian. Regional differences in drainage patterns and vegetation are due primarily to the seasonal distribution of rainfall. Most countries of the continent are richly endowed with natural resources. These resources include energy (hydropower, thermal and solar), agricultural, forest, mineral and petroleum, water and marine and human resources. Despite the abundance of these resources, the continent remains the most economically backward, having 26 of the world's 36 least developed countries. As of 1980, about 70 per cent of its population lived in rural areas, while a majority of the inhabitants lived in abject poverty.

The economic backwardness of the continent can be traced to its colonial past, the post-independence era and a combination of economic, political and endemic factors. These factors, among others, are: deficiencies and inadequacies in infrastructure, economic strategies and policies falling short of expectations and desired goals; disparities in urban and rural development and income distribution; insufficient, misplaced and under-utilized managerial and administrative capabilities; inadequate and inconsistent human resources development and management programmes, misplaced priorities, demographic factors, mismanagement of financial resources and political instability. The wealth, power and influence of any nation depend on its capability and capacity to utilize science and technology to galvanize development. The problem of the African continent is due to the low level of technology application for the development of its resources for the welfare of its teeming population. Consequently, it is dependent largely on the industralized world for wholesale importation of technology in terms of finished products. To reverse this trend, priorities must be placed on policies and programmes which would accelerate orderly development for self reliance. This can be achieved by mobilizing and optimally utilizing available local resources. In so doing, a conscious effort has to be made for a proper inventory of the resources of the continent to ascertain their type, extent, location and distribution. Surveying and mapping, including remote sensing, are basic tools for achieving these objectives.

---

* This paper, which was presented at the United Nations/Food and Agriculture Organization of the United Nations/European Space Agency Workshop on Microwave Remote Sensing Technology, held in Maspalomas, Canary Islands, Spain, 10-14 June 1991, does not necessarily reflect the views of the United Nations.

Surveying is one of the earliest professions, dating back to prehistoric times. The irony of the situation is that Africa, the home of Egypt, one of the leading countries of ancient civilization, should and ought to be in the forefront of development in surveying and mapping technology. After all, centuries ago, when the Nile river overflowed its banks annually, re-nourishing the farmlands on its banks but at the same time obliterating all landmarks, surveyors were called upon to re-demarcate land boundaries at their original positions. As far back as 5000 years ago, the Great Pyramid of Cheops, clearly the greatest single building ever erected by man, was set out in Egypt with a near perfect square base and sides built on cardinal points. Cadastral survey was introduced in Egypt by the eighteenth dynasty in about 1600 B.C. Although these ancient skills of demarcation of the earth, boundaries and property lines, limits and shapes of construction, the charting of the oceans, etc. were introduced to Africa long ago, the level of surveying and mapping in Africa remains low when compared with the rest of the world. Dr. Konecny in 1986 showed that only 24 per cent of Africa has been mapped at a basic scale of 1:50,000 and only at two per cent at the 1:25,000 and larger scales.

The early surveyors and mapping experts were mainly military men. Prior to the compartmentalization of the professions, the surveyor was the mathematician, the engineer, the architect, the planner, the builder, the cost consultant; and in some cases he was also the policy and decision maker. He understood the need - or surveying and mapping. Map scales were chosen to meet his

Table 1. Need for Surveying and Mapping Data and Information

TYPE OF ECONOMY	THE MAIN PRODUCTION	ENTIRE TERRITORY		PRIORITY AREA	
		USE	SCALE	USE	SCALE
Pre-Industrial	Agriculture	Transportation	1:200,000		
		Military and Defence	1:100,000	Tax Cadastre	1:5,000
		Resource Inventory	1:50,000		
Industrial	Consumer Products	Resources Management	1:50,000 Satellite Image Data	Construction Projects and Land Management	1:2,000 1:1,000
Post Industrial	Services	Regional Planning	1:10,000 Geographic Information System	Urban Planning	1:500 Urban Information System

immediate practical needs. Table I, taken from the work of Dr. Konecny, shows the need for surveying and mapping products. The first maps were compiled at the small scales of 1:200,000 and 1:250, 000 series to meet transportation needs. Later, 1:50,000 and 1:100,000 topographical maps were required for military use to control the tactical and strategic movements of troops and to determine the targets of military activities. Consequently, those countries which had been involved in wars are nowadays generally well and better mapped.

The benefits arising from surveying and mapping are difficult to quantify. Clearly, development can and does take place without surveys and maps, although, it could be haphazard.

On the other hand, it is also true that the lack of survey and mapping data and information outlay in all development planning and implementation can cause a national economic and social catastrophe on an unprecedented scale. Therefore, one would like to add that reliable, up to date and timely surveying and mapping data actually promotes development as well as expedites its planning and execution. Maps, map substitutes and map-like products in digital or graphical format are basic tools which aid the planning and realization of the goals and objectives of all sectors involved in promoting economic and social development. The level of development of a country is a measure of how well it is mapped. Most developed countries, that is, the service-oriented countries -- for example, the North American and European countries -- are well mapped at various scales ranging from the most widely accepted basic topographical scale of 1:50,000, 1:25,000 and 1:20,000 to the large scales of 1:5,000 and 1:10,000. On the other hand, the developing countries, with agro-based economies are yet to be fully mapped at the basic scale of 1:50,000.

Maps are needed for a number of reasons. Some of these reasons are:

- modernization, expansion, upgrading and development of transportation means, including roads, railways, ports and airports
- solving problems due to rural urban migration (presently 30 per cent of Africa's population live in urban centres, as against 8 per cent in 1920 and a predicted 50 per cent by the year 2000)
- security and defence - definition of national boundaries, exclusive economic zone (EEZ), defence from external aggressors, emergency service to reach disaster areas and relief

- development of telecommunication networks, and power transmission
- increased search for natural resources, problems of agricultural development, irrigation and water supply, increased food production to reduce starvation and nutrition shortage
- protection of the environment from ecological disasters such as flooding, desertification and erosion, etc.
- land use, land administration and management
- mining exploitation
- forecasting and prediction of shortages of natural resources and the necessity of undertaking more studies in planning of inventories and rational exploitation
- provision of cultural and social services

It is therefore expedient that a conscious effort should be made by all Governments of Africa to invest in surveying and mapping as against merely placing it as a footnote in the order of national priorities.

SURVEYING AND MAPPING IN AFRICA

Historical records show that surveying and mapping services and products in most countries of the world, including Africa, were produced on a routine basis. These services include: a network of first-order geodetic controls, using any of the conventional methods, triangulation, trilateralization, traversing, astro fixing, etc., their densification to lower order networks, geodetic levelling and benchmarking to provide the necessary height control data, aerial photography acquisition and subsequent mapping, usually by restitution of stereo photographic images in photogrammetric plotters and reproduction.

Until the last three decades, photogrammetric control extension was performed by analog methods. With the advent of computer technology in the 1950s, the analog methods gave way to analytical photogrammetry. Developed countries were competing in developing cost effective software for aerial triangulation. Dr. Schut at the National Research Council (NRC), Canada, developed a computer program for strip formation and adjustment for aerial triangulation. Ackermann at the ITC, the Netherlands and later at Stuttgart, Germany, developed the PATM43 Independent Model Method of Aerial Triangulation and Adjustments. Dr. Dwain Browne in the United States was in the forefront of research and application methods for bundle adjustment and associated computer software. Manual cartographic scribing gave way to direct scribing at the photogrammetric machine compilation stage of mapping. Later, automatic digital plotters, such as the Gestalt plotters, were introducted to the market. The raw materials of science and technology for the delivery of surveying and mapping services were therefore available for consumption by Africa.

In the paragraphs that follow an attempt is made to highlight the impact of these scientific developments in Africa. The period under review was the immediate post-independence period of most African countries. Surveying and mapping facilities, where available, were those left behind by the colonial masters. Most of the countries lacked indigenous manpower. The immediate post-independence preoccupation was, logically, the training of indigenous personnel at all levels and in all areas of specialization in surveying and mapping science due to the paucity of experts and support staff.

The state of the art in geodetic control networks, aerial photography coverage and topographical mapping of the continent. Most of these services, having been inherited from our colonial past, pre-independence, the relevant documents are, in most cases, filed in countries other than in the national Survey Department of each country. Even more disturbing is the fact that some of the original records have been lost or cannot be traced. Lack or shortage of survey and mapping data are often filled by isolated survey works based on local origin. To further compound the problem, the francophone African countries carry out the survey and mapping of their territories in metric units while most anglophone countries still operate in the imperial system. Relating surveys from one country to another thus creates a major problem, particularly at contiguous boundaries.

GEODETIC SURVEY ACTIVITIES

A network of ground control points is required as the basic framework on which all survey and mapping is tied. The surveys of the 30th meridian and the 12th parallel constitute the basic framework for the establishment of a unified geodetic network for the African continent. The distribution of geodetic control networks of Africa is shown in appendix 1.

THE TWELFTH PARALLEL SURVEY PROJECT

The survey of the 12th parallel linking Dakar to N'Djamena up to its connection with the survey of the 30th arc meridian which links Cape Town to Cairo and to the Red Sea was undertaken from 1967 to 1970 and funded by the United States Government. This project was first muted as far back as 1949 at the

Johannesburg African Scientific Conference, out of concern for possible harmonization and standardization of individual geodetic networks in the continent. The recommendation came up again in 1953 at the meeting of experts in cartography and map surveying held at Bukari, Zaire. It was later repeated by the General Assembly of the International Union for Geodesy and Geophysics (IUGG) and the International Association of Geodesy in 1960 and adopted by the African nations during the First Regional Conference of Cartography for Africa in 1963. This arc of parallel spanning over 4,658 km is divided as follows:

-	Chad	917 km
-	Cameroon	51 km
-	Nigeria	1191 km
-	Niger	275 km
-	Burkina Faso	719 km
-	Mali	837 km
-	Senegal	668 km

In Nigeria, local and indigenous surveyors jointly executed the project with their American counterparts.

The accuracy and relevance of the project in the current quest for a uniform geodetic base for Africa requires a fresh analysis and appraisal.

A study of the available data and records of the various geodetic networks shows that 16 datums are currently in use in Africa and four major ellipsoids, namely: Clarke in 1880, used in 27 countries, International Ellipsoid in three countries; modified Clarke 1880 used by one country and the Bessel Ellipsoid used by one country. The problem is further compounded by the fact that the accuracy of the networks is not known. These differences in datum are present even between neighbouring States. Hence, the need for a uniform datum so that all surveys can be related to one another.

SATELLITE GEODETIC SURVEY

African Doppler Survey (ADOS) - A Doppler Control Network for Africa

A Doppler Control Network Project for Africa was initiated as a result of the joint effort of Commission VIII (charged with the responsibility of Coordination of Space Techniques for Geodesy and Geodynamics (CSTAG)) and Commission II (on Geodesy for Africa) of the International Association for Geodesy (IAG). The project, which was sponsored by and executed in collaboration with the Canadian International Development Agency (CIDA), the United States Defence Mapping Agency (DMA) and the Directorate of Overseas Survey (DOS), the United Kingdom, under the auspices of the Commission for Geodesy in Africa, commenced in 1981. The aim of the project was to establish a network of Doppler points to which existing controls could be adjusted on a common datum. In addition, areas without exisiting controls can be filled in by rapid Doppler observations at a later date. Priority was given to Doppler points coinciding with the best and highest order existing control in the area so as to convert the new controls derived to a new datum. Forty-six of the 52 member States of the Organization of African Unity (OAU) participated in the project. A total of 307 Doppler points, well distributed over the continent, were accepted. However, the unification exercise is complicated because only 22 countries provided a number of ADOS points with geodetic coordinates and the datums used. The new Doppler data and database for the Doppler derived stations are archived at the Regional Centre for Services in Surveying, Mapping and Remote Sensing, Nairobi, Kenya. Preliminary coordinates of all the stations located in Benin, Burundi, the Central African Republic, the Congo, Djibouti, Egypt, Gabon, Guinea-Bissau, Mali, Namibia, Niger, Rwanda, South Africa, Togo and Burkina Faso were released to these countries.

As a follow to the project, two post-ADOS training seminars were organized in Nairobi, Kenya, and Yamoussoukro, Côte d'Ivoire, for anglophone and francophone countries respectively. The contents were:

- Applications of space techniques in geodesy

- Unification and strengthening of existing national geodetic control network through the use of Doppler satellite

- Geodesy to obtain corrections for scale and orientation distortions; and datum correction parameters

- Geoid and geodetic datum definition for each country and eventually for the African continent. Appendix III gives the status of the project as of 1984.

With the experience acquired in the ADOS project, a second Post-ADOS programme was to have commenced and aimed at:

(a) Detailed analysis of existing data and a programme of work to increase the basic geodetic infrastructure at the national level. This was to have been embarked upon directly by each country or through bilateral and multilateral cooperation;

(b) Connection of the networks at regional and sub-regional levels by direct cooperation between the countries of the region or with international cooperation.

It was envisaged that about 14 per cent of the existing networks are required as additional works to connect the main loops. The data when completed would have formed the basis of a continental geodetic data bank.

In the Directorate General Military Survey (DGMS), the United Kingdom carried out some lower order Doppler fixes in Sierra Leone, Liberia, Kenya and Djibouti. Unfortunately, in the short time at my disposal to conduct search into the records, I was unable to confirm any further action on the part of the African countries to put into proper use the experience and knowledge they had gained from the project on the realization of the objectives of the ADOS programme. In Nigeria, for instance, the Marconi and JMR receivers used on the project have been sent for repairs to Canada and the United States respectively since 1985. They have not yet been recovered.

COMMISSION FOR GEODESY IN AFRICA

The Commission for Geodesy in Africa, established by the International Association for Geodesy (IAG) was inaugurated in Lagos in 1977 with the following objectives:

- to make an inventory of the status of geodetic work in Africa, update and maintain such an inventory

- to stimulate and sustain interest of survey Organizations in Africa with a view to organizing geodetic control and gravity networks for scientific and cartographic purposes

- to encourage geodetic education and advise on curriculum development in geodetic science

- to establish and maintain data banks and make geodetic information available nationally and internationally.

The Commission at its inauguration established five sub-committees to conduct studies and research:

- Gravity
- Data Bank
- Education and Publications
- African Geoid and Datum Definition
- Inter-African Geodetic Projects Coordination

AFRICAN GRAVITY NETWORK

In the search for geodetic records, it was discovered that gravity data were missing or sparse in most African countries. In addition, most of the existing gravity nets are isolated and intended for prospecting purposes. They were thus established only in the areas of geological interest. However, the need to establish a uniform gravity network for Africa, to serve as reference stations for all gravity measurements for the detection of crustal deformations and detection of possible periodic errors in the gravity standard by IGSN, was identified. The project was to be jointly undertaken by African scientists and their Italian counterparts. Twenty stations were to have been established in the first instance in Benin, the Central African Republic, Ethiopia, Egypt, Ghana, Cote d'Ivoire, Kenya, Liberia, Senegal, the Sudan, Madagascar, Uganda, Burkina Faso and Nigeria. Unfortunately, the project was not implemented due to lack of funds and support from the expected donor country. Also, there is no serious commitment on the part of African Governments to fund research activities in gravity work despite the fact that the continent is seismically active and parts of it are prone to earth tremors and earthquakes. However, individual African countries still carry out isolated gravity surveys in their countries.

THE AFRICAN GEODETIC DATABANK

Commission XI of the International Association of Geodesy adopted a resolution to establish an African Data Bank (AGDB). A Committee charged with the responsibility to establish the Data Bank was constituted in 1977 with headquarters at Lagos, Nigeria. All national and international organizations were requested to release all the geodetic data, in their custody, to the Bank. Unfortunately, the Committee is plagued with numerous problems not unconnected with severe underdevelopment viz: lack of funds, general apathy of the relevant African Government towards promoting and facilitating the AGDB activities, lack of technical input by the international geodetic community, and the slow pace of introducing generalized and automated information management systems in the curriculum in institutions of higher learning of Africa.

APPLICATION OF GLOBAL POSITIONING SYSTEM IN NIGERIA

Ground control establishment using the Global Positioning System (GPS) techniques started in Nigeria in 1989 with the establishment of 100 No. GPS survey controls by the oil companies under the umbrella of the Nigerian National Petroleum Company (NNPC). Since then, the oil industry, notably Shell Petroleum

Development Company, Elf and Gulf, have also employed the technique to provide controls for map revision and updating of the 1:50,000 topographical maps of parts of southern Nigeria, their main areas of operation, using satellite remote sensing techniques. The National Petroleum Investment Management Services (NLAPIMS) of NNPC has also carried out some GPS surveys in the Chad Basin of Borno State of the country. A national campaign to establish a network of controls using the GPS was embarked upon at the Federal Surveys of Nigeria. All the State governments are participating in this scientific work. GPS is relatively new to the African market. Data on its application for control establishment on the African continent are not yet available. There is, however, no doubt that many countries of the continent, particularly the oil producing States, are already employing the technique to establish and densify controls.

AERIAL PHOTOGRAPHY ACQUISITION

Most francophone countries of Africa are covered by aerial photography at the 1:65,000 and 1:75,000 scales acquired between 1951 through 1981 while most anglophone African countries are covered with 1:40,000 and smaller-scale photography. These were used mainly for the production of the basic topographical maps at the scale of 1:50,000 and for planning purposes. Available records show that many African countries had aerial photographic capabilities before their independence. It is disheartening to note that despite the fact that some of the countries became independent as far back as the late 1950s to the early 1960s, only Burkina Faso, Ethiopia, Côte d'Ivoire, Liberia and Madagascar have developed indigenous facilities and capabilities for aerial photography acquisition. The other countries depend largely on foreign survey concerns operating locally on contract or under technical assistance for the execution of their aerial photographic projects. I must add, however, that a good number of the countries have local facilities for processing of the aerial films. Infrared and false colour photography have also been used for mapping.

Records would not be complete without due reference to and acknowledgement of the activities of the United Nations Economic Commission for Africa (ECA), a body which has played a major and crucial role in the development of cartography on the African continent. ECA is responsible for initaiting and coordinating cartography activities in Africa.

Activities of the United Nations Economic Commission for Africa in cartography

The United Nations set up an ad hoc Group of Experts on Cartography in 1949 to study cartographic policies and practices and recommend ways and means for its development. One of the major recommendations of the group which was adopted was that the United Nations should champion the promotion of cartography and take all such measures to establish and develop it in the regions where it was lacking. To this end, a separate United Nations Cartographic Conference for Africa was launched under the auspices of the United Nations Economic Commission for Africa. This is a forum whereby African cartographers make concerted efforts to discuss the role of their profession in economic development, including environmental monitoring. The first conference was held at Nairobi, Kenya, in 1963. The aim of the conference was to encourage the development of cartographic services in Africa with special emphasis on the role of surveying, mapping and remote sensing for meaningful planning and economic development. There is no doubt that surveying and mapping products are sine qua non for the economic development and powerful tools for environmental monitoring, detection and prevention of hazards. Subsequently, six other conferences have been convened, in Tunis, Tunisia, 1966; Addis Ababa, Ethiopia, 1972; Abdijan, Cote d'Ivoire, 1979; Cairo, Egypt 1983; Addis Ababa, Ethiopia 1986; and Ouagadougou, Burkina Faso, 1989. The outcome of the conferences have resulted in:

- the setting up of Regional Centres for Training in aerial survey, photogrammetry and airborne geophysical survey as well as conducting research in these areas within the African environment;

- the establishment of joint centres for specialized services in surveying and mapping. The strategy was to pool the resources of a group of countries within the region to execute projects beyond the executive capacity of any one of its members and to offer opportunity for shop-floor experience to African States so as to prepare them to eventually take full charge and control of the surveying and mapping of their regions. In addition, the Centres were also to provide servicing and maintenance of equipment to Member States, thus minimising delay, cost and saving scarce foreign exchange, as well as, providing services, employment and experience to a strong team of indigenous factory engineers;

- with the development of remote sensing, Regional Remote Sensing Centres were to be established within the African Remote Sensing programme;

- the declaration and celebration of 1986 as the Year of Cartography in Africa was aimed at englightening the Governments of African countries on the use and benefits of cartography so that they could rate cartography high among their national priorities;

- the establishment of the African Remote Sensing Council in 1975 and the subsequent merger of the Council with the African Association of Cartography in 1989 to form the African Organisation for Cartography and Remote Sensing to minimize duplication and overlap of activities of the two organizations and save cost on their maintenance;

- in cooperation with the Commission for Geodesy in Africa in the execution of the African Doppler Observation Survey (ADOS) programme, the ultimate objective of which is to provide zero-order controls and common datum to which African participating countries can adjust their national networks. It is envisaged that a common datum for Africa will facilitate the standardization of map specification which had hitherto not been practicable due to the different map projection systems of the countries within the continent;

- national, regional and international exchange of information and developing awareness horizontally among professionals and vertically to decision-makers as an effective tool in developing cartography and remote sensing. To this end, ECA Regional Centres were requested to organize seminars and study tours for decision makers to sensitize them through exposure to concrete and practical use of remote sensing.

Regional Centre for Training in Aerospace Surveys, Ile-Ife, Nigeria

The Regional Centre for Training in Aerospace Surveys in (RECTAS), Ile-Ife, Nigeria was established in 1972 to provide training courses at the professional and technician levels in various disciplines of cartography. This was to ensure that existing and newly established national surveying and mapping organizations were adequately staffed. The Centre has developed in terms of physical and academic expansion. Initially, training courses were offered at technician and operator levels in photogrammetry in both the English and French languages. Today, it offers training programmes in photogrammetry and remote sensing at the technician, technologist and post-graduate levels. It also organizes short-term training courses to meet specific user needs, particularly in remote sensing applications. It enjoys support and cooperation from the Swiss, French and the Netherlands Governments and the European Community (EC). In addition to its regular courses, the Centre conducts research and consultancy services in surveying, photogrammetry and remote sensing to member States and other African countries.

Regional Centre for Services in Surveying, Mapping and Remote Sensing, Nairobi Kenya

The Centre was established in 1975 to provide specialized services, in surveying and mapping to the eastern and southern African block. The centre inherited the regional remote sensing facility which the United States Government, through its Agency for International Development (USAID), had established to provide remote sensing services to the east and southern Africa regions. The following facilities are available at the Centre:

- user course in remote sensing
- short courses in remote sensing applications to resource exploitation and development and environmental monitoring
- distribution centre for satellite imageries
- archival of surveying and mapping data
- consultancy services and project execution
- topographic mapping at 1:250,000 using satellite imageries

Regional Remote Sensing Centre, Ouagadougou, Burkina Faso

The National Centre at Ouagadougou was regionalized in 1979 to offer user-assistance services in programmes in photogrammetry and remote sensing. It offers short-term introductory courses of three months' duration in remote sensing and project execution in application remote sensing in the areas of desertification control, agronomy and water resources development. It has a well-equipped photo-laboratory and a rich archive of satellite imageries. There has not been any student intake at the Centre in the last two years.

Remote Sensing Centres: Cairo, Egypt, and Kinshasa, Zaire

These two centres still operate as national centres. The centre in Egypt, located in the Academy of Sciences, is well equipped and modern. It is engaged in project execution in all areas of resources development. The Kinshasa Centre is embarking on a membership drive mission to convince African countries within that region to participate in the Centre.

The programme is to set up more centres as and when the need arises. A Remote Sensing Centre for north Africa is to be established at Tunis, Tunisia.

ORGANIZATION OF THE AFRICAN REMOTE SENSING COUNCIL

The Conference of Ministers of the Economic Commission for Africa (ECAK) unanimously endorsed the establishment of the African Remote Sensing Council in 1975. The initial programme included the establishment of two ground receiving and processing stations at Kinshasa, Zaire, and Ouagadougou, Burkina Faso. This decision was informed by the need for the reception to have at least 90 per cent coverage of the continent and the existence of tracking facilities (Intelsat network) in the locations. In addition, five Training User-Assistance Centres were to be established in Cairo, Egypt; Ouagadougou, Burkina Faso; Kinshasa, Zaire; Nairobi, Kenya and Ile-Ife, Nigeria. An intergovernmental meeting of experts held in Nairobi, Kenya 1977 prepared the draft constitution of the Council. This was ratified by the ECA Conference of Ministers in Kinshasa, 1977. The Constitution came into force in 1979 after the required number of signatories had been secured. The inaugural meeting of the Council was held at Ouagadougou, Burkina Faso, the same year. Initially, the headquarters operated from the ECA secretariat at Addis Ababa. It has been located at Bamako, Mali, since 1982. Unfortunately, the Council did not make any appreciable impact on remote sensing activities in the continent due to lack of funds.

Later, it became necessary to rationalize and harmonize the activities of the institutions sponsored by ECA and the OAU, because of the huge financial burden of running the institution and the fact that some of them were responsible for similar operations. The merger of the African Association of Cartogpahy and the African Remote Sensing Council gave birth to the African Organisation of Cartography and Remote Sensing (AOCRS) in 1988. The objectives of the Council include the promotion of the development of cartography and remote sensing in Africa and the coordination of major survey, mapping and remote sensing activities of the member States.

Developments in instrumentation witnessed rapid technological advancements. Analog instruments yielded way to analytical plotters. Rapid developments were also recorded in methodology and improved user products. Unfortunately, despite these developments, conventional surveying and mapping techniques still currently in use did not offer cheaper and faster production techniques. If available statistics are anything to go by, that is, 4 per cent growth rate in geodetic control network establishment and 3 per cent in mapping assuming that the necessary funds and facilities are available, using these conventional methods, the basic mapping requirement of the continent would only be met in another 50 years.

In order to implement the Lagos Plan of Action aimed at the rapid economic development of Africa between 1980 and the year 2000, as directed by the conference of Ministers of ECA member states in 1980, African countries must brace up to the challenge and take advantage of the new developments in remote sensing technology to ensure cartography for all by the year 2000. This entails the provision of basic surveying and mapping services for the inventory of natural resources, improvement of the land exploitation system and management of water resources.

Remote sensing applications in Africa

With the launching of Sputnik I in 1957 by the Soviet Union and Landsat Multispectral Scanner (MSS) in 1972 and Landsat Thematic Mapper (TM) in 1982 by the United States, research efforts shifted from photogrammetry to remote sensing for the production of thematic and resource maps and photographic images for various purposes, namely: regional, urban and rural planning and development, development of infrastructure, natural resources management, environmental monitoring and protection, etc. Although there was increased awareness of the vast potential of remote sensing technology among African scientists, cartographic applications of remote sensing were limited to the production of base maps at the scales of 1:250,000. Its use for resource mapping varied from country to country and was limited to special- purpose uses, particularly in forestry, agriculture, water resources and ecological studies, etc.

Due to the limited resolution of Landsat (MSS, TM resolution of 80m and 30m respectively), only rudimentary efforts were made in the application of remote sensing technology in the production of basic maps. This is partly due to the slow decision process and partly because the interest of photogrammetrists and mapping experts in remote sensing was limited to thematic cartography. Furthermore, despite the fact that the TM sensors on board Landsats 4 and 5 are superior to the multispectral scanner onboard Landsat 1-3 in terms of spectral range, spatial resolution, radiometric sensitivity and accuracy, Landsat is still inadequate for the mapping of cultural features at larger scales. However, institutions of higher learning offering courses in cartography have expanded their curricula to include programmes and courses in satellite geodesy, mapping and remote sensing technology in space techniques.

The launching of SPOT, with high spatial resolution of 10m-20m, stereo viewing capability and low repetitivity, in 1986, and the aggressive campaigns mounted by its proprietors, have created awareness and encouraged surveying and mapping establishments to take advantage of the vast potentials of the new technology for rapid production of maps of their countries. The last few years have witnessed a sharp upsurge in remote sensing activities in the continent. This sudden awakening of interest in the application of remote sensing is due largely to the capability of SPOT satellites to provide three-dimensional mapping capability by stereo imaging. Resource surveyors and mapping specialists have at last eliminated the staggering and frustrating problems of obtaining images and further information required for efficient performance of their duties in aiding resource inventory and environmental management for purposes of development. A number of African countries have now embarked on the upgrading and expansion of their institutional capabilities through a programme of intensive training of indigenous personnel in remote sensing technology and the acquisition of satellite image interpretation equipment and other satellite image processing facilities. Satellite remote sensing techniques are now being utilized for the production of topographical maps at the 1:100,000 and 1:250,000 scales and for the quick revision of the 1:50,000 basic topographical maps in many African countries.

The satellite data processing facilities available at the UNECA Centres in Nairobi, Kenya, Ouagadougou, Burkina Faso and at Cairo, Egypt, are well equipped to support these programmes.

Nigeria has also concluded preliminary studies on the establishment of a Satellite Ground Receiving and Processing Station at Panyam, Jos, Nigeria.

SUMMARY AND CONCLUSIONS

In the foregoing discourse, the factors responsible for the economic backwardness of Africa have been identified as being largely due to the low level of the applications of science and technology for the development of its natural resources, thus making African countries dependent on industrialized nations. To redress the situation, a significant proportion of all available resources must be mobilized and harnessed for development. In so doing, a complete inventory of the resources is required to determine their type, extent, location and distribution. Surveying and mapping provide an efficient means for such an inventory.

Looking back into the history of technological development in surveying and mapping, it has been established that there is no reason whatsoever why Africa should not have been in the forefront of development, if the pace of ancient civilization had been kept. We have noted that Africa is grossly undermapped having been only 20 per cent mapped at the basic scale of 1:50,000. The uses of maps as aids to development programmes were discussed. It was concluded that Governments of African countries must place high premium on surveying and mapping services and rate them high among their national priorities.

Technological developments in surveying and mapping science, in terms of instrumentation and methodology, were highlighted, ranging from high-technology satellites to basic techniques. Their application in the delivery of surveying and mapping services were also discussed. We have realized that conventional techniques do not adequately meet the current urgent needs. We identified the need to reorient our attitude and apply the best techniques to meet the tasks at hand, that is, the quick and timely production of maps, using efficient and cost effective methods, to meet our national goals and objectives. To this end, the philosophy for the delivery of surveying and mapping services in Africa is advocated as the provision, analysis, representation, translation and communication of spatial information which is central to the needs of a developing continent.

An analysis of the geodetic networks in Africa shows that there is a dearth of controls. We recognized the need to densify and adjust the multifarious geodetic networks to a uniform datum using one projection system if we are to map Africa together without any gaps or overlaps such that all surveys can be related to one another. To do this effectively, a programme of extension and densification of geodetic controls using the Global Positioning System needs to be embarked upon, either through technical assistance from willing donor countries, or directly by each country and in cooperation with other countries.

The Commission for Geodesy in Africa shall be noted and commended for mapping out course of action for the development of Geodesy in Africa and the integration and harmonization of the programmes of individual countries, particularly in the establishment of the African Gravity Network and the African Geodetic Data Bank. Unfortunately, the Commission has not been able to perform effectively due to lack of funds and other logistics problems. IUGG and the IAG are called upon to solicit adequate financial support for the programmes and activities of the Commission from its member nations as a measure of its commitment to ensuring that all African countries benefit from the new developments in satellite geodesy.

The state of the art in aerial photography coverage of the continent was reviewed. Almost the entire continent is covered with aerial photography at scales varying between 1:40,000, 1:65,000 and 1:75,000 and acquired between 1951-1981. However, we have also established that Africa is lacking in up-to-date photographic coverage at all scales. Facilities, technical know-how, executive capability and capacity are simply not on the ground. The continent continues to depend almost entirely on foreign expertise for the execution of its aerial photographic projects. What is even more distrubing is the nearly complete apathy on the part of African Governments. Africa is simply not competitive in an increasingly competitive world! This situation must be reversed. African Governments must invest in the acquisition of complete aerial survey systems expand, modernize and upgrade the existing aerial photographic processing facilities and train indigenous skilled human resources to operate the system.

We have examined the activities of the United Nations Economic Commission for Africa and the OAU *vis-à-vis* the fostering of the economic emancipation of Africa through the design and implementation of vibrant plans and programmes aimed at achieving self-sufficiency and self-reliance in cartography and remote sensing by the year 2000.

We embrace the elements of the Lagos Plan of Action, the Final Act of Lagos and the United Nations Programme of Action for Africa's Economic Recovery and Development and Africa's Alternative Framework for Structural Adjustment Programmes for Socio-ecocnomic Recovery and Transformation as a prescription for revamping Africa's battered economy. What use is a prescription if there is no will to accept the panacea? The realization of the objectives of these laudable programmes undoubtedly depends on the inventory and development of the vast and rich natural resources of the continent. The irrepacleable value of surveying and mapping as a *sine qua non* to this inventory has been re-affirmed.

The African Regional Cartographic Conferences have resulted in the establishment of the Regional Centres for training in aerospace survey, services in surveying, mapping and remote sensing. Three such centres, at Ile-Ife, Nairobi, and Ouagadougou, operate as regional centres while the Remote Sensing Centres at Kinshasa and Cairo operate at national level. African countries are called upon to take advantage of the facilities and expertise available at these centres to develop their capabilities and establish facilities in surveying and mapping science and technology.

The efforts and the achievement of many African countries in the applications of remote sensing techniques for their resource and thematic mapping have been reviewed. In this regard, all Governments should:

- Endeavour to strengthen and support all structures working in cartography and remote sensing, including training and educational institutions, and ensure that such institutions absorb this technology. To this end, a recycling of African nationals previously trained in foreign countries should be pursued as a means of continuous training and professional development. This would provide an avenue for updating of skills and knowledge in surveying, mapping and remote sensing technology;

- Take full advantage of the potentials of cartography and remote sensing in their development planning and programming;

- Mobilize and sensitize the international community, especially those countries possessing cartography and remote sensing technology, to the needs and limitations of African countries and spare no effort in ensuring that the African countries benefit from the advantages derived from the use of advanced cartography and remote sensing technology;

- Seek bilateral and multilateral cooperation on a South-South and/or North-South basis to develop facilities in surveying and mapping;

- Mount intensive and extensive enlightenment campaigns on the magic which cartography and remote sensing hold as the key to development.

The efforts of African countries to pool resources and share facilities in remote sensing technology through the establishment of the African Remote Sensing Council should be supported. Much as the Council had tried to make the desired impact, lack of funds had cramped its best endeavou rs.

Finally, in the words of John Kennedy and re-echoed by Barber Conable of the World Bank at the recently concluded 27th OAU Summit at Abuja, Nigeria, "Africa's problems are man-made and could be solved by man." All that is left, and this is all that needs to be said, is the will to do so.

Appendix I

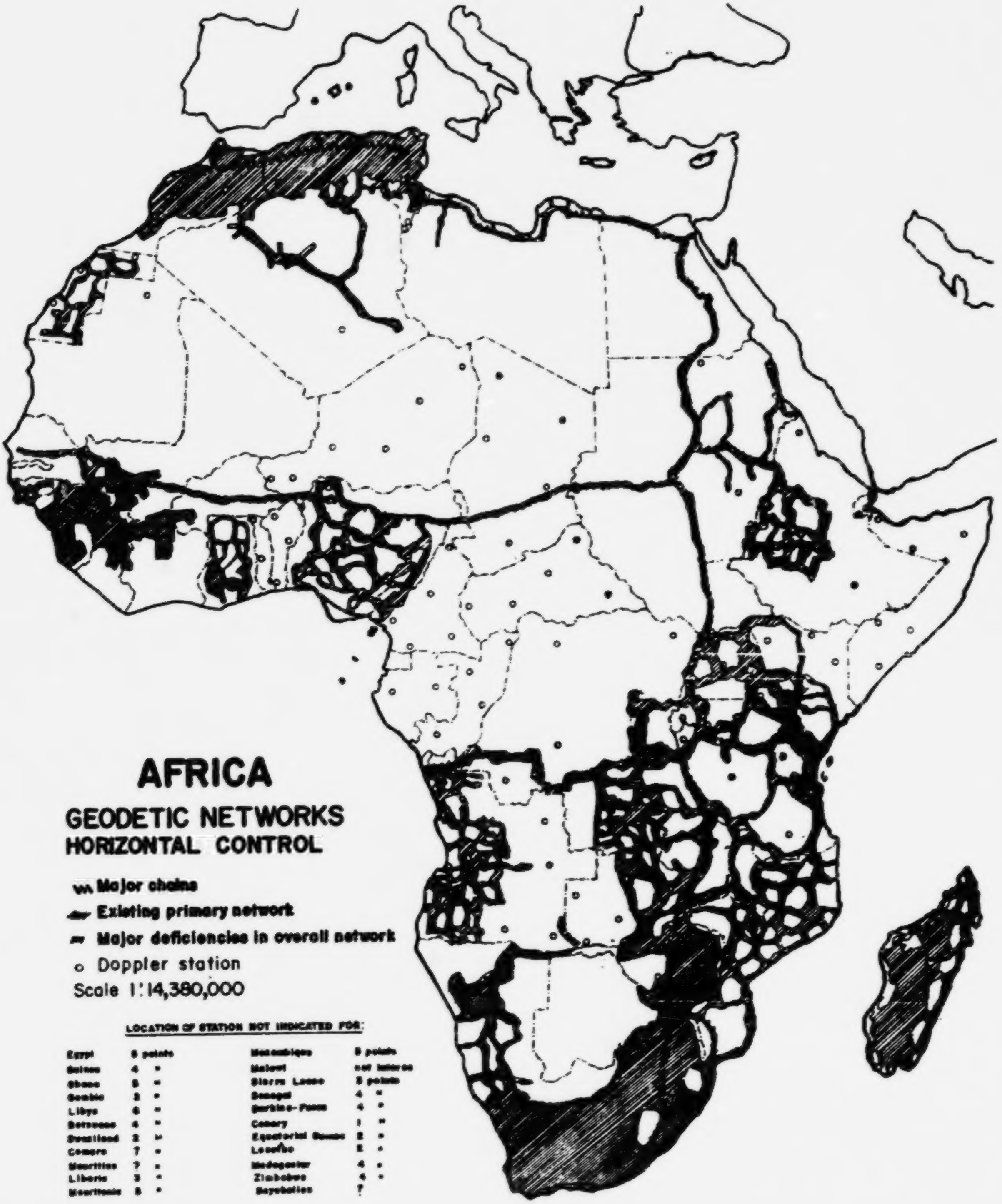
AFRICA
GEODETIC NETWORKS
HORIZONTAL CONTROL
Major chains
Existing primary network
Major deficiencies in overall network
○ Doppler station
Scale 1:14,380,000

LOCATION OF STATION NOT INDICATED FOR:

Egypt	8 points	Mozambique	8 points
Guinea	4 "	Malawi	not interes
Ghana	5 "	Sierra Leone	3 points
Gambia	2 "	Senegal	4 "
Libya	6 "	Burkina-Faso	4 "
Botswana	4 "	Canary	1 "
Swaziland	2 "	Equatorial Guinea	2 "
Comoro	? "	Lesotho	2 "
Mauritius	? "	Madagascar	4 "
Liberia	3 "	Zimbabwe	4 "
Mauritania	6 "	Seychelles	?

Appendix II

SOURCE: ECA REPORT E/ECA/NRD/CART/125

NAME OF COUNTRY	AREA IN SQ. KM.	POPULATION	TOPOGRAPHICAL MAPPING						INDIGENOUS MAPPING CAPABI-LITIES	AERIAL PHOTOGRAPHIC COVERAGE		REMARKS
			1/50,000 & LARGER SCALE	YEAR	1/100,000	YEAR	1/250,000	YEAR		1/25,000	YEAR	
Algeria	2,381,741	20,577,000	15%	50-79			100%	63-81	AVAILABLE	100%	79	
Angola	1,246,700	8,339,000	-				45%	78	No Data	40%	81	
Benin	112,622	3,719,500	52%	85			100%	85	Tech. Asst.	100%	66-75	
Botswana	582,000	1,007,000	45%	74-81			60%	74	ditto	90%	51-74	
Burkina Faso	274,200	6,607,000	-	-			100%	53-72	Available	100%	50-78	A.S.F.
Burundi	27,834	4,421,000	100%	82	100%	38	100%	79	Tech. Asst.	-	-	
Cameroon	475,442	9,164,775	100%	56-78	-		100%	53-78	Ditto	10%	58-70	
Cape Verde	4,033	313,000	-		-		-		No data	-	-	
Central Africa Republic	622,984	2,450,000	40%	63-79	-		100%	54-75	Tech. Asst.	100%	34-77	
Chad	1,284,000	4,789,000	10%	63	-		100%	51-76	No data	100%	54-65	
Comoros	2,171	431,000	-		-		-		ditto	100%	49-50	
Congo	342,000	1,651,000	20%	63-66	-		100%	48-78	Tech. Asst.	100%	51-67	
Cote D'voire	322,463	9,161,000	60%	78	-		100%	58-74	Available	50%	70-73	A.S.F.
Djibouti	22,000	330,000	-		20%	53	45%	68-72	No data	-	-	
Egypt	1,001,449	44,533,000	-		50%	b/54	-		Available	70%	-	
Equatorial Guinea	28,051	375,000	-		-		-		No data	-	-	
Ethiopia	1,221,900	42,500,000	22%	86	-		100%	65-72	Available	100%	63-73	A.S.F.
Gabon	267.667	1,127,000	50%	87	-		95%	87	No data	95%	54-75	
Gambia	11,295	618,000	100%	79	-		100%	80	Ditto	-	-	
Ghana	238,537	12,626,000	100%	72	-		-		Available	50%	57-76	
Guinea	245,857	5,177,000	100%		-		-		No data	100%	51-79	
Guinea Bissau	36,125	863,000	-				-		Ditto	-	-	
Kenya	582,644	18,960,000	53%	86	60%	59-66	100%	78	Available	80%	53-69	
Lesotho	30,335	1,444,000	100%	66	-		100%	69-78	No data	100%	75-76	
Liberia	111,369	2,057,000	30%	69	-		100%	72	Available	90%	79-82	A.S.F.
Libya, Arab Jamahiriya	1,759,540	3,342,000	25%	64-81	-		45%		No data	60%	68-79	
Madagascar	587,041	9,400,000	30%	84	95%	84	-		Available	100%	54-79	A.S.F.

Appendix II (continued)

Malawi	118,484	6,429,000	85%	50-78	-	84	100%	74-79	Available	100%	62-74
Mali	1,240,000	7,528,035	2%	85	-		100%	55-72	Tech.Asst.	100%	52-75
Mauritania	1,030,700	1,779,000	-		-		100%	55-78	No data	100%	53-64
Mauritus	2,045	992,855	-		-		-		Tech.Asst.	100%	75
Morocco	446,550	22,109,000	70%	86	84%	86	50%	86	Available	95%	53-75
Mozambique	801,590	13,311,000	85%	84	15%	71	100%	84	Tech. Asst.	95%	56-72
Niger	1,267,000	5,772,000	10%	56-78	-		100%	58-70	ditto	100%	50-65
Nigeria	923,768	89,022,000	95%	86	85%	86	64%	86	Available	100%	57-74
Rwanda	26,338	5,700,000	100%	52-58	100%	38	100%	63	No data	-	-
Sao Tome & Principe	964	92,000	-		-		-		ditto	-	-
Senegal	196,192	6,193,000	30%	78	-		100%	57-72	Tech.Asst.	100%	53-78
Seychelles	280	64,332	50%	80	-		-		No data	-	-
Siera Leone	71,740	3,472,000	100%	79	-		100%	72	Available	100%	56-76
Somalia	637,857	5,269,000	1%	50	100%	73-76	100%	73-76	No data	100%	73-75
Sudan	2,505,813	29,362,000	-		50%	49-76	-		Tech.Asst.	60%	41-79
Swaziland	17,363	605,084	100%		-		100%	76	No data	100%	71-72
Togo	56,785	2,756,000	100%	57-67	-		100%	51-67	Tech.Asst.	100%	49-66
Tunisia	163,610	6,886,000	50%	56-81	65%	56	100%	56	Available	55%	67-73
Uganda	236,036	14,625,000	100%	47-74	-		100%	78	Tech.Asst.	100%	54-65
Tanzania	945,087	20,378,000	100%	86	-		70%	78	Available	100%	52-73
Zaire	2,345,409	31,151,000	50%	50-63	-		50%	b/80	ditto	75%	52-59
Zambia	752,614	6,242,000	75%	57-79	-		98%	88	ditto	80%	55-81
Zimbabwe	390,580	7,740,000	100%	80	10%		20%	b/74	No data	90%	63-80
Namibia	823,620	1,000,000	-		-		-				
Western Sahara	1,552	550,000	-		-		-				

Note: A.S.F. - Aerial Survey Facilities

Appendix III

ADOS STATUS UP TO END OF MAY 1984

Source: Nairobi Centre, Kenya

COUNTRY	NO OF OBS. ADOS POINTS	ADOS POINTS TO BE OBSERVED	R E M A R K S
Algeria	unknown	some	INC has not reported on ADOS
Angola	-	12	No current contact
Benin	4	-	Observed by IGN
Botswana	9	-	Completed
Burundi	5		Observed by France
Cape Verde	7	-	Completed
Cameroon		-	Completed
Central African Rep.	6	-	Observed by IGN
Chad	Nil	6	No contact
Congo	6	-	Observed by IGN
Djibouti	2	1	Observed by IGN
Egypt	16	6	No current report
Equatorial Guinea	8	-	Completed by Spain
Ethiopia	Nil	12	No current report
Gabon	8	-	Completed
Ghana	Nil	6	No current report
Gambia	1	-	Completed
Guinea	3	-	Completed
Guinea Bissau	3	-	Completed
Cote D'Ivoire	9	-	Completed
Kenya	-	11	STRE to observe from Juil 1984
Lesotho	5	-	Completed
Liberia	4	-	Completed
Libya	-	15	No report from Libya
Madagascar	-	10	No current report
Malawi	6	-	Completed
Mali	7	-	Observed by IGN

Appendix III (continued)

Country	No of Obs. Ados Points	Ados Points To be Observed	Remarks
Mauritania	1	6	No current report
Mauritius	Nil	-	No contact
Morocco	14	Nil	Completed
Mozambique	Nil	11	No current report
Niger	6	-	Observed by IGN
Nigeria	Nil	13	USA and Nigeria started obs. 5/84
Rwanda	5	-	Observed by IGN
Sao Tome & Principe	Nil	2	No contact
Senegal	13	2	Completed
Seychelles	5	-	Information from DMA
Sierra Leone	Nil	4	Probably observed by UK
Somalia	Nil	12	No current report
Sudan	3	6	No current report
Swaziland	4	-	Completed
Tanzania	8	-	Completed
Togo	3	-	Observed by IGN
Tunisia	5	-	Completed
Burkina Faso	6	-	Observed by IGN
Uganda	Nil	5	No further development
Zaire	1	7	No current report
Zambia	5	-	Completed
Zimbabwe	6	-	Completed

Appendix III (continued)

OTHER POINTS

OTHER TERRITORIES OR COUNTRIES	N OF OBS. ADOS POINTS	ADOS POINTS TO BE OBSERVED	REMARKS
Canary Island	1	-	Completed
Comoro Islands	Nil	1	No contact
Namibia	Nil	7	No current report
Reunion	Nil	1	IGN to observe in 6/1984
South Africa	3	10	Information from DMA
Western Sahara	Nil	3	No current report
Total	4	22	

NOTES

1. Adedeji, Adebayo, Keynote Address, Symposium of Commission VI, Nigeria, International Archives of Photogrammetry and Remote Sensing, vol. 26-6 (1986), pp. 157-165.

2. Adekoya, O.L., "Science and Technology Policy in Nigeria-Existing programmes and with particular reference to Surveying and Mapping" (text of lecture at the Nigerian Institute of Policy and Strategic Studies, NIPSS Kuru, Nigeria, 1988), unpublished.

3. Ihemadu, S.O., International Archives of Photogrammetry and Remote Sensing, vol. 26-6 (1986), pp. 109-125.

4. Konecny, G., "The significance of photogrammetry and remote sensing in developing countries", International Archives of Photogrammetry and Remote Sensing, vol. 26-6, (1986).

5. Konecny, G., "The development and state of the art of remote sensing", ITC Journal (1987), pp. 153-156.

6. Olujohungbe, O., Remote Sensing Activities in Africa - International Archives of Photogrammetry and Remote Sensing, vol. 26-6 (1986), pp. 126-136.

7. Verstappen, H. Th., "Remote sensing applications; an outlook for the future", ITC Journal (1987), pp. 157-164.

8. Status of Topographical Mapping in Africa, ECA, E/ECA/NRD/CART/125, June 1989.

9. Cartography and Remote Sensing Bulletin, UNECA, December 1990.

10. Mapping for Development. Published by Ordance Survey of Great Britain, 1988.

11. Centre for Space Science and Technology Education Africa, SAP/90/001, United Nations, New York, 1990.

12. Sundry Reports: African Doppler Satellite Survey, Twelve Parallel Survey African Cartographic Association, Federal Survey Dept., Lagos, Nigeria, Archives.

13. "Your Guide to Surveying, Mapping, Land Tenure and Remote Sensing Inputs to Development Aid Projects - 1987. "Ordance Survey of Great Britain", 1987, pp. 14-16.

14. The Continental African Geodesic Nework - A Common Scientific Work. UNECA.

15. Economic Commission for Africa (ECA), Seventh United Nations Regional Cartographic Conference for Africa, Ouagadougou, Burkina Faso, 1989 draft report.

OCEANOGRAPHIC APPLICATIONS OF MICROWAVE RADAR DATA*

M. Cantón-Garbín
Universidad de Las Palmas, Spain

INTRODUCTION

The major drawback of visible and infrared imagery of the ocean is the problem of cloud cover. For the oceanographer, who would like as many uninterrupted views as possible of the ever-changing sea surface, the answer has been to move from visible and infrared wavelengths to microwaves which can penetrate cloud and, to a high degree, rain. Thus, during all weather conditions radar provides the capability to measure the environmental conditions at the ocean surface, providing high resolution and wide area coverage.

Though passive microwave radiometry is strongly influenced by the effect of surface roughness on the emissivity of the sea surface, enabling wind speed to be recovered from multifrequency sensors, it is the active microwave instruments which can remotely sense the most information about sea-surface roughness.

Microwaves transmitted by a downward looking satellite radar are scattered into many directions after striking the sea. A small portion of this scattered energy, carrying with it information about phenomena at the surface, is eventually received by the radar. To use radars to study the sea, it is necessary first to calculate the scattered electromagnetic field, knowing the properties of the surface (direct problem), and then, conversely, to infer the surface characteristics knowing the scattered field (inverse problem). Before looking in detail at particular sensors and their applications, we are going to consider how active radar sensors interact with the sea surface.

SPECULAR REFLECTION AND SCATTERING AT THE SEA SURFACE

Usually, the ratio between the reflected and incident energy is expressed by a scattering cross section σ is a function of the surface or target, frequency, polarization and of the electrical and physical sea-surface properties. It is measured by an active microwave remote-sensing device, and therefore, it is the dependence of σ on the environmental properties of the surface which enables the microwave sensor to be used as a remote-sensing instrument.

---

* This paper, which was presented at the United Nations/Food and Agriculture Organization of the United Nations/European Space Agency Workshop on Microwave Remote Sensing Technology, held in Maspalomas, Canary Islands, Spain, 10-14 June 1991, does not necessarily reflect the views of the United Nations.

The reflection mechanisms involved in surface scattering may include specular reflection and diffuse scattering, or a combination of both, depending on the surface roughness and the radar parameters. Reflection at the surface is strongly dependent upon the viewing angle. For near-nadir viewing (looking vertically down on to the surface), specular reflection is the principal process for returning energy to the sensor. The magnitude of O is proportional to the area of surface whose inclination is such as to directly reflect energy back to the sensor. For a flat calm, the surface as a whole will reflect energy back to a sensor emitting and viewing at nadir, but other incidence angles will result in no reflection back to the sensor. As it is roughened, the surface will present many facets reflecting in different directions, so that the radar returns to a nadir sensor will be reduced. Conversely, off-nadir sensors will now receive some reflected energy, but since even the roughest seas is unlikely to have slopes tilted at more and 20° - 25° from the horizontal, specular reflection is important only for viewing angles between 0 and about 150°.

For viewing angles greater than this, a return signal is only achieved by scattering at the surface, and this depends on the surface roughness. Figure 1 illustrates different degrees of surface roughness resulting in (a) purely specular reflection, (b) some scattering but a dominant reflection in the specular direction, and (c) complete scattering. The definition of roughness varies with radar wavelength λ_R and viewing angle θ. A smooth surface (a) can be considered to exist when the vertical height h_r of surface roughness irregularities is:

$$h_r \ll \lambda_R \cos\theta / 4\pi$$

A rough surface (c) is approximately defined as:

$$h_r \gg \lambda_R \cos\theta / 4\pi \qquad (1)$$

RESONANT BRAGG SCATTERING

For a smooth surface, oblique viewing of the surface with active radar yields virtually no return. If the surface is rough and contains periodic surface features comparable to the size of wavelength of the radar, then the regular lattice of roughness acts as diffraction gratings. Because scatter from the repeating lattice pattern adds coherently in the far field (far from the

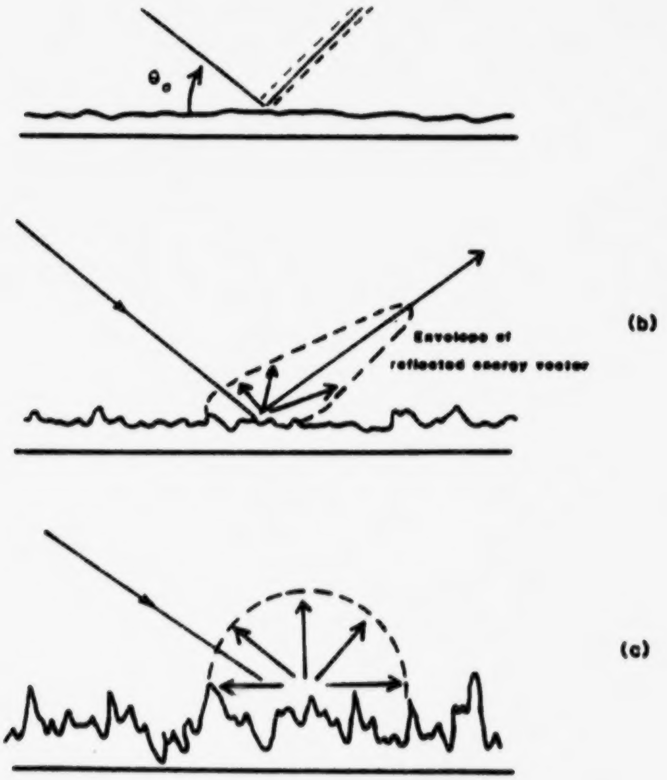
θ₀
Envelope of reflected energy vector
(b)
(c)

Figure 1. Reflection and scattering of radar waves.

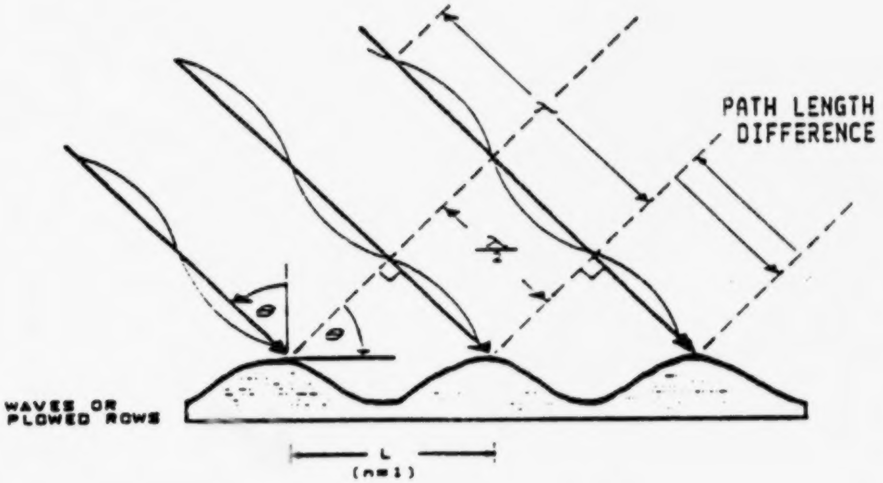
PATH LENGTH DIFFERENCE
λ/2
θ
θ
WAVES OR PLOWED ROWS
L
(n=1)

Figure 2. Bragg scattering at the sea-surface.

surface 0, the scatter is resonant and is called Bragg scatter. The return signal will be at a maximum, if the following condition is fulfilled (Figure 2):

$$L = \frac{n\lambda_R}{2\sin\theta}$$

For sea waves whose crests are at an angle 0 to the radar line of sight the criterion is:

$$L = \frac{n\lambda_R \sin\phi}{2\sin\theta} \qquad (2)$$

Examples of such conditions include wind-induced waves on water surfaces or plough rows in agricultural fields.

Because the ocean surface can be considered to be a superposition of plane waves, and because radio scatter is a linear process, each wave component can act independently as a diffraction grating. Within the limits set by the spectrum of ocean waves, all wavelength and angles are found on the sea surface, so all radio frequencies in resonance with these waves are scattered. σ is therefore an approximate measure of the amplitude of such waves.

The choice of radar wavelength is seen to be crucial in determining the sea-surface roughness which can be detected, both in controlling the height of roughness which can be detected through (1) and also the ocean wavelength, if any, which will dominate the backscatter return (2) (Table 1).

At the microwave frequencies used for active ocean remote sensing, the depth at which the radio energy is reduced to 1/e of its surface value is between 0.1 millimeter (mm) and 10 centimerer (cm) in water, which is much smaller than for dry land surfaces. Because of the very shallow penetration it has largely been assumed that backscatter occurs entirely at the sea surface, and is related to the shape of the sea-surface profile.

The scatter of short radio waves can be calculated by assuming the ocean surface has two scales: (a) short wavelength ripples, riding on (b) longer, larger waves. The Bragg scatter from each small area is calculated using the local small wave fields and the local orientation of the surface and integrating over the entire area.

When the wind is stronger than a few metres per second, sufficient to roughen the surface with high frequency ripples, the Bragg scattering is produced by the ripples which are modulated by the longer waves. In this way it is possible to

Table 1. Bragg wavelength L as a function of radar wavelength and incidence angle.

RADAR WAVELENGTH	INCIDENCE ANGLE			
	$\theta =$	20°	40°	60°
3.2 cm (X-BAND)	L =	4.7 cm	3.5 cm	1.9 cm
5.7 cm (C-BAND)	L =	8.3 cm	4.4 cm	3.3 cm
23. cm (L-BAND)	L =	33.6 cm	17.9 cm	13.3 cm

obtain information bout the longer waves. Furthermore, the scattered signal is shifted in frequency (the Doppler shift) by exactly the frequency of the ocean wave producing the scatter.

OCEANOGRAPHIC APPLICATIONS OF SYNTHETIC APERTURE RADAR

Synthetic aperture radars (SAR) accurately maps the radar reflectivity of the sea over areas 50 to 100 km on a side, with a resolution of 10-40m. A radar image of the ocean surface may be viewed as a map or snap-shot of short gravity wave field with wavelengths in the order of 1 cm to 30 cm, subject to Bragg resonances effects. Surface and internal waves, surface slicks, ship traffic, ice, ocean currents, fronts and eddies and signatures related to bottom topography can be studied by the radar. All of the above expressions of ocean dynamics may be observed by a SAR either directly or indirectly, because of their interaction with small-scale wind generated waves at the ocean surface. The intensity of the backscatter modulation from the ocean surface is dependent on parameters such as wave height and length, wind speed and direction, and on the radar parameters. The latter include spatial resolution, the angle of the incident radar beam and the integration time.

A SAR is a pulse-Doppler radar that transmits short radio pulses to obtain resolution in range, and that uses the Doppler shift of the scattered signals to obtain resolution in azimuth. Modern SAR systems that have been used for experiments in Oceanography operated at X, C and L-bands. However, most of the knowledge available to date is based on spaceborne SAR data, which were exclusively acquired at L-band (Seasat, SIR-A and SIR-B). Some C-band SAR systems are being prepared at present (Earth Resources Satellite (ERS)-1, SIR-C and RADARSAT).

Influence of target motion

A SAR radar assumes that targets are stationary and that the Doppler shift of the received signal is due entirely to the radar motion. But the ocean surface is always in motion, and interpretation of SAR images of the sea requires some understanding of the influence of this motion on the images.

In optically processed images the primary influence of target motion is a displacement of the target from its true position in the image to a new position appropriate to its velocity. Targets moving toward the radar are displaced in the direction toward which the radar is moving, and those moving away are displaced in the opposite direction (See figure 3).

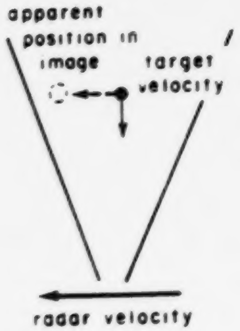
apparent position in image
target velocity
radar velocity

Figure 3. Influence of target velocity on its position in the radar image.

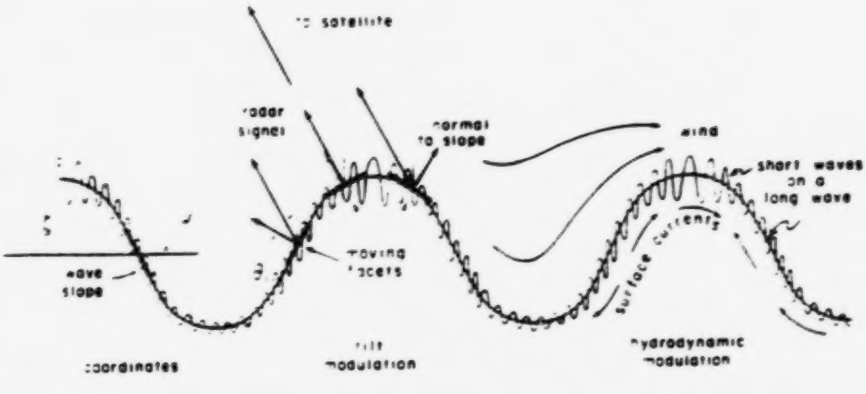
to satellite
radar signal
normal to slope
wind
short waves on a long wave
surface currents
moving facets
wave slope
coordinates
tilt modulation
hydrodynamic modulation

Figure 4. Some processes influencing SAR observations of ocean waves.

SAR imaging of ocean waves

Synthetic aperture radar images of the sea frequently show wavelike patterns, and this leads to the expectation that Fourier transform of SAR images can be used to obtain the spectra of longer waves on the sea. For this reason, the images have been examined to determine the conditions under which waves can be imaged, the correspondence between the wavelike patterns in the image and waves on the sea, and the accuracy with which the ocean-wave spectrum can be calculated.

A SAR does not directly measure wave height, but only the variations in the reflectivity of the surface and there is still not a complete consensus amongst ocean-wave and radar scientists as to the precise mechanisms whereby waves are imaged, whether waves are always imaged, and what direction and wavelength of waves are preferently imaged by SAR.

The variability in radar cross section is usually attributed to three processes: hydrodinamic interactions; electromagnetic interactions or tilt modulation; and motion effects.

Hydrodynamic interactions

The hydrodynamic mechanism incorporated all the fluid - dynamical processes that modulate the capillary waves by the phase of the longer gravity or swell waves. The non-uniform distribution of the short waves on the long waves is attributed to either positive or negative 'straining' of the short waves, depending on whether they propagate in convergent or divergent surface flow sections (figure 4). Convergent and divergent velocity patterns are created by the fluid orbital velocity field, associated with the progression of the swell wave. These surface movements affect the capillary waves, and the resulting interactions of capillary and gravity waves increase the amplitude of the ripples near the swell crest following the passage of a convergent surface velocity field on the rising edge of the wave. A corresponding reduction in the amplitude of the ripples may be observed near the wave troughs. Due to the fact that the occurrence of increased and decreased capillary wave energy is phase to the swell, patterns of strong Bragg scatter on the radar image correspond approximately to swell crests, and patterns of weak backscatter correspond to swell troughs. This theory only applies to low heights and range travelling waves.

Electromagnetic Modulation

Electromagnetic or tilt modulation represents a mechanism whereby the swell alters the way in which the radar beam responds to the roughness of the capillary waves as a function of incidence angle. The gravity waves presents the capillary waves to the radar at different incidence angles as the slope, or tilt, of the longer waves changes. The tilt effect occurs irrespective of hydrodynamic modulation and would still be noticeable if the capillary wave energy were uniformly distributed over the gravity waves. Backscatter related to tilt modulation tends to be very pronounced from slopes of gravity waves that face the radar and least effective from the slope facing away from the radar (figure 4). A parallel swell-wave field travelling in range direction either toward or away from the radar would appear as a series of parallel light and dark streaks, if the radar backscatter were to be modulated by tilt alone. On the other hand, there is no direction; in this case, the troughs and crests are oriented parallel to the radar look direction.

Velocity bunching

A moving sea surface distorts the formation of a SAR image. The effect on the image of target velocity in the range direction has been discussed previously. Garget velocity causes azimuth-image shift. The rising face of a wave is therefore shifted on the image in the positive azimuth direction, and the falling face in the negative azimuth direction. If the long wave amplitude is not too large, the displacement will be a fraction of the ocean wavelength, and the image of the wave will tend to be dark near the wave crests and bright near the troughs even if tilting and hydrodynamic interactions are negligible. If the wave amplitude is too large, however, the displacement can be more than a wavelength, resulting in a very smeared image (figure 5).

SAR images of the sea show many interesting features, including surface waves, internal waves, the influence of currents and bathymetry, ice floes, and ships and their wakes.

The ability of the Seasat SAR to image waves was investigated by comparing the images with measurements of ocean waves made by buoys and wave gauges in the area viewed by the radar. The primary observations were made during the Gulf of Alaska Experiment (GOASEX) and the Joint Air-Sea Interaction Experiment (JASIN).

A glance at many images showed that the SAR did not always image waves, even when they were present on the surface. Several factors are important for wave visibility:

(a) The wind at the sea surface must exceed some critical value:

$$U_{10} > 2\text{-}3 \quad \text{m/s}$$

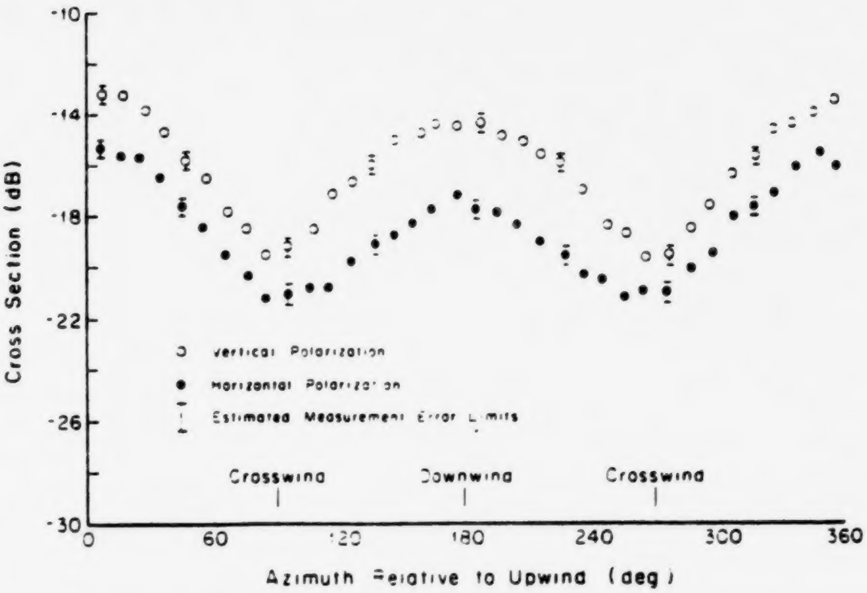

Figure 5. Variation of the scattering crooss section with the wind direction.

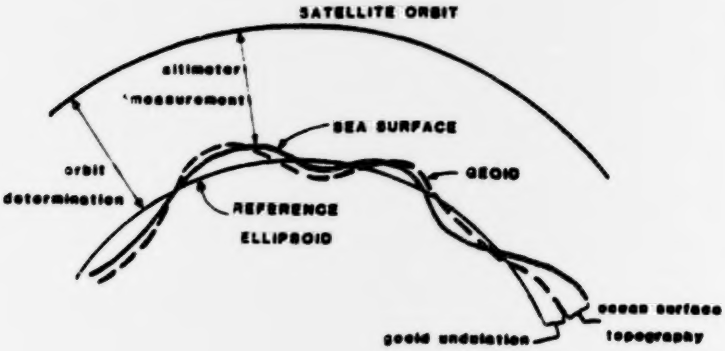
SATELLITE ORBIT
altimeter measurement
SEA SURFACE
orbit determination
GEOID
REFERENCE ELLIPSOID
ocean surface topography
geoid undulation

Figure 6. Contributions to the measured altimeter signal.

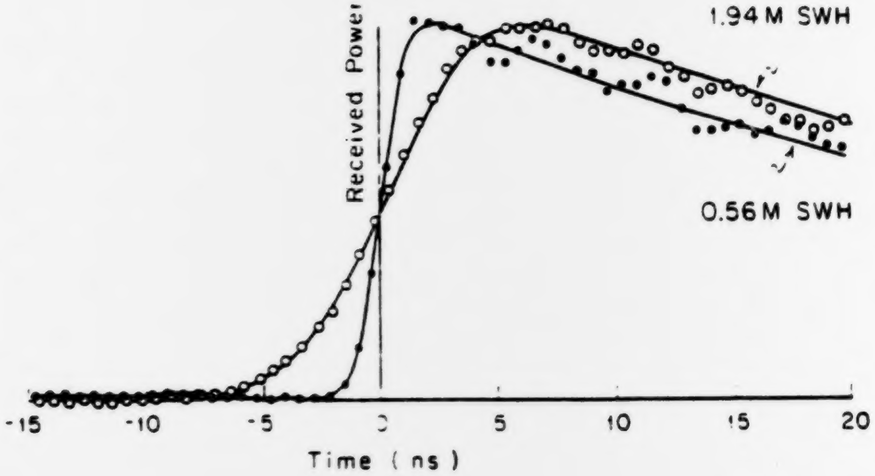

Figure 7. Pulse shapes for two different wave-height conditions.

(b) Nyquist sampling criterion: the wavelength L of the long waves must be at least twice the effective resolution of the radar.

(c) The significant wave height $H^{1/3}$ of the long wave must exceed some threshold, which is approximately

$$H^{1/3} > 1.4 \text{ m}$$

The physical characteristics of a given wave field may be presented in compact form by means of a directional wave spectrum. It reveals the direction and length of the dominant wave train(s), and, given proper calibration, it may even provide an estimate of wave height and energy. Conventional measurements for measuring the surface wave energy spectrum are based on point-measuring directional and non-directional buoy data. These are not very reliable for extrapolation over large areas and many do not supply directional information.

The directional wave component of a SAR image, however, can easily be extracted digitally by using a Fourier transform to compute the power spectral density. The resulting wave number spectrum is a polar plot which indicates wave direction; wave numbers are inversely proportional to wavelengths and increase radially with longest waves close to the centre of the plot and shortest on the periphery of the plot. A wave field observed over the JASIN experimental area 400 km northwest of Scotland. If the radar image is taken to be a direct representation of the surface long-wave distribution, it implies a dominant swell wavelength of the surface long-wave distribution, it implies a dominant swell wavelength of about 170 m in a direction 70° east of north. synoptic observations during the JASIN observed 152 m waves in a 50° direction. In general, agreement with surface observations is within about 10 per cent in wavelength and 25° in direction.

SAR observations of wave direction are ambiguous by 180°, but that the ambiguity can usually be resolved by assuming the waves are travelling downwind, or away from a storm, or toward land. This analysis is limited to those images where swell waves appear. Where they do not appear on images, it is not always possible to know whether it is because the swell was too high or too low, in the wrong direction, because there was no wind to cause ripples, or because the dominant wavelength was too short.

The generation of ocean wave spectra from SAR data is of both scientific and practical value. SAR derived ocean wave spectra could be used in scientific experiments for periodic updates and verification of regional and global wind-wave forecast models. The timely knowledge of directional wave spectra is of practical value. SAR derived ocean wave spectra could be used in scientific experiments for periodic updates and verification of regional and global wind-wave models. The timely knowledge of directional wave spectra is of practical value to operational offshore wave forecasting, marine transportation, fishing, and naval activities. Furthermore, the wave measurements and wave impact on coastal zones could also be useful for coastal erosion research.

Internal Waves

Next to surface waves, internal wave packets are most widespread and commonly occur on SAR imagery. They can be observed in near-coastal marine regions with a sharp, shallow, seasonal pycnocline (density interface). Internal waves are generated by the interaction of tidal currents and by abrupt changes in the topography of the sea bed, including shoals or sea mounts. The amplitude of these waves is in the range of 10 m up to 100 m. Internal waves owe their existence to vertical gradients of the water column, particularly at the density interface between two density layers (pycnoclines). It is of note, that internal waves, unlike surface waves, do not produce discernible elevation changes at the ocean surface and may only be detected by variations in the surface roughness. Internal waves cause flow convergence and divergence at the surface and thus compress or strength capillary waves.

Other oceanographic phenomena imaged by SAR

(1) In addition to waves, synthetic-aperture radars also observe variations of wind speed at the sea surface and are used to map the variability of winds over distances of 0.1 to 100 km. For these observations, the SAR operates as a high resolution scatterometer. Rapid change and spatial variations of surface winds and other atmospheric phenomena such as rain cells and storms, have a significant impact on the radar backscatter. The response time of capillary waves to wind stress is a very short, usually on the order of tens of seconds for moderate winds greater than 1 m/s. Therefore, SAR signatures of surface waves can be instantaneous expressions of local wind fields, and a strong correlation of image brightness and surface wind speed may be established. In a similar way, brightness variations are also caused by the impact of storms and heavy rainfall on the sea surface; this creates small-scale roughness features including Bragg resonance waves.

(2) Eddies have been seen near strong currents and downstream of points of land.

(3) Tidal flows at coastal inlets are prominent, and show the pattern of dispersal of near shore water into the offshore waters.

(4) Although microwave energy at radar wavelength does not penetrate the ocean's surface, certain bathymetric features of the sea floor topography can be seen indirectly on radar imagery. Bottom features are detected because of the flow variations in tidal currents induced by changes in bottom topography and wave refraction due to shoaling topography. This interaction results in a modulation of the capillary waves at the surface which in turn gives rise to changes in radar reflectivity.

(5) Ships and wakes are seen sometimes, but not always. Slowly moving ships tend not to be seen on windy days, but large ships with strong wakes are easily seen, as are slowly moving ships on calm seas. The Doppler shift induced by the ship's motion causes the image of the ship to be displaced from the ship's wake, and this displacement can be used to estimate the ship's speed.

(6) Ice of various types can be distinguished in radar images. The SAR responds primarily to surface roughness and can distinguish new from first-year and older ice.

SCATTEROMETERS

Scatterometers are radars designed to measure accurately the scattering cross section of the sea at particular incidence and azimuth angles. The purpose of these instruments is to obtain information on wind speed and direction at the sea surface. these wind vector data can then be incorporated into models, global statistics and climatological datasets.

Because the cross section is symmetric about the mean wind direction, it is difficult to determine wind direction unambiguously using observations of radio scatter made at a small number of different angles. If an area of the sea is observed from two different angles, up to four possible wind vectors satisfy the observations. A third observation can reduce the ambiguity; however, this requires very precise observations because the anisotropy of cross section is weak.

The particular configuration of a scatterometer arises from several constraints. First of all, scatterometers must observe the sea at several azimuth angles to determine wind direction; thus they must radiate a signal with a narrow beamwidth in azimuth. At the same time, the radar must map scatter from a wide swathe on either side of the spacecraft, so the beamwidth in the vertical must be broad. The two requirements can be met by stick antennas that radiate into a fan beam.

The number of fan beams determines the ability of the radar to estimate wind direction. Seasat observed the sea at two azimuth angles; but this was insufficient to define wind direction uniquely, and the Seasat estimates of wind velocity had an ambiguity that produced up to four possible vectors. On ERS-1, three antennas will be used at three azimuth angles to reduce the ambiguity, producing two possible wind estimates 180° apart. The 180° ambiguity can then be removed automatically with the help of a few independent surface measurements, or even by knowing the pattern of winds at the surface: by knowing, for example, that strong winds circle lows but not highs.

The comparisons of Seasat scatterometer and JASIN data indicated that the accuracy of the scatterometer measurements was ± 1.6 m/s in speed and ± 18° in direction for winds between 3 and 16 m/s at mid-latitudes. Global comparisons, particularly in tropical areas, have not yet been completed, and will probably produce different estimates of accuracy.

The greatest oceanographic gain from wind scatterometry are likely to be found in conjunction with the numerical modelling of dynamical ocean processes. The type of processes whose study will benefit from satellite-derived wind-stress vectors range from localised upwelling to global ocean circulation. Another ocean-wide phenomenon is the complex ocean-atmosphere interaction which occurs in the Equatorial Pacific, in which an anomaly in the wind-stress field on the Western side can trigger off a wave which propagates eastwards and ultimately causes a significant rise in sea temperature off Ecuador and Peru, with disastrous consequences for the local fisheries and a marked change in the coastal weather patterns. El Niño, as it is called, has attracted a great deal of scientific attention recently. If the mechanisms which produce it can be adequately modelled it may be possible to predict the consequences several months ahead. Finally, the wind data represents a very great improvement in data coverage for the large areas of sea which are rarely traversed by shipping and even less often sampled for oceanographic and meteorological parameters, like in the Southern oceans.

ALTIMETER OBSERVATIONS OF THE SEA

Altimeters have been used to measure geotrophic currents, tides, winds and waves. Satellite altimeters are nadir viewing radars which transmit short pulses toward the earth's surface. The return time of the pulse after reflection is measured, and this yields the height of the satellite with accuracies of about 10 cm under normal conditions.

Measuring the distance between the satellite and the ground is only the first step in a longer procedure which must be followed before oceanographically-useful information is obtained. The aim for oceanographic applications is to obtain the sea-surface height relative to the geoid (the equipotential surface at mean sea level), (see figure 6). The height of the ocean surface above or below the geoid, the ocean surface topography, is therefore a parameter containing oceanographic information about ocean currents or about the tides.

The measurement of currents are particularly important because the slope of the sea surface can be directly related to surface geostrophic currents. Both, orbit errors and uncertainty in the height of the geoid constrain the accuracy of the observations, however, and studies so far have been limited to observations of the temporal variability of currents, the position of strong permanent currents, and the distribution of the larger features in the mean circulation of the ocean basins.

The same techniques used to observe ocean currents have also been used to observe oceanic tides. If the altimeter signal is not corrected for tides, as is done for studies of currents, the position of strong permanent currents, and the distribution of the larger features in the mean circulation of the ocean basins.

The same techniques used to observe ocean currents have also been used to observe oceanic tides. If the altimeter signal is not corrected for tides, as is done for studies of currents, then the topography observed by the altimeter varies from day to day due to time-variable currents and to tides. But the tides have definite, known frequencies, and that part of the signal coherent with the tidal potential is assumed to be the tide.

The observations of winds and waves by altimeters is considerably easier than the observations of current and tides. The heights of waves is calculated from the shape of the reflected pulse. An initially short transmitted pulse is lengthened upon reflection, first from wave crests and then from wave (figure 7). The slope of the leading edge of the reflected pulse is inversely proportional to the significant wave height. The Seasat altimerter had an accuracy of±10 per cent for waves higher than 1 m, but it tended to overestimate the height of large waves.

The altimeter observation of wind speed are based on measurements of the scattering cross section at nadir. The stronger the wind, the lower the cross section and the weaker the reflection from the surface. Comparisons of winds measured by the altimeter with winds measured by ships and buoys indicated that altimeters are able to give a fair estimate of wind speed, probably within about 1 m/s of the true value.

The Seasat and Geos altimeters could track the height of continental ice sheets, and the data from the former were used to map the height of the ice covering Greenland and portions of the Antarctica.

Perhaps the most remarkable use of remote sensing over the oceans is in mapping the sea floor. This is not because the altimeter can actually penetrate the ocean-it cannot. But ridges and trenches on the ocean bottom create variations in the height of the sea level, and these persist after the much smaller variations caused by currents have been averaged out over time. Changes in sea-surface height of up to 30 meters, compared with only about 1 meter for currents. The sea surface varies by two or three meters for every kilometer of change in sea-floor depth. Even kilometers by deep-laying mass concentrations under the sea floor, and these variations must be analyzed to reveal the sea-floor topography. Potentially, accuracies in sea-floor depths to within half a kilometer are achievable. The more accurate altimetric data that will be produced by the Topex mission should provide a better view of the sea bottom by filling void areas in the data.

NOTES

1. Cantón M., and A. Hernández-Guerra. "La teledetección de los océanos desde el espacio: Principios físicos y aplicaciones". Revista Española de Física. (1991) In press.

2. Colwell, R.N. (ed.) Manual of Remote Sensing, 2nd ed. American Society of Photogrammetry (1984).

3. Cracknell, A.P. (ed.). Remote Sensing in Meteorology, Oceanography and Hydrology. (New York, John Wiley and Sons 1981).

4. Gower, J.F.R. (ed.) Oceanography from Space. (New York, Plenum Publishing Corporation 1980).

5. Hibbs, A.R., and W.S. Wilson "Satellites map the oceans". IEEE Spectrum, (1983) October, pp. 46-53.

6. Maul, G.A. "Introduction to Satellite Oceanogrpahy". (Dordrecht, Netherlands, Martinus Nijhoff Publishers 1985).

7. Robinson, I.S. Satellite Oceanography. (New York, John Wiley and Sons 1985).

8. Stewart, R.H. Methods of Satellite Oceanography. (Univesity of California Press 1985).

9. Werle, D. Radar Remote Sensing. A Training Manual. (Ottawa, Canada, Dendron Resource Surveys Ltd. 1988).

10. Wooding, M.G. Imaging Radar Applications in Europe. (The Netherlands, ESA Publications Division 1988).

THEORY OF SAR*

R. Keith Raney
Canada Centre for Remote Sensing
Ottawa

INTRODUCTION

The objective of this paper is to provide a theoretical description of a Synthetic Aperture Radar (SAR) sufficient to allow a user, interested primarily in the potential information content of an image, to appreciate the capabilities and limitations of the basic imaging system. Whereas the material is theoretical in principle, a descriptive approach is taken in the text: readers are assumed to be more interested in results than in the elegance of mathematical arguments. All SAR system properties described rest on rather solid theoretical analyses, some having roots in the previous century and before. In the view of this writer, however, there exists no previous source that clearly (much less adequately) discusses the subject from the point of view of this lecture... Hence this modest attempt.

A rumour persists that SAR is difficult to understand, and that its properties are endowed with a certain impenetrable mystique. The rumour is not true! A SAR is simply an imaging system, and as such, has much in common with other imaging systems. Its geometry differs from that of conventional optics, but to understand that requires only a shift in one's point of view. As a radar, a SAR provides its own illumination, a fact that has obvious consequences. Likewise, as a radar, the illumination is essentially at one frequency or "colour" again, with consequences. These properties and the first basic rule of conservation of energy that governs SAR imagery may be considered without trying to look at the inner workings of the end-to-end imaging system. Thus, the approach taken in the section below to examines a SAR as a certain kind of imaging device.

Additional properties of SAR are evident when one looks inside the system. This is done in section 3. For the curious of mind, the "synthetic aperture" principle is explored. After all, it is this feature which makes SAR such a suitable instrument for space-borne Earth observation platforms. In addition, a consequence of SAR signal processing is that a kind of "noise" is generated, known as speckle, that is unique to coherent systems...more on these important concepts below. These characteristics are captured in the second basic rule for SAR image formation (conservation of confusion).

---

* This paper, which was presented at the United Nations/Food and Agriculture Organization of the United Nations/European Space Agency Workshop on Microwave Remote Sensing Technology, Maspalomas, Canary Islands, Spain, does not necessarily reflect the views of the United Nations.

The paper closes with a few observations regarding assumptions, conditions and additional effects that are of interest from a theoretical point of view.

SAR AS AN IMAGING SYSTEM

The basic objective of an imaging radar system is deceptively simple: we wish to derive an "image" which is a (two-dimensional) mapping of the reflectivity of a scene illuminated by the radar using microwave energy. In model language, a scene in the real world is estimated as an image through a microwave transducer (MT). It is the purpose of this section to enlarge on the implications of this model for an orbital SAR. We are concerned in this section with the first-order geometrical and brightness properties of the image. These are summarized in the first principle of SAR image characterization that closes the section.

Geometrical considerations

SAR systems "work" because of the different mechanisms used to scan the two dimensions of the image. When a pulse is transmitted by the radar, it propagates at the speed of light, approximately $c = 10^5$/km/sec. Upon reflection, a small part of the incident energy is bounced back towards the radar, which then receives it, in effect measuring its relative strength and time delay. The range spatial dimension in the image results from such range calibrated scanning. The second dimension in the scanning process, and hence in the resulting image, is due to the spacecraft velocity along its orbital path, typically about $V_{s/c} = 7$ km/sec. The radar continuously transmits and receives pulses as it progresses along its path, thus accumulating a sequence of received signals which are processed to form the azimuth dimension of the image. The difference in range and azimuth scan rates, by a factor of nearly 10^5 allows the two-dimensional image to be formed.

These basic ideas need elaboration for the geometrical environment of a spacecraft. The important new element is that the radar is looking down at the Earth from an orbit typically 800 km above the surface. In contrast to an optical sensor, however, a radar looks not straight down but rather down to one side of the orbital plane. This is necessary for the transmitted pulse to scan terrain at increasing distances from the radar, and thus to provide the range dimension of the image. The natural "range" coordinate for the radar is slant range R_s, in effect the line of sight between the radar and each reflecting element on the surface. Most users, however, are interested in a map projection on the surface, which needs to be expressed in ground range R^g One of the tasks of a SAR processor is to make the needed geometric conversion from slant range delay to ground range, and for most of the following, we assume that such conversion has been done. From this geometry, an important parameter appears, namely the incidence angle 0 measured from the vertical, which is typically in the range of 20° to 50° for spacecraft SARs.

The sphericity of the geometry enters the azimuth of the image as well. Since the spacecraft is in a near circular orbit and looking downwards towards the Earth, the rate V_G at which the illumination footprint scans along the surface is smaller than the spacecraft velocity $V_{s/c}$. The ratio of these two velocities is a fundamental parameter impacting SAR performance as well as geometry 1/ a fact which emerges again later in the discussion.

As the radar moves along the orbit, it continues to accumulate data. The range extent of the imaged region is known as the swath width, quoted in ground range or across track distance, typically on the order of 100 km. The along track length of the imaged swath may be many hundreds of kilometres, although for most SAR processors, image products are generated on a frame-by-frame basis. Each such frame is, typically, 100 km long. Different radars and processing choices offer some variety in these numbers, of course.

To visualize the image that results from this geometry, we need to "change our point of view". If the sensor were an optical one, the geometry illustrated would result in an oblique image, seen from the spacecraft position as, literally, from the side. It would appear in the perspective characteristic of oblique aerial photography. A radar is not an optical sensor, however. The "point of view" appropriate to this radar geometry is orthogonal to the (instantaneous) slant range direction. Thus, the effective radar viewpint is oblique, but from the opposite side of the image from the radar. Note that the illumination still comes from the actual location of the radar. Thus, the radar image has some similarity with an oblique photograph for which the illumination is also oblique, but from the opposite side.

Following slant range to ground range conversion, this geometry results in imagery which resembles vertical viewing for reasonably level terrain, but for mountainous terrain local distortions in the image occur. These distortions are analogous to those encountered in oblique optical imagery if taken from the radar viewpoint. The underlying effect is elevation displacement, whereby reflecting objects higher than the datum plain are imaged as if they were closer to the radar than in fact they are. (Again, this is one-to-one equivalent to the optical case, for which taller objects are imaged as if they were further from the nadir point on the surface.) These effects may be exploited to achieve radar stereo viewing, just as would be the case for an optical instrument. For stereo viewing, two different radar images are required, each gathered using a different incidence angle over the scene.

In extreme cases, for which the local slope is greater than the slope of the incident wave front from the radar, the upper portions of the terrain are imaged as if they were closer to the radar than the bottom (which for the radar slant range measuring coordinate is strictly true), giving rise to the effect known as layover. Conversely, if the slope of a terrain feature on the side away from the radar is steeper than the slope of the radar line of sight, then a radar shadow appears. A consequence of these considerations is that for radar imagery of mountainous terrain, there is always a trade-off between layover and shadow: one may be decreased only at the expense of the other.

Impulse response

For an optical system, a fundamental characteristic of the "goodness" of the instrument is the point spread function which describes the detailed image brightness distribution arising from an arbitrarily small object in the scene. The corresponding fundamental characteristic of a imaging radar is called the impulse response, terminology brought into use from the field of systems analysis in electrical engineering. Any imaging system, even if perfect, images detail only to up to limits set by system capacity (measured by parameters such as signal bandwidth). The impulse response of a SAR may be observed as the image of a reflecting object that is smaller than the nominal resolution of the system. Since a SAR images in two dimensions, the impulse response is likewise two-dimensional. A good impulse response has been described as a "thumbtack", sharply pointed, and having very low response otherwise. (The energy outside the main response is known collectively as side-lobes, constrained by design of the radar and its processor to be as small as possible, although it is theoretically not possible to reduce them to zero.)

The most important parameters describing the impulse response are its widths in range and in azimuth. A high resolution radar (or other imaging system) is characterized by a relatively small impulse response width. The width of the impulse response generally is measured at a relative strength which is half of the power represented at the peak.

Range resolution of a SAR is determined by built-in radar and processor constraints. For this discussion, the most important fact is that these constraints act on the signal in the slant range domain. In slant range, range resolution is in effect a constant of the system. However, when the image is projected onto the ground range plane, the effective range impulse response is stretched. The increase in ground range resolution over that of the slant range is determined by the local incidence angle θ_L. As such, the effective range resolution is a function of the radar incidence angle as well as any local trend in terrain slope along the radar line of sight. Thus, the range impulse response width is

$$IRW_{RG} = \frac{IRW_{RS}}{\sin(\theta_L)} \qquad (1)$$

where IRW_{RS} may be taken as constant. Note that for most SARs, a "range resolution" is quoted that is in terms of ground range seen at a nominal incidence angle, usually near the centre of the intended image, and assuming locally level terrain.

Azimuth resolution of a SAR is determined primarily by the settings used in the SAR processor on the ground, although there is a resolution limit set by the radar system itself. The highest (that is, the finest or smallest) azimuth resolution that may be achieved is on the order of one-half of the size A_H of the azimuth antenna aperture of the radar. (For typical space radars, the antenna length is on the order of 10 metres). Indeed, it is the azimuth resolution feature that sets "SARs" apart from other radars, as we shall see below. SAR processing achieves an azimuth impulse response width that is hundreds of times smaller than the patch of terrain illuminated by the radar in the azimuth direction. The azimuth resolution limit, known as the single look azimuth impulse response width, is

$$IRW_{A1} = \frac{V_G \quad A_H}{V_{S/C} \quad 2} \qquad (2)$$

where the velocity parameters are as introduced above. Note, due to spherical geometry unique to orbital SARs, for antennas of equal size, that somewhat better azimuth resolution is available than from airborne SARs for which the vehicle velocity and the beam footprint velocity are essentially equal. 2/ Azimuth resolution is nominally constant across the range swath of an image. (Technically, one effect of the velocity parameters is to cause a small variation, although it is seldom of importance in practice.)

In general, a SAR processor usually is not set to achieve this degree of resolution in azimuth. For reasons explained below, there are benefits to be realized by intentionally trading azimuth resolution for other aspects of image quality.

At this point it is important to distinguish between resolution and pixel spacing. The impulse response is displayed as if the response function is present in an image at a continuous sequence of points. For SAR imagery, whether in digital form or in a photographic display, the image is represented as an ensemble of digital picture elements, or pixels, with a given inter-pixel spacing. Typically, pixel spacing is smaller than (nominal) resolution by a factor of approximately two. Resolution is a fundamental property of the radar, whereas pixel spacing is the fundamental parameter of importance in image interpretation. It is usually set by considerations such as desired image scale. The distinction is pertinent, because most people with an optical imaging background think of resolution and pixel as being the same quantity, and representing the same physical process such as the "instantaneous field of view". This is definitely not true for a SAR.

Scene reflectivity

The role of the impulse response is fundamental to the process of image formation. The impulse response is in effect the shape of the system function that scans the reflective scene in two dimensions. Image features such as brightness, contrast and spatial detail are expressed in the image as an additive combination of elementary reflections each of which have been shaped in the image by the impulse response function. The formal statement of this fact is through the convolution relationship

$$\acute{\sigma}_o = |r_o^2| ** G_{IRW} \qquad (3)$$

where G_{IRW} is the two-dimensional impulse response as described above, ** demotes convolution in the range and in the azimuth directions, r_o is the complex reflectivity of the scene being observed and $\acute{\sigma}_o$ is the estimate of scene reflectivity as observed in the image. These are several new ideas introduced in this expression.

This expression is typical of that used to describe most imaging devices. It is presented in the "power" domain. The "brightness" or relative strength of a pixel in the image is proportional to the magnitude of this expression, and is proportional to the electromagnetic energy per pixel gathered and processed by the radar. For an optical system used with solar illumination, for example, equation 3 could be used to express the relative exposure of a photographic film...the stronger the reflection, the brighter the image. At this level there is rather little subtlety for an optical system.

For a radar, however, the situation is different. The microwave signal transmitted by a the radar and thus sent out to scan the illuminated scene is not like solar illumination. It is essentially a single frequency, or monochromatic, to use the optical analogy. Furthermore, since there are many scatterers illuminated simultaneously, reflections from each of these combine coherently when received by the radar. Thus, the radar does not directly observe the energy reflected by each scatterer, but rather the combined energy following coherent signal combination. Coherence implies that the phase of these different reflections is important. In effect, the radar acts as an interferometer, whose input is a linear sum of complex signals with dimensions of complex voltage. The appropriate representation of the reflectivity process is in terms of the complex voltage r_o, magnitude squared. The output of the radar imager is designed to be power; or, equivalently, energy radar cannot measure energy reflectivity of the scene directly. It is only able to estimate average reflected energy, expressed in terms of the quantity σ_o. There are several important consequences of this fact, to which we return in section 3.

In general, scenes observed by a SAR consist of two kinds of reflecting objects: discrete scatterers. Discrete scatterers are characterized by a relatively simple geometric shape, such as a building. The classic element used to represent discrete scattering is corner reflector, a shape such as is formed in the inside corner of a room, having three sides intersecting at (nearly) right angles. Radar illumination striking such a shape, from the open side, of course, is very strongly reflected back along its incoming path. Such reflections appear as bright responses in the resulting image. When the electrical and geometric properties of such an object are known, the strength of the reflection, its so-called radar cross-section (σ), may be predicted. Larger and more complicated scenes, such as from an urban area, may be well represented by groups of such scattering centres.

For many Earth observation applications, however, the more interesting class of scattering is distributed over many reflecting elements, such as from a tropical forest. In detail, distributed scattering is made up of countless small discrete scatterers, but since there are so many of these per resolution cell, or per pixel, for that matter, the concept of individual radar cross-section is not helpful. For scenes with distributed scatterers, the average scattering cross-section, or reflectivity per unit area, applies. Such is the definition of sigma nought, σ_o.

In summary, there are two aspects of importance to equation 3: consequences following from the behaviour of the reflectivity r_o inside the $| |^2$/operator; and those outside of the $| |^2$ operator. For average image brightness properties, the outside consequences are applicable. For the present discussion, therefore, equation 3 may be understood to represent the ability of the SAR to represent in the image the mean reflectivity and the spatial detail present in the scene. Consequences that follow from signal behaviour inside the operator are considered in the section below.

Conservation of Energy

The imaging behaviour of equation 3 shows that the average reflected power in the scene is mapped into the image faithfully, subject to the amount of spatial detail allowed by the impulse response. Thus, (average) scene contrast, such as between a lake (which in general has low reflectivity) and a surrounding forest (which has larger reflectivity) may be well estimated in the image. The transition between these two regimes, however, will appear no more precisely than dictated by the impulse response limit. For example, if the actual change from "lake" to "forest" takes place in, say, 1 metre, the image will represent this as 25 metres, to use a number typical of spaceborne SARs. The main point is, however, that a SAR is capable of rendering a reasonably good estimate of average reflected energy from distributed scatterers.

It turns out that this relationship is a fundamental property of synthetic aperture radars, and may be expressed 3/ as the principle of conservation of energy: For a region in the scene having nominally constant average reflectivity, the average value of the SAR image is also constant, and independent of system focus, system coherence or scene coherence, assuming that all available data are used in the SAR processor in each case. This is an important feature of SAR imagery, and will be relevant to further discussion below.

INSIDE THE SYSTEM

A SAR is interesting, and an important instrument for satellite platforms, because of what happens inside the "black box". The primary interest is in the azimuth direction, for which formation of a synthetic aperture and subsequent SAR processing are the basic operations required. In order to achieve the azimuth impulse response described above, data collected by the radar along its orbital path are stored in a memory and processed. The idea for such an approach was first proposed by Carl Wiley in 1951 4/ and has been studied, refined, and put to work ever since. The method works because of the detailed behaviour of the complex reflectivity term inside of the $\| \; \|^2$ operator of equation 3, and the way in which the radar, the memory, and the processor are used to take advantage of the detailed structure of the complex reflectivity r_o as observed by the radar moving along its path. There are "good" consequences and "bad" consequences that result. The good result, of course, is a narrow (high resolution) azimuth impulse response. The bad result is the generation *speckle*, of a kind of noise unique to coherent imaging systems such as a SAR, although speckle has some good features as well. In this section we develop these ideas, closing with the second principle for SAR image characterization.

Principle subsystems

These are three "subsystems" needed for SAR operation: the *radar* (on board the spacecraft); data telemetry to a ground station recorded into a *memory* format; and the SAR *processor* (on the ground), sometimes called the "preprocessor". The SAR image, of course, is a product of the processor.

The key idea is that the data from the radar, as received at the radar or as collected in memory, is most definitely not like an image at all! This is the main distinction between "SARs" and optical imaging sensors such as SPOT. For an optical sensor, the output of the device itself is essentially an image: any processing applied is simply to clean it up, align the various bands or channels, put it in a suitable geometric format, etc. For a SAR, however, the output of the radar is a highly dispersed, even "totally unfocused", data stream, essentially meaningless without further processing. The radar is only half of the "sensor". The processor, which requires substantial data in memory on which to work, is the other half of the "sensor", and is an essential element in the image formation sequence.

The *radar*'s role is data collection. Like other radars, the on-board portion of a SAR transmits pulses of microwave energy, a small fraction of which, after reflection, is received back at the radar. Radar design is beyond the purpose of this paper, but a few comments are in order. Nature places tight constraints on the way in which SAR can work. These limit the resulting range swath width and azimuth resolution. Since all radars must be designed by the same basic rules, it is not surprising that the SAR systems now planned for this decade all have similar performance, at least in terms of resolution and swath width. There are greater degrees of freedom in the choice of wavelength (microwave frequency), incidence angles, polarization and, budget allowing, flexibility. Whatever the design details, however, the on-board portion of the SAR must accomplish one thing: to gather the data while preserving the phase of the complex reflecity r_o of every signal received. In effect, the data collection takes place inside of the $| |^2$ operation of equation 3.

Data collected by the radar must be arrayed in a memory format for the processor to work. Signals received at the radar may be digitized, formatted and sent via telemetry to a ground station directly, or may be temporarily stored in an on-board tape recorder for subsequent telemetry transfer to a ground station. In either case, the key memory function is that which is serving the SAR processor, hence on the ground. Since the phase of the data sequence must be preserved, this implies that all digital representations of the data be in pairs for each sample, the so-called in-phase and quadrature components, or I and Q for short. Again, the main task of the memory, like that of the radar, is to maintain the phase structure as well as the organization of the entire data set. This is not small task, as the amount of digital data is generally very large. For example, the digital down-link data rate for the Earth Remote Sensing Satellite (ERS-1) is 105 megabits per second, consisting of sample pairs (I and Q) of 5 bits each. The memory required for such a data volume dictates that high density tape recorders be used. For subsequent processing, portions of the data required for the image to be produced are transcribed to CCT, then to (a large) hard disk or cache memory interfacing with the processor.

The task of the processor is to operate on the sorted data so as to produce an image. In terms of equation 3, the processor uses the phase information associated with each and every signal element of r_o to create the desired azimuth impulse response, and plays this function over the information in memory to focus the data. The processor also performs the I I^2/energy, not in terms of complete voltage. Finally, the processor needs to perform certain geometric and radiometric correction, which, to first order, are analogous to those used in processing for optically sensed data.

In summary, the task of the radar and the memory subsystems, simply stated, is to preserve the phase fidelity of the signal sequence, nothing more. All of the "work" is done by the processor. Thus we turn our attention to the task confronting the processor, and its implications.

The Synthetic Aperture

For all imaging systems, indeed, for all systems that may be described by analogous mathematics, a fundamental rule applies: the Rayleigh diffraction limit. Lord Rayleigh, in a monumental little book on the theory of sound (!) published over 100 years ago, showed that the ultimate (angular) resolution of a system was determined by the ratio of the wavelength λ used to the size of the aperture D according to λ/D. Simple. It states that for higher resolution (at a given wavelength), a larger aperture is required. Radar must follow this natural law. It has given rise, for example, to the radar telescope used for planetary observation that may be found at Arecibo, Puerto Rico. The aperture of that instrument is 1/5 of a mile in diameter.

The Rayleigh diffraction limit may be used to show a C-band radar ($\lambda = 5.6$ cm) that an aperture about about 5 km long is needed in space to achieve a resolution on the surface of the Earth of 25m. There is no remote sensing programme, no matter how ambitious, that would put an antenna like that in space!

There is a way around the problem. The diffraction limit applies, strictly speaking, not to the aperture itself, but rather to the data used to focus the resulting beam of energy. Thus, if data corresponding to a 5-km segment of an orbital radar's path were collected in memory, then that data may be processed, or focused, to achieve the desired resolution. This is the concept of the synthetic aperture, and is at the heart of Wiley's innovation. The digital signals arrayed in memory represent the data distributed across an aperture that does not physically exist, but which in memory, and taken together, builds or synthesizes an ensemble of signals that may be focused to the limit of the data length.

Processing

The task of the processor is to focus the data to an image. In concept this is a straightforward operation. Consider a simple model, a stone tossed into a calm lake. The stone causes a set of concentric waves to spread out from the centre. If we visualize the whole scene, we see the waves and the centre splash as being related. With only a small amount of experience, however, one can reconstruct the whole scene by observing just a small part of the radially propagating wave set. (A closely related method was used for more than a thousand years by natives of the South Pacific Islands for navigation: by observing the patterns of the ocean swell and its variations in direction caused by wave diffraction around the islands, they were able to navigate accurately far beyond the limits of eyesight and the horizon.)

SAR data to be processed represent a small part of the set of microwaves reflected back to the radar from each scattering element, just as water waves spread from a dropped stone. The SAR processor is based on a mathematical model of the wave front structure expected from scatterers at each range element to be imaged. In order for the processor to work, however, it must be able to "see" the wave structures buried in the data. This requirement is satisfied if the phase each of the reflected signals is preserved, where here, the idea of phase is one-to-one equivalent to being able to observe a wave crest on the water.

The complex reflectivity r_o of equation 3 carries the required information. The phase of this term is determined by two factors: (i) the phase that the scatterer imposes on the reflected signal; and (ii) the phase imposed by the systematic change in range distance caused by the movement of the radar along its orbital path. We look at the consequences of (i) below, and concentrate on (ii) at this point.

The phase of the complex reflectivity due to the time carrying distance R(t) between the scatterer and the radar is $4\pi R(t)/\lambda$. Since the geometry of the orbit/Earth relationship is known, this phase may be "matched" in the processor. This phase function must be applied to every pixel (at a given range) over the synthetic aperture, of which there are thousands in general. Furthermore, a (slightly) different phase function is required for each different range pixel, of which there may be on the order of 4000. Thus, the task may be straightforward, but it requires many complex operations and some precision to perform correctly. It is not always done rapidly! Processing speed is an importanat SAR specification.

An interesting and fundamental consequence follows from such processing. This is because for greater ranges, there more data over which to process, in proportion to R. Application of the Rayleigh angular diffraction limit, and multiplication by R to find azimuth spatial resolution, leads to (nearly) constant azimuth resolution for a SAR. A similar argument shows that the SAR azimuth resolution is not a function of radar wavelength. Both of these results are in contrast to the way in which an optical imaging system works. They are the major reasons that SAR is such an important instrument for use in space where the imaging distances are so large.

There is a further consequence that is less obvious, but equally important. The image geometry and Earth location does not depend on accuracy in spacecraft pointing. This is true because the image is formed from data that seems to originate in the scene itself. However, there are requirements placed on the detailed design of the processor so that this inherent SAR geometric fidelity may be realized.

Additive noise

Like all radars, a SAR is an active system, that is, it depends on its own radiated power to get the desired imagery.

Signals received at the radar have a strength which is proportional to the transmitted power. Simultaneously, however, there is always a small amount of electromagnetic energy present in the radar receiver. Of course, this may not be used to form a useful image since it is unstructured noise, but it manages to find its way into the image since the receiver and the processor have no way of distinguishing "signal" from "noise". One aspect of image quality is the signal-to-noise ratio, and is usually specified in terms of noise equivalent sigma nought. This quantity expresses the noise as if it were a true signal from distributed scatterers of a given reflectivity. Typical numbers are in the range of -20dB or less. This might be compared to the strength of signals expected from actual terrain, such as for forests ($\sim$-8 dB), or rough water ($\sim$-14 dB). The issue gets more important when trying to image smooth surfaces having low radar reflectivity, such as new ice ($\sim$-20 dB)! The system signal-to-noise ratio is controlled at the outset by designing the radar to transmit adequately high power. For nearly all applications of SAR data, the user may assume that the system design is such that additive noise is not of concern, except for specialized or very quantitative analyses.

The issue of how to predict additive noise level in radars in general and in a SAR in particular has received considerable attention in the literature. 5/

Speckle

We now turn to the main remaining issue, and related considerations. As treated above, the SAR processor operations needed to focus the data were described. There is one more essential operation: detection. The processor's task is not complete until it has calculated the (estimated) energy per pixel, to which the desired σ_0 at each point in the image is proportional. This step completed the $| \, |^2$ operation. It is a simple calculation, but has many and deep consequences.

Recall the discussion of complex reflectivity in section 3.2, at which time the phase that the scatterer imposes on the signal was introduced. (We assume, as is usually true, that the second component of phase, due to changes in radar range over the observation interval, have been well matched and thus "cancelled" in the focusing operation.) Each scattering element, after focusing but before detection, still retains its own phase. This intrinsic scatterer phase has two parts: any phase shift due to electrical properties of the scattering material; and an additional phase term due to the position of the scatterer with an imaged pixel. This second part is by far the most important for the present discussion. At this level, a SAR is an extremely precise instrument, since it measures scatterer position, as expressed in phase, to a fraction of a wavelength! Of course, such precision is not maintained through the impulse response since radar wavelengths are much smaller then pixel size, but it is the phase consequences that concern us now. The precise location of an individual scatterer, such as the leaf of a tree, is not known, and in fact is a rather random, even accidental, quantity. Thus, the intrinsic phase of each focused (but as yet undetected) scatterer is a purely random quantity.

The consequence of performing magnitude squared detection over the large number of signals from scatterers found in any given pixel is that the complex signals may cancel themselves out. If so, then the resulting estimate of energy for that pixel would be ...ZERO. For the SAR processor described to this point, zero is the most likely result. Of course, there is a variety of possible results for each pixel, and these may be described rather well mathematically. It should be satisfying, however, that the average of the possible estimates is σ_0, the quantity desired. The fact remains, however, that seen at the individual pixel level, imagery with such wild expected variation, in response to nominally a scene of "uniform" reflectivity, is not very satisfying.

This behaviour is typical of any coherent imaging system in which the various scene elements have phases which interfere with each other at the last stage of image formation. In SAR parlance, the effect is known as speckle, a term carried over from astronomy. Speckle is a multiplicative noise, as it is proportional to the strength of the imaged segment under consideration. Increasing radar transmitted power cannot improve things...we are stuck with it. Thus we have the following dilemma: scatterer phase is extremely good in that it allows formation of an image through the synthetic aperture process, but is extremely bad in that it creates a noise inherent to the SAR image itself. What to do?

Fortunately there exist options that are helpful, options which easily may be accommodated in the design of the radar and the processor. The main approach is to do more averaging of the data after detection. As long as the image sets over which the averaging is done are statistically independent, then the averaging reduces the amount of speckle. The important description of speckle is its variance compared to its average or squared mean, where variance is a useful measure of the variation of a quantity with respect to its mean value. Let the speckle process have a mean value of one. (Since it is a multiplicative noise, the actual image mean value is carried in σ_0). The rule is, for N statistically independent post-detection images to be averaged, the resulting variance V_N is given by 1/N.

The images on which this averaging is based must come from the available data, and furthermore must be statistically independent. This may be done in more than one way, but the most widely used approach is the following. The data found in the synthetic aperture are used to form N different images. If data for each of these is taken from non-overlapping parts of the available data, then the resulting images may be shown to be statistically independent. Each such image is called a look, which are combined following detection of each one of them individually. Thus, an N-look image results that has a speckle variance of 1/N. Typical space radars use about four such looks, with a consequence that the speckle is reduced to acceptable levels. Speckle may be further reduced by a user, however, since additional averaging over image pixels produces a similar result. Seen from this perspective, it should be clear that a consequence of this is degraded resolution. More on this aspect in the following section.

There are several good features represented by speckle, when appropriately addressed. Speckle carries information primarily about the radar itself, even though it derives from the detailed phase structure in the scene. The spatial correlation function of the speckle is a good estimate of the impulse response potential of the SAR/processor combination. This property is preserved even though the processor may be out of focus. Thus, the performance of the system may be verified and monitored through, among other things, speckle analysis. Second, the speckle may be analysed to determine the effectiveness of speckle suppression. Estimating the speckle variance actually achieved at the output of the processor is a measure of the effective number of looks N_{eff}. Most processors use data for multi-looking that overlap to some extent, thus retaining some inter-look correlation. The most important speckle figure of merit is N_{eff}, not simply the number of looks implemented in the processor. For example, for Seasat, $N = 4$, yet $N_{eff} = 3.3$, typically. This was a consequence of the shape of the azimuth antenna pattern, details of processor operation, etc. It is N_{eff} that is of most interest to users.

Finally, speckle is an expression of the underlying coherence of the system, and gives a hint that there are available clever ways to take advantage of these systems to accomplish rather specialized radar measurements. One rather intriguing application is to create speckle interference between two different data collection sets from the same radar, but from two different passes along the same (or similar) orbit. Such interferometry may be processed to yield a map of terrain elevation countours, as has been demonstrated by researchers at the Jet Propulsion Laboratory, in Pasadena, California, for example.

Conservation of confusion

SAR performance is characterized by excellent resolution (for a radar), but with the attendant nuisance of speckle. Speckle may be reduced by averaging after detection, but only at the expense of resolution. The consequence of breaking up the available data into N looks is that each of the resulting looks, and hence of the final image, has its resolution degraded by the same factor N. This is true for averaging done in either the range or in the azimuth direction, and for data segmentation in either the synthetic aperture data set or in the final image. The key relationship is expressed by the principle of conservation of confusion: the product of the angle and azimuth resolutions divided by the total number of effective looks is a constant.

For a system such as multi-look SAR, image properties cannot be adequately described by "resolution" or "number of looks" alone. Resolution and number of looks must always be specified together. The principle of conservation of confusion is an expression of this fact. There is a logical trade-off between rsolution and speckle suppression, but if all data are used in the processor for each case, the amount of "information" carried by the image is invariant in response to allocating signal resources in either direction.

Increasing the number of looks is one way of intentionally decreasing the coherence of the processor. Thanks to the principle of conservation of energy, the estimate of average scene reflectivity, σ_o, is the same number, independent of how the resolution/look trade-off is accomplished, assuming, as before, that all available data are used in each case. This is a very important property of a SAR system.

COMMENTS AND CONCLUSIONS

SAR theory as outlined in this paper is based on certain assumptions, generally valid, but which deserve to be mentioned. The key results cited require (with the exception of detection) that the system be *linear*, that is to say, provide additive results for additive signals at the input. Now, a true linear system does not exist, only systems that are linear over a given signal dynamic range! SARs and processors are generally designed to be "linear" under most circumstances, but not always. Image artifacts may be generated if there is a saturation, limiting or other processes impacting the relative signal levels throughout the system. This is particularly true for fixed point digital stages, as is found, for example, in the Earth Resource Satellite (ERS)-1 SAR data down-link telemetry. The dynamic range of this link is 5 bits, no more. Dynamic range limitations in the signal domain, however, are much less troublesome than in the image domain.

Likewise, the discussion assumes that the gain and other performance characteristics of the SAR and processor are constant over time. In practice there are likely to be variations. It is the responsibility of the agencies sponsoring SAR systems to provide data products that are reasonably stable over the life of each mission.

All SAR systems being built or operating in orbit use a long coded pulse for the ranging signal. Processing is required to transform such a long pulse to a sharp impulse response analogous to that discussed for azimuth processing, but of course is much simpler since there is no range parameter (other than relative delay) to contend with. A detailed discussion has not been included since such pulses are not essential to understanding the main features of SAR.

Quantitative characterization of the radiometric and geometric performance of SARs generally requires calibration procedures to be done, as is the case for any measurement device. Calibration of a SAR is complicated by the important role played by the antenna, consequences of which may only be measured once in orbit, and by instruments designed for the purpose placed on the ground. These measurements are aided by self-check systems built in to the radar, and included in the processor.

The discussion has been based on treating the output of the processor as an image whose pixel digital values are proportional to reflected power. Often this is not true. The reader is cautioned that many processors use a magnitude detection scheme rather than magnitude squared. This is sensible from an image "appearance" point of view, and saves dynamic range and hence reduces the number of digital tapes required to store the images. The main disadvantage is that it makes the mathematics used to describe quantitative SAR performance more awkward. It has no impact, of course, on whether or not speckle appears!

The approach of this discussion assumes that only spacecraft SARs are of interest. For those with aircraft radar experience, the few differences that may be evident should not be offensive. In general, the aircraft SAR case is more complicated, as it implies the need for extra effort, in the radar and/or in the processor, to compensate for the motion of the aircraft, and the viewing geometry is more of an issue since the incidence angle may change so much over the imaged swath.

For most SAR processors, the prime product is as described, with pixels at a "standard" map scale spacing, but the orientation of the resulting image in most cases is parallel to the spacecraft orbit path rather than aligned with the latitude/longitude grid. Usually, special image products are available that are matched to standard map projects where required.

Some readers may have noted the omission of the term "Doppler" in this paper. Doppler, named after a German engineer of the nineteenth century, refers to the shift in a signal's frequency due to relative motion between the signal source and an observer. It is usually invoked as an "explanation" for the inner workings of SAR azimuth signal structure. The wavefront approach taken here is, in the view of this writer, more direct, and certainly is fundamentally correct. (The Doppler interpretation is the derivative of the wavefront model.)

Likewise, there has been no discussion of the "frequency domain", nor of frequency analysis operations such as the Fournier transform. Whereas it is essential to efficient implementation of SAR processors, and useful for analysis and design of such systems, the concept is not always an effective means of communicating new and sometimes subtle ideas. The author hopes that the discussion as presented is not disappointing to the reader in this regard.

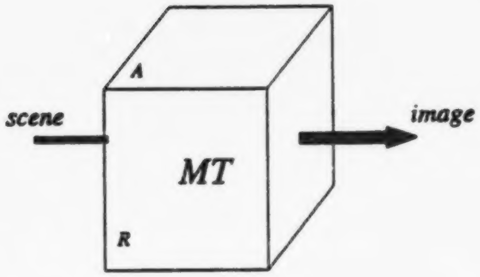
A
scene
image
MT
R

Figure 1. Conceptual Model of a Radar Imager

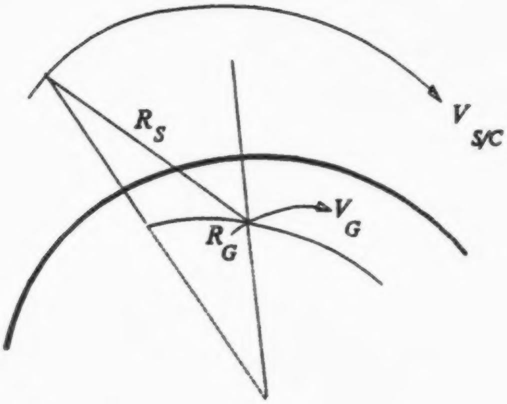

Figure 2. Geometry for an Orbital SAR

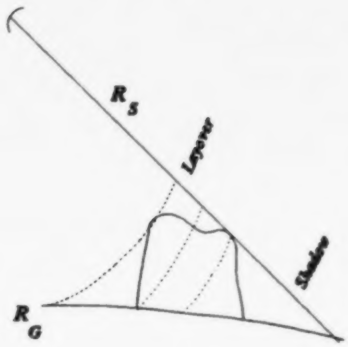
R_S
Layover
Shadow
R_G

Figure 3. Severe Terrain Variation may lead to Lay-over and Shadowing

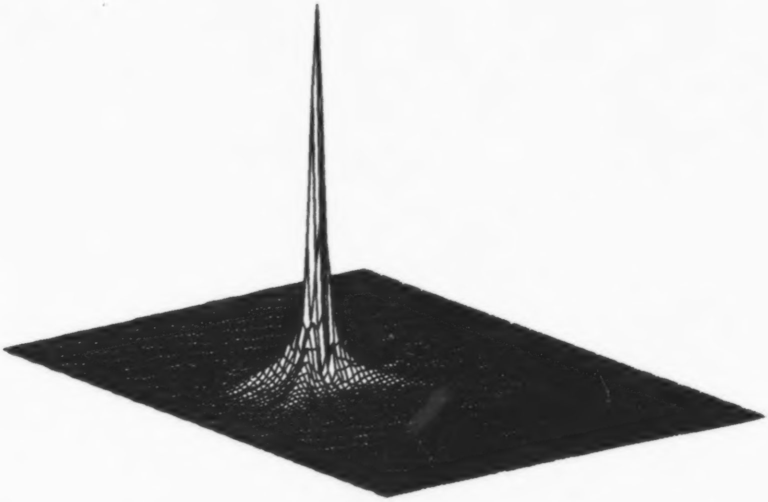

Figure 4. Example of Two-dimensional Impulse Response

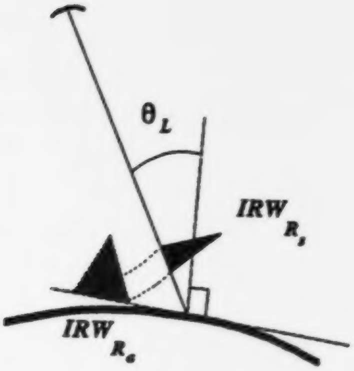
θ_L
IRW_{R_s}
IRW_{R_g}

Figure 5. Range Pulse Enlargement due to Slant Range/ Groud Range Projection

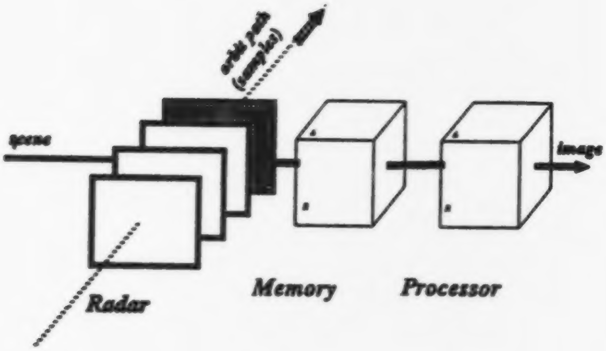
orbit path
(samples)
scene
image
Radar
Memory
Processor

Figure 6. Three Basic Sub-systems Central to SAR Imaging

NOTES

1. Raney, R.K. "A Paradigm Shift in SAR Processing," Keynote Address, TRIO.CRL 3rd Annual Radar Symposium, Hamilton, Ontario, 1 October 1990.

2. Raney, R.K. "Coniderations for SAR Image Quantification Unique to Orbital Systems," IEEE Transactions on Geoscience and Remote Sensing, (to be published).

3. Raney, R.K., "Theory and Measure of Certain Image Norms in SAR," IEEE Transactions on Geoscience and Remote Sensing, Vol. GE-23, No. 3, May, (1985) pp. 343-348.

4. Raney, op.cit. (1990).

5. Ulaby, F.T., R.K. Moore, and A.K. Fung. Microwave Remote Sensing, vol. II, (Reading, MA, Addison-Wesley 1982).

6. Raney, op.cit.. 1991.

NDVI - CROP MONITORING AND EARLY YIELD ASSESSMENT OF BURKINA FASO*

Suzanne M.E. Groten
International Institute for Aerospace Surveys and Earth Sciences (ITC)
Enschede, The Netherlands

INTRODUCTION

A number of studies on crop monitoring and yield estimation based on Normalized Difference Vegetation Index (NDVI) regressions in the Sahelian countries have been published so far. 1/, 2/, 3/, 4/ In addition, strategies for the establishment for NDVI-yield regressions were clearly analysed. 5/ Most of the existing studies, however, were still fragmentary and did not aim at establishing operational nationwide procedures. For this case study, a time series of the National Oceanic and Atmospheric Administration (NOAA)-NDVI data with a pixel resolution of 7.6 km that covered the whole country of Burkina Faso in the years 1984 to 1989 was performed. The data were obtained from the Africa Real Time Environmental Information System (ARTEMIS) system of the Remote Sensing Centre of the Food and Agricultural Organization of the United Nations (FAO) 6/. The main objectives of the case study were: (1) to identify the best NDVI parameters for millet/cereal yield regressions on a limited data set of selected provinces and years; (2) to determine the time when forecasts start to become useful; (3) to test the regressions on data from the whole country and for another year; and (4) to work out spatial Geographic Information Systems (GIS) models to improve the quality of input data and of presentation.

---

* This paper, which was presented at the United Nations/Food and Agricultural Organization of the United Nations/United Nations Environment Programme Seminar on Remote Sensing for Decision Makers, Nairobi, Kenya, 26-31 August 1991, does not necessarily reflect the views of the United Nations.

APPROACH TO NATIONAL CROP YIELD FORECASTING AT THE PROVINCIAL LEVEL

In establishing the approach for national crop yield forecasting, the objectives were developed during an FAO International Institute for Aerospace Surveys and Earth Sciences (ITC) seminar in 1988 and during extensive discussions with the Ministry of Agriculture of Burkina Faso. Therefore, for national crop yield assessment the following should be taken into account:

(a) The estimates must be available before harvest or at least before official yield statistics become available. Therefore, approaches of mathematical modelling of time series curves 7/, 8/, which are applicable only after the growing season are not relevant for operational near-real time monitoring. Also, deterministic simulation modelling 9/ usually does not yield timely results because of the high number of parameters involved which may be difficult to measure operationally. Regression analysis, therefore, has been applied more frequently in regional yield estimations 10/. Therefore, most of the methods applied in the present study were based on a statistical approach, combined with spatial modelling in a GIS.

(b) The forecast must be quantitative, precise and cross-checked with independent data sources. This means that methods must be tested on the basis of independent data sets and errors must be analysed. If possible, the historical database used for the establishment of yield regressions should include dry, normal and wet years, so that the results can be expected to be valid under a wide range of conditions. For example, the Burkina Faso data set for 1984 and 1987 showed drought years in parts of the country, for 1988 it showed a wet year and for 1985 and 1986 it showed "normal" years. Also, monitoring information was cross-checked visually with rainfall maps, NDVI soil moisture diagrams from 21 rainfall stations and with agrometeorological background information supplied by the Burkina Faso Transportation and Communications Ministry (MTC) between 1984 and 1989. The possibilities of digital cross-checking of ARTEMIS rainfall and NDVI data in logical GIS-models have been described. 11/

(c) The method should be applicable countrywide and give complete area coverage. Traditional yield estimates based on spatial interpolation and modelling of rainfall point data suffer from very high spatial variability of rainfall in the Sahel 12/, 13/, 14/. According to a study performed by scientists of FAO and the Center for Agrometeorology and Operational Hydrology (AGRHYMET) 15/, rainfall data can only be used for crop yield modelling in a surrounding of 2 to 3 km around meteorological stations in the Sahel. Therefore, satellite NDVI monitoring based on 9040 pixel values for one ARTEMIS image of Burkina Faso instead of a maximum 128 data recordings from rainfall stations has a potentially higher spatial representation compared to conventional approaches. The study results were based on NDVI values which were averaged for each of the 30 provinces. Also, from the pixel values, the regional NDVI averages for each of the 30 provinces was calculated.

(d) The information should be objective, transparent and reproducible. Regressions described in this article have also been established by African meteorologists and agronomists during an FAO/ITC course in Nairobi, confirming the results achieved by FAO/ITC in 1990.

(e) The use of a satellite early warning system should ease the work of responsible organizations during the growing season, so that real harvest measurements can be prepared and carried out more carefully. It should be pointed out that yield forecasts derived from a satellite early warning system must never be confused with or influence actual yield statistics. If this were the case, there would be the danger of producing higher correlation coefficients and "better forecasts" each year. Therefore, the methods of crop yield forecasting and of yield measurements (area frame sampling) must be developed independently.

Separating drought and atmospheric effects on 10-daily NDVI images: additional preprocessing using the conditional temporal interpolation method

The preprocessing of ARTEMIS data derived from the NOAA-Advanced Very High Resolution Radiometer (AVHRR) sensor has been described 17/. Maximizing NDVI over a certain period should lead to a removal of clouds and other atmospheric effects 18/. Although monthly images of Burkina Faso proved to be cloud free, it was found that one quarter of 180 10-day daily images were not entirely without clouds. Of the 60 per cent of all clouded images, only less than 1 per cent were affected by cloud pixels (see figure 1).

Clouded image series produce dips in NDVI time series diagrams. These image series are derived by the calculation of regional averages which can be confused with real drought stress. Smoothing of the extracted curves 19/, 20/ may lead to a loss of valuable information about the growing season. Strongly smoothed curves look very much like monthly or mathematically modelled curves and represent the same disadvantages for real-time monitoring of temporary drought situations. Moreover, according to the philosophy of the maximization of the NDVI, all disturbing factors tend to reduce the NDVI. Therefore, only certain negative deviations from the curve caused by clouds and other disturbing factors would need to be eliminated. Peaks of the

NDVI give important information about the quality of the growing season. Smoothing these peaks in the curve would make the data set unsuitable for yield regressions based on maximum NDVI values. It may very well be the case that earlier maximum-value regressions in the literature sometimes gave rather unsatisfactory results because of insufficient cloud correction during the image processing phase. Therefore, a more selective method is proposed which only eliminates negative deviations according to a user-defined criterion: a conditional temporal interpolation. This correction is applied during image processing, before the extraction of tabular NDVI data used in numerical analysis. The processing of all data has been one Integrated Land and Watershed Information System (ILWIS), a personal computer (PC)-based GBIS system with a very flexible map calculation programme). 21/ Batch programmes were written which allow the automatic application of the methods.

The conditional temporal interpolation method replaces pixel values satisfying a "cloud" criterion by the average of the corresponding pixel values of the preceding and the following 10-day period. These "cloud" pixels, including other atmospheric disturbances like dust storms, were considered all NDVI values which were either lower than zero (= 127 digital value) or which negatively deviated from the average values of the preceding and the following 10-day period by more than 10 per cent. This is an empirical percentage which was found after evaluating NDVI decreases due to real drought or senescence. A smaller percentage deviation may be applied, but would increase the risk of eliminating the effects of real drought stress. For the extreme case in which three or more consecutive pixels are clouded, the method is applied in three or more steps (see figure 2). The effect of this image correction on derived time series diagrams is demonstrated in figure 3.

Due to the fact that this method requires the availablility of images following 10-day periods, it is only applicable to the analysis of historical NDVI data for yield regressions. In real-time monitoring, other methods (excluding zero values in data agregation, etc.) have to be applied. But to what extent can "cloud" and drought effects really be separated? An evaluation of the method, applied to heavily clouded NDVI data of the Southern Province of Zambia under rainfall conditions of 800 to 1,500 mm is shown in table 1. It was found 22/ that 90 per cent of 60 cases of a NDVI decrease during the main growing season. This could be explained by a soil moisture deficit in either the same or the previous dekad (a 10-day period). A soil moisture deficit was defined when: (a) the soil moisture index (P + S)/ETC at a water holding capacity of 60 mm was lower than 1, or (b) when a relative decrease occurred in both NDVI and the soil moisture curve. 23/, 24/ In this case it was assumed that

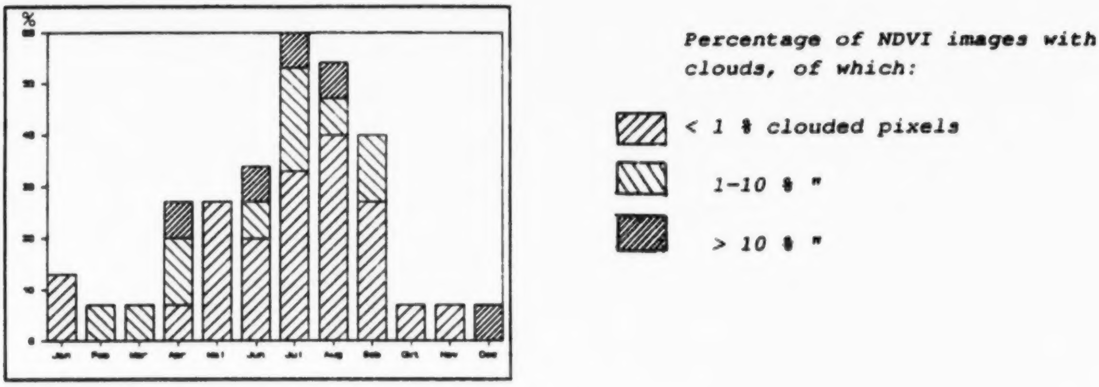

Figure 1. *Percentage of clouded 10-daily NDVI images of Burkina Faso*

Table 1

CASES OF NDVI-DECREASE	N	PERCENTAGE total (N = 60)	PERCENTAGE with clouds (N = 19)	PERCENTAGE without clouds (N = 41)
Dekads with clouds	19	32 %		
Dekads without clouds	41	68 %		
Dekads only with clouds, without soil moisture deficit	6	10 %	32 %	-
Dekads with clouds and soil moisture deficit				
. time delay 0 dekad	3	5 %	16 %	-
. time delay 1 dekad	6	10 %	32 %	-
. time delay 0 + 1 dekad	4	7 %	21 %	-
Total: time delay 0 - 1 dekad	13	22 %	68 %	-
Dekads without clouds and with decrease soils moisture				
. time delay 0 dekad	17	28 %	-	41 %
. time delay 1 dekad	14	23 %	-	34 %
. time delay 0 + 1 dekad	10	17 %	-	24 %

Evaluation of cloud- and drought effects in 60 cases of NDVI-decrease on 10-daily NDVI images, to which a supplementary cloud correction procedure has been applied; data for 3 x 3 pixel windows around the meteorological stations Monze, Magoye and Livingstone, Southern Province, Zambia (after MSc thesis Masialeti, 1990)
Soil moisture index = (P + S) / ETp; P = Precipitation (mm/dekad); S = Storage (mm) from the previous dekad; ETp = potential evapotrasnpiration (mm/dekad)

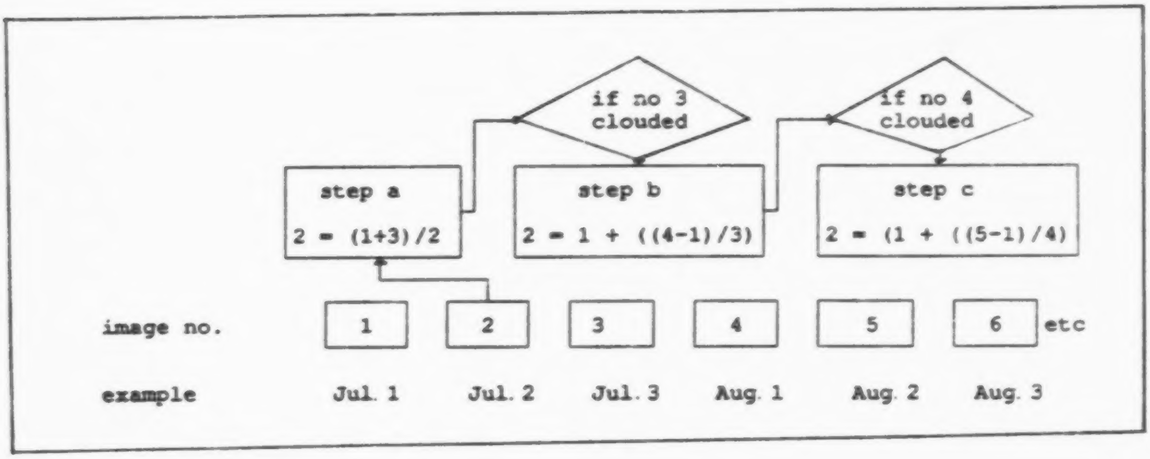
if no 3
clouded
if no 4
clouded
step a
2 = (1+3)/2
step b
2 = 1 + ((4-1)/3)
step c
2 = (1 + ((5-1)/4)
image no.
1
2
3
4
5
6
etc
example
Jul. 1
Jul. 2
Jul. 3
Aug. 1
Aug. 2
Aug. 3

Figure 2. *Schematic representation of the conditional temporal interpolation for the removal of residual cloud effects on 10-daily images*

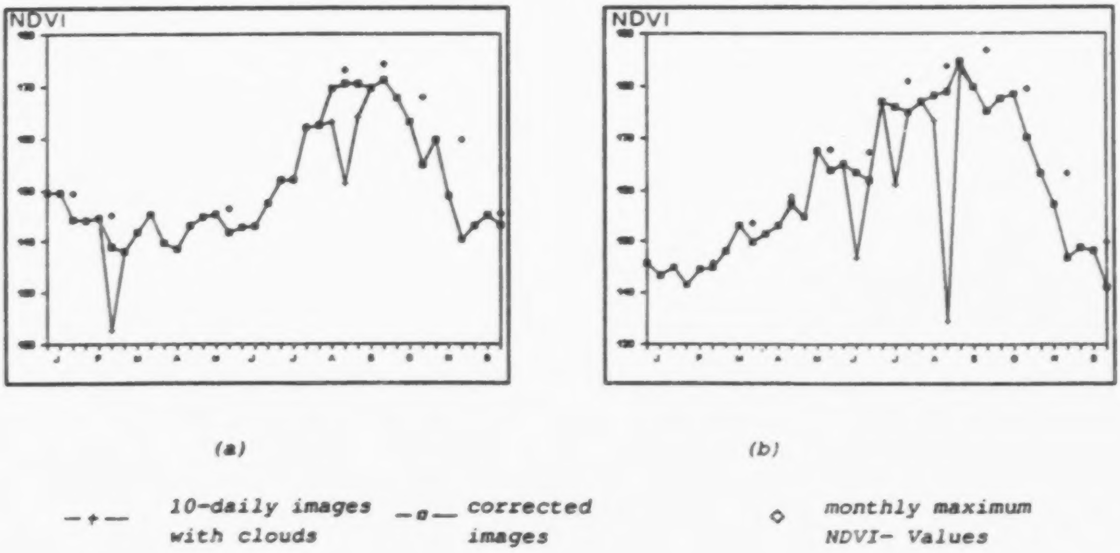

Figure 3. *The effect of the correction of cloud effects on derived NDVI profiles of (a) a central and (b) a southern province of Burkina Faso in 1988*

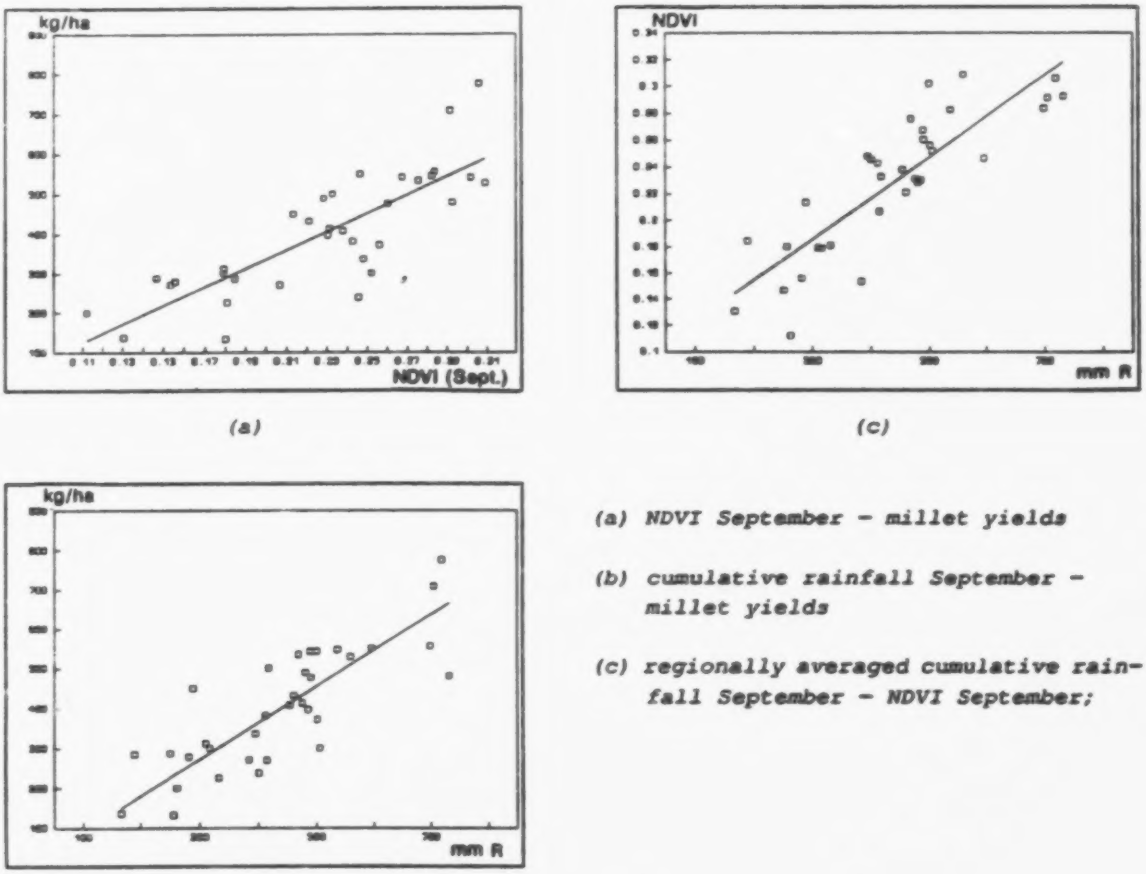

(a)

(c)

(b)

(a) NDVI September - millet yields

(b) cumulative rainfall September - millet yields

(c) regionally averaged cumulative rainfall September - NDVI September;

Figure 4. *Correlations between millet yields, rainfall and NDVI in seven northern provinces of Burkina Faso 1984 - 1987*

Table 2: Regressions between NDVI, Millet yields and rainfall

Ymillet = 0.91 * R	$r^2 = 0.67$	std. err. 87 kg/ha
NDVI = 0.093+0.00030763* R	$r^2 = 0.73$	std. err. 0.02790
NDVIdig= 138 + 0.03938 * R	"	"
Ymillet = -131.64 + 2334.93 * NDVI	$r^2 = 0.66$	std. err. 89 kg/ha
Ymillet = -2448 + 18.24 * NDVI(dig. val.)	"	"
Ymillet = -1276.16 + 0.48*R + 9.4*NDVIdig	$r^2 = 0.72$	std. err. 83 kg/ha

comment
n=34; 7 north. Provinces 1984-1988 minus Yatenga 1984 (yield data lacking)

R = cumul. rainfall until september R (mm)
Ymillet = average millet yields per province (kg/ha)
NDVI = regionally averaged maximum NDVI of september
NDVIdig, dig. val. = NDVI (-1 to +1) rescaled to digital values 0 - 255

during the main growing season a drought stress can occur at a soil moisture index of>one.

In only 10 per cent of the cases does cloud cover represent the main cause for a decrease of the NDVI. Part of this 10 per cent can, however, also be caused by a time delay greater than one dekad between a soil moisture deficit and the subsequent decrease of the NDVI. In all 41 cases of cloud-free images, the NDVI directly reacts on a soil moisture deficit. This proves that the fluctuations in the NDVI diagram produce much less "noise" than may be expected. Excessive smoothing of curves and images series therefore should be avoided.

A wrong interpretation of NDVI anomalies in an early warning system is more dangerous, if a drought is not recognized, than if a false alarm is given (this should however not happen too often). This is another reason to use interpolation criteria which lead to relatively little smoothing. For security reasons it is also recommended to cross-check NDVI information on drought areas with data on cloud cover. For cross-checking, cold cloud duration images from ARTEMIS should not be used exclusively. For these images, a low thermal threshold is applied which is designed to filter out only cold and rain bringing clouds. It is better to use the original non-corrected NDVI data and meteorological information for the verification of NDVI anomalies.

Establishment of relationships between crop yields, rainfall and vegetation index

Rain-fed crop production and rain-fed crop yields normally show trends similar to the cumulative yearly rainfall. Exceptional situations can, however, be caused by locusts, social unrest or by drought during senstive stages of crop development. A careful analysis of figure 4 proves that anomalies in the NDVI-yield diagram are also rainfall anomalies. This is not surprising, since the regionally averaged seasonal rainfall explains 73 per cent of the variations of the NDVI (see figure 4 c). Because of the relatively good relations between NDVI and rainfall in Senegal it has even been proposed to estimate rainfall from the NDVI. 25/ This relation is, however, only applicable for regionally averaged values and not on the pixel levels.

Sixty-seven per cent and 66 per cent of the variation of average provincial millet yields can be explained respectively by rainfall or the maximum NDVI of September. This compares well with a study that found that 50 to 70 per cent of the yields were explained by rainfall parameters in central Sudan.26/ The slight difference in correlation between rainfall and NDVI should not be overestimated, because known rainfall conditions may have played a role in yield assessments, whereas the NDVI is a completely independent data source. Together both variables explain 72 per cent of the yield variation with a standard error of 83 kg/ha at the end of September (see table 2).

Mapping the dekad of the start of the growing season and of sowing dates

Monitoring and mapping the start of the growing season is important for the estimation of sowing dates which are related to crop yields, especially for photosensitive varieties. In the Sahel, a very late or interrupted start of the growing season can lead to a complete failure of the crop season, if the latest possible sowing data for crop varieties with a minimum maturation cycle has passed. Therefore, monitoring the start of the growing season is important to complement a statistical approach to crop yield forecasting. Mapping the start of the growing season and of sowing dates could also be important for defining the starting time for dynamic crop simulation modelling. Agrometeorologists have defined the start of the growing season as the dekad, when rainfall exceeds half of the potential evapotranspiration ($R > ET/2$). This corresponds to 25 to 30 mm rainfall per 10-day period.27/, 28/ The start of the growing season in Ethiopia has been defined as the first dekad with positive NDVI increments, which is followed by a positive trend leading to an NDVI maximum. 29/ A disadvantage of this method is that the start of the growing season can not be identified in real time monitoring, because the continuation of the growing season is unknown. Moreover the start of the growing season shows a high spatial variation, so that not only a tabular-graphical, but also a cartographic method is required.

A calculation in map format of the start of the growing season based on 10-daily NDVI increments is demonstrated in figure 5. The growing season was defined to have started if during two consecutive dekads positive NDVI increments have occurred with a defined minimum increase. The method was only applied for the period relevant for sowing in the centre and in the north of the country (for the south, the earliest sowing period in April could have been included). This time limitation also helped to avoid a secondary NDVI, slightly bimodal rainfall regime. The calculation period ends after the latest possible sowing time, which is towards the end July for grain crops in large parts of the country. The criteria for the establishment of minimum NDVI increments were based on a study of rainfall, evapotranspiration and NDVI curves from 21 meteorological stations in Burkina Faso. It was found that:

-when $R \geq$= ETp/2, 10-daily NDVI increments are$\geq$1 digital value (0-255);

-when $R >$ ETp during the first part of the growing season, increments are$\geq$3 digital value. The maximum 10-daily increments are 8-10 dig. val. in the north and the centre and up to 15 digital value in southern savanna areas.

The NDVI in Burkina Faso responds after one to four dekads following a good rainfall in the beginning of the growing season. Time delays of two to four dekads, however, only occur in some years in agricultural areas (due to land preparation) and in areas with natural vegetation but unfavourable infiltration conditions. The difference in behaviour of cultivated and non-cultivated areas, and between different years appeared to be rather inconsistent, which causes some problems for the estimation of the start of the growing season from NDVI increments. More phenological information would be required for a full understanding of the underlying processes. Knowing the location of agricultural areas, a possible delay of the response of the NDVI to the onset of the rains could however be anticipated and included in a logical model. When no differentiations are made between cultivated and non-cultivated areas as in figure 5, it is possible that pixel collocations will have errors at the per pixel interregional level. A smoothing filter was not applied to the maps in figure 5 in order to allow a critical interpretation.

The high regional and annual variability of the start of the growing season is shown in figure 5. A visual analysis allows the conclusion that an early start of the growing season is no guarantee of a good continuation of it, as has been learned from the drought years of 1984 and 1987. On the other hand, figure 5 shows that in some areas and years the onset of the growing season was very late (e.g., in parts of the Sahel, so that sowing conditions probably have been unfavourable). On the basis of NDVI increments also sowing dates could be estimated spatially. In Burkina Faso sowing is done as early as possible at about 4 ETp/3. 30/ This is even earlier than the definition of the growing season cited above. Farmers have to profit as much as possible from the scarce rainfall and even apply dry seeding in case of need. In this case, there is practically no time delay between the greening of fields and of natural vegetation. Since sowing has to be spread over several days and over rainfall events in manual land preparation, it can however quite safely be assumed that any signficant NDVI increment in the beginning of the growing season reflects favourable seeding or reseeding conditions. The refinement of the calibration has to be carried out during an experimental phase of implementation of satellite monitoring the national level.

Monitoring of the continuation of the growing season

The qualitative monitoring of a current growing season is done by comparing observed current NDVI data with historical data, and optimum or averaged reference curves. The impact of negative deviations from a reference curve on yields, however, depends on critical stages of crop development. The average crop calendars of three provinces compared to the NDVI profiles of several years is shown in figure 6. The crop calendars were compiled from MTC 1984 and 1989 and by our own observations. A decrease of the NDVI during the early vegetative phase, the flowering stage and the early ripening stage is known to be particularly harmful to yields. The location of the provinces described is indicated in figure 7.

NDVI-yield regressions for seven northern provinces, 1984-1988

A group of seven provinces of the Sahelian zone and the Sudano-Sahelian border was assumed and confirmed to be a homogeneous data set for which early forecasting would be very relevant. Regressions were elaborated between millet yields and various parameters of the NDVI, which was corrected for shifts in the sensor characteristics by adding a year-specific constant1/ The development of correlation coefficients between millet yields and monthly NDVI parameters in the course of the growing season is shown in figure 8. It appeared that the highest correlations were obtained by multiple linear regression (up to $r^2 = 0.87$) at the end of the growing season). Similar results as for millet yields were obtained for the average yields of rainfed cereals (millet, sorghum, maize and fonio). A regression for sorghum along gives unfavourable results ($r^2 = 0.6$), probably because of cropping of sorghum varieties under very different ecological conditions, such as, in depressional areas, which are less rainfall dependent.

Regressions based on simple averaged maximum values gave better results than regressions based on integrated NDVI or growth rates using different periods of integration. Including additional easily measurable parameters like geographic latitude did not improve the result. Satellite rainfall data from the ARTEMIS system were not included in the model, since a comparison of satellite and ground rainfall estimates of Burkina Faso showed a structural underestimateion of seasonal rainfall of about 100 mm. Recalibration studies of satellite rainfall estimates are, however, ongoing.

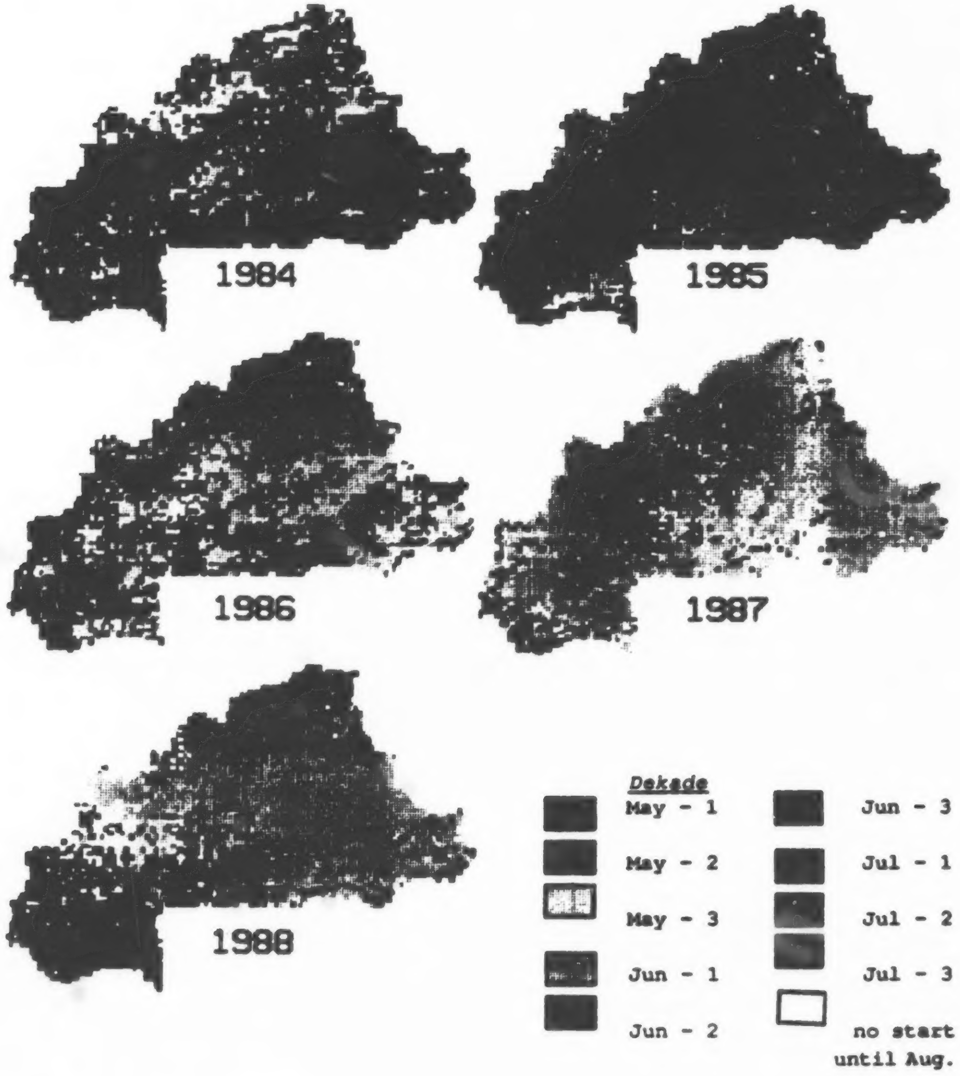
1984
1985
1986
1987
1988
Dekade
May - 1
May - 2
May - 3
Jun - 1
Jun - 2
Jun - 3
Jul - 1
Jul - 2
Jul - 3
no start until Aug.

Figure 5. *Dekad of the start of the growing season calculated from 10-daily NDVI increments.*

Definition of the start of the growing season: The dekad with an NDVI increment of ≥ 1 digital value (NDVI stretched from 0 - 255), followed by another dekad with an NDVI increment of ≥ 3 digital values. In this figure, only the dekads between the third dekad of April to the first dekad of August were included in the computation.

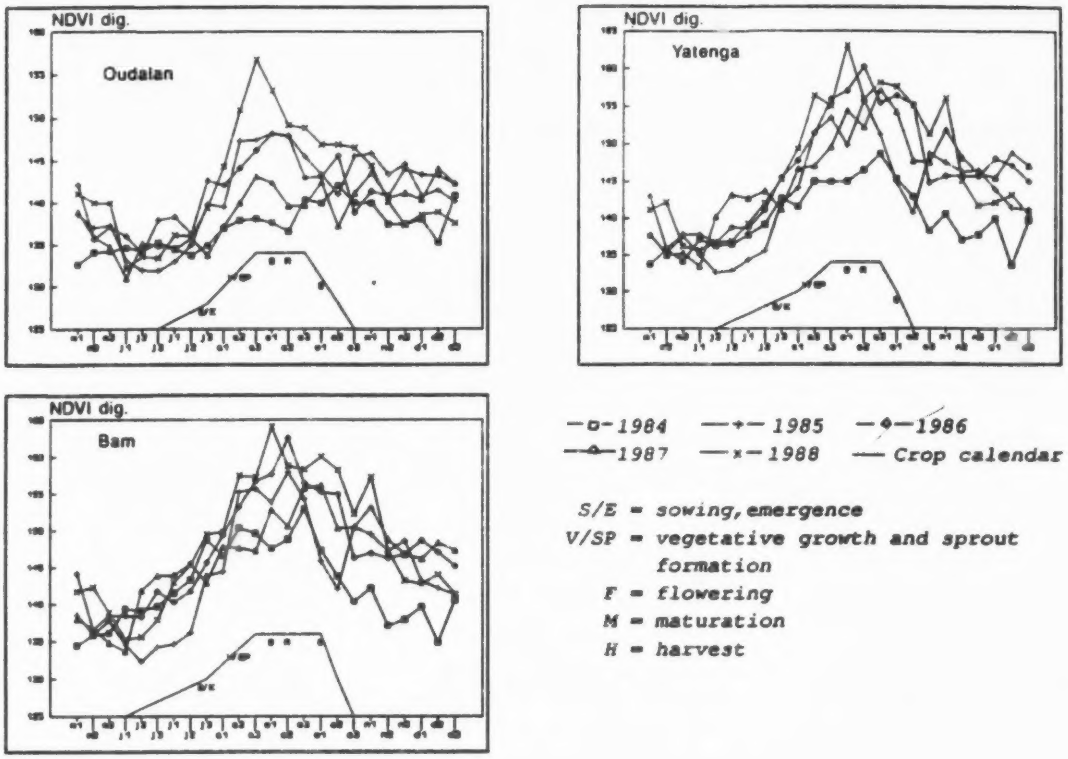

Figure 6. *NDVI profiles and crop calendars of 3 northern Provinces of the Sahelian and the Sahelo-sudanian zone of Burkina Faso*

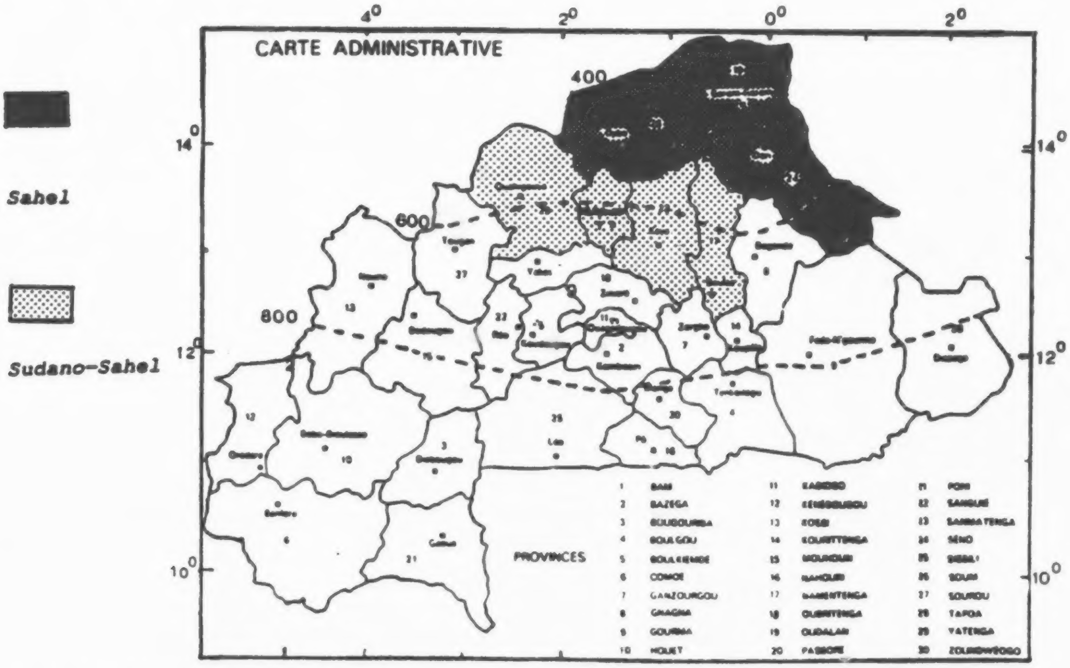
CARTE ADMINISTRATIVE
4°
2°
0°
2°
14°
12°
10°
400
600
800
Sahel
Sudano-Sahel
PROVINCES
1 BAM
2 BAZEGA
3 BOUGOURIBA
4 BOULGOU
5 BOULKIEMDE
6 COMOE
7 GANZOURGOU
8 GNAGNA
9 GOURMA
10 HOUET
11 KADIOGO
12 KENEDOUGOU
13 KOSSI
14 KOURITTENGA
15 MOUHOUN
16 NAHOURI
17 NAMENTENGA
18 OUBRITENGA
19 OUDALAN
20 PASSORE
21 PONI
22 SANGUIE
23 SANMATENGA
24 SENO
25 SISSILI
26 SOUM
27 SOUROU
28 TAPOA
29 YATENGA
30 ZOUNDWEOGO

Figure 7. *Province Map of Burkina Faso*

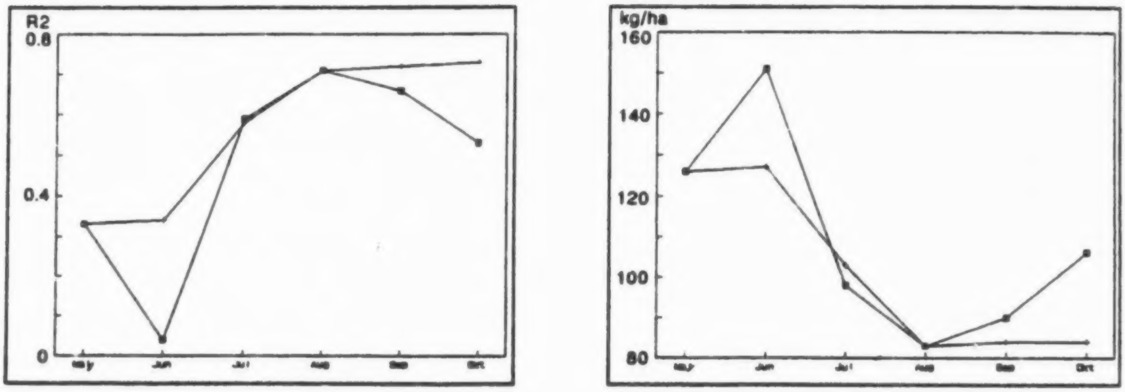

(a) Correlation (R²) monthly NDVI- millet yields

(b) Standard error of regression NDVI- millet yields (kg/ha)

-□- simple correlations ¬+-multiple correlations (with optimum number of variables)

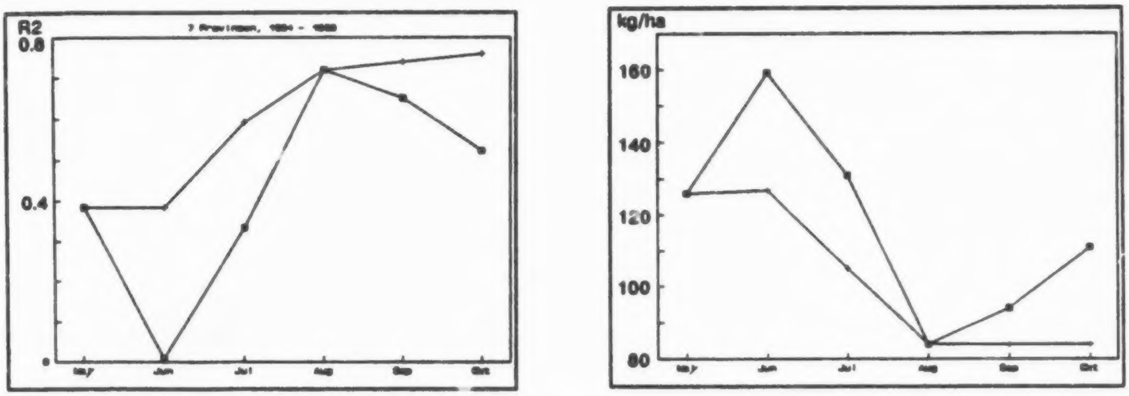

(c) Correlation (R²) monthly NDVI - average cereal yields (Millet/Sorghum/Mais/Fonio)

(d) Standard error of regression NDVI- cereal yields (kg/ha)

Figure 8. *Development of the correlation (r²) between monthly NDVI values and millet yields in the course of the growing season, and the corresponding standard error of estimate*

n = 34 (Provinces Oudalan, Soum, Seno, Yatenga , Bam, Sanmatenga and Namentenga, 1984 bis 1988, exept Yatenga 1984 (no millet data)
Source: MAE (1989): digital data bank Ministery; revised data Nov. 1989, exept: Sahelian provinces 1984 and Seno (1987): provincial reports

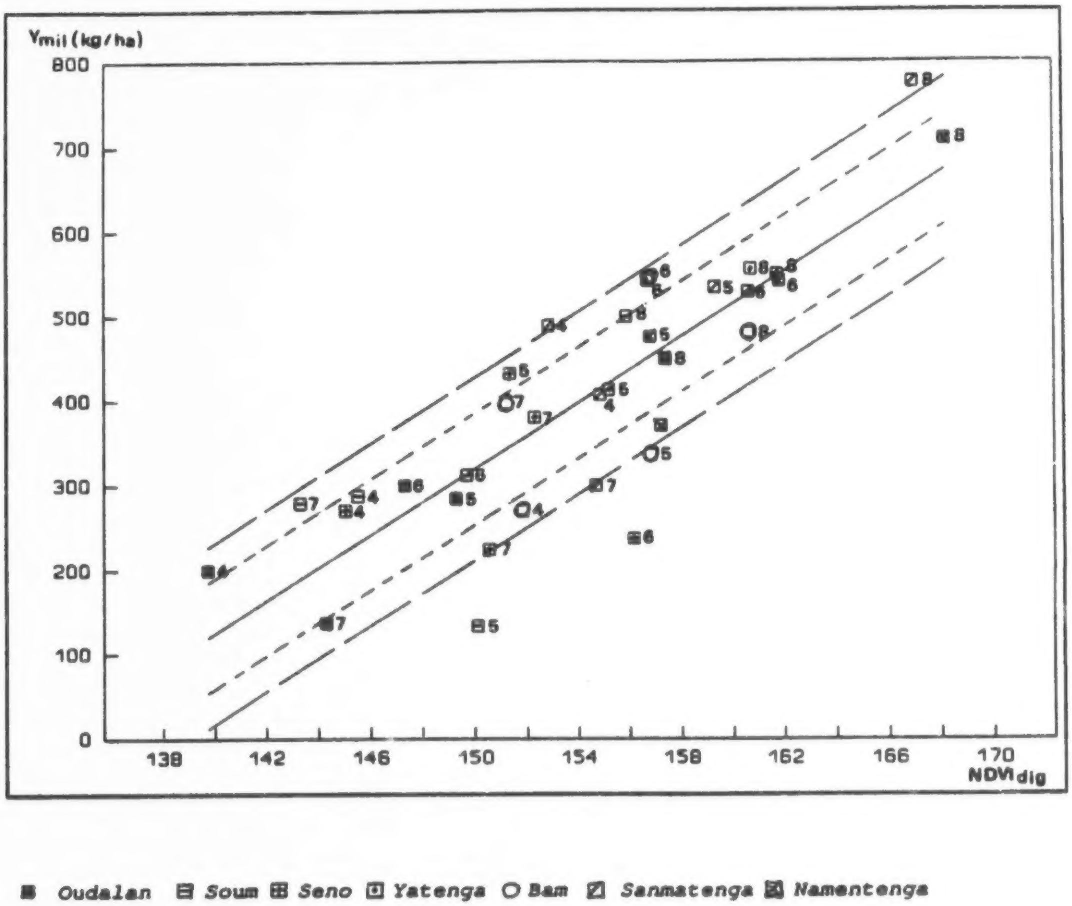

Figure 9. NDVI of August and millet yields in 7 northern provinces of Burkina Faso 1984 - 1988

Regression: Ymillet = - 2602 + 19.48 * NDVIaug ; $r^2 = 0.71$, Std. err. = 83 kg/ha

Confidence interval: p = 90 % --> Y +/- 108 kg/ha
p = 80 % --> Y +/- 66 kg/ha

Using a correlation coefficient of $r^2 = 0.71$, a reasonable forecast can be derived from the month of August onwards can be (see figure 8). After August, multiple correlations only improve the results slightly and come relatively late for crop yield forecasts. The optimum forecast time based on August data corresponds to approximately two months before harvest and three months before the first official production data become available. In figure 9, the August regression is given for the seven northern provinces. A statistical evaluation showed that the NDVI and yield variables are normally distributed at the 84 per cent (yields) and at 97 per cent (NDVI) significance level. A simple sign test proved that with 80 per cent significance none of the provinces and non of the years differed significantly from the general trend. Anomalies found in figure 9 and other diagrams will be analysed below.

On 10-daily data higher correlations were obtained (up to r2/= 0.87) but they do not lead to an increased accuracy of the forecast due to the increase of NDVI parameters and the decrease of the degrees of freedom involved in multiple regression (see figure 10). Therefore, a standard error of 80-85 kg can be considered the limit of accuracy.

Similar or slightly less favourable correlations with millet yields are found for integrated NDVI values, when different cumulation periods are tested in the months of June and July, and for other critical periods of plant growth. An effort to correct for possible interannual changes in average vegetation cover of the provinces by subtracting dry-season NDVI minima also did not improve the results.

Anomalies of the regression were investigated with the help of 10-daily national agrometeorological bulletins. Knowledge about the residues reveals agromomic factors which may improve of the regression model. It was found that one province, Soum was hit in 1985 by drought and locust and by borer in September. In parts of the province in 1986 the start of the growing season was detected through these agronomic factors (figure 5) as well as by personal field observations. In addition, the Water Requirement Satisfaction Index (WRSI) of FAO in 1986 gave only 72 per cent satisfaction of crop water requirements, according to the Ministry of Transportation and Communications in 1989. In the province of Bam, yields in 1985 were lost due to flooding in June through August, aggravated by the fact that farmers had started to grow millet in depressional areas after the drought of 1984. In 1987, the provinces of Oudalan, Seno, Sanmatenga and Namentenga were affected by a regional drought, which is well recognizeable on seasonal NDVI anomaly maps but was less pronounced in August.

Extension of the data set to the south

To test whether the type of relation changes in the central and southern parts of the country, where rainfall conditions and yields are much less variable than in the Sahelian zone, a random sample of eight additional provinces was joined to the database analysed under six provinces. From these eight provinces, five confirmed the linear August regression determined for the north, which includes Kadiogo, Komoé, Ganzourgou and Zoundweogo with the exception of Gnagna in 1985, which cannot be explained (see figure 11). Three other provinces however distinguished themselves from the data set by relatively low yields compared to the NDVI in Mouhoun, Boulgou and Houet. In this case, a non-linear regression (second-order polynomial regression) is more appropriate. This regression does not differ much from the linear regression except in the high NDVI/biomass classes. The difference in NDVI-yield relations between certain provinces can either be due to low average yields related to extensive farming systems and bad soils or to a comparatively high vegetation cover.

Test of the regressions with 1989 data for all provinces

Operational yield forecasting should produce timely and precise countrywide results. Monthly regressions were more easily applicable (not requiring additional cloud correction) and provided results nearly as good as 10-daily data. Therefore, of the regressions found in six and seven the following regressions were selected for a test:

(a) linear regression on monthly data of August, see figures 9 and 11;
(b) multiple regression on monthly data of May to September;
(c) non-linear regression on monthly data of August 1989.

Both the linear and the non-linear regressions strongly overestimated the millet yields of the groups A, C and E of the provinces (see figure 12). The question remains, however, whether it is a structural overestimation due to an incorrect sensor calibration or there are regional discrepancies.31/ The low overall yield values indicate the latter. For instance, are the yields of the 10 provinces which were used for the non-linear regression in 1989 15 per cent below the level of the yields of the preceding years? Figure 13 indicates that forecast errors are regionally distributed, pointing to the following different error sources for groups of provinces:

Group A comprises all seven provinces belonging to the northern data set, analysed in six. The deviation has been caused by a locust invasion which was recognized only late in the growing season. 32/ Locusts can selectively attach millet grains in the sensitive milk-ripening stage, preferring it to the green vegetation. A rainfall map also indicates some deficit areas in the north.

Group B is well represented by both the linear and non-linear regression. It represents the "normal case" for central provinces with rainfall conditions between 600 and 1000 mm.

Group C comprises three neighbouring central provinces, which may also have been affected by the locusts, the northeastern part of the country seemed to have suffered less than the northwestern part. Detailed information about the extent of the locust plague is lacking. An estimation of the impact of the locust plague can be derived by assessing the "yield gap" between the regression forecast and the served yields. Drought which affected large parts of the country in September according to a rainfall map does not explain this regional anomaly sufficiently.

Group D is a larger group of central and southern provinces, which is well represented by the non-linear regression. This clearly shows that in the majority of these provinces an increase of rainfall and NDVI only leads to a minor increase in yields. Although this may be due to the effect of increasing vegetation cover affecting the NDVI, it is probably more affected by the nutrient limitations in extensive cultivation under high rainfall conditions.

Group E differs from group D by significantly lower yields compared to the high NDVI. The three most southern and moist provinces belonging to this group. The agrometeorological bulletins mention problems due to excessive rainfall in July and August in these provinces as well as in the Nahouri province. This latter province probably has suffered from greater waterlogging than neighbouring provinces because of heavier volcanic soils.

SUMMARY AND CONCLUSIONS

Historical records of partially clouded 10-daily NDVI images can be improved by applying a conditional temporal interpolation. The application of this method, which leaves peak values of the NDVI unsmoothed, allows a successful application of NDVI-yield regressions based on simple maximum 10-daily NDVI values. The use of other NDVI parameters like integrated NDVI and increments showed no comparative advantage. For a homogeneous data set of seven Sudano-Sahelian provinces and five years high correlation coefficients were obtained, which allow forecasts from 2 to 3 months before harvest. An extension of the data set to the central and southern provinces of Burkina Faso indicates at least two statistical groups of populations with different agroecological conditions and NDVI-yield relationships. This data set was based on a test of regressions of 1989, with all errors being less than then 15 per cent. In the other provinces regional forecast errors were caused by drought in September, by late sowing, by flooding and by locust problems. Some NDVI and used for the improvement of the regression model:

- local flooding from extreme regional NDVI increases;
- monitoring of migratory pests, especially locusts (possibly also weaver birds, rats);
- drought at sowing time using the spatial modelling of sowing dates similar to the modelling of the start of the growing season as demonstrated;
- drought during the ripening stage can only be taken into account at the end of August regression after the first quantitative forecast.

Until specific studies have been carried out, empirical correction factors for extreme events have to be applied in close cooperation with plant protection and other relevant organizations.

NOTES

1. Dijk, A. van, S.L. Callis, and C.M. Sakamotto et. al. "Smoothing vegetation index profiles: An alternative method for reducing radiametric disturbance in NOAA/AVHRR Data" Photogrammetric Engineering and Remote Sensing, Vol. 53, No. 8 (1987) pp. 1059-1067.

2. Comte, D.M. le, F.N. Kogan et al. "Assessment of crop conditions in Africa" NOAA-Technical Memorandum NESDIS AISC 13, Washington (1989) pp. 66.

3. Barthoholomé, E. "Radiometric measurements and crop yield forecasting: Some observations over millet and sorghum experimental plots in Mali", International Journal of Remote Sensing Vol. 9, Nos. 10 and 11, (1988) pp. 1552-1593.

4. Oxenstierna, A. "Productivity estimation in the Sudan using NOAA NDVI GAC-Data Paper of RS and GIS Laboratory, (Dpt. of Phys. Georg. Univ. of Lund, Sweden, 1990) pp. 10.

5. Malingreau, J.P. "The vegetation index and the study of vegetation dynamics" Toselli (ed.) Applications of Remote Sensing to Agrometeorology (1989) pp. 285-303.

6. Hielkema, J.R., J.A. Howard and C.J. Tucker et al., "The FAO/NASA/NLR ARTEMIS system: an integrated concept for Environmental Monitoring by Satellite in Support of Food/Feed Security and Desert Locust Surveillance," Proc. 20th Int. Symp. on Remote Sensing of Environment, Nairobi, Kenya, 4-10 December 1986 (1986) pp. 147-160.

7. Badhwar, G.D. and H.K. Henderson "Application of Thematic Mapper Data to Corn and Soybean Development Stage Estimation", Remote Sensing of Environment, Vol. 17, (1985) pp. 197-201.

8. Dijk op. cit.

9. Penning de Vries, F.W.T., D.M. Jansen and H.F.M. Ten Berg et al. "Simulation of ecophysiological processes of growth in Several Crops", Simulation Monographs Vol. 29, Wageningen (1989) pp. 271.

10. Liverman, D.M. "Forecasting the impact of climate on food systems: Model testing and model linkage", Climatic Change 11, (1987) pp. 267-285.

11. Groten, S.M.E. "The Design of Spatial Models," Proc. of FAO/ITC Seminar on ARTEMIS and GIS Applications for Food Security Early Warning, 12 Nov.-7 Dec. 1990, Nairobi.

12. Flitcroft, I.D., V. McDougall and J.R. Milford et. al. The calibration and interpretation of Meteosat based estimates of Sahelian rainfall, Proc. Remote Sensing Workshop "Ground truth", Nottingham, GB (1986).

13. Milford, J. and Dugdale, G. "Estimation of rainfall using geostationary satellite data in: Applications of remote sensing in agriculture", Proc. of the 48th Easter School of Agricultural Science, University of Nottingham, April 1989.

14. Diallo, A.A. and Turpeinen, O.M. Estimation de la pluviométrie pentadaire au Burkina Faso par l'indice de précipitation ESOC (EPI), ESA Journal 1987, Vol. 11 No. 12, (1988) pp. 68.

15. FAO "Evaluation préliminaire de la production cérealière de 1987 en Afrique de l'ouest", GIEWS, 16 November 1987, report W/S5988.

16. Sivakuman, M.V.K., and J. Gnoumou Agroclimatology of West Africa, Burkina Faso, ICRISAT Information bulletin No. 23, (Andra Pradesh, India, 1987) pp. 192.

17. Hielkema, *op. cit*.

18. Holben, B.N. "Characteristics of maximum value composite Images From Temporal AVHRR Data," *International Journal of Remote Sensing* Vol. 11, No. 8, (1990) pp. 1511-1520.

19. van Dijk, A., *op. cit*. *et. al*.

20. Azzali, S. "Analysis of crop production in Zambia with the help of remote sensing, meteorological data and mathematical models", ICW nota 1907, (Wageningen, Netherlands, 1988) pp. 43.

21. Valenzuela, C.R. and M. Meijering "Aerospace Imagery and Geo-information systems for Watershed Management", *5th Int. Soil Conservation Conference*, Bangkok (1988).

22. Masialeti, I. The Use of ARTEMIS-Vegetation Index NDVI Data for monitoring land cover dynamics and yields in the Southern Province, Zambia. MSc-thesis ITC (1990) pp. 785.

23. Kowal, J.M. and Kassam, A.H. Agricultural Ecology of Savanna - a Study of West Africa. (University Oxford Press, 1978) pp. 403.

24. Henricksen, B.L. and J.W. Durkin. Moisture availability, cropping period and the prospects for early warning of famine in Ethiopia, *ILCA Bulletin*, Vol. 21 (1985), pp. 9.

25. Henricksen, B.L., and J.W. Durkin. "Estimating Vegetation Growing Periods in Africa using Meteorological Satellites; *Outlook on Agriculture*", Vol. 16, No. 4 (1987), pp. 160-166.

26. Kerr, Y.H., Imbernon, J. et al. "NOAA-AVHRR and Its Use for Rainfall and Evapotranspiration Monitoring, *International Journal of Remote Sensing 10*,No. 4 and 5 (1989), pp. 847-857.

27. Ahlcrona, E. "Remote sensing with Ancillary Data for Land Degradation Studies in Central Sudan," *Proc. 20th International Symposium on Remote Sensing of the Environment*, Nairobi, Kenya, (1986) pp. 127-139.

28. Mellaart, E.A.R. "Stimulations des effects de la variabilite de la disponibilite hydrique en fonction de la pluviosite sur la production de sorgho et de mil," Report project AGRISK, Ouagadougou, Groningen (1988), pp. 75.

29. Henricksen and Durkin, op. cit. (1987).

30. CILSS-PDP/Min. Agric. Niger "La collecte et le traitement des informations nécessaires au suivi de la stratégie alimentaire", Atélier (Niamey, Niger, 1986) pp. 20.

31. Holben, B.N., Y.J. Kaufman and J.D. Kendall "NOAA-11 AVHRR Visible and Near-IR Inflight Calibration", International Journal of Remote Sensing, Vol. 11, No. 8 (1990), pp. 1511-1520.

32. Ibid.

REMOTE SENSING FOR RURAL WATER SUPPLY IN INDIA*

M.G. Chandrasekhar, A.K. Gupta, J. Krishnamurthy,
P.P. Nageswara Rao
Indian Space Research Organisation Headquarters
Bangalore, India

INTRODUCTION

The amount of fresh water that is more or less readily available on land is less than 3 per cent of the total amount of terrestrial water. The terrestrial surface water comprises less than 0.15 million km^3/(0.25 per cent) and the rest is all underground water. These water sources in principle should be adequate to meet foreseeable human needs on this planet. However, the uneven distribution of these water resources combined with the explosive growth of population, the increase in demand for agriculture and industry and rapid urbanization in developing countries has resulted in the severe scarcity of freshwater availability in many areas. As a 1989 United Nations Children Education Fund (UNICEF) study revealed, "over 800 million people in developing countries live without access to a safe potable water supply and 1.8 million lack adequate sanitation services." In many developing countries, nearly 35 per cent of the people do not have easy access to drinking water.

India receives annually an estimated precipitation of about 400 million hectares metres (M ha m), of which about 70 M ha m is lost to the atmosphere as evaporation and about 115 M ha m flows as surface runoff. Of the remaining 215 M ha m that soaks to the ground, about 165 M ha m is retained as soil moisture allowing 50 M ha m to be stored as groundwater. In addition, lateral seepage of 5 M ha m from irrigation systems and 30 M ha m from rivers and streams together constitute about 85 M ha m of ground water. As per the estimates by the Indian Central Groundwater Board, India's annual exploitable groundwater potential is about 42.3 M ha m. At present, the groundwater utilization in the country is about 13.5 M ha m of which 85 to 90 per cent is used for irrigation and the remainder is used for other purposes.

---

* This paper, which was presented at the United Nations/ International Astronautical Federation and the Government of Canada Workshop on Space Technologies for Development, 2-5 October 1991, Montreal, Canada, does not necessarily reflect the views of the United Nations.

Notwithstanding this fact, due to uneven distribution in space and time of these water resources, there have been about 165,000 villages without adequate supply of potable water since the 1980s in India.

The majority of the minor irrigation programmes in rural India are achieved through groundwater development. Groundwater systems provide an instant and reliable source of irrigation. Nearly 50 per cent of the cropped area under irrigation (68 million hectares) is irrigated through groundwater. This dependence of groundwater became a necessity owing to the high cost and long time required to construct major irrigation projects and dams, as well as from environmental considerations. Thus, there is a constant increase in the demand for groundwater resources.

A closer look at the groundwater development indicates that: (a) there are areas where groundwater development has already attained a maximum; (b) there are areas endowed with high ground water potential but the utilization has remained at a low level; (c) even in most of the drought-prone areas, ground water development and utilization has not been commensurate with natural replenishment potential (recharge); (d) there are areas where the ground water has declined and sea water ingress has taken place in coastal areas due to overexploitation of ground water. It is in this context that scientific methods of source finding and optimum utilization of this resource for meeting the rural water supply needs became very relevant.

India has made great strides in using the sophisticated remote sensing technology for rural development. Even with the relatively modest investment made, the nation has established a self-reliant base in this technology, which is now playing a crucial role in the management of natural resources. India is developing space and ground segments indigenously as well as the necessary expertise and infrastructure for implementing various remote sensing application projects.

Remote sensing applications in India, under the umbrella of the National Natural Resources Management System (NNRMS), cover diverse fields such as agricultural crop acreage and yield estimation, drought warning and assessment, mapping and damage assessment of flood-affected areas, mapping for agro-climatic planning, waste management and water resources management. Thus, it touches almost all facets of national development. Active involvement of the users in the government ministries and departments, including both Central and State, has ensured effective harnessing of this technology in solving problems relevant to the country.

APPLICATION OF REMOTE SENSING IN GROUNDWATER EXPLORATION

Groundwater occurrence

Groundwater holding capacity and yield of hard-rock terrain depends on compactness of rocks. Compactness in turn depends on presence of pore spaces within rocks (porosity) and their interconnectedness (permeability), which is enhanced by the presence of weak planes (fractures, joints, rock contacts, shear zones, etc.) and weathering of rocks. Groundwater movement within rocks and sediments is controlled by permeability of the rocks, and geological structures. Groundwater occurrence in the semi-consolidated sandstone formations and unconsolidated alluvial plains is determined by the porosity and permeability. Remote sensing techniques provide a synoptic view of the interactions of physiographic and hydrogeological factors contolling the occurrence and movement of groundwater. One of the advantages of using remote sensing techniques is that certain features which are often missed in ground surveys, for want of a synoptic view, could be easily identified.

Remote sensing satellites such as Landsat, the Indian Remote Sensing Satellite (IRS) and the Système Probatoire l'Observation de la Terre (SPOT) have been extensively used in the survey and exploration of water resources. Sometimes information is supplemented by aerial photos. Hydrogeologists have explored various spatial and spectral data offered by these satellites in addition to microwave regional and thermal remote sensing data (10.3 - 12.5 micrometer region) for differentiating the moist from the dry lineaments.

Scale and resolution of satellite data

The scale of satellite data for mapping of groundwater-related features depends on the degree of details required on various factors controlling the occurrence of groundwater. Whereas small scales (1:250,000 or 1:125,000) have been found useful for regional scale mapping of groundwater features, the 1:50,000 scale has been found suitable for detailed mapping and ground follow up of the identified groundwater prospective zones for further developing. Mapping on a 1:50,000 scale has, however, been found to be about 8-10 times (Rs.25 per sq. km.) which costs more than mapping 1:250,000 (Rs.2.70 per sq. km.) or 1:125,000 (Rs.3.67 per sq.km.) scales and is also equally time consuming. 1/ Low resolution satellite data was found suitable in mapping of ground water features at a regional scale (1:250,000 and 1:125,000 scales) while higher resolution data have been found adequate to map the potential groundwater zones at a 1:50,000 scale. However, the use of high- resolution data (20-40 m) for small scale (1:250,000/1:125,000) mapping provided more details that are not seen on low resolution remotely sensed data (70-80 m) on the same scale.

Image interpretation and data analysis

Inferences regarding the occurrence of groundwater are derived by identifying the hydrogeomorphological features on the satellite images or aerial photographs through visual interpretation and digital analysis. Various visual interpretation elements such as tone, texture, pattern and association are used in identification and delineation of various surface expressions which are indicative of groundwater occurrence. Using these techniques groundwater prospective zone maps of all of India have been prepared on a 1:250,000 scale. Image processing technqiues such as filtering, linear stretching, rationing, principal component analysis, band combination, specific colour composites, etc., are useful for extracting the various groundwater related features. A flow chart of methodology adopted for ground water exploration is given in figure 1.

The approach used involved stratification of the prospective zones into relative groundwater yield potential areas/zones (viz., Excellent, Good, Moderate, Poor, Nil) with likely yields assigned to each of the prospective zones based on the ground data. This stratification is supported by information on drainage, topography, landforms (geomorphology), rock types and their composition and compactness, nature of aquifers (weathered, fractured, jointed, etc.) through which the groundwater moves, weathering status of rocks, presence of geological structures (lineaments, fractures, faults, joints, shear zones, intersection of lineaments, sink-holes, etc.), annual recharge, rainfall status, nature of soils (sandy, clayey, loamey, etc.), hydrologic characteristics of rocks such as porosity, permeability, grain sizes, etc. The presence of anomalies indicative of groundwater, such as vegetation, fracture pattern, lineament intersection, cut-off meanders, sand bars, burried paleochannels, abandoned channels and valley fill, are identified.

National Drinking Water Mission

The experience gained in the use of remote sensing for groundwater resource development prompted the Government of India to adopt this technology for scientific source finding of groundwater under the National Technology Mission on Drinking Water. This mission is aimed at providing 40 litres per capita per day (lpcpd) of potable water (with an additional 30 lpcpd for cattle in desert areas). The water should be available within a distance of 1.6 km from the village for about 1.62 lakh problem villages where potable water in adequate quantity or of acceptable quality was not available. The approach adopted had three components, viz.: (i) remote sensing based investigation; (ii) conventional hydrogeological investigation, and (iii) ground geophysical investigation. A combination of all three led to identification of an aquifer. For the first time, the entire country was mapped on a 1:250,000 scale for groundwater potential zones using satellite data, and the maps are being used by the concerned state government agencies for further exploitation of groundwater resources. The approach for development of drinking water sources is shown in figure 2.

Success rate of borewells

Comparison observations have shown that groundwater prospect maps prepared using remote sensing methods, having success rates of locating borewells with good yield have gone up to about 90 per cent, as against 45 to 55 percent achieved using conventional methods alone. This feedback was received through many state governments and the Directorate of the National Drinking Water Mission. The success rates of wells drilled in different states (see table 2) have thus proved the capability of satellite remote sensing as a scientific source location methodology for groundwater exploration.

Time and cost effectiveness of remote sensing technology

Information contained in groundwater potential zone maps prepared from remote sensing methods has been very useful in narrowing down the target areas for groundwater exploration in a given region. Detailed hydrogeological and geophysical investigations on the ground are carried out based on information extracted from these maps/satellite data. This approach significantly saved time and money for ground water exploration. Use of groundwater potential zone maps along with the conventional system of locating well sites has resulted in a very high success rate in locating wells with good yield. Experience has shown that remote sensing surveys are about 10 times faster and cheaper than the conventional groundwater surveys.

Site location for water harvesting structures

Apart from mapping of Groundwater Prospect Zones, remote sensing has been found highly successful in the location of favourable areas for water harvesting structures such as check dams, anicuts, subsurface dikes, percolation/recharge tanks and inverted wells, etc., for augmenting the groundwater recharge. Sites for water harvesting structures have been located with the help of remote sensing imagery in several states under the National Drinking Water Mission.

Role of remote sensing in conjunctive use of surface and ground water

Conjunctive use of surface and groundwaters is fast emerging as an important water management issue, since several of the existing irrigation projects suffer from inadequate supplies. It has been observed that the available supply in many of the canal systems is one fourth to one third the amount equidistant for intensive agriculture; nor is it supplied satisfactorily in time. Moreover, neglect of the groundwater component in irrigation planning is one of the main causes of waterlogging and the attendant problems of salinity in the command areas (as it causes the water table rise in the process bringing up the subsoil salts). Therefore, conjunctive use of both the surface and groundwater resources is of the utmost importance to avert water abuse, to make optimum use of available water resources and avert problems caused due to mismanagement of water resources such as waterlogging, fall of the groundwater table, salinity/alkalinity of soils, salinization of aquifers in coastal zones, etc.

WATER MANAGEMENT IN COMMAND AREAS

Nearly 80 per cent of rural water needs are for irrigation of agricultural crops. Most of the green revolution in the developing countries is essentially due to the increase in irrigated area. Notwithstanding the fact that the majority of the irrigation projects have brought tremendous prosperity, the associated problems of salinity/alkalinity, waterlogging, etc., call for a scientific approach to the management of these water resources. Remote sensing technology can play a useful complementary role in managing the land and water resources of command areas to maximize production.

Reservoir operational and storage assessment

By combining the waterspread area of a reservoir obtained from satellite data with the area-storage curve of the reservoir, the storage volume may be estimated. This information, together with the crop types and acreage information, is used to develop reservoir optimization models for determining the reservoir operating schedules. Repetitive coverage permits estimation of volume change in reservoir storage during the crop growing period. Quantitative estimates of demand and supply enable determination of a number of irrigation schedules possible from the reservoir (see figure 3).

Irrigation scheduling

Management of water supplies for irrigation in command areas is an essential component in increasing agricultural production and efficient water use management. The usefulness of remote sensing techniques in making an inventory of irrigated lands and identifying of crop types, including their extent and condition and production estimation, has been demonstrated in various investigations 2/ 3/.

Multi-date satellite data was used to inventory a surface water tank water spread area, irrigated cropland and their acreage. A water tank inventory was conducted of Araniar-Kortaliyar basin of Tamil Nadu using aerial photographs on 1:60,000 scale. Water spread areas, cropland and catchment areas of tanks were estimated and compared with those of conventional data.

Irrigation requirements of crops are determined by assessing the soil moisture and crop condition over an area so that the crop water demand can be estimated and irrigation scheduling planned accordingly. The measurement of canopy temperature and spectral reflectance of the crops through remote sensing techniques is an indirect method of assessing the plant stress. Studies on crop canopy temperature and spectral indices revealed that estimates of leaf area index (LAI) as well as evapotranspiration could be integrated into irrigation scheduling programmes. Microwave remote sensing would be useful for the detection of soil moisture 4/. It has been found that the scattering coefficient for microwave radar could be related to soil moisture, crop classification and plant moisture.

INTEGRATED LAND AND WATER RESOURCES STUDIES

A unique area where satellite remote sensing has been effectivey utilized for resource management is in surveys for rural development. It is ideally suited to bring out the inter-relationships of various disciplines. These surveys involve preparation of a set of resource maps using remotely sensed data, such as surface water bodies, groundwater potential zones, zones requiring groundwater recharge, types of soil, salinity/alkalinity and erosion status, existing land use and distribution of wastelands, etc. Based on these maps, an integrated land and water resource map, highlighting priority areas for agriculture development, fuel and fodder development, soil conservation and afforestation, etc., is prepared in order to arrive at a package of practices and strategies to address the local problems at the village/tehsil/district level.

Making use of such surveys, strategies can thus be worked out for ensuring all round development of vast rural areas of the country without upsetting the ecological balance. This integrated approach has been effectively used in India for combating/mitigating the effects of drought. Integrated resource maps are being prepared to assist in optimum management of land and water resources in drought-prone districts of India.

USE OF GIS IN THE MANAGEMENT OF WATER RESOURCES

The Geographic Information System (GIS) is an important tool for efficient storage retrieval, analysis and presentation of geographical data. This technology has tremendous potential in almost every discipline concerned with spatial information management. GIS is emerging as an important technology for natural resources management in India. As part of NRIS, under NNRMS (National Natural Resources Management System), several GIS projects in specific resources management areas, viz., wasteland development, hill area development planning, land use planning, district level planning, groundwater development and environmental management of watersheds have been taken up.

A pilot study for a wasteland development programme carried out by the Space Applications Centre (SAC) in parts of the Palitana taluka in the Bhavnagar district of Gujarat yielded encouraging results on the socio-economic aspects, fodder requirements of (village-wise) and identification of wastelands for the purpose of agricultural development. Work done in these projects and experience gained are indicative of the fact that GIS is rapidly becoming one of the most useful and powerful analytical tools of resource planners and managers.

One of the GIS projects specific to water resources development has been taken up for the Subarnrekha River Basin, for the development of water resources on a regional scale. GIS will also be applicable to the micro and detailed level of water management. The project involves planning for water resources development, sharing of water by riparian states, regional economy, environmental management, watershed management, watershed prioritization, water quality assessment, flood monitoring and site location for dairy and poultry development.

In addition to spatial data provided by remote sensing socio-economic and meteorological data are integrated using GIS techniques. GIS is being used in carrying out locale-specific packages of practices to provide better management of water resources in drought-prone areas such as identification of sites for groundwater recharge, rainwater, harvesting, etc.

FUTURE THRUST AREAS

The future research areas in the field of remote sensing of groundwater will require the development of remote sensing models for prediction of groundwater depth and yield. Hydrogeological medels are being developed for quantifying the groundwater yields. Such models are based on correlations between various parameters that govern the groundwater regime. The zones identified using remote sensing data are correlated with well yield data available from the wells already existing in the area. Yield test/pump test data of borewells with a minimum density of at least one well in every 50 sq. km. is being used in developing the model.

Efforts have been made to quantify the likely yield of the groundwater prospect zones delineated from space imagery 5/. Efforts are being made by the Department of Space for depth-yield estimation of groundwater prospect zones by combining remote sensing information with the well data. Other recent areas include the use of artificial intelligence for groundwater prospect zone mapping, depth-yield estimation and the use of GIS for optimum management of groundwater resources.

Several studies have been made using images in the thermal infrared and microwave (radar) region, indicating the usefulness of these spectral regions for geological and groundwater applications. Estimation of groundwater quality, especially salinity, of aquifers from remote sensing is yet another important area of research. Also, salinization of aquifers is a common problem in coastal areas.

CONCLUSION

In India, remote sensing has been successfully used to provide information on groundwater potential zones of the country and to meet the supply requirements for drinking water of the rural population. The use of remote sensing for mapping of groundwater potential zone as part of National Drinking Water Mission has resulted in considerable time and cost saving. The groundwater potential zone mapping has been completed in a record time of one year for the entire country on 1:250,000 scale using satellite data. The maps prepared from remote sensing have been effectively used to locate high yielding groundwater sources for further development by respective state governments. Use of maps (prepared from interpretation of remote sensing data) has shown about a 90 per cent success rate of borewells, as against about 45-50 per cent achieved conventionally. The success story of the use of remote sensing for ground water mapping and surface water monitoring to meet rural water demand in India is very relevant in the context of using remote sensing for rural development. Methodologies developed for watershed prioritization, integrated resources development at the micro level and crop production forecasting and command area water management are equally important for developing nations.

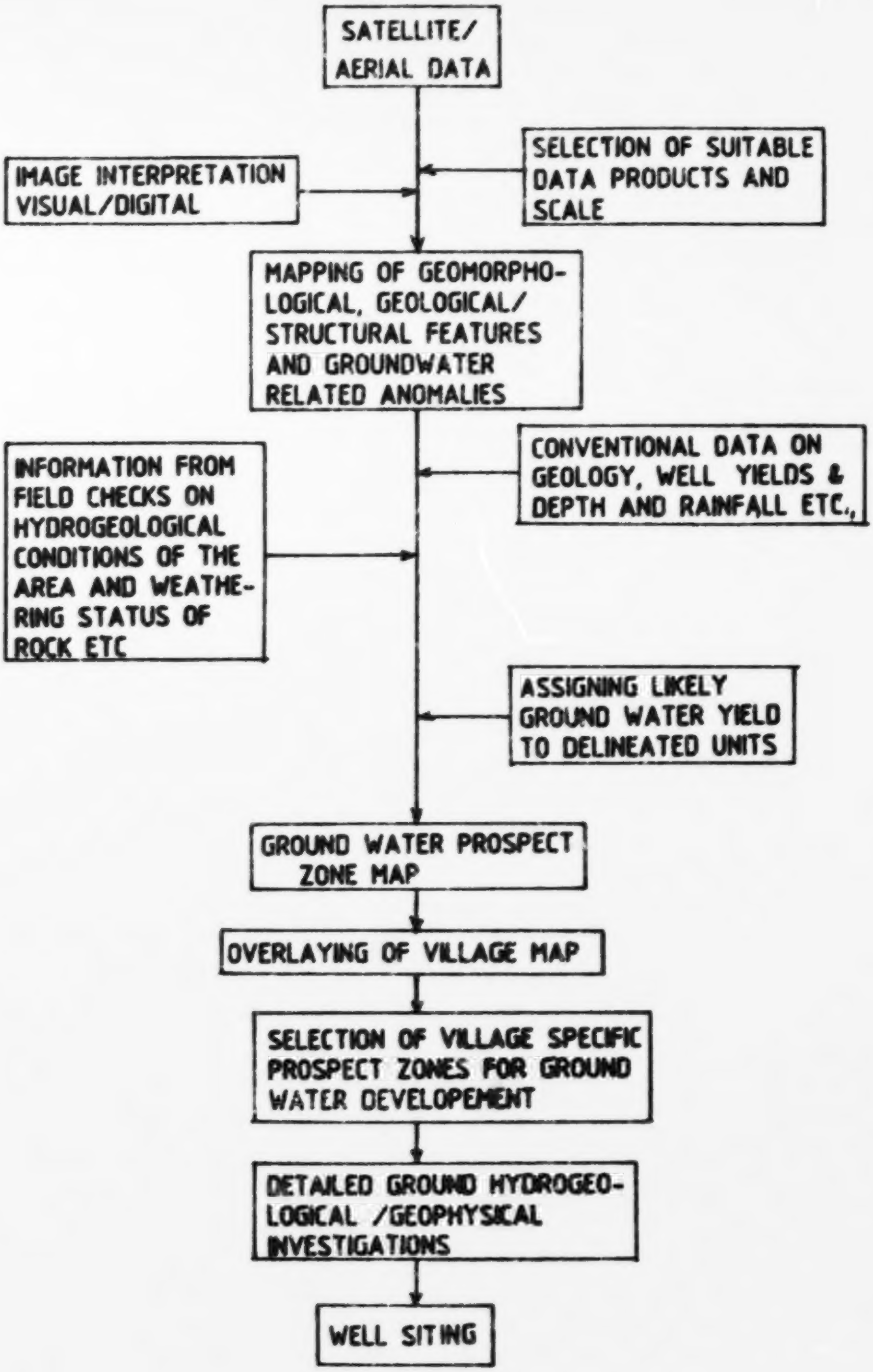
SATELLITE/ AERIAL DATA
IMAGE INTERPRETATION VISUAL/DIGITAL
SELECTION OF SUITABLE DATA PRODUCTS AND SCALE
MAPPING OF GEOMORPHOLOGICAL, GEOLOGICAL/ STRUCTURAL FEATURES AND GROUNDWATER RELATED ANOMALIES
INFORMATION FROM FIELD CHECKS ON HYDROGEOLOGICAL CONDITIONS OF THE AREA AND WEATHERING STATUS OF ROCK ETC
CONVENTIONAL DATA ON GEOLOGY, WELL YIELDS & DEPTH AND RAINFALL ETC.,
ASSIGNING LIKELY GROUND WATER YIELD TO DELINEATED UNITS
GROUND WATER PROSPECT ZONE MAP
OVERLAYING OF VILLAGE MAP
SELECTION OF VILLAGE SPECIFIC PROSPECT ZONES FOR GROUND WATER DEVELOPEMENT
DETAILED GROUND HYDROGEOLOGICAL /GEOPHYSICAL INVESTIGATIONS
WELL SITING

GROUND WATER PROSPECT ZONE MAPPING THROUGH REMOTE SENSING FOR RURAL WATER SUPPLY

Figure-1

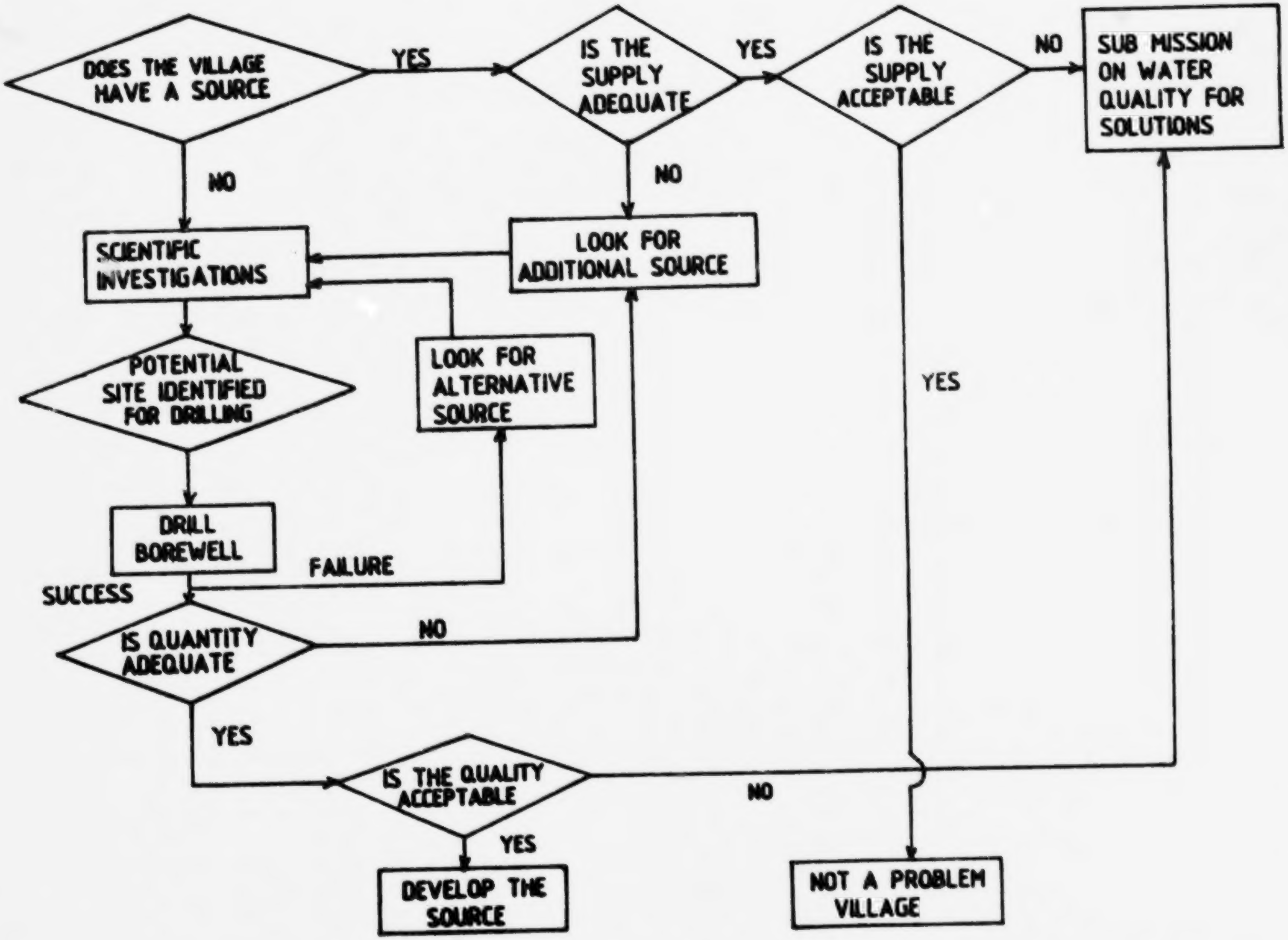
DOES THE VILLAGE HAVE A SOURCE
YES
IS THE SUPPLY ADEQUATE
YES
IS THE SUPPLY ACCEPTABLE
NO
SUB MISSION ON WATER QUALITY FOR SOLUTIONS
NO
NO
SCIENTIFIC INVESTIGATIONS
LOOK FOR ADDITIONAL SOURCE
POTENTIAL SITE IDENTIFIED FOR DRILLING
LOOK FOR ALTERNATIVE SOURCE
YES
DRILL BOREWELL
FAILURE
SUCCESS
IS QUANTITY ADEQUATE
NO
YES
IS THE QUALITY ACCEPTABLE
NO
YES
DEVELOP THE SOURCE
NOT A PROBLEM VILLAGE

FIGURE 2 : **Flow chart of village wise activities for development of drinking water sources**

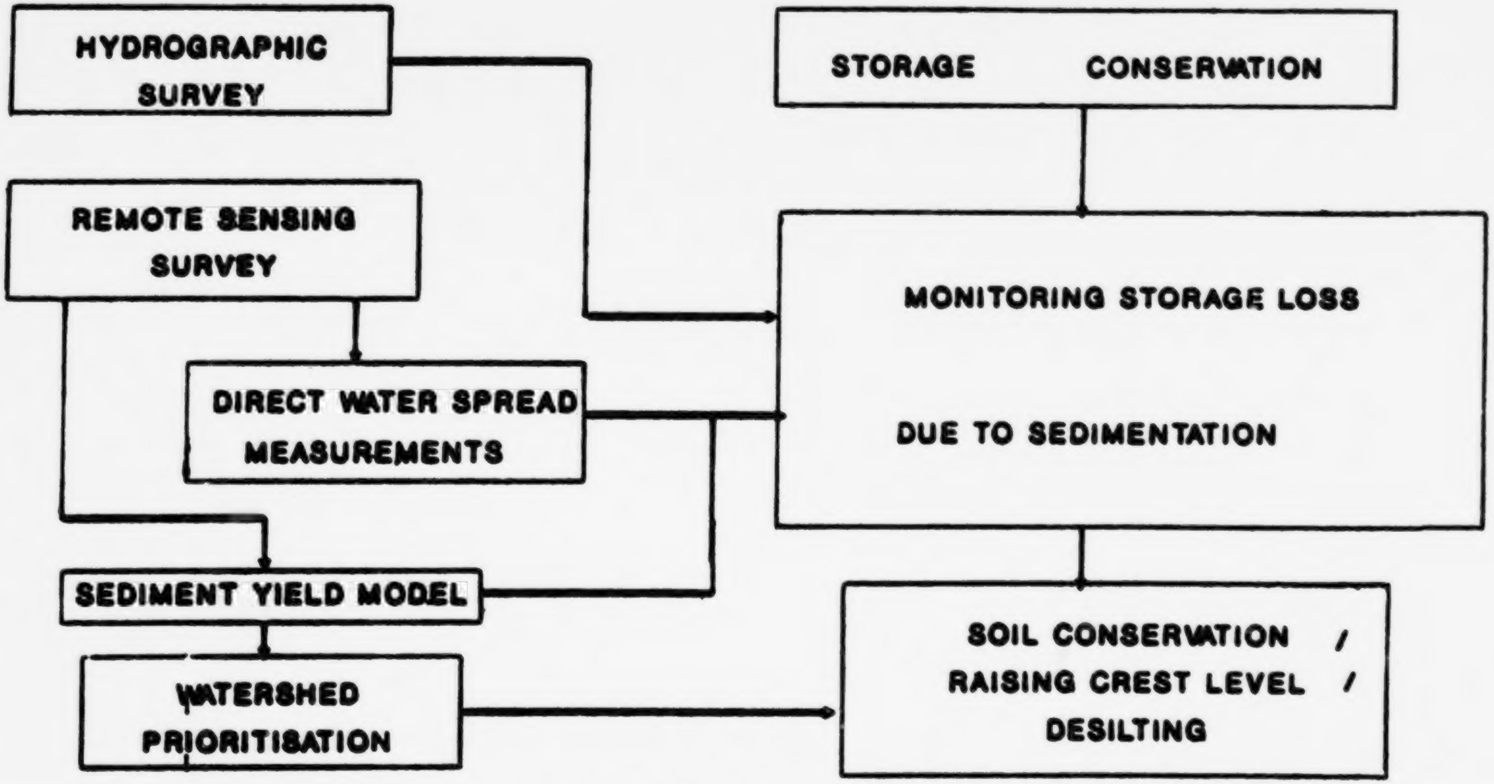
HYDROGRAPHIC SURVEY
REMOTE SENSING SURVEY
DIRECT WATER SPREAD MEASUREMENTS
SEDIMENT YIELD MODEL
WATERSHED PRIORITISATION
STORAGE CONSERVATION
MONITORING STORAGE LOSS
DUE TO SEDIMENTATION
SOIL CONSERVATION /
RAISING CREST LEVEL /
DESILTING

RESERVOIR STORAGE LOSS ESTIMATION AND CONSERVATION

FIGURE-3

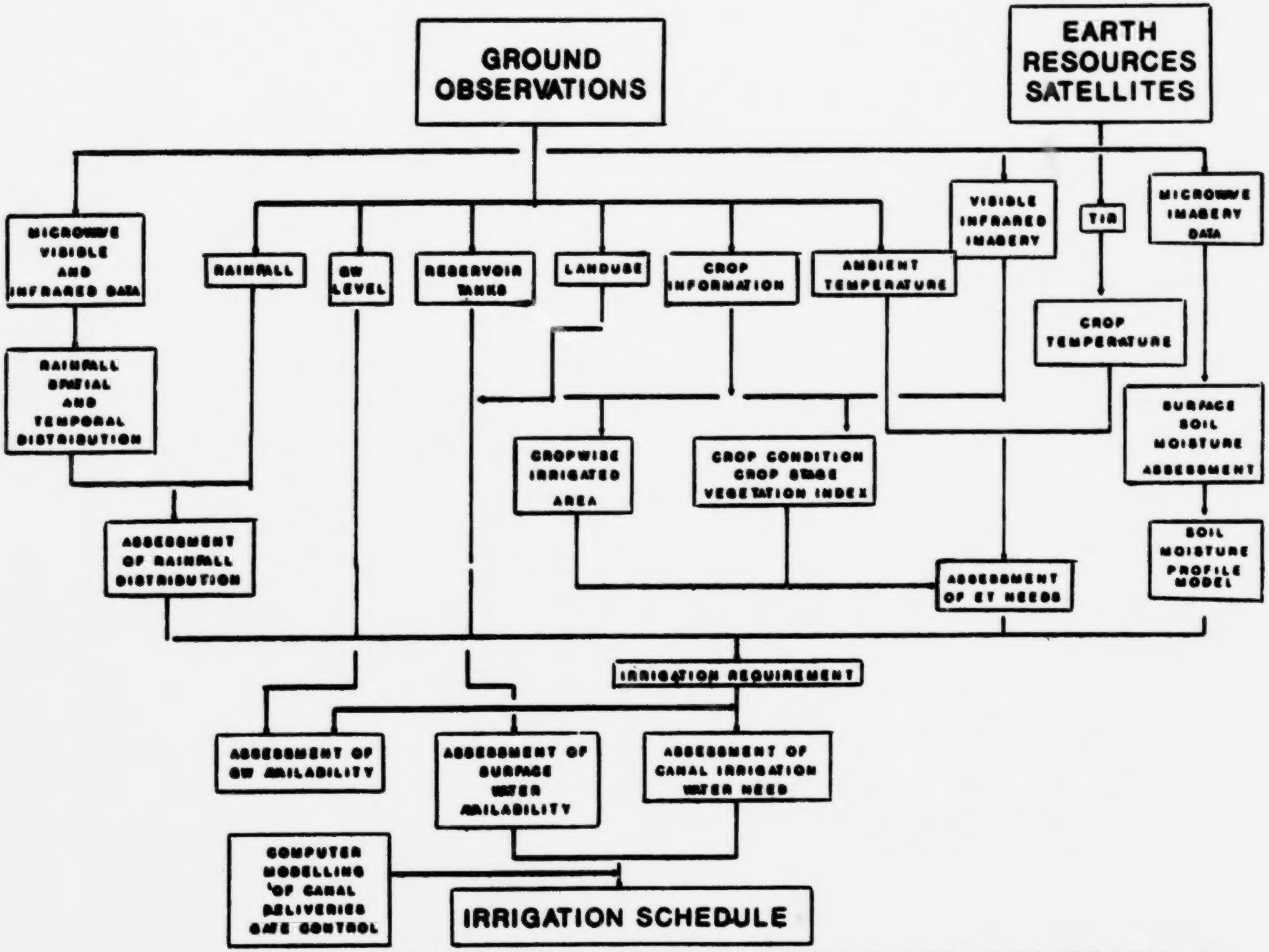
GROUND OBSERVATIONS
EARTH RESOURCES SATELLITES
MICROWAVE VISIBLE AND INFRARED DATA
RAINFALL
GW LEVEL
RESERVOIR TANKS
LANDUSE
CROP INFORMATION
AMBIENT TEMPERATURE
VISIBLE INFRARED IMAGERY
TIR
MICROWAVE IMAGERY DATA
CROP TEMPERATURE
RAINFALL SPATIAL AND TEMPORAL DISTRIBUTION
CROPWISE IRRIGATED AREA
CROP CONDITION CROP STAGE VEGETATION INDEX
SURFACE SOIL MOISTURE ASSESSMENT
SOIL MOISTURE PROFILE MODEL
ASSESSMENT OF RAINFALL DISTRIBUTION
ASSESSMENT OF ET NEEDS
IRRIGATION REQUIREMENT
ASSESSMENT OF GW AVAILABILITY
ASSESSMENT OF SURFACE WATER AVAILABILITY
ASSESSMENT OF CANAL IRRIGATION WATER NEED
COMPUTER MODELLING OF CANAL DELIVERIES GATE CONTROL
IRRIGATION SCHEDULE

ROLE OF REMOTE SENSING IN IRRIGATION SCHEDULING

FIGURE-4

Table-1: Statistics on success rates of borewells

Sl. No.	State	Total No. of Bores drilled	Total No. of Successful bores	% Success
01	Gujarat	13667	12912	94.47
02	Rajasthan	116	108	93.10
03	Orissa	136	134	98.53
04	Andhra Pradesh	216	169	78.24
05	Bihar	1044	951	91.09
06	Goa	628	560	89.17
07	Karnataka	397	288	72.54
08	Madhya Pradesh	290	282	87.24
09	Meghalaya	112	99	86.39
10	Uttar Pradesh	437	421	96.33
	Total	17043	15924	93.43

NOTES

1. Nagesware Rao, P.P., Jayaraman V. and Chandrasekhar, M.G. "The Economics of Remote Sensing for Natural Resources and Environment Development projects: an Indian perspective". The Economics of Remote Sensing, Economic and Social Commission for Asia and the Pacific (ESCAP)/United Nations Development Programme (UNDP) Regional Remote Sensing Programme, ST/ESCAP, (1990(a)), pp. 992.

2. Thiruvengadachari. Photogrammetric Engineering and Remote Sensing, vol. 48, No. 10 (1981), pp. 1493-1499.

3. Nageswara Rao, P.O., Mohankumar, A. and Chandrasekhar M.G. "Cropland inventory in the command area of Krishnarajsagar project using satellite data", Proc. National Symposium on Remote Sensing for agricultural applications (New Delhi, 6-8 December 1990), pp. 357-363.

4. Mohan S., Mehta V.S., Meta, R.L. et al. "Multifrequency microwave measurements of soil moisture" Proc. National Symposium on Remote Sensing for agricultural applications (New Delhi, 6-8 December 1990), pp. 357-363.

5. Gupta A.K. and Ganesh Raj, K. "Study of Groundwater Potential Zones of Pavagada taluk using Two Different Scales of Landsat TM Imagery and Borewell data", ISRO Technical Report No. ISRO NNRMS-TR-81-89.

THE GREAT IMPACT OF THE EDUCATIONAL SATELLITE SYSTEM IN CHINA*

Fuwen Gao
Institute of Modern Educational Technology
Beijing Normal University
Beijing, China

ABSTRACT

As a developing country, China has the goal of developing its industry, agriculture, science and technology and national defence. The Chinese Government, however, faces various problems in reaching this goal. Among its problems, the education of the Chinese people is the most important task, since on a vast scale education is the way to speed up the economic development of a country. The Chinese Government chose satellite television broadcasting to deliver educational programmes. So that a countrywide educational satellite system has been established in a very short period of time. The practice and experiences in China have proved that using a satellite can offer educational programmes to the people throughout China efficiently and rapidly. Through the promotion of education, the economics and society of China have been promoted significantly. Further applications of space technology are considered to offer integrated services in the rural areas. An interactive satellite education system is also under consideration.

INTRODUCTION

Due to the fact that China is a developing country with a huge population, the Chinese Government has been seeking methods to increase access to education. Correspondence study and radio broadcasting have been widely used since 1949, when the People's Republic of China was founded. The people who are working in government, schools and factories are allowed to study new laws, new policies, new technology, and new skills in the workplace. When television (TV) technology became available in the big cities in 1960, the earliest TV universities were established in Beijing, Shanghai and Shenyang. Courses in the natural sciences, engineering and the humanities were offered to primary and secondary school teachers and people working in industrial areas. Because there was only one TV channel per city at that time, courses were broadcast in the early morning and late at night. Students were urged to absorb knowledge, so they went to their workplace, the only place equipped with a TV set, to watch programmes at 5 am.

---

* This paper, which was presented at the United Nations/ International Astronautical Federation/Canada Workshop on the Space Technologies to Development, held in Montreal, Canada, 2-5 October 1991, does not necessarily represent the views of the United Nations.

In the late 1970s an evolutionary change began. The country attempted to modernize industry, agriculture, science and technology and national defence. Also, a new "open-door" policy to the world began to be implemented. In this new situation, great educational demands are being made of the Government and educators. After studying other countries' distance education programmes, such as the Applied Technology Satellite (ATS) educational programmes in the United States and India, the programmes of TV Ontario in Canada and Learn Alaska in the United States, the Government decided to build a satellite television based multimedia education system.

After only a few years, the largest distance education network in the world is running successfully. Students are taking courses every day. The impact of distance education on the development of China has been significant. Also, what happened in China is also very important for the entire world.

Demand for education in China

When China opened its door to the world, the gaps between the developing countries and the developed countries were recognized. We realized the need for economic, scientific and technologogical development to catch up to the advanced countries. Modernization of industry, agriculture, science and technology has become our goal. How to reach that goal, however, was the big question. Investing a lot of capital to import equipment, assembly lines and factories represented one method for modernization in a short time. But high technology cannot be imported so quickly. The people must have basic knowledge and skills to master the use of new machines. That is to say, we can buy modern equipment easily, but we cannot buy technological knowledge in the same way. We need to educate personnel to control new technology. Obviously, there is a link between education and social economic progress. Education on a vast scale is the way to bridge the gaps between China and the developed countries. First, education will be used to raise the cultural level and understanding of people and this in turn will stimulate their desire for modernization. Secondly, the knowledge and skills necessary to qualify personnel at various levels will be offered through different kinds of education. A highly skilled labour force will be prepared through education for production of advanced industry and agriculture.

But in a country like China, which has 1.2 billion people, the demand for education is so great that the traditional education cannot be expected to meet the needs. For example, according to the census of 1986, there are 8 million primary and secondary schoolteachers in China. Three million of them are not qualified. These teachers should be retrained first, because the quality of the school depends mainly on them. There are not, however, enough places for these teachers in traditional universities. Also, because these teachers are the only available people in their respective areas to teach, they cannot leave school to study. Even if they could enter a university, it would take too long to finish their studies, and students would be left without teachers. Distance education appears to be the only available solution to this problem.

Satellite TV based multimedia education system

In 1986, the first satellite TV channel began offering education at a distance. Since then a satellite TV education-based multimedia distance education system has written a new chapter in the history of Chinese education.

Different kinds of media are used in distance education in the world, but it was necessary to analyse which one was most suitable for our situation. The media should be made easily available and convenient for teachers and students. In our case, 1 billion people are distributed in an area of about 9.6 million square kilometres. About 80 per cent of the territory is mountain and desert. The farthest distance from east to west or from north to south is as much as 5,000 kilometres. Transportation in remote areas, mountain regions, islands and deserts is poor, and communication is difficult. There is no telephone, television or mail service. It is also difficult to establish cable, microwave trunk or television stations there. Satellite TV broadcasting is an ideal medium to overcome the difficulty in delivering programmes directly to the learners located all over the distance education system based on satellite transmission. Taking advantage of the social system, the Chinese Government devoted considerable effort, money, materials and human resources to make television education available.

The project was planned to have three phases. In the first phase, a series of pilot programmes for distance education was carried out by leasing and purchasing transponders from the INTELSAT. The success in the programmes has shown that a 6-meter antenna for a C-band TV receiving Earth station can meet the requirement of television relaying on the condition of the hemispheric beam transponder of International Telecommunications

Satellite Organization (INTELSAT). Four-metre antennas, even three meter antennas can still meet the needs of TV transmission for signal quality when they use a domestic coverage beam. This has resulted in promoting greatly the development of a ground network. China has mature techniques to produce lower cost Earth stations for educational uses. In the second phase, China's communications satellite was made and launched. This satellite is complemented by the leased and purchased transponders. A second Chinese-made communication satellite with 24 transponders will be launched to form the domestic satellite communication system. Additional channels will be devoted to distance education. The Chinese Government provides a space segment for distance education continuously and increasingly.

The whole satellite delivery system is a hierarchical structure. At the highest level, the State Educational Commission has established the China Education TV (CETV) Station, which is responsible for editing and broadcasting educational programmes that use a satellite. Cooperating with the Post and Telecommunications Ministry, CETV manipulates an Earth station to up-link programmes into INTELSAT V and CHINASAT. These satellites cover all of China and some countries in South-East Asia, such as Thailand and Myanmar. Every day the two channels broadcast for 31 hours in total. The rest of the broadcast day is shared by provincial educational stations that broadcast their own programmes.

At the local level of the delivery system, TV relay stations are built in big cities and population centres. People can receive programmes using their TV sets at their workshops and at home. Because of the country's varied geography, it is more efficient to build many TV relay stations with small transmitting power rather than fewer stations with great power. Television receiving only (TVRO) Earth stations are widely used in small towns, villages or organizations and schools. Usually these stations are equipped with video cassette recorders. Programmes are recorded for later viewing or for delivery to learning centres. Print materials, including textbooks, reference books, and study guides, are combined with videotapes to form a learning package.

At the bottom lowest of the delivery system are the learning centres, which provide the study places, where people gather together to watch tapes if they do not have access to a TVRO. There they meet tutors and classmates to discuss their lessons. They have opportunities to ask for clarification and explanation of material covered in the TV programmes. For some courses, tutorials are also used for assigning and correcting homework and for assigning projects for which credit is given.

By the end of 1990, the delivery system had broadcast 36,000 hours of educational programmes through two TV channels. More than 600 TV relay stations and 4,000 TVRO stations have been set up in 29 provinces. About 20 million people view educational programmes or take courses either at home or at 30,000 learning centres.

Administrative system

The administrative system is also a hierarchical structure, with two parallel subsystems. China TV Normal College (CTVNC) and China Central Radio and TV University (CCRTVU) are at the highest level.

CTVNS's main task is primary and secondary school teacher retraining. Professional education is also included. CTVNC is responsible for formulating teaching guidelines, programme planning, adopting relevant regulations and rules and broadcasting lectures. It is also in charge of setting norms and standards for each category and level of students for organizing the production of teaching materials. CTVNC works in very close partnership with universities. CTVNC asks the university, with its high-quality video production team, video studios and better teachers, to produce video programmes. Outstanding teachers in secondary schools are invited to teach as good role models.

At the local level of the administrative system, the executive organizations of teacher training projects are the institutions and schools in provinces, counties and districts.

CCRTVU is at the apex of the second subsystem. It serves a radio and TV university providing a large number of people with access to higher education through distance education. Its responsibility included evaluating curricula, offering courses, producing syllabuses, offering reading materials, administering examinations and training teachers and administrative staffs.

There are 37 branch TV universities in provinces, autonomous regions and municipalities. A total of 1,550 work stations are located in all counties to organize students to study TV courses.

During the 10 years from 1978 to 1988, the TV University published 150 million copies of textbooks which are used to teach 300 courses in twenty-one specifications. The results include: 20,000 hours of video programming have been produced; 1.2 million students have graduated from CCRTVU, 37 per cent of the total number of graduates from traditional higher education. About three million people have taken continuing educational courses from CCRTVU.

CCRTVU has produced 10,000 hours of video programming. Over 1 million teachers are enrolled in courses and 1 million teachers watch teaching demonstration programmes. One million principals of primary and secondary schools attend workshops to update their administrative capabilities.

Contents of distance education in China

The first satellite TV broadcasting channel is used primarily for the delivery of training courses. When the second channel was added, professional, vocational and continuing education for adults became the three aspects of Chinese distance education programming.

Courses for teacher training are emphasized. Mathematics, physics, chemistry, history, geography, Chinese language and literature, physical training and English are offered. Students can select a group of courses which are closely related to their area of teaching. After two years, they can be qualified in one subject.

Teachers chosen from Beijing represent a good teaching model. Teachers and students in the remote areas watch the programmes and practice in their classes what is demonstrated.

The State Education Commission has organized training courses to train the principals of primary and secondary schools. They study educational policy, evaluation methods and administration methods, etc. There are 120 million young people who have finished school and returned home to work. They need to study literature and to learn new technology to improve the country's production and economic development.

Channel II offers courses, lectures and video programmes to teach science and technology in agriculture. The programmes are interesting, easy to understand and of relevance to actual agricultural problems. A wide variety of continuing education courses are offered in engineering, including computer programming, electronics, graphics, mechanical, chemical, civil and architectural engineering (advanced computer technology courses are taught on weekends). There are also courses in economics and administration, such as business, accounting, statistics, finances and taxation and banking. CCRTVU also offers a continuing education programme for engineers.

Impact of distant education on the development of China

Over a few years the scale of distance education in China has expanded considerably and its impact on the development of China has been tremendous. Distance education offers the Chinese people access to educational opportunities, which have raised their levels of literacy and updated their skills. They have become more knowledgeable and qualified. Therefore, the levels of the economy, literature, industry and agriculture have been raised.

Due to the fact that more people have recognized that distance education is an efficient way to develop society, more money is being spent to establish TV relay stations or TVRO stations. Usually, in a developing country backwardness of education leads to an underdeveloped economy, which leads to backwardness of education; it is a vicious circle. But now this pattern is changing. We see a bright future for education in China.

During the period of eighth five-year plan, one more satellite TV channel will be dedicated to primary and secondary students. More TV relay stations will be established so that 70 per cent of the areas in all counties will be covered. The distance education system will be set up so as to be completely supplemented by correspondence education, radio and TV education. We now are thinking of ways to build and to integrate the satellite system for the rural areas in China, which will include offering better education opportunities for school students and adults, and improving the communications between these areas and big cities. An interactive tele-teaching and teleconferencing system using space technology is also research phase.

The education system has a great impact on the development of the economy, literature and society of China. We are sure that the more space technology we use, the more progess we will have.

OPERATIONAL ENVIRONMENTAL SATELLITE REMOTE SENSING FOR FOOD SECURITY AND LOCUST CONTROL BY FAO*

THE ARTEMIS AND DIANA SYSTEMS

Jelle U. Hielkema
Senior Remote Sensing Officer (Environmental Monitoring)
FAO Remote Sensing Centre
Rome, Italy

INTRODUCTION

Since 1975, the Food and Agriculture Organization of the United Nations (FAO) has been pioneering the developing of the use of satellite remote sensing techniques for improving the surveillance and foreccasting capabilities of FAO's Global Information and Early Warning System (GIEWS) on the Food and Agriculture and Centralized Desert Locust Reporting and Forecasting Service at its headquarters, as well as those of related organizations at the regional and national levels, primarily in Africa.

On the basis of findings from experimental activities on the use of Landsat, National Oceanic and Atmospheric Administration (NOAA) and Meteosat satellite data for vegetation monitoring and precipitation assessment, FAO defined an operational system for largely automated satellite environmental monitoring for the above programmes, based on the use of hourly Meteosat thermal infrared and daily NOAA Advanced Very High Resolution Radiometer (AVHRR) data covering Africa, the Near East and South West Asia. The system, the Africa Real Time Environmental Monitoring Information System (ARTEMIS), was developed as a result of close technical cooperation between the FAO Remote Sensing Centre, the FAO Global Information and Early Warning Service, Plant Protection Service, NASA Goddard Space Flight Center (GSFC), the universities of Reading and Bristol and the National Aerospace Laboratory (NLR) of the Netherlands, with financial assistance from the Government of the Netherlands through an FAO Trust Fund.

---

* This paper, which was presented at the United Nations International Training Course on Remote Sensing Applications for Environmental Assessment and Monitoring, Sioux Falls, South Dakota, United States, 9 September-4 October 1991, does not necessarily reflect the views of the United Nations.

The ARTEMIS system was installed in the FAO Remote Sensing Centre in Rome during August 1988 and has since then operationally generated an increasing number of information products on the occurrence of rainfall and vegetation development, on a 10-day and monthly basis, which are currently being used by a number of programmes at FAO headquarters by regional and national food security early warning and locust control organizations in the Intergovernmental Authority on Drought and Development (IGADD) (eastern Africa) and Southern African Development Coordination Conference (SADCC) (southern Africa) regions.

In order to make ARTEMIS output products and other relevant data available in a timely manner at regional and national levels, a dedicated satellite communications system, DIANA (Data and Information Available Now in Africa), is currently being developed by the European Space Agency (ESA) in cooperation with the FAO Remote Sensing Centre.

The DIANA system will, by early 1992, provide a capability for high-speed (64 kilobits/sec) two-way transfer of facsimile images of documents and maps, character-coded text documents and digital images in raw or processed form from computers at FAO headquarters to personal computer-based terminals of recipients, initially in Africa, by using the commercial International Telecommunications Satellite Organization (Intelsat) satellites through the facilities of Telespazio in Italy.

SATELLITE REMOTE SENSING SYSTEMS FOR FOOD SECURITY AND LOCUST CONTROL

The satellite systems carrying sensors with spectral, spatial, temporal and radiometric resolution characteristics suitable for precipitation and vegetation detection and monitoring, including agricultural production environment and desert locust habitat stratification, can be broadly divided into two major groups:

(a) Environmental satellites

This group consists of both geostationary and polar orbiting satellites which are characterized by relatively low spatial (1-5 km) and high temporal (30 minutes - 12 hours) resolutions. The European Meteosat, United States Geostationary Operational Environment Satellite (GOES) and NOAA satellites and the Japanese Geostationary Meteorological Satellite (GMS) belong to this group. The sensors of these satellites were designed for observing atmospheric processes to support weather forecasting, including snowcover and precipitation assessment. Moreover, the Advanced Very High Resolution Radiometer (AVHRR) sensor on the NOAA satellites has spectral and radiometric characteristics suitable for vegetation detection and monitoring. Environmental satellite data allow monitoring of dynamic atmospheric and terrestrial phenomena. Facilities for receiving and processing these types of data are of relatively low cost and the spatial characteristics of the data, combined with the orbital characteristics of the satellites, permit simultaneous observations on regional and continental scales.

(b) Earth resources satellites

This group of satellites is characterized by relatively high spatial (10-80 metres) and relatively low temporal (16-18 days) resolutions. The United States Landsat, French Satellite Probatoire d'Observation de la Terre (SPOT) and Japanese Marine Observational Satellite (MOS) polar orbiting satellites belong to this group. Their sensor characteristics make them suitable for stratification purposes and for detailed vegetation monitoring at a local scale.

At present, some of the above satellite systems for example, Meteosat, NOAA, Landsat and SPOT, provide data on a fully operational basis generally within the time constraints of applications requiring real time or near real time data to satisfy user information needs.

REMOTE SENSING TECHNIQUES AND METHODOLOGIES FOR FOOD SECURITY EARLY WARNING AND DESERT LOCUST HABITAT MONITORING OPERATIONS

In the fields of food security, early warning and desert locust control, the parameters of soil moisture, as provided by precipitation, and quantity of green vegetation distribution are significant indicators of agricultural production conditions and the ecological potential for the development of desert locust populations.

Remote sensing of soil moisture in desert regions is possible with microwave sensors and by thermal techniques. 1/ 2/ 3/ However, no satellite-based soil moisture remote sensing system, using microwave techniques, is currently available on an operational or semi-operational basis for an area the size of the desert locust recession area; thermal remote sensing techniques that use Meteosat data are still in the research phase.

Remote sensing of meteorological events that cause soil moisture changes relevant for agricultural crop production and locust population development can be undertaken from geostationary environmental satellites, e.g., Meteosat for Africa and the Near East. The high temporal frequency of these types of data in the visible and thermal infrared wavelengths permits detailed monitoring of weather systems likely to produce the rainfall necessary to support crop development and initiate locust breeding.

Various schools have developed and tested remote sensing techniques for estimating rainfall quantitatively from Meteosat data. FAO has been closely involved in these developments, as undertaken by the universities of Bristol and Reading. 4/ 5/ 6/ 7/ The technique developed by the University of Reading, 8/ based exclusively on the use of Meteosat thermal infrared data, was selected by FAO for implementation on the ARTEMIS system. The technique is based on the observed linear relationship between the vertical extent of a cloud in the atmosphere, as evidenced by the temperature of its top, which can be measured by the satellite at frequent intervals, and the amount of rain which falls from the bottom of the cloud. This technique is particularly suitable for application in tropical and arid environments where generally over 90 per cent of the annual rainfall comes from strong convective activity, i.e., strong vertical development of clouds.

Remote sensing of green vegetation biomass is a well-developed technique for which several satellites frequently collect data on a worldwide scale. The technique involves measuring reflected spectral radiance resulting from the interaction between the green-leaf vegetation cover and incident solar spectral irradiance. These measurements can be made from any altitude above the surface (1 m, 10,000 m, 1,000 km) depending on the remote sensing system in question (ground-based, aircraft or satellite, respectively). Spectral estimation of green-leaf biomass generally involves the use of two wavelength regions, the red (0.6-0.7 um) and near infrared (0.75-1.1 um), although the specific wavelengths used often vary slightly between instruments. The 0.6-0.7 um region corresponds to the in vivo red region of chlorophyll absorption and is inversely related to chlorophyll density. 9/ In the 0.75-1.1 um region, reflectance is proportional to green-leaf density. Ratio combinations of these two wavelength regions thus contain information related to the chlorophyll-green-leaf density. Use of the two bands for making plant canopy inferences by non-destructive techniques is facilitated by the proximity of the two bands in the electromagnetic spectrum. This proximity enables simple band ratios or other combinations to be used to compensate for difference in solar flux intensities. Linear or ratio combinations of red/near infrared spectral data have been used to quantify a variety of vegetation types. 10/ 11/

The choice of suitable satellites for remote sensing observations for particular applications depends upon satellite spectral, spatial, temporal and radiometric resolutions, orbital considerations and the spatial-spectral-temporal characteristics of the objects to be observed.

Moreover, successful monitoring of crop conditions and desert locust habitats, relevant to FAO's programmes, requires a satellite that can at a given time detect the presence and assess the quantity of green-leaf vegetation biomass with a suitable spatial resolution over very large areas on continental and intercontinental scales, while radiometrically maintaining the integrity of spectral contrast of the surface materials, and do so at frequent intervals. 12/ Furthermore, satellite detection of vegetation cover at high temporal intervals requires the elimination of often considerable cloud cover, which is generally present during the typical monitoring periods for above applications, i.e., the rainy seasons. A technique for compositing largely cloud-free NOAA AVHRR vegetation index data from multiple daily NOAA orbits over 10-day and monthly periods, while maintaining data/information integrity, was successfully developed and tested by the NASA Goddard Space Flight Center (GSFC). 13/

Landsat Multispectral Scanner (MSS) data have been evaluated for mapping and monitoring desert locust habitats, 14/ by using both visual and digital image analysis techniques. 15/ 16/ These studies showed that Landsat MSS data could accurately detect the presence of green vegetation and monitor its phytodynamics. In addition, Landsat MSS data can make an important contribution to the systematic mapping of potential desert locust habitats on thorough visual interpretation of suitably enhanced imagery at a scale of 1:250,000. The imagery provides synoptic and yet detailed information on the geomorphology and soil characteristics of an area. At present, FAO is undertaking, following the 1986-1988 desert locust plague, a systematic mapping of potential desert locust habitats in the recession area using a methodology developed by Popov, in which the use of Landsat MSS data is paramount.

The AVHRR sensor on the NOAA satellites, providing data at 1.1 and 4 km spatial resolutions, is ideally suited for routine and cost-effective monitoring of vegetation development over large areas, such as the desert locust invasion area, extending from the West African Coast to North west India and from Turkey to the United Republic of Tanzania as well as the continental scales of FAO GIEWS.

The NOAA AVHRR based vegetation monitoring technique, developed and tested by NASA GSFC in cooperation with the FAO Remote Sensing Centre was implemented on the operational ARTEMIS system. NOAA AVHRR data are operationally available at 4 km resolution on a global basis from the NOAA in the United States. The full 1.1-km resolution data can be obtained from regional direct readout receiving stations as established in Maspalomas, Canary Islands, Spain; Niamey, Niger; Nairobi, Kenya; and Islamabad, Pakistan.

ARTEMIS SYSTEMS CHARACTERISTICS

The ARTEMIS system, which became operational at the Remote Sensing Centre at FAO headquarters in August 1988, was conceived and developed as a highly automated, dedicated satellite data acquisition, thematic processing and production system, based on the use of high-frequency Meteosat and NOAA AVHRR data. It consists of a number of integrated hardware and software components, which are summarized as follows. 17/

(a) Hardware

(i) A Meteosat Primary Data User Station (PDUS) for direct, automated reception of high-frequency (hourly), full-resolution digital Meteosat data in the visible, thermal infrared and water vapour channels through a 3-metre dish antenna, down converter and receiver. the PDUS is controlled by a dedicated VME 68000 microprocessor and stores data on two 150 megabite (Mb) disks before transfer of data through an ethernet link to the central system computer for mapping and thermatic processing.

(ii) A computer unit consisting of a Hewlett-Packard (HP) 1000 A900 minicomputer, supported by a high-speed 6250/1600 bpi tape drive, three disks (132, 404 and 571 Mb), a clock, a system console, a printer and a modem. The system is currently being expanded with a second tape drive, an optical disk drive and additional memory for the HP 1000 A900.

(iii) An interactive image analysis workstation, consisting of a Ramtek interface to the HP 1000 A900 with a 1,280 x 1,024 x 16 bit display memory, a 19-inch high-resolution colour monitor, a graphics terminal with touch screen capability, trackball and a printer.

(iv) An output sybsystem, consisting of a hard colour copy camera for 10 x 15 inch polaroid and 35 mm film products, HP Vectra microcomputer for IBM personal computer (PC) and ERDAS compatible output on floppy disk, the 6250/1600 bpi tape drive and a six-pen colour plotter. Colour and black and white laser printers are being installed.

Furthermore, the Integrated Land and Watershed Information System (ILWIS) GIS software package, developed by the International Institute for Aerospace Survey and Earth Sciences (ITC), 18/ was implemented on the system in December 1988 for combination and manipulation of ARTEMIS digital data products with data from other sources.

ARTEMIS remote sensing terminal connections within FAO headquarters, through dedicated lines linked to microcomputers of users, are currently being established in the Emergency Centre for Locust Operations (ECLO) (IBM compatible PC with IDA/ILWIS software and VGA graphics), FAO (GIEWS) (IBM Compatible PC with VGA graphics serving a network of microcomputers with IDA software and EGA graphics capability) and the Centralized Geographic Information System (GIS) Group (IBM AT with ERDAS/ArcInfo software). Two additional remote terminal ports to support other in-house users are still available on the present system configuration. In a planned upgrading of the system, two further remote terminal ports will be added.

(b) Software

The ARTEMIS system software can be divided into the following groups, according to function: 19/ 20/

(i) Meteosat PDUS operating system and communications software for controlling data reception, quality control, quick-look display, data storage and transfer to HP 1000 A900;

(ii) HP 1000 A900 operating system software for operating the computer subsystem and related peripheral equipment;

(iii) Operational applications software for mapping and thematic processing of Meteosat and NOAA Global Area Coverage/Local Area Coverage:/High Resolution Picture Transmission (GAC/LAC/HRPT) data and for generation of output products in specific user formats;

(iv) General applications software for image processing for operational and development purposes (NASA GIMMS software);

(v) Database management and communications software for manipulation and integration of various ARTEMIS system databases with other data and for retrieval and archival functions;

(vi) Software for definition and extraction of sub-area and point data from the ARTEMIS product database and for archival of raw.

ARTEMIS DATA PROCESSING

The ARTEMIS system acquires and processes Meteosat thermal infrared data for rainfall estimation, according to the TAMSAT methodology of the University of Reading, chronologically as follows: 21/

(i) Acquisition and preprocessing of Metosat digital TIR data for Africa and the Near East on an hourly basis through pre programmed Meteosat PDUS reception schedule and calibration data as provided by the European Space Operational Centre (ESOC), Germany;

(ii) At selected daily intervals, at 2100h and 0300h, activated by the system clock, transfer of available digital Meteosat images to central system computer for processing;

(iii) Image selection for rainfall processing programme by using predefined image quality control parameters;

(iv) Computer mapping of selected images to ARTEMIS common geographic format, i.e., Hammer Aitoff equal area projection and resampling from 5 km input data resolution to 7.6 km ARTEMIS output product resolution;

(v) Execution of programme MIRPOINTS, which extracts digital Meteosat themal infrared counts for specified point locations (some 1,200 meteorological stations and other locations in Africa) from available hourly images and archives extracted data in a database;

(vi) Execution of programme HRPRO, involving processing of available, in principle hourly, Meteosat images to determine cold cloud duration (CCD) for each pixel on the basis of satellite calibration data, cloud top temperature thresholds for specific geographic regions and time intervals between successive images; product: daily CCD images;

(vii) Execution of programme DAYPRO for determination of cumulated cold cloud duration (DCCD) and number of rainfall days (DNRFD) for 10-day periods; stores results in ARTEMIS database;

(viii) Execution of programme DECPRO, which converts 10-day CCD maps into 10-day estimated rainfall (DERFF) maps, by using predetermined linear regression relations; stores result in ARTEMIS database;

(ix) Execution of the programme MNTPRO, once a month, which adds the three 10-day DERF and DNRFD maps and stores the created monthly map in the ARTEMIS database; furthermore, this programme compares the monthly estimated rainfall map (MERF) with long-term normal rainfall reference maps and generates absolute and relative rainfall anomaly maps (NRFANABS/REL); stores results in the ARTEMIS database.

The above nine processing steps are executed in a fully automated sequence, primarily during the evening and night hours, thus leaving the system free for other operational and developmental processing tasks during the day.

NOAA AVHRR data for vegetation assessment is acquired by FAO on magnetic tape from two sources:

(i) NOAA AVHRR Global Area Coverage (GAC) (4 km resolution) data, covering Africa, the Near- East and South-West Asia, as received by the satellite during daily mid-afternoon overpasses and transmitted to the receiving and archiving facilities of NOAA in Washington, D.C. After quality control by NASA GSFC, data are transmitted to FAO by courier and received for thematic processing generally within 7-10 days after data acquisition by the satellite.

(ii) NOAA AVHRR High Resolution Picture Transmission (HRPT) (1.1 km resolution) data, covering West Africa, as received by the ESA receiving station at Maspalomas, Canary Islands. Data are transmitted to FAO by express mail and generally received within 10-14 days after acquisition.

Processing of NOAA AVHRR GAC and HRPT data is done automatically by the ARTEMIS system as follows:

(i) Mapping of channel 1 (red), 2 (near infrared) and 5 (thermal infrared) data of daily available orbits to the ARTEMIS common geographic format projection and resampling of 4 km resolution input data to 7.6 km ARTEMIS product output resolution;

(ii) Calculation of normalized difference vegetation index: ch 2 + ch 1/ch 2 - ch 1 and identification of cloud-covered areas, by using thermal infrared channel 5 data;

(iii) Generation of 10-day vegetation index composites (DNDVI) by using a maximizing technique on all available daily data;

(iv) Storage of the resulting DNDVI images in the ARTEMIS database;

(v) Once a month, generation of a monthly vegetation index composite (MNDVI) through maximizing three DNDVI images;

(vi) Storage of the resulting MNDVI image in the database.

For processing of the NOAA AVHRR HRPT data at 1.1 km resolution, essentially the same sequence of processing steps is followed. At present, this is not an automated programme and requires operator intervention.

ARTEMIS OUTPUT FOR SUPPORTING FOOD SECURITY EARLY WARNING AND DESERT LOCUST MONITORING AND FORECASTING

Since August 1988, the ARTEMIS system produces the following products on a routine basis:

(i) Ten-day and monthly cold cloud duration (D/MCCD) maps for the continent of Africa and the Near East, based on hourly Meteosat data;

(ii) Ten-day and monthly estimated rainfall (D/MERF) maps for the southern Sahara, Sahel, Sudanian and tropical countries of West Africa, obtained through regression relationships between CCD and ground observed rainfall;

(iii) Ten-day and monthly estimated number of rainfall day (D/MNRFD) maps for Africa and the Near East;

(iv) Ten-day and monthly NOAA AVHRR GAC based composite vegetation index (D/MNDVI) maps for Africa, Southern Europe, the Near East and South-West Asia.

The above products all have a spatial resolution of 7.6 km and are available in both photographic and digital IBM PC compatible formats.

(v) Ten-day-NOAA AVHRR HRPT based composite vegetation index maps for the desert locust recession area of West Africa.

The above product has a spatial resolution of approximately 1.1 km and has been operationally available since mid-August 1989. Detailed information about the current ARTEMIS data based is provided in appendix I.

At present, in cooperation with NASA GSFC, the ARTEMIS vegetation index data coverage is being expanded to cover the rest of Asia and Central and South America. Operational data product availability is expected by the end of 1991.

ARTEMIS PRODUCT USER COMMUNITY

The following entities are currently receiving the ARTEMIS output products on a 10-daily and monthly basis.

A. At FAO Headquarters:

(i) Global Information and Early Warning System (GIEWS) on Food and Agriculture;

(ii) Emergency Centre for Locust Operations (ECLO);

(iii) Office for Special Relief Operations (OSRO);

(iv) Agrometeorology Group of the FAO Remote Sensing Centre.

B. At the regional and national levels:

Since 1 January 1989, ARTEMIS data products in both photographic and digital formats have been routinely supplied to regional and national food security early warning systems in the IGADD region, comprising the countries Djibouti, Ethiopia, Kenya, Somalia, Sudan and Uganda; and in the SADCC region, comprising Angola, Botswana, Lesotho, Malawi, Mozambique, Namibia, Swaziland, the United Republic of Tanzania, Zambia and Zimbabwe. The development of the use of ARTEMIS products at regional and national levels, including further calibration and training programmes, is being undertaken through close cooperation between the FAO Remote Sensing Projects, funded by the Government of Japan, based in Nairobi, Kenya, for the IGADD region; and at Harare, Zimbabwe, for the SADCC region. For the calibration and training programmes, active cooperation has been developed between the FAO Remote Sensing Centre and the Department of Meteorology of the University of Reading and the International Institute for Aerospace Survey and Earth Sciences.

SATELLITE TELECOMMUNICATIONS DEVELOPMENT: THE DIANA SYSTEM

The ARTEMIS system, located in Rome, serves primarily the environmental information needs of the Global Information and Early Warning System (GIEWS) and Emergency Centre for Locust Operations (ECLO) of FAO, which communicate analysed information, combined from a number of sources, to recipient and donor countries in the form of telexed summaries and GIEWS and ECLO bulletins and publications.

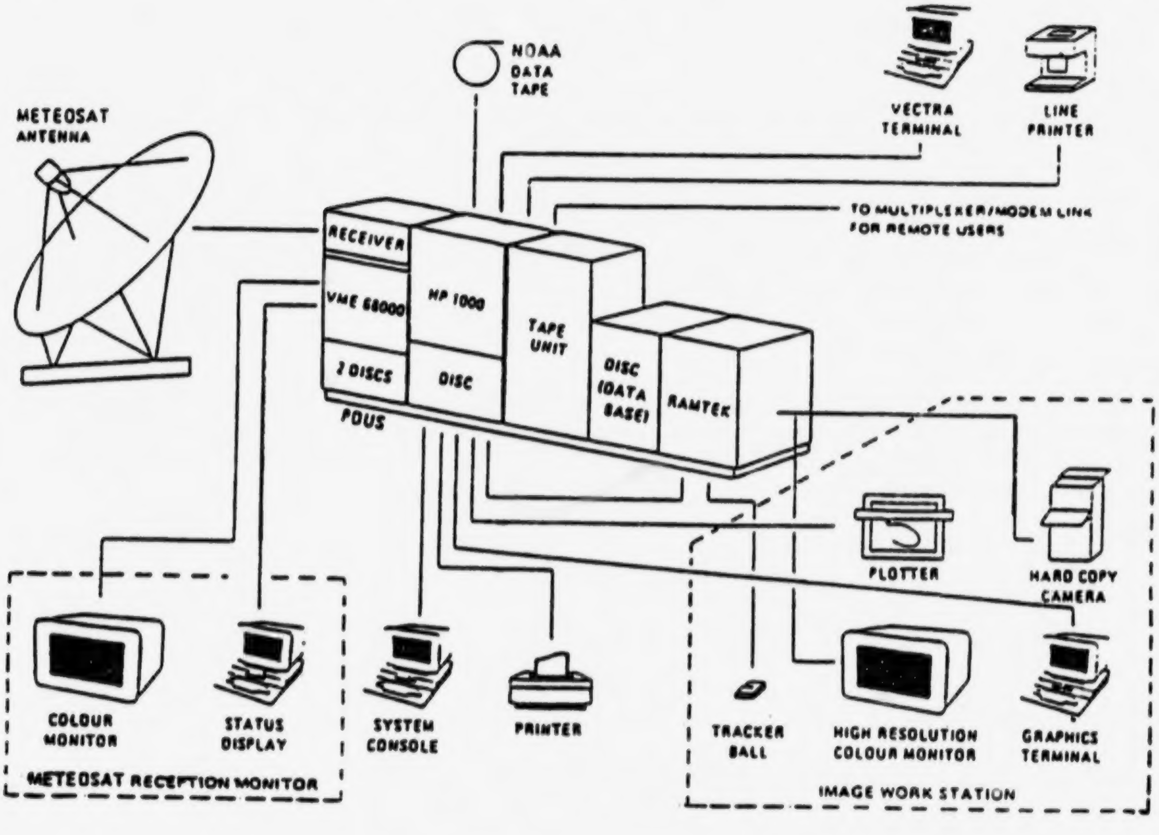
NOAA
DATA
TAPE
VECTRA
TERMINAL
LINE
PRINTER
METEOSAT
ANTENNA
TO MULTIPLEXER/MODEM LINK
FOR REMOTE USERS
RECEIVER
VME 68000
2 DISCS
HP 1000
DISC
TAPE
UNIT
DISC
(DATA
BASE)
RAMTEK
PDUS
PLOTTER
HARD COPY
CAMERA
COLOUR
MONITOR
STATUS
DISPLAY
METEOSAT RECEPTION MONITOR
SYSTEM
CONSOLE
PRINTER
TRACKER
BALL
HIGH RESOLUTION
COLOUR MONITOR
GRAPHICS
TERMINAL
IMAGE WORK STATION

Figure 1. ARTEMIS system configuration.

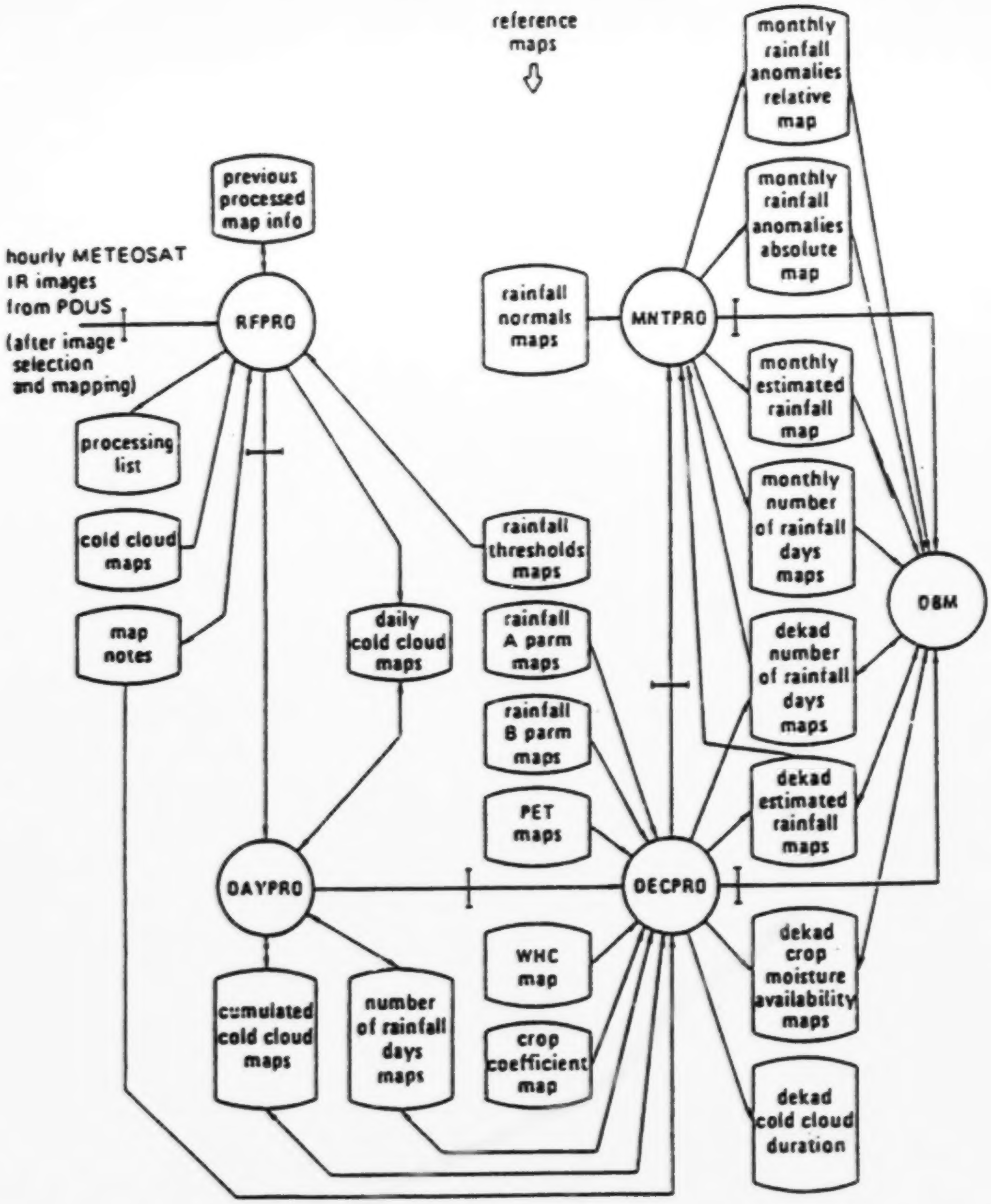
reference maps
monthly rainfall anomalies relative map
previous processed map info
monthly rainfall anomalies absolute map
hourly METEOSAT IR images from POUS
(after image selection and mapping)
RFPRO
rainfall normals maps
MNTPRO
processing list
monthly estimated rainfall map
monthly number of rainfall days maps
cold cloud maps
rainfall thresholds maps
map notes
daily cold cloud maps
rainfall A parm maps
DBM
dekad number of rainfall days maps
rainfall B parm maps
dekad estimated rainfall maps
PET maps
DAYPRO
DECPRO
WHC map
dekad crop moisture availability maps
cumulated cold cloud maps
number of rainfall days maps
crop coefficient map
dekad cold cloud duration

Figure 2 a. ARTEMIS rainfall assembly overview.

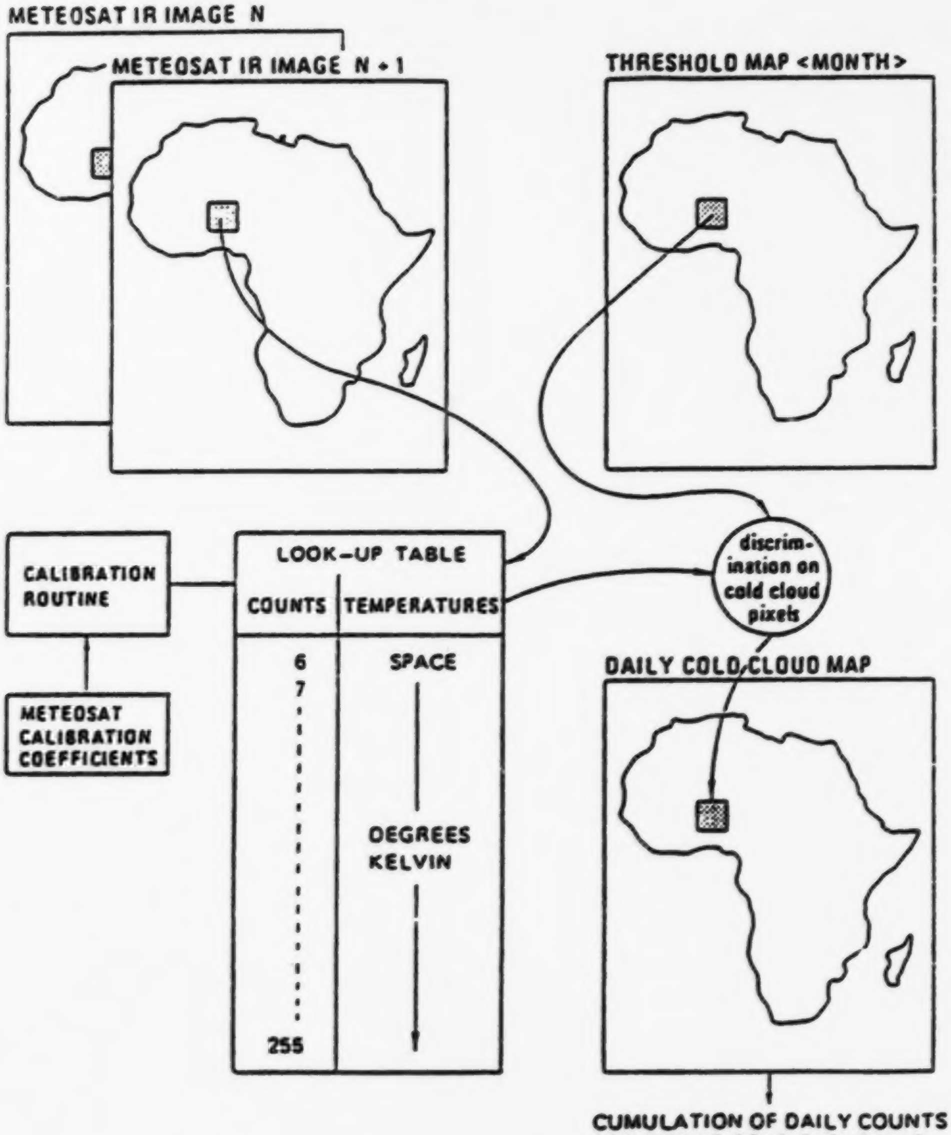
METEOSAT IR IMAGE N
METEOSAT IR IMAGE N + 1
THRESHOLD MAP <MONTH>
CALIBRATION ROUTINE
METEOSAT CALIBRATION COEFFICIENTS
LOOK–UP TABLE
COUNTS
TEMPERATURES
6
7
255
SPACE
DEGREES KELVIN
discrimination on cold cloud pixels
DAILY COLD CLOUD MAP
CUMULATION OF DAILY COUNTS FOR DEKAD COLD CLOUD MAP

Figure 2 b. ARTEMIS cold cloud discrimination.

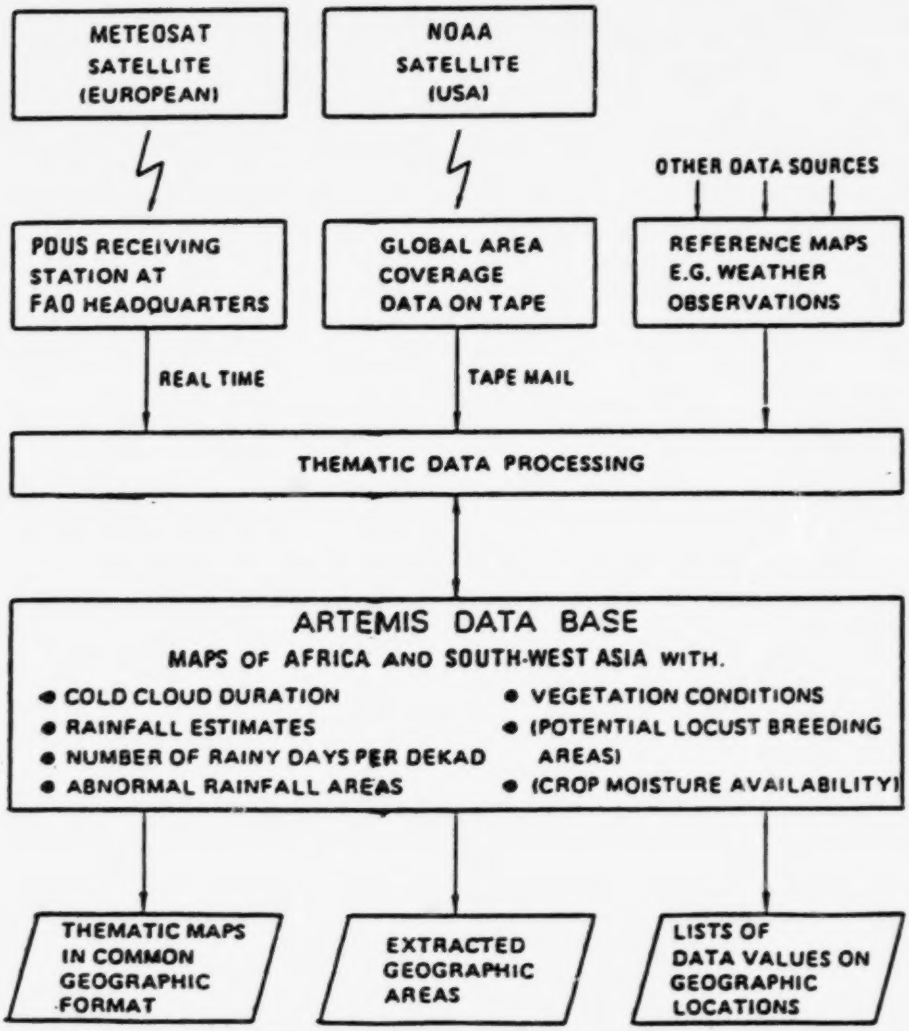
METEOSAT
SATELLITE
(EUROPEAN)
NOAA
SATELLITE
(USA)
OTHER DATA SOURCES
PDUS RECEIVING
STATION AT
FAO HEADQUARTERS
GLOBAL AREA
COVERAGE
DATA ON TAPE
REFERENCE MAPS
E.G. WEATHER
OBSERVATIONS
REAL TIME
TAPE MAIL
THEMATIC DATA PROCESSING
ARTEMIS DATA BASE
MAPS OF AFRICA AND SOUTH-WEST ASIA WITH.
● COLD CLOUD DURATION
● RAINFALL ESTIMATES
● NUMBER OF RAINY DAYS PER DEKAD
● ABNORMAL RAINFALL AREAS
● VEGETATION CONDITIONS
● (POTENTIAL LOCUST BREEDING AREAS)
● (CROP MOISTURE AVAILABILITY)
THEMATIC MAPS
IN COMMON
GEOGRAPHIC
FORMAT
EXTRACTED
GEOGRAPHIC
AREAS
LISTS OF
DATA VALUES ON
GEOGRAPHIC
LOCATIONS

END-PRODUCTS ON PHOTOGRAPHIC MEDIA, COMPUTER TAPE, FLOPPY DISK OR AVAILABLE VIA REMOTE TERMINAL AND IN FUTURE VIA SATELLITE LINK

Figure 3. ARTEMIS system outline.

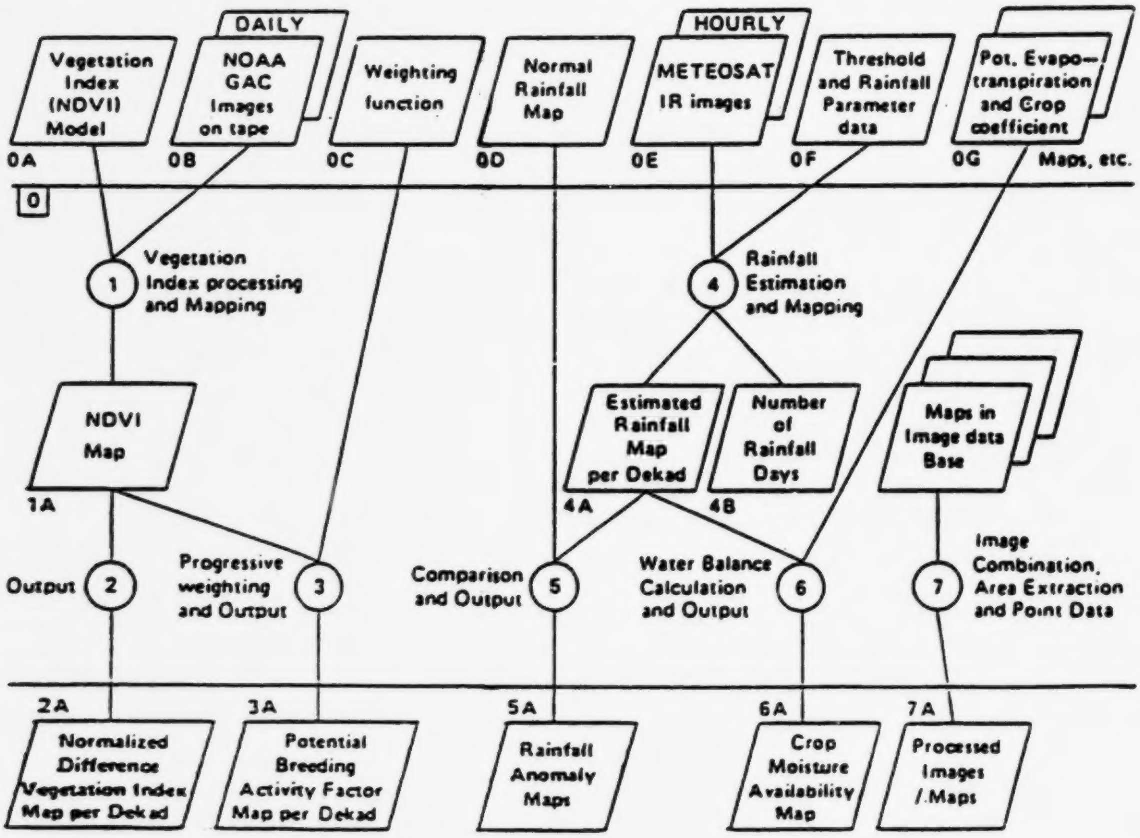
DAILY
Vegetation Index (NDVI) Model
NOAA GAC Images on tape
Weighting function
Normal Rainfall Map
HOURLY
METEOSAT IR images
Threshold and Rainfall Parameter data
Pot. Evapo-transpiration and Crop coefficient
0A
0B
0C
0D
0E
0F
0G
Maps, etc.
0
1
Vegetation Index processing and Mapping
4
Rainfall Estimation and Mapping
NDVI Map
1A
Estimated Rainfall Map per Dekad
4A
Number of Rainfall Days
4B
Maps in Image data Base
Output
2
Progressive weighting and Output
3
Comparison and Output
5
Water Balance Calculation and Output
6
7
Image Combination, Area Extraction and Point Data
2A
Normalized Difference Vegetation Index Map per Dekad
3A
Potential Breeding Activity Factor Map per Dekad
5A
Rainfall Anomaly Maps
6A
Crop Moisture Availability Map
7A
Processed Images /Maps

Figure 4. Survey of ARTEMIS information sets and processing functions.

Rapid communication of the high volume ARTEMIS system information products to users at regional and national levels requires special communications facilities.

Jointly with the European Space Agency (ESA), the FAO Remote Sensing Centre has formulated a project for the development, implementation and demonstration of a dedicated satellite communications system, DIANA, based on low-cost microcomputer technology and by using the commercial Intelsat satellites through the facilities of Telespazio in Fucino, Italy (Hielkema, 1988).

The DIANA system will provide a capability for high speed, two-way transfer of facsimile images of documents and maps, character-coded text documents and digital images in raw or processed form from FAO headquarters to microcomputer based receiver terminals of users at the regional or national level.

This capability will enable regional organizations and national early warning units and plant protection services to receive processed satellite information and other relevant communications from FAO headquarters in near realtime. The DIANA system, which is funded by ESA member countries: Italy, Belgium, Spain, Ireland, Norway, the United Kingdom and Finland is being developed industrially under ESA management. The industrial phase will be completed by June 1991, followed by a testing and training period. Subsequently, three DIANA terminal stations, linked to the central hub station at FAO headquarters, will be installed at selected locations in Africa and demonstrated for various applications a the period of one year from February 1992 through January 1993. Currently, confirmed DIANA terminal locations are: Nairobi, Kenya; Harare, Zimbabwe; and Accra, Ghana.

NOTES

1. Schmugge, T. "Remote sensing of soil moisture with microwave radiometers," Paper 81-4503, Am. Soc. Agr. Engng. 1881 Winter Meeting, Chicago.

2. Wetzel, P.J. and Atlas, D. "Inference of Precipitation through Thermal Measurement of Soil Moisture; Precipitation Measurement from Space," Workshop Report, 28 April-1 May 1981, NASA/Goddard Space Flight Center, pp. 170-172.

3. England, C.E., Gombeer, R., Hechinger E., *et.al*. "Applications of Meteosat data for rainfall, evaportation, soil moisture and plant-growth monitoring in Africa," *ESA J.* (1983) p. 3.

4. Barrett, E.C. "Mapping Rainfall from conventional Data and Weather Satellite Imagery Across Algeria, Libya, Morocco and Tunisia, AGP/DL/RS/1/77. (Rome, FAO, 1977).

5. Barrett, E.C. Harrison, A.R. "Rainfall monitoring by Meteosat in Africa." Consultants Report GCP/INT/432 NET. (Rome, FAO, 1986).

6. Hielkema, J.U. "Remote sensing techniques and methodologies for monitoring ecological conditions for desert locust population development", FAO/USAID Final Report. GCP/INT/349/USA. (Rome, FAO, 1980).

7. Barrett, E.C. and Harrison, A.R. "Rainfall monitoring by Meteosat in Africa," Consultants Report GCP/INT/432 NET. (Rome, FAO, 1986).

8. Milford, J.R. and Dugdale, G. "Rainfall mapping over West Africa in 1986, 1987," Consultants' Report GCP/INT/432/NET. (Rome, FAO, 1987).

9. Tucker, C.J. "Red and Photographic Infrared Linear Combinations For Monitoring Vegetation," *Remote Sensing Environ*., vol. 8 (1979), p. 127.

10. Tucker, C.J., Hielkema, J.U. and Roffery, J. "The Potential of Satellite Remote Sensing of Ecological Conditions for Survey and Forecasting Desert Locust Activity," *Int. J. Remote Sensing*, vol. 6 (1985), p. 127-138.

11. Curran, P.J. "Multispectral Remote Sensing for the Estimation of Greenleaf Area", *Phil. Trans. R. Soc.* B 309 (1983), p. 257.

12. Tucker, C.J., Hielkema, J.U. and Roffery, J. "The Potential of Satellite Remote Sensing of Ecological Conditions for Survey and Forecasting Desert Locust Activity," Int. J. Remote Sensing, vol. 6 (1989), pp. 127-138.

13. Helben, B.N. "Characteristics of Maximum-Value Composite Images From Temporal AVHRR Data", Int. J. Remote Sensing, vol. 7, (1986), pp. 1417-1434.

14. Pedgley, D.E. "Testing feasibility of detecting locust breeding sites by satellite," Final report to NASA. 1973.

15. Hielkema, J.U. Applications of Landsat Data in Desert Locust Survey and Control", AGP/LCC/77/11. (Rome, FAO, 1977).

Hielkema, J.U. "Advanced Training and Research on Satellite Remote Sensing Techniques and Applications in the United Kingdom and the United States," AGLT/RSU series 2/79. (Rome, FAO, 1979).

16. Hielkema, op.cit. (1980).

Hielkema, J.U. "Operational Environmental Monitoring and Information Dissemination by Satellite at FAO: The ARTEMIS and DIANA Systems," USAID/NOAA International Workshop on Satellite Techniques for Estimating Precipitation, Washington, December 1988.

Hielkema, J.U. Howard, J.A., Tucker, C.J. etal. "The FAO/NASA/ARTEMIS system: An Integrated Concept for Environmental Monitoring By Satellite In Support of Food/Feed Security and Desert Locust Surveillance," Proc. 20th ERIM Symposium on Remote Sensing of the Environment, Nairobi, Kenya, December 1986a.

17. van Ingen Schenau, H.A., Venema, J.C., Spaa, J. etal., "ARTEMIS system Overview and Presentation of ARTEMIS Products," Paper ITC/FAO Seminar, 14-25 November 1988, Enschede, Netherlands.

18. Meijerink, A.M.J., Valenzuela, C. and Stewart, A., "ILWIS: The Integrated Land and Watershed Management Information System", ITC Publication No. 7 (Enschede, Netherlands, ITC, 1988).

19. van Ingen Schenau, op.cit.

20. Hielkema, op.cit. (1986a).

21. van Ingen Schenau, op.cit.

REMOTE SENSING APPLICATIONS IN WATER RESOURCES WITH CASE STUDIES IN SAHEL AREAS, WEST AFRICA*

M. Antoninetti, P.A. Brivio, M.A. Gomarasca and E. Zilioli

CNR-IGL, Remote Sensing Department
via Ampère 56, 20131 Milan, Italy

INTRODUCTION

The Sahelian area of Africa is currently the focus of a large number of studies as a consequence of the severe drought experiences throughout the region. International and national agencies are concentrating their attention on understanding the drought impact on the indigenous population and solving the problems of improving the management of systems of these arid and semi-arid rangelands with an effective inventory and control of the land.

Remote sensing techniques offer an important contribution to recording and understanding the actual surface conditions above all in the agricultural and pastoral zones where the survival of the human and animal populations is strictly related to the availability of water and forage. Mainly, three characteristics of the data have contributed to the great interest aroused in the satellite images: the availability of a multiyear archive made possible new types of investigations; the temporal frequency of data acquisition, which enables a constant control of dynamic phenomena.

This paper deals with some results of two research projects on hydrologic subjects concerning the prediction of water availability of the Senegal river flood zone and with the identification of the geomorphic units of hydrologic interest in the inland delta of Niger.

SENEGAL RIVER FLOOD ESTIMATE

Geographically, the study area is framed within longitude 9° to 13° West and latitude 10° to 15° North (see figure 1). The precise area of interest occupies the greater part of the

---

* This paper, which was presented at the Third United Nations Training Course on Geological Sciences, Potsdam, Germany, 7-25 October 1991, does not necessarily reflect the views of the United Nations.

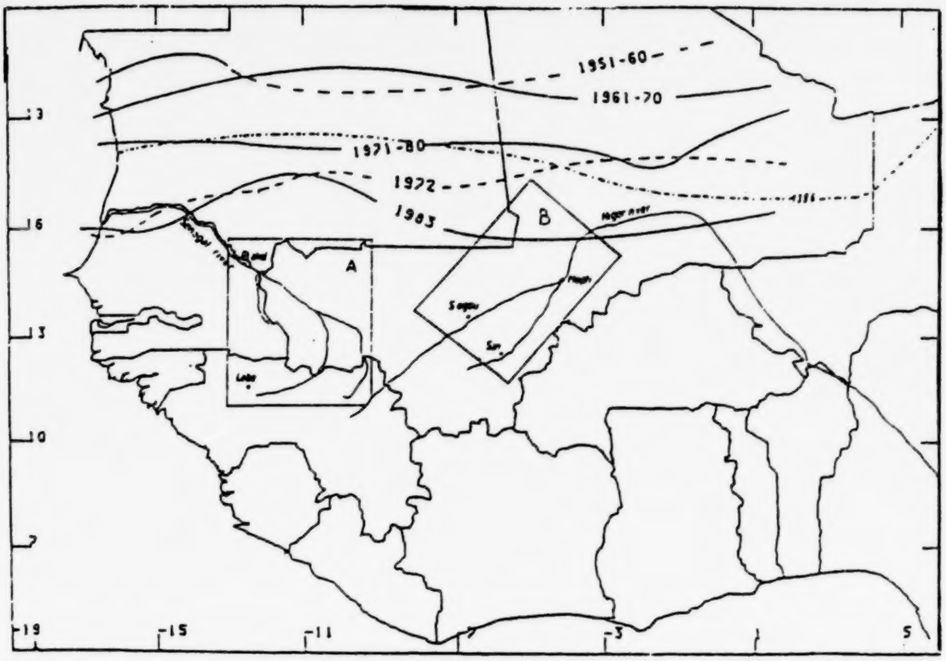
1951-60
1961-70
1971-80
1972
1983
B
A
Niger river
Senegal river
Bakel
Segou
Mopti
San
Labe
19
16
13
10
7
-19
-15
-11
-7
-3
1
5

Figure 1. Location of the studied areas: A, Senegal river; B, Niger river. The 100 mm isohyet represents the theoric limit of the desert.

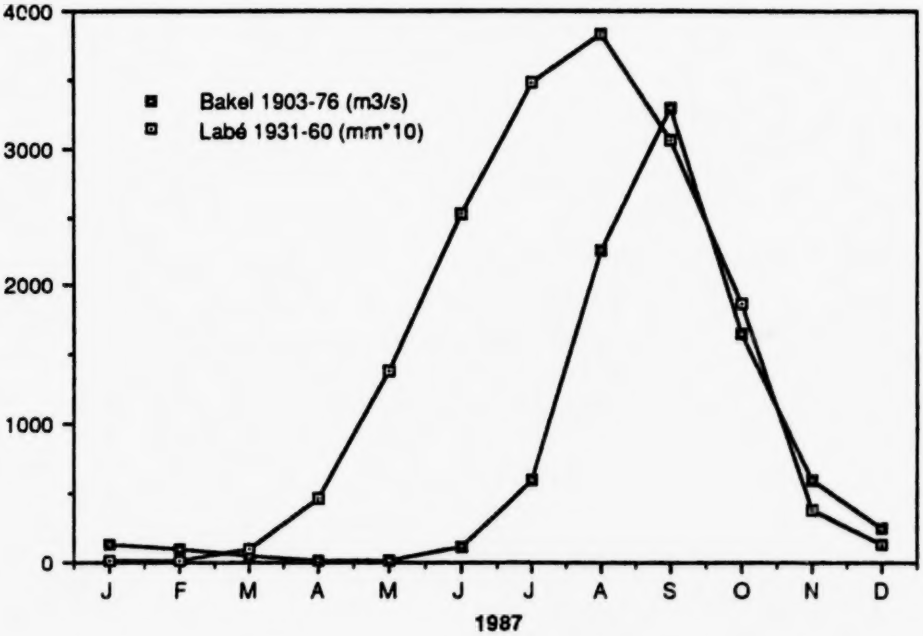

Figure 2. Diagrams of rainfall P and riverflow discharge Q, at the stations of Labé and Bakel, from a historical basis of 70 and 30 years, respectively.

mountainous area of Fouta-Dajalon (Guinea), which is considered the "water castle" of West Africa, from which the affluents of the greatest African rivers originate. The upper part of the Senegal river basin under consideraton is fundamentally constituted by three main tributaries: the Falémé, the Bafing and the Bakoye rivers.

From the south to the north, four phyto-climatic belts are represented: the forested Guinean zone, the dry-forested Sudano-Guinean zone, the tree-savanna Sudanian zone and the prairie-savanna Sahelian zone. Climate is characterized by a rainy summer season (April to October) and a dry winter season (November to March).

Hydrometeorology is expressed by the diagrams in the form of a historical sequence analysis, at the main stations of Labé, in the Fouta-Djalon, for precipitations and of Bakel, sited some 500 miles downstream the Senegal river, for riverflow discharge, as illustrated in figure 2. The delay-time between the feet of the diagrams of the two events turns out to be more than 60 days; this is of great advantage, because it permits the application of an early warning strategy by the methodology proposed.

Schematically, the study area can be subdivided into two distinct geomorphologic zones:

-In the South, granitic-doleritic lands at different plateaux (Infracambrian - Ordovician), covered by discontinuous laterites, 1000 to 3000 metres (m) high (Fouta Djalon), are cut by the drainage in a V-shaped valley succession;

-In the Northern area, formed by Infracambrian sandstones and Birrimian schists, the main rivers cut the overlying lateritic soil with banks 5 to 20 m deep.

All the upper Senegal basin formations can be considered impervious; it is possible to find reduced aquifers in the sandstone levels, included between granites and schists, and in the detrital cones present at the foot of the doleritic-sandstone escarpments in the Fouta Djalon area. The vegetation features (from south to north: forest, savanna, prairie) are strictly connected to the special kind of soil and climate. The vegetation, on the other side, can influence, directly or indirectly, the hydrogeological evolution of the underlying soil. The human presence, marked by extensive fires to obtain new grazing and cultivable areas, greatly contributes to the alteration process of the environmental balance.

Since The European Space Agency (ESA) ground receiving station, located at Maspalomas (Canary Islands) and covering West-Africa countries, became operative in acquiring National

Oceanic and Atmospheric Administration (NOAA) Advanced Very High Resolution Radiometer (AVHRR) data in July 1986, we decided to start our study taking into account satellite data of spring 1987, just at the beginning of the rainy season of a new hydrologic year.

In order to evaluate a long-term data set of NOAA-AVHRR images, which would incorporate more than one hydrologic year, a standard procedure of digital preprocessing was implemented on a mainframe computer. The procedure includes some operations and corrections. In particular:

- Extraction of satellite navigation parameters from CCTs;
- Panoramic correction of the geometric distortion caused by Earth curvature, scan angle and satellite altitude;
- Radiomnetric correction of sensor data by means of calibration values and coefficients as suggested by Price, 1987.

Processing

Two physical quantities were derived from satellite data, according to relations checked by referenced authors.

NDVI (Normalized Difference Vegetation Index)

First, we tried to correlate the hydrometeorological data with the NDVI, defined as the ratio of spectral absorption caused by chlorophyll in the AVHRR channel 1 (0.58-0.68 micrometer (μm) and high reflectance due to the leaf structure in channel 2 (0.72-1.1 μm):

$$NDVI = ch2 - ch1)/(ch2 + ch1) \qquad (1)$$

where NDVI was evaluated in terms of equivalent spectral albedos of channels 1 and 2 of the AVHRR, instead of DN's (digital numbers) readable from CCTs. The solar spectral constant, this approach is preferable and it gives the possibility to compare vegetation indexes (VI) from different satellites. 1/ 2/

Surface temperature (Ts)

Surface temperature has been computed starting from the radiance measured by the AVHRR and obtain from the digital numbers of the imagery files through a linear conversion and suitable calibrations. Successively, radiance values have been converted into brightness temperatures (or black-body temperatures) lower (Tb) by inversion of the Plank equation. In order to reduce the influence of the atmospheric absorption on the radiance measured, *we adopted the "split window algorithm"* (SWA) that expresses Ts by the following relation:

$$T_s = a_1 \, T_{ch4} + a_2 \, (T_{ch4} - T_{ch5}) = a_0 \qquad (2)$$

where T_{ch4} and T_{ch5} are the brightness temperatures from the AVHRR thermal infrared channel 4 (10.3-11.3 µm) and channel 5 (11.5-12.5 µm), respectively. Coefficient values a_0=0, a_1=1 and a_2=3.168 have been chosen on the basis of suggestions by Price (1984) according to his experimental checks in the continental United States. No correction has been brought for the emissivity influence.

Finally, the dividing lines of the Senegal river main tributaries, including Bafing, Falemé and Bakoye, were digitized from a topographic map in vector format, using a minicomputer-based image processing system.

These data have been overlaid on the full set of NOAA-AVHRR sub-frames and single sub-basin area sorted and cut out in order to evaluate the influence of each basin over the total flood zone of Senegal river.

The predictive role of the satellite derived quantities and rainfalls in relation to the fluvial discharge Q has been tested by correlating each of these quantities to the heights of the river waters. In particular, fourteen 10-day data (an 11 image set and 3 interpolations) have been considered in the regression analysis, covering different periods, on the basis of the temporal relationship between occurrences recorded in the upstream Fouta-Djalon NDVI, T_s and P, starting with the beginning of the rainy season, in springtime, and the riverflow discharge Q, at Bakel, from July, about 90 days later. The diagrams of the resulting correlations are shown in figure 3. Correlation coefficients show the same appreciable values of r = 0.98 (see figure 3).

The hydraulic significance of the vegetation cover seems to be confirmed and appears to be able to play a very significant role in the near future, especially for applications in the arid and semi-arid regions.

Some useful considerations can be derived at this stage:

-Temporal and spatial resolution of NOAA-AVHRR Local Area Coverage (LAC) data are suitable to study these kinds of phenomena at basin scale. Also, the cloud cover appears to be greatly reduced in respect to the higher spatial resolution satellite sensors (Landsat multispectral scanner (MSS) and

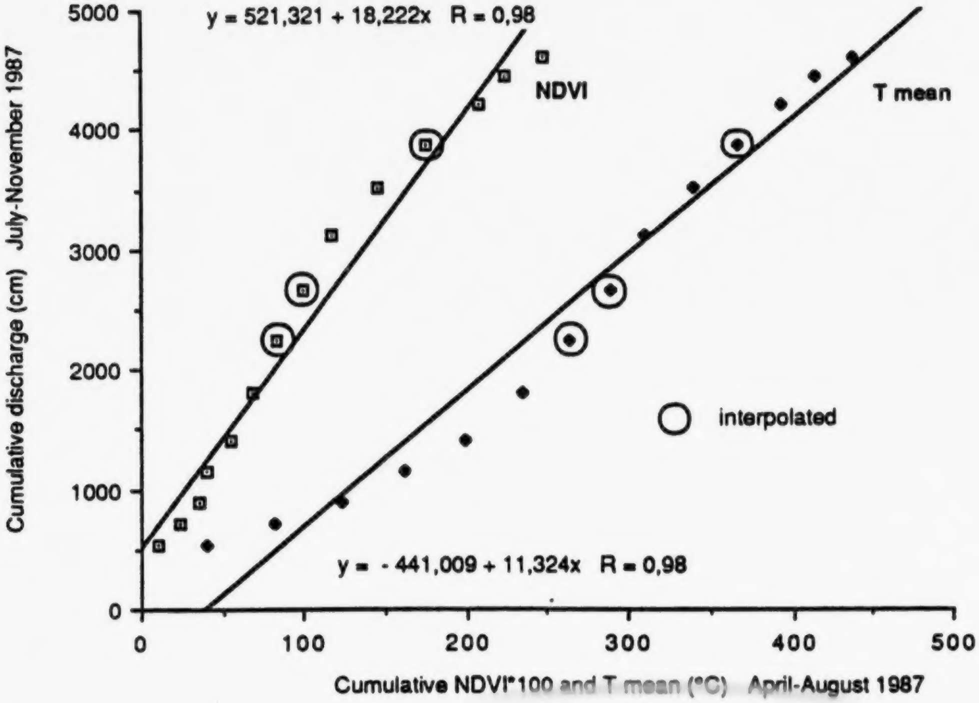

Figure 3. Correlation diagrams between cumulative functions of NDVI and T_S with Q

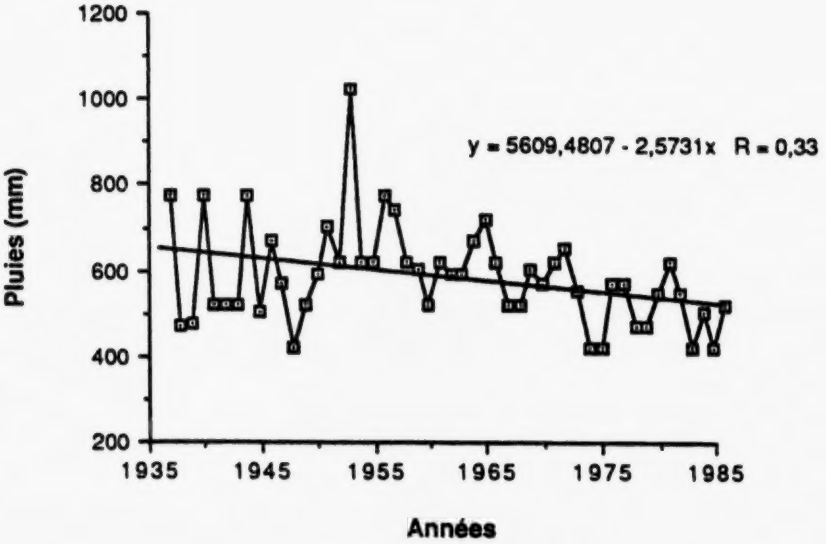

Figure 4 - Interannual variability of rainfalls at Mopti in the last 50 years.

thematic mapper (TM), Satellite Probatoire pour l'Observation de la Terre (SPOT));

-The Bafing river basin can offer the more complete environmental information owing to its extension from the Fouta Djalon to the sub-Sahelian zone, embracing all the phyto-climatic belts;

-Simple analysis of NDVI and T_s values enable the definition of the hydrologic behaviour of a rivershed.

For proper completion of the research project, some development activities are needed:

-Examination and comparison of other hydrologic years;

-Contribution to understanding further basin features (evapotranspiration, thermal inertia, etc.) by means of day/night NOAA-AVHRR thermal infrared data;

-Exploitation of NOAA-AVHRR General Area Coverage (GAC) and LAC format data already acquired by NOAA (historical backdated series 1981-1986), because of the influence on the area and onto the river regime exerted at present by the activation of the Manantali dam, sited just before the confluence with the Senegal river, which became operative early in August 1987.

Niger river inland delta

The inland delta of the Niger river in Mali represents one of the greatest features of fluvial morphology in the world. The inland delta, at least that part defined as the "alive delta", covers the territory that is seasonally flooded and it includes a large portion of the Sahel, 400 km long and 150 km wide, which overlaps the southern border of the Sahara desert. It extends into the north-central part of Mali, within 13° 30′ and 15° 30′ latitude North (see figure 1).

The results for the region included the 700 millimetre (mm) and 450 mm of annual rainfall rate, so that it is placed between the Sudan and the Sahelian regions; the rainy season lasts about four months, from May/June to August/September.

Air temperature varies causing double peaks: two maxima in April/May and November and two minima in January/February and in August. The latter coincides with the peak of the rainy season; in just the month of August, one half of the total year rainfall occurs. 3/

The deltaic landscape influences the air temperature. It has been proved that it causes a 1 to 2 ° C temperature difference in comparison to the surrounding regions.

Of course, particular attention must be given to the quantity and distribution of precipitation. The rainfall pattern shows a constant decrease from the south to the north; the means that the rainy season is shorter for about one month between Mopti and Diré. The Sudan-Sahelian regime is marked by a great inter-annual variability of rainfall. At Mopti, the records for the last 50 years show a variability which ranges between 1000 mm and 400 mm as shown in figure 4.

The circulation model and exchange of water at the surface and in the ground is a matter of great interest. Some hydrologic features are still concealed, without no apparent explanation.

As far as the river Niger discharge is concerned, we would recall only the extraordinary dissipating action played by the deltaic system. Only 2 per cent of the incoming waters located at Segou, at the opening of the delta, succeed in reaching Gao, where is placed the first gauging station after the delta, is located. Although a large loss is due to evaporation, some questions must still be resolved about the groundwater seepage and supply.

Nevertheless, it seems that important contributions derive from deep aquifers coming from the desert zones of the north-west, where drought in the river channels, unexplainably, appears subject to delay more than elsewhere.

The origin of the inland delta of the Niger river is associated with the action of intensive subsidence, probably of tectonic nature, and to the obstructing action by the fossil dunes which control the downstream course of the river.

The African craton forms the substratum covered by sedimentary bodies deposited during a Precambrian sea transgression, and later during the Eocene and Quaternary era.

The hydrologic network of the inland delta is influenced by the geologic and morphological units. The alluvial plain is formed by the accumulation of the thin material eroded from the sandstone reliefs and deposited by the Niger and Bani rivers, flowing toward the north with a typical meandering shape.

On the western plateau the Yame river and its tributaries, which continuously deepen their river-beds in the rocky substratum, are controlled by the pre-existent tectonic lineaments. The extension of the region does not permit planning of ground surveys. Thus, it can actually be considered an example of very inaccessible and severe environment reachable only by canoe during the wet season and exposed to very hot temperatures in the dry period.

At the same time, the geographical location of the delta, whose largest portion belongs to the Sahelian belt, makes it a large and promising water reservoir that after the flooding inevitably disappears into the depths of the Earth and into the sky, by circulation and evaporation.

In order to follow the evolution of the flooding in the Niger delta we adopted the concept based on interpretation of data analysis where landscape indicators are found at different sites and the water expanses become rather legible although no quantitative information is given. 4/, 5/ Also, a comparison between the rainy and the dry seasons was conducted by the use of false colour composites (FCC) of MSS Landsat data. 6/

On the basis of the simple consideration of spectral reflectance variations observed in the region of the lakes it is possible to follow the flooding stages and the successive period of décrue. Our procedure involved a computer-assisted analysis on a large window from the Landsat frame 197-50, 82 km x 155 km sized, concerning the central part of the delta ("alive delta"), in relation to the dry and the wet seasons, taken on 21 March 1986 and 15 October 1986, respectively.

The first objective of the investigation has been the comparison between the observed environmental features and the known hydrological evidences.

The first step of the image analysis was the photo-interpretation of FCC products to distinguish the principal geomorphological and environmental features which characterize the landscape.

A remarkable limit is visible along the borders of the western cliffs of the Dogon plateau, where the sandstone formations gently dip beneath the Quaternary fluvio-lacustrine deposits of the delta. Indeed, on looking at the dry season image we perceive it as some specimen in geomorphology or structural geology. It shows the fracture patterns and rock type as distinct with sharp contrasts which seldom occur.

In order to enhance and to better understand the action played by the fracture system, a map of lineaments has been drawn by photo-interpretation, at successive stages of the following image files. 7/

(a) wet season/MSS 5 (0.6-0.7 micron);
(b) wet season/MSS 7 (0.8-1.1 micron);
(c) dry season/directional derivative (- 45°);
(d) dry season/directional derivative (+ 45°).

The result is the area description of the highest frequency and cross-density of lineaments, where the highest capacity of water retention and infiltration into the ground would be concentrated, and the assessment of the great neotectonic features in the delta basin, corresponding to probable active lines of subsidence. The digital multiplication of MSS 6 (0.7-0.8 micron) by MSS 7 was performed to increase the difference when it appears to be too feeble between the two of the seasons considered.

The NDVI profiles outline the particular contrasting aspects between the dry season, when it is smoothed and almost flat, and the wet season, where the relative low peaks relate to the flooded areas. The NDVI values have been calculated using (1) where ch1 is the MSS and ch2 is the ch4 (see table 1).

The two MSS images have been successively analysed to produce classified land cover/land use maps reflecting the geo-hydrological units of this area.

An unsupervised approach 8/ was used for the definitions of the training statistics, applying the following procedure:

-to reduce computational time, five cluster areas are selected such that each one contains several of the cover types of interest and all cover types were represented in the clustering areas;

-the clustering algorithm is run independently for each area;

-the collected ground truths are used to associate the spectral classes of enhanced in the images with the informational classes; the various levels of vegetation density were defined based upon calculation of NDVI 9/

-the spectral classes are evaluated and selected to be retained for the classification;

-all the images are classified by means of a Maximum Likelihood algorithm.

Results show the relationships between informational classes and geo-hydrological patterns in the study area. A comparison of both seasons show a distinctive variation in vegetation patterns with moisture. However, in the wet season image a strong

Satellite		AVHRR	LANDSAT-MSS
Altitude		853 km	705 km
Cycle duration		1 day	16 days
Ground coverage		3000 km	185 km
Ground resolution nadir		1.1 km	80 m
Spectral bands	ch1	0.58-068 µm	0.50-0.60 µm
	ch2	0.72-1.10 µm	0.60-0.70 µm
	ch3	3.33-3.93 µm	0.70-0.80 µm
	ch4	10.3-11.3 µm	0.80-1.10 µm
	ch5	11.5-12.5 µm	==========
Radiometric resolution		10 bit (1024 dig. lev.)	8 bit (256 dig. lev.)

Table 1: Characteristics of the AVHRR and MSS sensors

relationship among training and test classes presented some confusion. On the other hand, in the dry season image the results indicate a good classification for bare soils and confusion for vegetation and water classes in relation to a better exposure of the rocks and soils during that time of the year.

In any case, the classification accuracy for the defined classes is not high due to the limited spectral coverage of the MSS sensor. The number and the high correlation among the bands limit the choice of the appropriate training sets for the classification, particularly during the dry seasons, in regard to the water classes.

It was not possible to perform the analysis of temporal variation of water filling in the mares in agreement with the groundwater flow. To do that, we also need to further process an image selected between April and August of the same year.

As a matter of fact, the "alive delta" at the end of March, (date of the pass utilized for the dry season) still represents the hydrographic tail of the previous hydrological year. The results obtained at the end of this phase of the research indicate that it could be possible to plan:

-a study of the evolution of the seasonal flooding both in space and time, monitoring the quantity of water involved in the region and its impact on the landscape;

-a possible estimate of flood prediction with some useful advance; so that with a long term type of prediction an economic profit can also be derived for agricultural purposes. 10/, 11/

-a better knowledge of the water circulation model, either at the surface or in the depth. That would be of great interest, it could improve the knowledge of the relations between the surface drainage and the aquifers, so that it could be of great benefit and provide a framework for the programmes currently being carried out in the region for water resources exploitation.

The possibility for obtaining good results also may be found in the analysis of drainage and in the detection of both geomorphic and landscape units in the surroundings of the lakes, because water level, clearly detectable on the images, is in direct relation with the water table piezometry.

We expect to find some unexpected ground waterflow of a certain degree of importance, especially in the dry season, in the framework of the general planning for water resources exploitation in the region.

NOTES

1. Price, J. "Calibration of satellite radiometers and the comparison of vegetation indices", Remote Sensing of Environment, Vol. 21 (1987).

2. Price, J. "An update on visible and near infrared calibration of satellite instruments", Remote Sensing of Environment, Vol. 24 (1988).

3. Gallais J., "Le délta interieur du Niger", IFAN, (Tome II, Dakar 1967).

4. Guyot L., 1986 "Intérpretation visuelle des "quick looks" d'images LANDSAT pour l'étude de la crue annuelle du fleuve Niger dans son delta inférieur au Mali," Bull. Soc. Française Photogramm. et Télédé., (1906) n. 104.

5. Bossard M. and Guyot L., Utilisation des "quick-looks" d'images MSS LANDSAT pour des suivis de phénomènes évolutifs en Afrique: Photointerpretation, (1987) n. 1987-4.

6. Guyot L., 1985 "Le suivi de la crue du fleuve Niger dans le delta intérieur", (lac Débo, Mali): IGN, Paris, 1985.

7. Zilioli E. and Antoninetti M., 1987 "Geostructural evolution of the Southern Alps: lineaments trends detected on Landsat images", Remote Sensing of Environment, (1987) n.23.

8. Fleming M.D., Berkebile J.S. and Hoffer R.M., "Computer aided analysis of Landsat-1 MSS data: a comparison of three approaches including a modified clustering approach", LARS Information Note 972475, (Purdue University, West Lafayette, IN 1975).

9. Antoninetti M., Brivio P.A., and Tomasoni R., "Contribution of different satellite data to the study of hydrological parameters in the Senegal river basin for the early assessment of the flood regime", 22nd ERIM Symposium, Ivory Coast, 20-26 October 1988.

10. Brivio P.A., Grégoire J.M. and Zilioli E., "Use of Landsat imagery to detect hydrologic indicators of the Niger river regime," ITC Journal, (1984) p. 3.

10. Grégoire J.M. and Kohl H.G., "Space technology and predictions of the availability of flood water in the Niger river", International Workshop Hydrologic Applications of Space Technology, Cocoa Beach, 18-24 August 1985.

11. Price, J. "Land surface temperature measurements from split window channels of NOAA 7 AVHRR data", *Journal of Geophysical Research*, (1984) n. 89.

REMOTE SENSING APPLICATIONS IN TROPICAL AFRICA: ENVIRONMENTAL GEOLOGY, SOILS AND VEGETATION COVERAGE*

Mikko Punkari
Research Director
Finnish Earth Resources Group (FERG)
Veklahti, Kirkkonummi, Finland

INTRODUCTION

A general statement of the rate of soil erosion, vegetation coverage and environmental degradation in Africa is presented on the basis of previous investigations, field studies and different kinds of remote sensing data. Field investigations were carried out in Tunisia, Western Sahara, Gambia, Senegal, the United Republic of Tanzania, Zanzibar, Kenya, Zimbabwe and Botswana. The remote sensing data used were National Oceanic and Atmospheric Administration (NOAA) Advanced Very High Resolution Radiometer (AVHRR) Normalized Difference Vegetation Index (NDVI) imagery, Landsat and Satellite Probatoire pour l'Observation de la Terre (SPOT) imagery as well as aerial photographs. 1/

Deforestation, fuel wood collection, over-grazing, savanna burns as well as inappropriate cultivation methods and management have resulted in severe soil erosion and degradation, which may be irreversible. The reduction of vegetation coverage leads to removal of the most fertile upper soil followed by decreasing biomass production. Further on, the siltation of rivers destroys natural water ecosystems and decreases the life span of reservoirs.

Soil erosion, disappearance of vegetation coverage, including deforestation, and general environmental degradation are slow processes and are very difficult to identify. One of the key questions is, how to prove these environmental changes? Remote sensing techniques have been proposed as one of the most effective methods to monitor these events.

NOAA NDVI imagery show clearly the amount of green biomass. The annual and phenological changes in biomass production can be measured and these help to map the area most vulnerable to soil erosion. The more detailed Landsat and SPOT imagery can be used to map, for example, deforestation, vegetation types, land use and eroded areas. A map depicting main ecological zones and erosion risk in Africa produced by using remote sensing data is presented in this study.

---

* This paper, which was presented at the Third United Nations Training Course on Remote Sensing Applications to Geological Sciences, Potsdam, Germany, 7-25 October 1991, does not necessarily reflect the views of the United Nations.

REMOTE SENSING METHODS

The satellite imagery used were NOAA AVHRR data and calculated NDVI pictures the tones of which are highly related to the amount of green vegetation.

Landsat colour composite imagery was interpreted in particular from all the regions visited. Also, some high quality SPOT scenes were used. The purpose of the high resolution image interpettation was to identify the areal distribution and magnitude of soil erosion in action. It was also possible to estimate the volume of deforestation, overgrazing and cultivation, all related to soil erosion.

By using modern remote sensing and additional Geographical Information Systems (GIS) techniques, four different research scales can be obtained to realize, to estimate and to monitor soil erosion. These research scales are the following:

Level 1: The weather satellites such as NOAA, Nimbus-7 and Meteosat having spatial resolution of 1 to 5 km give the possibility to monitor green biomass production and phenology in wide areas as from all of Africa at one time. 2/, 3/, 4/, 5, 6/

Level 2: The earth resources satellites (eg. Landsat and SPOT) the spatial resolution being 10-100 m can be applied to the mapping of vegetation types and eroded areas in a general scale. 7/, 8/, 9/, 10/, 11/

Level 4: Field work is necessary for detailed reconnaissance of the soil systems. Field observations serve also as control points for interpreting remote sensing data.

The NOAA NDVI images that show the amount of green vegetation are appropriate tools to estimate carrying capacity of the arid and semi-arid areas. The time series of NDVI images show how much green vegetation is available and what are the phenological and yearly changes. The problem, however, is that the images tell little about the slopes, soil types and population pressure. More detailed aerial and satellite imagery can be used to produce maps on carrying capacity by interpreting land-use, topography, vegetation, soils and erosion.

The areal distribution of savanna burns is clearly displayed in satellite imagery. It is not easy, however, to recognize burns older than one month. In some cases the spectral characteristics of burnt arreas return in five to ten days to the normal level. 12/ As discussed below, the imagery illustrates that in some areas more than a half of the savanna vegetation is burned every year.

NOAA NDVI Data

One of the sensors of NOAA satellites is AVHRR with the spatial resolution of 1.1 km local area coverage (LAC) and in a generalized form about 4 km global area coverage (GAC). Colour composites were made by using the NOAA/AVHRR data of the northern half of the globe collected in the office of NOAA in the United States. The data were received during 23 to 29 August 1982 and 21 to 27 March 1983. The AVHRR GAC data were connected to a data matrix to form a global vegetation index (GVI) with the spatial resolution of 15 km in NOAA. The vegetation index NDVI was counted from that data by using the formula:

$$NDVI = (R - IR)/(R + IR)$$

In this formula, R is the reflectance of the red wavelength from channel 1 and IR near infrared from channel 2. The atmospheric correction has been made by using an algorithm which corrects the effects of solar zenith angle, Earth-sun distance and Rayleigh scattering counts as an approximation for the effects of aerosols. To avoid the cloud effect, only the satellite measurements taken on the clearest day were accepted. The counted NDVI ratio also minimizes the effects of topography and shadows.

By using remote sensing data and the vegetation index formula the vegetation amount and green leaf area index (LAI) and productivity are obtained. 13/, 14/ The NOAA ND0-14VI technique has been verified in the estimate of green biomass by United Nations Environment Programme/Food and Agricultural Organization of the United Nations (UNEP/FAO), for example, in Senegal, 15/ in Ethiopia 16/ and also in Tunisia. 17/ It has been found that satellite measurements in the red region of the spectrum and the spongy mesophyll structures of vital leaves cause high reflectance in the near-infrared region. Strong correlations have been found between NDVI and green biomass (r = 0.85) 18/ as well as NDVI and percentage vegetation coverage.

The remote sensing image produced shows clearly the sharp boundary of the Sahara desert. In the south, it shows the latitude of 15° North. Only the rainy mountains of Eritrea have promoted vegetated areas north of that latitude in the border of Ethiopia and Sudan. Eastern Ethiopia, northern Kenya and Somalia except for the coastal area south of Mogadiscio can be classified as desert according to the image. The basic data collected by the satellites are stored and cover the whole globe. Since 1979, comparable data have been received, which has enabled the monitoring of the changes of vegetation cover and biomass production. 19/

In the Burkina Faso region, the light tones in a remote sensing image indicate very low green biomass production before the rainy season. Based on the Landsat imagery interpretation, the area of grass burns cover more than 50 per cent of the area of the savanna vegetation. Numerous fires can be seen also in an image taken in the thermal band of NOAA/AVHRR. 20/ Also, the area of bare agricultural land is wide in this densely populated area (31 inhabitants/sq. km.). According to the remote sensing data, a threat to soil erosion is exceptionally high in Burkina Faso and the surrounding areas.

Also, many other NOAA NDVI composites from Africa published in other papers 21/, 22/, 23/ were used to estimate the phenological effects, volume of green vegetation and areas sensitive to soil erosion. In the last mentioned paper, the vegetation amount of the dry year 1984 in the Sahel has been compared to the two following years by subtracting the NDVI values of that year from the latter ones. The outcome is a picture showing only the changes occurred. The data show that in 1984 the eastern part of Sudan, the eastern part of Chad and the northern part of Senegal were exceptionally dry. The boundary of a certain amount of biomass shifted back after that year 50-200 km back northwards. A north-south oscillation in vegetation boundaries in the Sahelian zone amounting to 50-250 km interannually or over a period of a few years appears to be fairly normal. 24/ The detailed results of the image interpretation are presented below, together with the description of areas investigated in the field.

In southern Africa, UN/FAO and the Food Security Unit of the nine member countries of the Southern African Development Coordination Conference (SADCC) have established the project entitled "Remote Sensing Component of the Early Warning System of SADCC Countries". The project is producing agrometeorolgical maps and other outputs by using NOAA and European Meteosat data. The maps produced depict the number of cold-cloud-duration and rainy days as well as rainfall estimates. The monitoring of vegetation cover and vigour is done by means of NOAA NDVI data.

Nimbus-7 data

The Nimbus-7 polar orbiting satellite was launched in 1978 to an altitude of 955 km from the United States. The Scanning Multichannel Microwave Radiometer (SMMR) 37 GHz data of the Nimbus-7 satellite have been used to monitor vegetation and desertification. This imaging microwave sensor of the satellite receives data from each area in about every sixth day, and the spatial resolution of this frequency is 25 km.

The difference of the vertically and horizontally polarized brightness temperatures in the frequency of 37 GHz correlates well with vegetation coverage. Vegetation emits largely depolarized radiation and absorbs polarized radiation emitted from the soil. This difference is non-linearly related to the green leaf area index. This difference is sensitive to the water content of plants, while NDVI is sensitive to chlorophyll absorption. The microwave difference method is also sensitive to soil moisture and therefore is most relevant in arid and semiarid environments. These SMMR data do not suffer from a loss of sensitivity in areas of low vegetation density and thus complement the AVHRR/NDVI data in such situations. 25/, 26/, 27/ The NDVI method is problematic in poorly vegetated areas especially in the areas of salt-crusted loams; in southern Tunisia, for example, the near infrared reflectance from the soil has been observed to be high. 28/

Measurements of this 37 GHz difference have been made 29/ from the Senegalese Sahel and Burkina Faso between 1979 and 1985. Rainy periods and green vegetation can clearly be seen from the curves representing the difference mentioned. Starting in 1981 the amount of vegetation has radically decreased, especially in Senegal (from 15 to 25 K). In the beginning of the period, the value corresponding to vegetation during that time fell from 11 to 16 K. In Texas and Australia, the corresponding trend has not been demonstrated.

The investigations made by using 7 SMMR data clearly show the possibilities of modern technology to monitor the problems related to changes in vegetation cover and erosion. The period of the satellite observations received is too short for conclusions to be drawn from these data alone. However, the rapid increase in human activity and soil erosion observed in the areas investigated is the most probable explanation for the trend of the 37 GHz curves. Also, a decrease of annual precipitation resulting in a lesser amount of green vegetation can explain the curves.

Landsat and SPOT imagery

With Landsat and SPOT imagery it is possible to map many characteristics of geology, hydrology, soils, vegetation and landuse in Africa. General vegetation types, landuse eroded areas have been mapped from the Sahelian zone, 30/, 31/, 32/ from Tunisia, 33/ Tanzania 34/ and Botswana. 35/ The vegetation index NDVI can be calculated also by using this kind of data and monitoring of the biomass production. 37/ The changes in the distribution of cultivated land in the central Sudan has been mapped by using remote sensing methods. 38/ Also, the amount of fuelwood in the Sudan has been estimated by using Landsat data. 39/, 40/ In Botswana, Landsat imagery has been used to map vegetation types and areas of range degradation and desertification. 41/ In Botswana, the existence of savanna burns have been compiled based on Landsat imagery. 42/ During the last few years, many investigation programmes studying vegetation and soil erosion in African countries and by using satellite imagery have been established.

Deforestation has indisputably been the most important factor increasing the vulnerability of the land to soil erosion. For example, in Ethiopia over 40 per cent of the country had been forested. Subsequently, three decades ago, 16 per cent was forested, and 10 years ago only 3.1 per cent of the country was forested. According to the interpretations made by using Landsat satellite imagery taken in 1979, only 1.8 per cent of the land surface is forested. Currently, the country ranks as one of the lowest in terms of soil erosion, land degradation and starvation.

Information on forests, soils, erosion, water, pastures and carrying capacity has been obtained from Mauritania through fieldwork, by applying Landsat imagery and putting the data into a computerized geographical database or GIS. The main characteristics of geology, geomorphology, soils, hydrology, surface water quality, vegetation, cultivation, forest management, savanna burns as well as details of remarkable erosion patterns can be interpreted. The degradation of the environment can be interpreted in the presence of surrounding natural areas which can be used as control areas.

Also, vegetation damage caused by over-grazing, such as steppification or bush encroachment, is difficult to detect if the vegetation cover has remained. The same problem of analysing environmental changes, however, exists also in fieldwork. The amountss of green vegetation and unvegetated areas are easy to interpret by using the red and near infrared bands. The most striking man-made features in satellite imagery are deforested areas, fields, roads, burnt areas and highly overgrazed and eroded areas.

Northern Africa and Sahelian zone

NOAA NDVI data reveals that in the mountainous area north of Gafsa, Tunisia, there are reasonable seasonal variations in vegetation coverage followed by little rain in winter. In the Sahara plain of central Tunisia, south of Gafsa, seasonal change in NDVI is fading. The climate there is extremely arid, and the biomass is low (less than 500 kg dry biomass/ha) and vegetation consists of scarce perennial shrubs which producce leaves at different times. The desertification threat is very severe.

The average vegetation coverage of 10-21 per cent in central Tunisia is so low, that the NDVI method is not sensitive enough to reveal any changes in green biomass.

The erosion caused by big herds of commercial cattle in Senegal can easily be seen in the field and from remote sensing data. Observations show that cattle paths have deeply eroded the organic topsoil exposing the sandy mineral deposits. In the conservation areas enclosed by a fence, dense grass vegetation and trees protect the soil. Such protected patches surrounded by eroded and deforestated areas are striking features in the satellite imagery. The same phenomenon can be seen in the aerial photographs taken from Tunisia.

Landsat images from the Linguere and Ferlo region, in northcentral Senegal, were interpreted by the author. The area is situated between the isohyets of 250 to 400 mm. The image analysis was made by using the control areas observed in the field. The image was taken during the catastropic drought period of 1968-1974. Observations indicated that the worst soil erosion occurred in the wide shallow wadi basins filled with sandy loam. Roads, villages and cattle pastures are located in these wadis.

The evolution of albedo in the same area has been measured applying Application Technology Satellite (ATS), Meteosat and Landsat satellite data. In Ferlo albedo increased markedly from 1968 to 1973 and decreased again after some normal years to a value below that for 1968. However, in Mauritania albedo remained at a higher level, which probably indicates desertification.

NOAA NDVI images show the sharp boundary of vegetation zone following the Senegal river in the area investigated. This phenomenon can more clearly be seen from the full resolution NOAA LAC NDVI images published. During the rainy season almost the whole area od rhw Senegal is covered by green vegetation and after the dry season the vegetation is withered throughout the country. The desert border can be seen from Landsat images. The desert border was checked also in the field. The most striking boundary is between grass covered land and ground surface covered by occasional trees, shrubs and grass patches surrounded by aerolian sand. This boundary corresponds well to satellite imagery interpretations and is situated about 50 km south of the Senegal river. The total dry biomass in 1981 was less than 800 kg/ha in the northern side of the boundary and usually more than 1200 kg/ha in the southern side of the boundary.

Landsat imagery hase revealed the occurrence of seasonal burning of grasslands in the Sahel. South of the 400 mm isohyet, 20-60 per cent of the land was burnt. Just north of the boundary, in the area interpreted from Landsat imagery, only some small patches were found to have been burnt in the autumn of 1972.

Desert encroachment has been overestimated in many general articles, where shifts in desert margin have been described as being about 100 km over 20 years. This idea is not supported by Landsat satellite imagery and other data from Kordofan, the Sudan. 54/, 55/ No evidence has been found either for large shifts in ecotype borders or systematic growth of "desert patched" villages. However, the temporary expansion of the cultivated areas during the end of the Sahelian drought has been observed. In the present study it was not possible to monitor the changes of the vegetation and erosion. Many observations, both in the field and through the use of Landsat imagery, however, support the concept that in the western Sahel, overgrazing and cultivation have resulted in extensive desertification and soil degradation, at least in places within the semi-arid zone where the annual rainfall is 250 to 350 mm. These observations, however, were made after the drought of 1974. The estimation of these kinds of complex environmental changes is extremely difficult.

East Africa

Landsat images taken on 27 July 1975 of the Morogoro region, in the central part of the United Republic of Tanzania, show that about 15 per cent of the rangelands of the Mkata plain were burnt in the beginning of the dry season. These fire scars were so clearly visible that they could not have been more than one month old. This kind of burning during the dry season should be considered as bad land management. The grassland of the Mikumi National Park has been clearly eroded by wildlife compared to adjacent sparsely populated areas. However, in the densely populated areas of the plain, the savanna has also been strongly eroded.

Landsat imagery shows strikingly the effect of commercial firewood collection around the Tanzanian town of Dodoma. 59/ A treeless circle of 40 km radius can be seen around the town. A secondary reason for that is the other land-use activities like over-grazing and agriculture. Also, severe indications of land degradation occur in that desertificated area. The circle is widening and the firewood transportation distance is increasing. This phenomenon is quite typical for the whole semi-arid area investigated.

The high population pressure can clearly be seen from satellite imagery. The boundaries of the national parks, such as, Nakuru, can be outlined due to the deforestation of the other areas. Forest growth on steep mountain slopes are also still untouched. There is no doubt that the greater of the present steppe area has been forested before the increase in human activity in the area. The southern part of Kenya was found to be one of the worst areas in terms of deforestation and soil erosion among the localities studied in the field.

Southern Africa

The SPOT image from the Gaborone district showed in sharp relief the clear-cutting of the trees and overgrazing problems. Inside the fence surrounding the town area which keeps the cattle out, dense low acacia thorn trees, shrubs and grass are growing. On the other side of the fence numerous cow and goat herds have browsed and grazed the leaves and grass and trampled the organic soils. It is possible to see in the field that under thick thorn trees the soils are not eroded and the land surface is up to 20 cm higher in such places compared to cattle tracks and overgrazed areas. In the areas of trampling erosion, the formation of stony desert pavement has also begun. Thus, the rehabilitation of vegetation is difficult because of the soil degradation.

Mapping of the areas exhibiting land degradation and desertification in Botswana has been made using Landsat imagery. 60/ In that map, 10-40 per cent of the land surface has been presented as areas of range degradation and potential desertification. The map shows that land degradation also occurs in areas mainly used by wildlife, possibly as a result of the reduced land available for them. Wildlife immigration routes of are blocked by 'buffalo fences' and concentration of grazing by wildlife occurs next to the fence; wildebeest and hartebeest are especially migratory in dry years. The same phenomenon of wildlife erosion occurred in the United Republic of Tanzania and Kenya, where large amounts of wildlife have been forced into the national parks. Human land-use activities beginning of the borders of the parks may be closing the natural immigration routes.

Map of high erosion risk

Based on the facts presented above a map depicting the main ecological zones of Africa, and especially the area of high erosion risk, was produced by using satellite data. The zones were interpreted by using mostly NOAA GAC NDVI multi-temporal satellite data. Between the deserts (C) and evergreen forests (B) there is a zone of vegetation withering during the dry season (A) which is most vulnerable to soil erosion (see figure 4). During the dry season in zone A, the vegetation coverage decreases radically because of overgrazing and drying of the vegetation. This results in encroaching desert patches, which are a common occurrence, and soil degradation may take place due to water and wind erosion.

CONCLUSION

Mmodern data collection techniques, including GIS and digital image processing systems, are needed to verify the slowly progressing environmental degradation in Africa. The sources of data should be field measurements and observations involving erosion and vegetation coverage and composition. Data collected by remote sensing methods on both a local and a global scale are most useful. The data on vegetation coverage obtained by using remote sensing techniques give an idea about the areal distribution and intensity of the soil erosion and degradation processes in the African savanna environment. It is also possible to produce detailed maps depicting vegetation coverage and erosion by using Landsat and SPOT data.

The United Nations/United Nations Environment Programme (UNEP) programme Global Environment Monitoring System (GEMS) provides global environmental data management services. A part of this programme, the "Global Resource Information Database" (GRID), collects geographical databases based on, for example, satellite data. These kinds of programmes make it possible to keep a continuous and progressive watch over the productivity of the vegetation. Databases containing systematic data on climate, vegetation, soils and land-use are necessary to monitor the trends possibly leading to reduction of biomass production in Africa. The databases could be combinations of remote sensing data and field observations.

It is possible that an observation period of some 10 years is required to prove, for example, that a given shift of an ecological border is permanent. However, the massive data acquired by the remote sensing systems, such as the NOAA NDVI data, can reveal inter-annual trends immediately and accurately. Efforts to prevent the destructive development leading to erosion and soil degradation should be strengthened immediately.

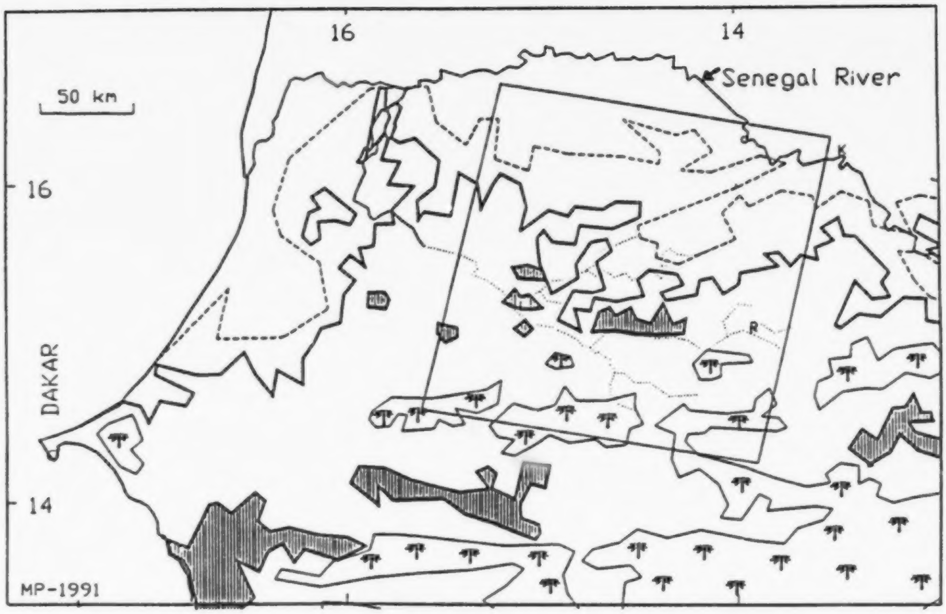
16
14
Senegal River
50 km
16
14
DAKAR
R
MP-1991

Figure 1. A map depicting desert border and desert patches inside vegetated areas (hatched areas) in Senegal interpreted by using NOAA LAC NDVI images received in September 1981 (see Justice et al. 1985). On the northern side of the hatched line the vegetation was extremely poor and thick line separates the sandy area with scattered vegetation and grass covered area. The square represents the location of Landsat image used.

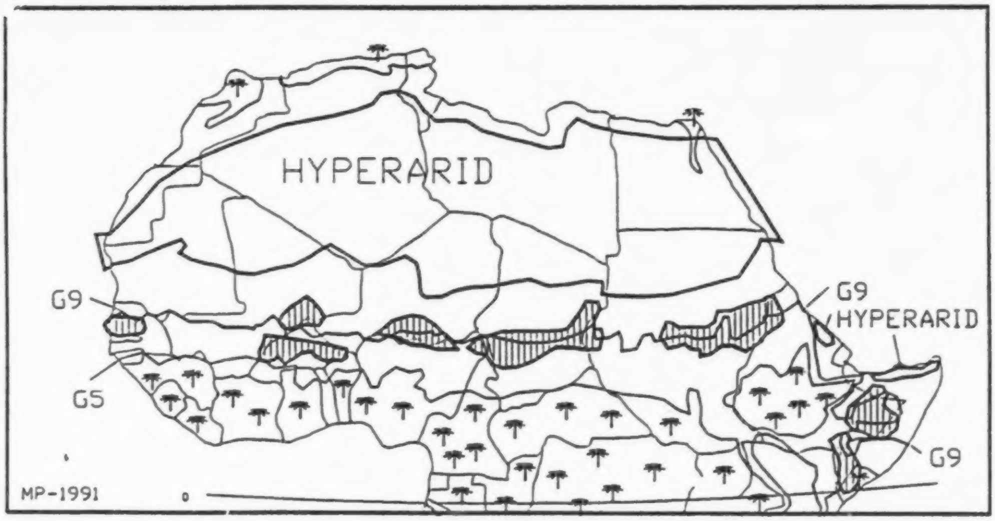
HYPERARID
G9
G9
HYPERARID
G5
G9
MP-1991
0

Figure 2. A map depicting hyperarid areas and areas of very high degree of desertification hazards (FAO et al. 1977). The two other lines correspond to the limits of green vegetation in September (G9) and May (G5 and tree symbols) interpreted from NOAA GAC NDVI images.

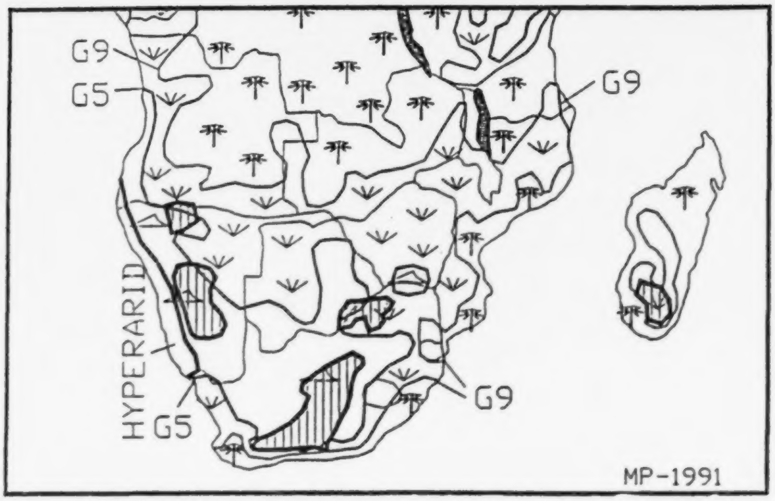

Figure 3. A map depicting hyperarid areas and areas of very high degree of desertification hazards (FAO et al. 1977) in the southern Africa. The two other lines correspond to the limits of green vegetation in September (G9) and May (G5 and tree symbols) interpreted from NOAA GAC NDVI images.

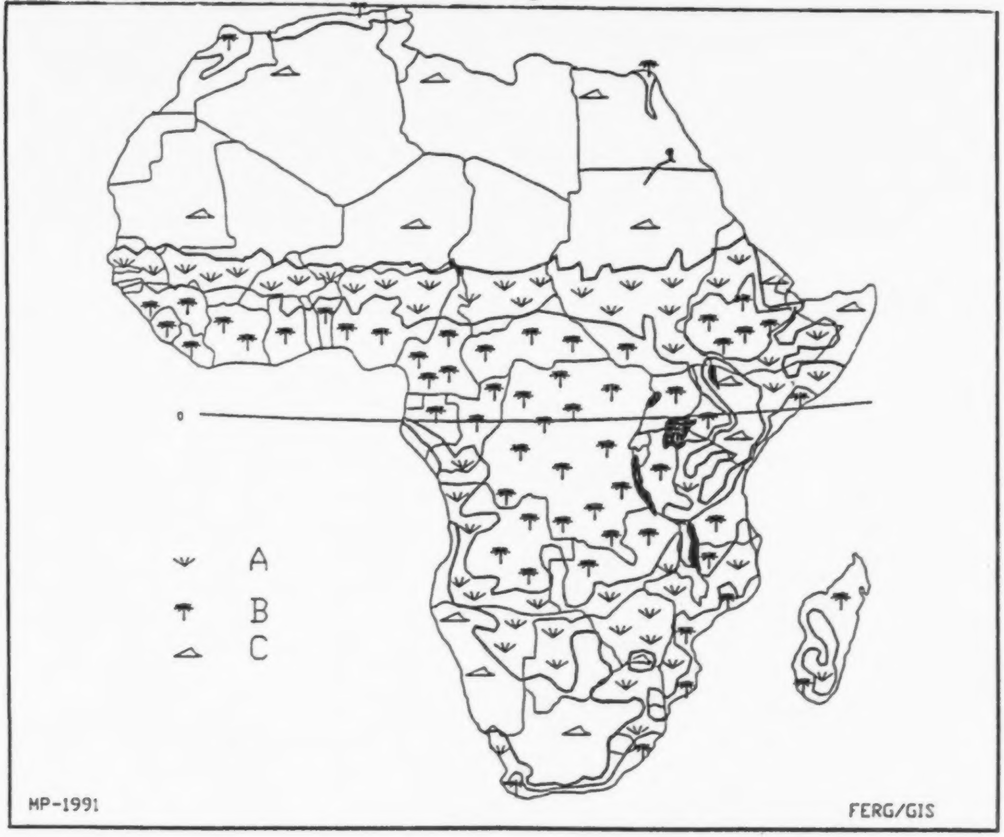

Figure 4. The main ecological zones of Africa interpreted by using NOAA satellite data. Between the deserts (C) and ever-green forests (B) there is a zone of vegetation withering during dry seasons (A) which is most vulnerable to soil erosion. During the dry season in this zone (A) the vegetation coverage is decreasing radically when over-grazing of the dry vegetation prevails. Encroaching desert patches are common.

NOTES

1. Punkari, M. "Monitoring of soil erosion, vegetation coverage and environment degradation in Africa: A review. Finnish Earth Resources Group". Report of Investigation. (Kirkkonummi, Finland 1991), p. 51.

2. Justice, C.O., J.R.G. Townsend, and B.N. Holben _etal_. "Analysis of the phenology of global vegetation using meteorological satellite data," _International Journal of Remote Sensing_ vol. 8, No. 8 (1985), pp. 1271-1318.

3. Choudhury, B.J. and C.J. Tucker. "Monitoring global vegetation using Nimbus-7 37 GHz data", _International Journal of Remote Sensing_, vol. 8, No. 7 (1987a), p. 1885-1890.

4. Tucker, C.J. and B.J. Choudhury. "Satellite remote sensing of drought conditions," _Remote Sensing of Environment,_ vol. 23 (1987), pp. 243-151.

5. Hellden, U. and L. Eklund. _National Drought impact monitoring - a NOAA NDVI precipitation data study of Ethiopia_. Lund Studies in Geography, Ser. C 15. Lund, Sweden. (1988), p. 55.

6. Kennedy, P.J. Monitoring the phenology of Tunisian grazing lands. _International Journal of Remote Sensing,_ vol. 10, No. 4-5 (1989a), pp. 835-845.

7. Hellden, U. "Evaluation of Landsat-2 Imagery For Desertification Studies in Northern Kordofan, Sudan. Lunds Universitets Naturgeografiska Instit.", Rapporter och Notiser 38. (Lund, Sweden, 1978), p. 40.

8. Hellden, U. "An assessment of woody biomass, community forests, lands use and soil erosion in Ethiopia," _Lund studies in geography_. Ser. C14. (Lund, Sweden 1987) p. 75.

9. Hellden, U. and M. Stern. "Monitoring Land Degradation in Southern Tunisia - a test of Landsat Imagery and Digital Data," Lund University Naturgeografiska Institute, Rapporter och Notrser 48 (Lund, Sweden, 1980) p. 42.

10. Kihlblom, U. and D. Johansson. _Satellite monitoring of vegetation and geology in semi-arid environments_. SWECO Consulting Engineers Architects and Economists. (Stockholm, Sweden, 1989) p. 74.

11. Dalsted, K.J. "The use of Landsat-based soil and vegetation survey and graphic information system to evaluate sites for monitoring desertification." Desertification Control Bulletin, No. 16. (UNEP, Nairobi, Kenya 1988) pp. 20-26.

12. Langaas, S. and R. Kane. "Temporal spectral signature of fire scars in savanna woodland", 11th Annual International Geoscience and Remote Sensing Symposium IGARSS'91. Presentations. (Helsinki University of Technology, Finland). (1991) pp. 1157-1160.

13. Curran, P.J. "Multispectral remote sensing for estimating biomass and productivity," In Plants and the daylight spectrum. Smith, H. (ed.) (Orlando, FL, Academic Press, 1981) pp. 65-99.

14. Curran, P.J. "Multispectral remote sensing for the estimation of green leaf index". Philosophical Transactions of the Royal Society, Ser. A 309. (1983) pp. 257-270.

15. Justice, op.cit.

16. Tucker, op.cit.

17. Hellden, U. and L. Eklund, op.cit.

18. Kennedy, P.J. "Monitoring the vegetation of Tunisian grazing lands using Normalized Difference Vegetation Index". Ambio, vol. 18, no. 2, (1989) pp. 119-123.

19. Hellden, U. and L. Eklund, op.cit.

20. Malingreau, J.P., C.J. Tucker and N. Laporte. "AVHRR for Monitoring Global Tropical Deforestation", International Journal of Remote Sensing (1989), pp. 855-867.

21. Justice, op.cit.

22. Tucker, C.J. and C.O. Justice. "Satellite remote sensing of desert spatial extent". Desertification Control Bulletin, No. 13. UNEP, Nairobi, Kenya. (1986) pp. 2-5.

23. Tucker, C.J. and B.J. Choudury, op.cit.

24. Dregne. H.E. amd C.J. Tucker. "Desert Encroachment," Desertification Control Bulletin (UNEP, Nairobi, Kenya, 1988) No. 16, pp. 16-19.

25. Choudhury, B.J. and C.J. Tucker, op.cit.

26. Choudhury, B.J. and C.J. Tucker. Satellite-observed seasonal and inter-annual variation over the Kalahari, the Great Victoria Desert, and the Great Sandy Desert: 1979-1984. Remote Sensing of Environment, vol. 23. (1987b) pp. 233-241.

27. Becker, F. and B.J. Choudhury. Relative sensitivity of Normalized Difference Vegetation Index (NDVI) and Microwave Polarization Difference Index (MPDI) for Vegetation and Desertification Monitoring. 24. Remote Sensing of Environment (1988), pp. 297-311.

28. Curran, op.cit. (1981).

29. Becker and Choudhury, op.cit.

30. Hellden, op.cit. (1978).

31. Hellden, U. "Drought impact monitoring - A remote sensing study of desertification in Kordofan, Sudan." Lunds Universitets Naturgeografiska Instit., Rapporter och Notiser Lund, Sweden. (1984) pp. 61.

32. Helleden U., op.cit (1987).

33. Dalstead, op.cit.

34. Hellden, U. and M. Stern, op.cit.

35. Kihlblom and Johnson, op.cit.

36. Ringrose, S. and W. Matheson. Desertification in Botswana: progress towards a viable monitoring system. Desertification Control Bulletin, No. 13. (UNEP, Nairobi, Kenya. 1986) pp. 6-11.

37. Helleden, op.cit. (1984).

38. Ahlcrona, E. "Monitoring the Impact of Climate and Man on Land Transformation," Lunds Universitets Naturgeografiska Institution, Rapporter och Notiser 66. Lund, Sweden. (1986) pp. 88.

39. Hellden, U. and K. Olsson, "The potential of Landsat MSS data for Wood Resources Monitoring - A Study in Arid and Semi-Arid Environment. In Kordofan, The Sudan, Lund Universitets Naturgeografiska Institution, Rapporter och Notiser 52 (Lund, Sweden, 1982) p. 35.

40. Olsson, K. "Fuelwood Demand and Supply in the Umm Ruwaba/Er Rahad region," In N. Kordofan, The Sudan- A study based on field data and Landsat MSS information. Lunds Universitets Naturgeografiska Institution, rapporter och Notiser 64. Lund, Sweden. (1985) p. 74.

41. Ringrose, op.cit.

42. Darkoh, M.B.K. "Combating desertification in the southern African region: an updated regional assessment," (UNEP, Moscow, 1989) p. 371.

43. Kuru, A. "Roots of deforestation problems in Ethiopia", In Deforestation or development in the Third World? Palo, M. and G. Mery (eds.), vol. 3, Bulletin 349 of the Finnish Forest Research Institute (Helsinki, Finland, 1990), pp. 71-79.

44. Dalsted, op.cit.

45. Lundholm, B. "Domestic animals in arid ecosystem," In Can Desert Encroachment Be Stopped? Rapp, H.N. le Houerou and B. Lundholm (eds.). Ecological Bulletins 24, Swedish Natural Science Research Council, Stockholm, Sweden. pp. 29-42.

46. Kennedy, op.cit.

47. Choudhury, B.J. and C.J. Tucker, op.cit.

48. Nouikoft, G. "Traditional Grazing Practices and Their Adoption to Modern Conditions in Tunisia and the Sahelian Countries". Can Desert Encroachment Be Stopped? Ecological Bulletins (Swedish Natural Research Council, Stockholm, Sweden, 1976) No. 24, pp. 55-69.

49. Courel, M.F., R.S. Kandel and S.I. Rasool. "Surface albedo and the Sahel Drought," Nature, vol. 307, No. 9 (1989), pp. 528-531.

50. Justice, op.cit.

51. Tucker, C.J. and C.O. Justice, op.cit.

52. Justice, op.cit.

53. Rapp, A. "A review of desertification in Africa - water, vegetation, and man". SIES Report 1. Secretariat for International Ecology. (Stockholm, Sweden, 1974) pp. 77.

54. Helleden, op.cit. (1984).

55. Helleden and Eklund, op.cit.

56. *Ibid*.

57. Dregne, *op.cit*.

58. Langaas, *op.cit*.

59. Idris, H. "Energy problems in arid countries." *Can desert encroachment be stopped*? In Rapp. A., H.N. le Houerou and B. Lundholm (eds.) *Ecological Bulletin* (Swedish Natural Science Research Council, Stockholm, Sweden, 1976) No. 24, pp. 103-112.

60. Arntzen, J.W. and E.M. Veenendaal. *A Profile of Environment and Development in Botswana*. Institute for Environmental Studies (IES) (Amsterdam, Netherlands, 1986), p. 172.

ADVANCE WARNING AND EVALUATION OF DAMAGE CAUSED BY CYCLONE, FLOOD AND OTHER METEOROLOGICAL PHENOMENA IN BANGLADESH*

Md. Atiar Rahman and Suraiya Begum
Bangladesh Space Research and Remote Sensing Organization
(SPARRSO)

INTRODUCTION

Being situated in the humid tropical zone, Bangladesh is one of the most disaster prone countries in the world. The country is affected by almost all the bad weather phenomena occurring in the tropical regions around the globe. About 110 million people of the country experience the havoc of natural calamities in the form of atmospheric floods, cyclones, etc., and geologic earthquakes, landslides, etc., every year. The influence of geologic hazards, however, is comparatively less than atmospheric hazards.

Physiographically, the country is almost flat deltaic plain formed by old and new alluvium except its northeastern Barind Tract and eastern hilly region. The plain lies almost at sea level in the south and rises gradually towards the north. Geographically, the Himalayas in the north and the funnel-shaped coast of the country touching the Bay of Bengal in the south causes not only monsoons but also catastrophic revenges of cyclones, Nor'westers, tornadoes, floods and other calamities. These regular meteorological phenomena causing damage to life and property are a barrier for economic prosperity of the country. As a developing country, Bangladesh can not overlook the burden of such damage without taking appropriate precautionary measures to reduce the severity of losses. Unprecedented damage caused by the floods of 1987 and 1988 and cyclones of April 1991 has led the Government of Bangladesh to give new thought to strengthening its early warning, forecasting and disaster management system.

---

* This paper, which was presented at the United Nations/ Economic and Social Commission for Asia and the Pacific/Office of the United Nations Disaster Relief Coordinator Workshop on the Application of Space Techniques to Combat Natural Disasters, organized in cooperation with the Government of China, 23-27 September 1991, Beijing, does not necessarily reflect the views of the United Nations.

Tropical cyclones

Cyclone occurring in the tropical regions of the Earth (lying between 30° North to 30° South) are called tropical cyclones and those occurring outside the tropical regions are called extratropical cyclones. Bangladesh is prone to frequent destructive tropical cyclones associated with tidal surges, particularly in the pre-monsoon months of April and May and post-monsoon months of October and November.

A cyclone is a relatively small and intense low-latitude warm-core low-pressure area having wind circulation in counter-clock wise direction in the Northern Hemisphere and clockwise direction in the southern hemisphere. Warm ocean temperatures (more than 27°c), absence of strong vertical wind shear and presence of a low pressure region are the prerequisites for development of cyclones.

Cyclones in the Bay of Bengal originate mostly over the South Bay and the Andaman Sea from the travelling easterly wave. Because of the funnel-shaped coast, Bangladesh very often becomes the landing ground of cyclones formed in the Bay of Bengal. The Bay of Bengal cyclones also move towards the eastern coast of India, towards Burma and occasionally into Sri Lanka. But they cause serious damage when they enter into Bangladesh. There are, on the average, six cyclones formed in the Bay of Bengal every year.

Classification of cyclones

Cyclones in the Indo-Bangladesh subcontinent are classified according to their intensity and the following nomenclature is in use:

(a) Depression: wind speed up to 50 km/h.
(b) Deep depression: wind speed from 51 to 61 km/h.
(c) Cyclonic storm: wind speed from 62 to 87 km/h.
(d) Severe cyclonic storm: wind speed from 88 to 118 km/h.
(e) Severe cyclonic storm with hurricane intensity: wind speed above 119 km/h.

Cyclone data receiving facilities

At Bangladesh Space Research and Remote Sensing Organization (SPARRSO)

SPARRSO has established an Advanced Meteorological Satellite Ground Receiving Station at Dhaka. The meteorological ground station receives in real time both high-and low-resolution imagery from the United States National Oceanic Atmospheric

Administration (NOAA) and the Japanese Geostationary Meteorological Satellite (GMS) satellites. These data are received at six-hours and one-hour intervals respectively every day. Besides, it has established an advanced data processing system comprising two VAX 11/750 computers, two microwave 3499, I^2s image processing systems having two 512 X 512 size display monitors and two 1024 X 1024 size display monitors.

SPARRSO has also established a very powerful Geographic Information System (GIS) VAS-11/750 based advanced Earth Resource Information Management (ERIM) - GIS system. The system can accommodate 32 overlays in Raster format and has the capability to process the information along with other databases for various environmental applications/modelling. Micro Vax based complete modules of ARC/INFO GIS has been procured and is to be installed in one of the Micro Vaxes 3400 soon.

The Bangladesh Meteorological Department (BMD) has a network of 35 surface observatories and 12 air observatories distributed all over the country which are providing information about different meteorological parameters. BMD also has a network of three, Eather Surveillance Radars located at Dhaka, Khepupara and Dox's Bazar. The radars at Cox's Bazar and Khepupara are mainly used for cyclone monitoring/tracking purposes. The radar at Dhaka is a hydrology-cum-meteorological one which is used to monitor Nor'westers, tornados, hails and rainfall intensity over different parts of the country. Each of these radars has an effective range of 400 km.

Cyclone tracking and forecasting

SPARRSO receives pictures from Japanese GMS capable of surveillance of weather over one third of the Earth's surface. From this satellite, SPARRSO monitors the formation, growth and movements of depressions, tropical cyclones and monsoons that affect Bangladesh's weather. The ground station also receives High Resolution Picture Transmission (HRPT) data from NOAA satellites and processes the NOAA Advanced Very High Radiometer (AVHRR) (1.1 km) and TIROS Operational Vertical Sounder (TOVS) data for mapping and monitoring the weather (monsoon and cyclones). An automatic grid, i.e. latitude, longitude and national boundary can be fitted in the picture with the help of the present analysis system. These facilities provide all possible data to detect the cyclones, determine their position, track their motion and analyse their intensity. Wind speed of cyclones can also be determined from the degree of organization of the cloud pattern and their sizes.

Determining the path of the cyclone in advance is one of the most difficult tasks in meteorology. The classical method for forecasting cyclone tracks is a judicious method for consideration of current of the atmosphere. Tropical cyclones often show different preferred paths at different times of the year. Hence, climatology of cyclones provides some insight to guess the initial forecast. However, as there are large numbers of exceptions, forecasts based on climatology alone can not be entirely relied upon. Recently, various statistical and numerical dynamical methods have also been introduced for the forecast of cyclone paths. SPARRSO has installed a model named TYAN (Typhoon Analysis) for predicting the track of a cyclone based on climatology of the Bay of Bengal.

The tropical cyclone intensity is determined from the satellite imagery by examining the spiral structure of the cloud and Central Dense Overcast (CDO) patterns of the cyclone's cloud system. This may be done from the visible and thermal imagery. Through examination of the imagery, an intensity number called Tropical (T) number is determined. The T number has a direct relationship with the maximum wind of the cyclones. These are as follows:

T number	Highest wind speed (km/h)
1.0	47
1.5	47
2.0	56
2.5	64
3.0	82
3.5	101
4.0	121
4.5	143
5.0	167
5.5	188
6.5	213
7.0	259
7.5	287
8.0	316

SPARRSO disseminates low resolution facsimile cloud picture and high resolution laser print cloud pictures to the Bangladesh Meteorological Department for regular weather forecasting and cyclone warning and to the Bangladesh Water Development Board for flood forecasting.

Cyclone warming

Besides the normal function BMD ensures the following action in case of cyclone formation in the Bay:

(i) To issue early warning for cyclone as early as possible and endeavours to do so between 24 and 36 hours ahead as soon as depression forms in the Bay of Bengal;

(ii) To inform the cyclone preparedness programme about existence of a depression in the Bay of Bengal;

(iii) To issue alert messages to the listed officials;

(iv) To issue suitable special weather bulletins to Radio Bangladesh and Bangladesh Television to broadcast and telecast respectively and also to the national press for the benefit of the public;

(v) To transmit the special weather bulletins to the Control Room of Relief and Rehabilitation, Cyclone Preparedness Programme and Bangladesh Red Crescent Society for taking necessary action.

Cyclone warning signals:

There are 11 storm warning signals meant for the maritime port. The same signal numbers are also applicable to the public in general. Explanations of the signals are as follows:

(i) Distant Warning Signal Number One: This means that there is a region of squally weather in the distant sea where a storm may form;

(ii) Distant Warning Signal Number Two: This means that a storm has formed in the distant sea;

(iii) Local Cautionary Signal Number Three: This means that the port is threatened by squally weather;

(iv) Local Warning Signal Number Four: This means that the port is threatened by a storm but it does not appear that the danger is as yet sufficiently great to justify extreme precautionary measures;

(v) Danger Signal Number Five: This means that the port will experience severe weather from a storm of slight or moderate intensity that is expected to cross the coast to the north of the port in the case of Chittagong and Cox's Bazar and to west of the port in the case of Mongla;

(vi) Danger Signal Number Six: This means that the port will experience severe weather from a storm of great intensity that is expected to cross the coast to the south of the port in case of Chittagong and Cox's Bazar and to the east of the port in the case of Mongla.

(vii) Danger Signal Number Seven: This means that the port will experience severe weather from a storm of slight or moderate intensity that is expected to cross over or near the port;

(viii) Great Danger Signal Number Eight: This means that the port will experience severe weather from a storm of great intensity that is expected to cross the coast to the south of the port in case of Chittagong and Cox's Bazar and to the east of the port in the case of Mongla;

(ix) Great Danger Signal Number Nine: This means that the port will experience severe weather from a storm of great intensity that is expected to cross over or near to the port.

(x) Great Danger Signal Number Ten: this means that the port will experience severe weather from a storm of great intensity that is expected to cross over or near to the port.

(xi) Failure of Communication Number Eleven: This means that communications with the Meteorological Warning Centre have broken down and the local officers consider that a devastating cyclone is following.

There are four signals for the river ports, which are as follows:

(1) Cautionary Signal Number One: This means that the area is threatened by squally winds of transient nature;

(2) Warning Signal Number Two: This means that a storm is likely to strike the area (vessels of 65 feet and under in length are to seek shelter immediately);

(3) Danger Signal Number Three: This means that a storm will strike the area (all vessels will seek shelter immediately);

(4) Great Danger Signal Number Four: This means that a violent storm will soon strike the area (all vessels will take shelter immediately).

Evaluation of cyclone damages:

Cyclones cause severe damage when they enter into Bangladesh. This is because of its low flat terrain, high population density and poorly structured houses. Most of the damage occurs in the coastal district and offshore islands. A list of severe cyclones that visited Bangladesh since 1960 is presented in table I with official casualty figures, storm surge heights and wind speeds. Among them the 12 November 1970 cyclone and the 29 April 1991 cyclone were the most severe. According to satellite pictures, the cyclone of 1970 began to form on 8 November and hit Bangladesh on 12 November (figure 1) with a wind speed of about 140 km/hr and storm surge height of about 30 ft. The cyclone coincides with the high tide period and thus the surge height was influenced. Officially the death figure due to this cyclone was 500,000 but in reality it could have been more. It was estimated that about 46,000 fishermen living in the cyclone affected area lost their lives.

The cyclone of 29 April 1991 can only be described as a supercyclone. Its severity was indescribable. It had a dimension of more than two times that of Bangladesh. The maximum wind speed estimated from the NOAA-11 satellite picture was recorded at 1338 hours. On 29 April it was about 240 km/hr. The cyclone was first detected as a depression on 23 April in the satellite pictures taken at SPARRSO from NOAA11 and GMS-4 satellites. The cyclone in its initial stage moved slightly north-westward and then northward (figure 1). From 29 April it started moving in a north-easterly direction and crossed the Bangladesh coast north of Chittagong port during the night of 29 April. The cyclone started affecting the coastal islands of Nizum Deep, Bhola and Sandwip from the evening of that day. The maximum storm height during this cyclone has been estimated to be about 20 to 25 feet. The loss of lives and property has been estimated to be $2,500 million and the death figure about 1,38,000. The death figure would have been more but early and timely action taken by various agencies of the Government considerably reduced the casualties.

The meteorological satellite data provide the track, the diameter and wind speed of the cyclone. This information is also useful to assess the probable storm surges. Thus, if the topographic and resource information are known prior to the landfall of the cyclone, the information derived from the meteorological satellites is quite useful to assess the preliminary damage. However, for detailed mapping of the damaged area and more accurate assessment of the damages we are to depend on the use of higher resolution data from SPOT/Landsat TM, aerial photos and ground data collection. Since real time is not capable of acquiring aerial photographs just after the disaster, to access actual damages, it has to depend on the field officer's statements.

FLOOD

Flood is the most common and regular phenomenon of Bangladesh. It is predominantly a result of high inflows of three major rivers, Ganges-Padma, Brahmaputra-Jamuna and Meghna, and the flash flows from tributaries originating from neighbouring countries. The combined drainage area of the three mighty rivers is about 15,55,260 sq. km., only seven and a half per cent of which lie within Bangladesh. Most of the rivers of Bangladesh are characterized by limited depth, sandy bottom, flat slopes, meandering, erodable banks and shifting channels. Thus, heavy incessant rain may cause flooding due to drainage congestion. High ocean tides and cyclones also cause serious flooding in the coastal areas by obstructing drainage of upland discharge.

Floods occur in every year during the monsoon period from June to October. Generally, all the rivers start rising in April and May. By June, the low and medium lands are normally flooded. The floods reach their peak in August and September when the Brahmaputra and the Ganges combine simultaneously. In an average year about 20 per cent of the country (25,600 sq. km.) is flooded with a flooding of 3 to 12 feet. In Bangladesh, normal floods are considered to be a blessing because they provide vital moisture and fertilizer for the soil. Only abnormal floods that inundate large areas and cause widespread damage to crops and property are considered hazardous.

Past floods in Bangladesh

Bangladesh has a long history of floods. Reliable information about floods is received has been received since 1922. Prior to 1954 the floods were not recorded properly. It is known that during the period of 1923 to 1953, several severe floods occurred. Floods that occurred from 1954 to 1988 are well recorded (table II). Statistics show that high floods (inundation up to 28,000 sq. km.) have occurred every three years in the past, severe floods (inundation up to 36,000 sq. km) occurred in every six years and catastrophic floods (inundation more than 50 sq. km) have occurred once every nine years. There has not been any significant change over the period of about 100 years of moderate floods. Severe and catastrophic floods, however, have been occurring more frequently in recent times.

Flood forecasting activities

Flood forecasting and warning activities were initiated by the Bangladesh Water Development Board (BWDB) after the flood of

1974 with the immediate objective of setting up of a nationwide flood forecasting and warning service. The Flood Forecasting and Warning Division is responsible for providing flood information bulletins covering the greater part of Bangladesh after analysing data received from field stations during the flood season. The division also forecasts floods along the Ganges-Padma and Brahmaputra-Jamuna river courses based on data received from India.

Flood data collection and processing

SPARRSO receives information and cloud distribution pictures over large areas by acquiring imagery from GMS and NOAA satellites in six and one hour intervals respectively. The clouds could be translated into rainfall in different areas of the catchment. For flood forecasting, catchment rainfall could be used as input data. On a real time basis, water level data from 35 stations and rainfall data from 34 stations are collected by BWDB for the purpose of flood monitoring and forecasting. Flood forecasting and warning centres used to visualize radar monitor cloud movements at five-minute intervals through a microwave link with BMD.

Data received from different sources are processed by a microcomputer based data management system developed for the Flood Forecasting and Warning Centre. Three microcomputers, a hard disk, a floppy disk drive, printer, plotter and digitizer constitute the system. Based on the information received from different organizations regarding water level and rainfall data, a flood forecast is formulated and computer printouts are produced. Quantitative forecasts are limited to the Ganges, Brahmaputra, Buriganga and Lakhya. For the other rivers, qualitative forecasts are issued.

Techniques of flood forecasting

The existing forecasting techniques followed by the Flood Forecasting and Warning Centre are based on available data on water discharge, water level and rainfall records. Historical data have been analysed to develop different models. At present, the warning centre is using Gauge to Gauge Correlation, the Muskingum/Cung Routing Model, Water Level Trend Analysis and the Antecedent Precipitation Index Catchment (APIC) Model. Gauge to Gauge Correlation and Muskingum/Cung Routing Model are applied for flood forecasting in major rivers by correlating water level or discharge between upstream and downstream stations. The water Level Trend Analysis method is being used successfully for streams with no tendency towards flash flooding for forecasting floods with a lead time of 12 to 48 hours. The Antecedent Precipitation Index Catchment (APIC) Model is a method of estimating the excess rainfall of a rainstorm. The model is suitable for flood forecasting in flash flood-prone areas. But due to some calibration problems in the radar at BMO, it gives only qualitative forecasts.

By incorporating SPARRSO satellite data in the flood forecasting model, prediction lead time can be increased by several days. Present flood forecating data provide information only water level changes in the river. Information on flood extent and depth of inundation is important for proper preparedness measures. SPARRSO's present GIS will be used by the Flood Action Plan for the above purposes.

Evaluation of flood damage

The synoptic and repetitive coverage provided by the satellite remote sensing system has the advantage of being able to monitor the extent of flood and post flood damage assessment. The meteorological satellites such as GMS and NOAA obtain data of a coarser ground resolution compared to those from resources satellites like the United States Landsat, French Satellite Probatoire Observatoire de la Terre (SPOT), Russian Sojuzkarta, etc., but the former have the advantage of providing nearly continuous monitoring of the environment over relatively large areas.

High-resolution SPOT and Landsat imagery are not available on a real time basis in Bangladesh. Moreover, they visit a particular area every 16 or 26 days. Thus, they have limited capability of providing flood time data. Since Bangladesh is not capable of acquiring aerial photographs during flood periods, it has to depend on NOAA AVHRR data for flood mapping and damage assessment.

In resource satellite and meteorological satellites, infrared sensors are common. As infrared radiation is strongly absorbed by water, dark tones on hardcopy imagery will represent water. During the flood of 1988, imagery of the passes with relatively clear sky were processed and have been used to estimate the inundation area which is about 78,00 Sq. km. NOAA Satellite data can be analysed for the study of the health of crops. SPARRSO estimated the main crop damage due to the 1987 and 8 floods. Areas of heavy damage to crops in 1988 floods were identified analysing the post-flood image from NOAA - 10. SPARRSO is using NOAA-AVHRR data of channel 1 (0.55 - 0.68 micrometre) and channel 2 (0.725 - 1.10 micrometrr) for a greenness or Vegetation Index. The normalised Vegetation Index (NVI) is defined as:

$$\text{NVI} = \frac{\text{Channel 2} - \text{Channel 1}}{\text{Channel 2} + \text{Channel 1}}$$

Here channel 1 is in the visible wavelength and channel 2 is in the infrared wavelength. The numerator of these is always negative for water, whereas for vegetation the NVI value is always positive. By assigning the negative value of the NVI, flooded areas on the imagery appear to be dark and can be easily identified. If some clouds are present, a better results is achieved by making a composite of channels 1 and 2 and the NVI[1] when relief contours are available, the depth of floods can be displayed through the GIS installed at SPARRSO.

Floods of 1987 and 1988

Among the four most severe floods during the past 35 years, the flood of 1988 is the most severe. Very high casualties and losses were reported. In the affected area, green agriculture fields have gone under deep water, with railways, highways, bridges and culverts being washed away, causing a total deadlock in the communications system. Many important towns were totally inundated. The country's sole international airport had to close down because its runways were flooded. Seventy per cent of the capital city's land mass was under water and mechanized and country boats were the only means of transportation on the submerged highways. The on-rush of flood waters started on 30 August 1988 and entered the SPARRSO campus. By 1 September, the flood waters entered the main laboratory building and the receiving station had to stop its operations due to lack of electricity. In 1988, the damage due to flooding totaled approximately $1,200 million. The following causative factors were identified for the catastrophic flood of August and September 1988.

- Excessive rainfall in the catchment area in the last week of August;
- Synchronization of the peak water levels of the Ganges, Brahamputra and Meghna rivers;
- The solar eclipse of 11 September 1988;
- The earthquake of 21 August 1988;
- Deforestation in the upper catchment.

The 1987 flood was catastrophic but the devastating and unprecedented August/September 1988 flood was perhaps the worst flood in our recorded history. During 1987 an area of 56,600 sq. km. was inundated whereas the 1988 an area of 81,831 sq. km. was inundated (figure 2). The 1987 flood was the result of heavy rainfall both in Bangladesh and adjoining areas. But the catastrophic flood of 1988 was caused mostly by rainfall in the catchment area lying outside Bangladesh.

Nor'wester

Nor'westers generally come from the north-westerly direction towards the south-east. For this reason, these are called Nor'westers. In the pre-monsoon season, i.e., March, April and May, warm moist southerly currents from the sea at 1,000 to 10,000 feet (at different levels) blows over Bangladesh and cold, dry air blows from the north-east/northerly direction. Nor'westers originate in the encounter between these two airspaces. Nor'westers are characterized by strong surface winds up to a maximum of 113 to 129 km/h accompanied by heavy rain, thunderstorms and occasional hail. According to the BMD sources, Nor'westers hit Dhaka area in the month of April, May and June frequently. Nor'westers caused widespread damage throughout Bangladesh every year.

Tornado

A tornado is also a low pressure region where storm winds blow around a centre in a counter-clockwise direction in the northern hemisphere and a clockwise direction in the southern hemisphere. It forms on land. Tornadoes are more severe than Nor'westers. They occur within very small areas and vary from a few feet up to a maximum of 1.5 km. and travel few km. They carry all the trees, houses, buildings and other things that are within its path. Tornadoes in Bangladesh occur mostly during March-June and in the afternoon. Every year different parts of Bangladesh are struck by a large number of tornadoes, causing a lot of damage to life and property. It is difficult to recognize a tornado either in surface weather maps or in the satellite picture and thus forecasting of a tornado well ahead of its occurrence becomes very difficult.

Conclusion

Although we have no way to stop natural disasters, we can do a lot to prepare ourselves better to face such disasters. Loss of human lives and damage to property can be minimized if necessary precautionary measures are taken and warnings are given well in advance. Bangladesh is a disaster prone country. Floods, cyclones and other disasters are common phenomena in every year. As such, a very advanced disaster management system is required. Due to the catastrophic floods of 1987 and 1988 and severest cyclone of 29 April 1991, the Government of Bangladesh has taken a new look to the improvement of non-structural methods of disaster warning, preparedness and management besides the structural measures. Since almost all the rivers and streams of Bangladesh have their headwaters outside

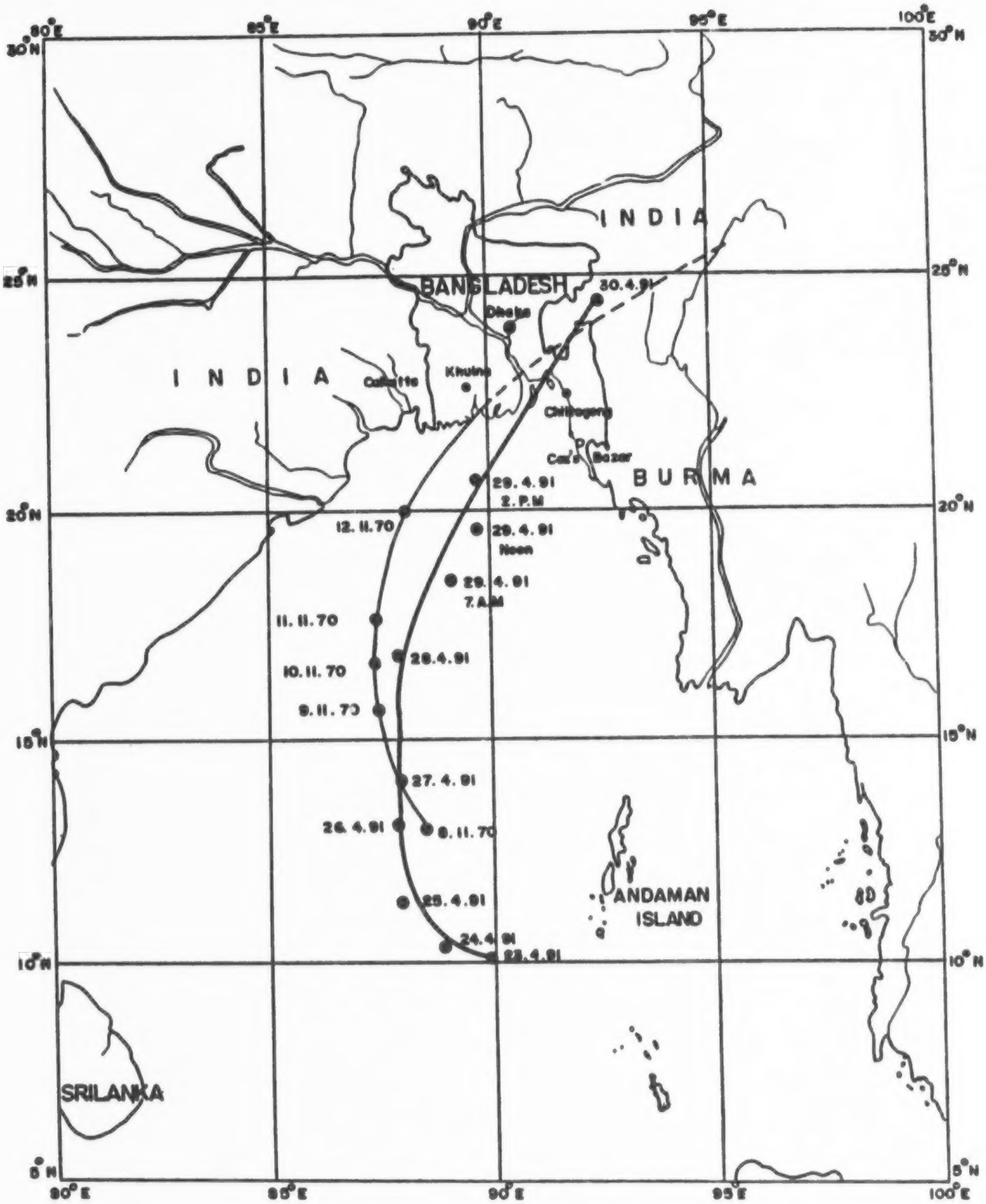
80°E
85°E
90°E
95°E
100°E
30°N
25°N
20°N
15°N
10°N
5°N
INDIA
BANGLADESH
Dhaka
Khulna
Calcutta
Chittagong
Cox's Bazar
BURMA
INDIA
ANDAMAN ISLAND
SRILANKA
30.4.91
29.4.91 2.P.M
29.4.91 Noon
29.4.91 7.A.M
28.4.91
27.4.91
26.4.91
25.4.91
24.4.91
23.4.91
12.11.70
11.11.70
10.11.70
9.11.70
8.11.70

Figure 1. Track of cyclones of 1970 and 1991

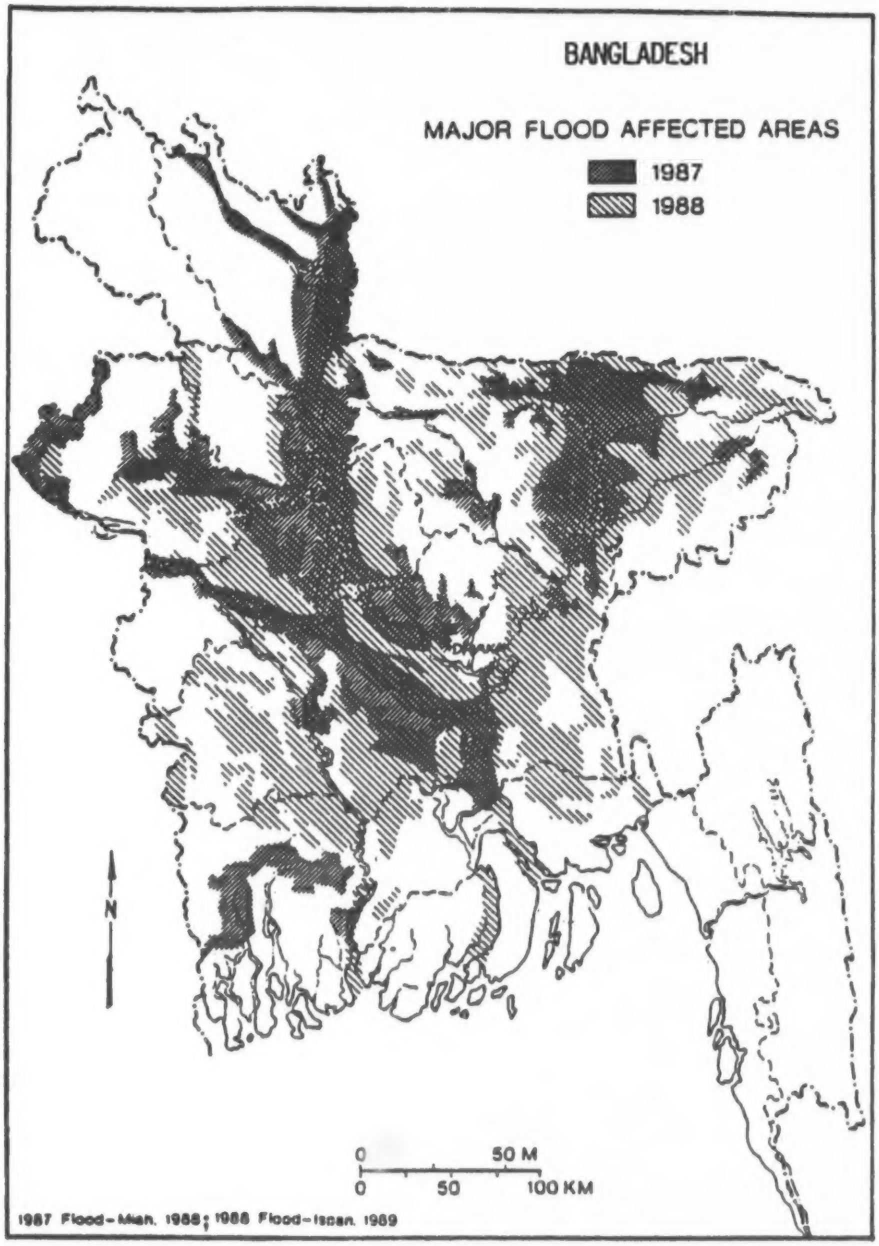
BANGLADESH
MAJOR FLOOD AFFECTED AREAS
1987
1988
DHAKA
N
0
50 M
0
50
100 KM

1987 Flood-Mian. 1988; 1988 Flood-Ispan. 1989

Figure 2. *Major flood affected areas, 1987 and 1988.*

TABLE I

Cyclones affecting Bangladesh since 1960

Date	Max. wind speed in Kms/hr	Storms surge ht. (in ft.)	Deaths
9 Oct. 1960	162	10	3,000
30 Oct. 1960	210	15-20	5,149
9 May 1961	146	8-10	11,466
30 May 1961	146	20-29	
28 May 1963	203	14-17	11,520
11 April 1964	-	-	196
11 May 1965	162	12	19,279
31 May 1965	-	20-25	-
14 Dec. 1965	210	15-20	873
1 Oct. 1966	146	15-30	850
11 Oct. 1967	-	6-28	-
24 Oct. 1967	-	5-25	-
10 May 1968	-	9-15	-
17 April 1969	-	-	75
10 Oct. 1969	-	8-24	-
7 May 1970	-	10-16	-
23 Oct. 1970	-	-	300
12 Nov. 1970	223	20-30	5,00,000
8 May 1971	-	8-14	-
30 Sept. 1971	-	8-14	-
6 Nov. 1971	-	8-18	-
18 Nov. 1973	-	8-13	-
9 Dec. 1973	122	5-15	183
15 Aug. 1974	97	5-22	-
28 Nov. 1974	162	7-16	a few
21 Oct. 1976	105	8-16	-
13 May 1977	122	-	-
10 Dec. 1981	97	-	02
15 Oct. 1983	97	-	-
9 Nov. 1983	122	-	-
3 June 1984	89	-	-
25 May 1985	154	10-15	11,069
29 Nov. 1988	162	5-10	2,000
29 April 1991	225	20-25	1,38,000
2 June 1991	100	6	-

TABLE II

STATISTICS ON BANGLADESH FLOOD
Area affected by flood in Bangladesh

Year	Thousand Sq. Km.
1954	36.4
1955	49.9
1956	35.1
1960	28.2
1961	28.4
1962	36.9
1963	42.5
1964	30.7
1965	28.2
1966	33.0
1967	25.3
1968	36.9
1969	41.0
1970	42.0
1971	35.8
1972	20.5
1973	29.0
1974	52.0
1975	16.4
1976	27.9
1977	12.3
1978	10.8
1980	32.5
1982	3.1
1983	11.0
1984	27.9
1985	11.3
1986	3.1
1987	56.6
1988	81.8

the country, regional cooperation and exchange of hydrometeorological data among the neighbouring countries are of extreme importance for better disaster preparedness programmes.

NOTES

1. Chaudhury, A.M. "Flood plain mapping and flood monitoring using SPARRSO facilities", *Proceedings of the Workshop on the Application of Remote Sensing to Flood Plain Mapping and Monitoring*, Dhaka, Bangladesh, December 1989.

DROUGHT PREPAREDNESS MONITORING AND MAPPING FOR PENINSULAR MALAYSIA*

Mustafa Kamal Baharuddin
Department of Agriculture, Malaysia
and
Nazlan Hashim
Malaysian Centre for Remote Sensing

INTRODUCTION

Peninsular Malaysia experiences humid tropical climate. The mean annual daily temperature is about 27°C and the daily relative humidity ranges from 94 per cent to 100 per cent. Peninsular Malaysia receives high rainfall with the maximum annual rainfall exceeding 5,000 millimeter and the minimum of about 1,750 mm. However, its distribution with respect to time and area is highly varied. In the extreme north-western region of the country, there is a distinct dry season from December to February; whereas, the east coast region receives a high rainfall in the months of November to March. During the South-West Monsoon period from May to August, the west coast receives relatively little rainfall as it lies within the rainshadow area of the mountains of the neighbouring Indonesian island of Sumatra. Many other areas receive high rainfall in the intermonsoonal period when there is considerable atmospheric instability and convective activity.

Drought is said to occur when rainfall amounts and distribution, soil water reserves and evaporation losses combine to cause crop or livestock yields to diminish markedly. With so much rain, drought is not considered a major disaster in Malaysia. It is less of a catastrophe than a flood, for instance. A severe drought only occurs once in six years. More than 80 per cent of Malaysian agriculture is made up of tree crops which are relatively unaffected by the drought. This, however, does not mean that drought has not been a problem. Tree crops establishment have been affected by drought. Rubber replanting schemes under RISDA (Rubber Industry Small Holder Development Authority) suffer a high percentage of crop failure due to drought, especially in the northern states of Peninsular Malaysia.

---

* This paper, which was presented at the United Nations, Economic and Social Commission for Asia and the Pacific (ESCAP)/United Nations Disaster Relief Co-ordinator (UNDRO) Workshop on the Application of Space Techniques to Combat Natural Disasters organized in co-operation with the Government of China, 23-27 September 1991, Beijing, China, does not necessarily reflect the views of the United Nations.

Drought also affects short-term crops which are dependent on soil moisture such as rice paddy (rice plant). Although rice paddy only makes up 10 per cent of Malaysia agricultural land use, it is a very important crop, as rice is the staple food, and paddy is the crop that is most affected by drought. Unfortunately, the major rice growing areas of Malaysia are found in the northern states where drought occurrences are more frequent and usually more severe. During a bad year, the paddy yield could drop by as much as 50 per cent. Therefore, even though drought may not be considered a major disaster, nonetheless, drought management still plays a very important role in Malaysia particularly the agricultural planning programmes. This paper reviews the conventional drought early warnings method and the newly introduced space-based drought monitoring and mapping.

Drought Preparedness Programme

Naturally the major consideration in the Malaysian programme for drought preparedness is for paddy management of major agricultural crops such as paddy and other major crops that are important to the Malaysian economy. Paddy is grown in Malaysia, and as in most Asian countries, has only small holdings of about two to three hectares. However, in Malaysia almost all the paddy grown are concentrarated on a few large schemes. Muda, the largest is one contiguous growing area extending to over 100,000 hectares. All the schemes are provided with irrigation facilities, either using dams as in Muda or water is drawn from major rivers as in Kemubu Scheme. The provision of irrigation facilities were not meant primarily for drought but rather for two crops of rice to be grown per year. But these facilities have also been instrumental in preventing or reducing damages due to drought. There is no major problem during normal dry spells; but once every few years, a prolonged drought occurs. When this occurs, insufficient rain falls for the whole year, and there is not even enough rain during the wet season. In this instance, the dams can not be filled up during the first seasons and there would be no water to draw upon for the second season. Currently, canals are being used as temporary reservoirs and cloud seeding during favourable atmospheric conditions are carried out. However, the success of cloud seeding operations are still questionable. There is perhaps a need for other more effective means of solving this problem. other short term crops also suffer the effects of drought, and preparations have to be made to minimize them. Until recently, not much attention was given to this problem. But as the importance of these crops to the Malaysian economy began to be more appreciated, planners started to grapple with the problems.

Basically, two approaches are followed. One is to delineate agro-ecological zones and confine certain crops to a particular zone according to their abilities to withstand long spells of dry weather. The other is to draw-up a crop calendar for each area whereby different crops are grown at different times of the year, according to the water requirement of each crop. In either case, an Agricultural Rainfall Index (ARI) has to be drawn up first, to determine the locations of wet and dry areas and the severity of wetness and dryness. At the moment, an ARI map has only been drawn for Peninsular Malaysia.

AGRICULTURAL RAINFALL INDEX

Agricultural Rainfall Index (ARI) is defined as to the ratio of the monthly rainfall (at 80 per cent probability) to the monthly potential evapotranspiration taken as a percentage.[1] Empirically, ARI can be represented by:

$ARI = R80/Eo \times 100\%$
Where
R80 is the monthly rainfall at 80% probability of a station
Eo is the potential evaportranspiration of a station.

To determine the ARI for an area, rainfall measurements for that area for at least 20 years, preferably 30 years, are arranged in decreasing order. For a 20 year period, the last four figures are cutoff (for a 25 year period, the last five are cutoff). This constitutes 80 per cent of the readings. The mid-point value of the lowest figure retained, and the highest figure cutofff, is taken as the rainfall value, at 80 per cent probability (R80), for that area. Practical example for computing ARI is elaborated in Appendix 1.

The operational mechanism of drought mapping and monitoring using ARI starts with the computation of ARI at 830 rainfall station distributed all over Malaysia. The 830 rainfall station is managed by Drainage and Irrigation Department (DID) and the Malaysian Meteorological Service (MNS). ARI values for each month are then plotted on a map and isolines are drawn for ARI values of 40 per cent and 200 per cent. Finally, the twelve monthly maps are superimposed to form a composite map and is known as the ARI map of Peninsular Malaysia as shown in Appendix 2.

AGROCLIMATICAL ZONATION

The ARI map is self-explanatory and can be used to produce a crop zone map. If the rianfall amount in a particular month is less than the monthly evaportanspiration, the deficit may be covered by soil moisture storage.[2] Studies have shown that when the rain is down to half Eo, crop can still be sustained by soil moisture storage. However, when the amount is reduced to four tenth of Eo (ARI = 40 per cent), drought conditions can be expected. These same studies have also shown that if rainfall exceeds the water retaining capacity of the soil, the soil becomes saturated and surface runoff takes place. Where drainage is poor, flooding occurs. This is likely to take place when the ARI values exceed 200 per cent. Thus, for our purpose, those zones that have an ARI value of 40 per cent or less are considered dry zones and those with ARI value greater than 200 per cent are considered wet zones; those zones with ARI values ranging between 40 per cent and 200 per cent are considered zones suitable for crop planting.

For the purpose of delineating crop zones, the ARI map is superimposed on a Soil-Crop Suitability map to produce an agroclimatic map. The agroclimatic map does not take into consideration such factors as present land utilization, socio-economic considerations, national strategic crop development policies or other national policies. When all these factors were taken into account, the areas can be zoned for specific crops (Table 3). Such a map of Peninsular Malaysia produces 26 climatic zones, each suitable for a particular number of crops (Department of Agricultural).[3] [4] Extension workers may use this map to advise farmers to grow only crops recommended for their area. If farmers follow this advice, then they are not likely to face the problem of drought.

DROUGHT MONITORING

Apart from the ARI and agroclimatization method, a scheme to monitor drought in the Muda scheme has been also developed by the Malaysia Meteorological Service. It starts with the calculation of monthly rainfall values at various percentiles. The area is said to have "severe rainfall deficiency" if its total rainfall (represented by the selected rainfall station) for at least three consecutive months is within the lowest five per cent of the historical rainfall record. It has "serious deficiency" if the rainfall is between five and ten per cent. For the area, the drought is considered broken, if either or both of the following criteria are met:

(a) rainfall for the past month equalled or exceeded the 30th percentile historical amount for a 3 month period starting that month; and

(b) rainfall for the last 3 months equalled or exceeded the 70th percentile historical record for the same 3 months.

SATELLITE TECHNOLOGY IN DROUGHT MONITORING

Using satellite technology to monitor drought is not a very new approach introduced to Malaysia. The use of National Oceanic and Atmospheric Administration (NOAA) Advanced Very High Resolution Radiometer (AVHRR) satellite data was introduced in 1984 through the 'Satellite Crop Monitoring' as part of drought early warning programme for South and Southeast Asian training programme initiated by the United Nations/Economic and Social Commission for Asia and the Pacific (ESCAP) and NOAA. The introduction of the satellite technology is aimed at enhancing the analyses of the Climatic Impact Assessment project. The programme also known as Agro-climate Assessment or AGROCIA.

Project AGROCIA

The long-term objective of AGROCIA project is to establish a stand-along basis within each recipient country a crop monitoring tool to be used by food security decision-makers on a near real-time basis. There were nine recipient countries of this cooperative program including Malaysia. The other eight recipient countries are namely Bangladesh, India, Indonesia, Nepal, Pakistan, the Philippines, Sri Lanka and Thailand. The technical expertise for this project was provided by the Climate Applications Branch (CAB) of the NOAA; and the Cooperative Institute for Applied Meteorology (CIAM).

The institutional arrangement for implementation of this AGROCIA at Malaysian national level comprising of two level committees - the National Implementation Committee and the Working Group. The National Implementation Committee comprising of senior officers from the Department of Agriculture (DOA) Malaysia, Meteorological Service (MMS), National Paddy and Rice Board, Ministry of Science, Technology and the Environment; and the Drainage and Irrigation Department; with the Ministry of Agriculture (MOA) as the Secretariat. The working group, on the other hand, consisting of three officer, one each from DOA, MMS and MOA, which was trained and entrusted with the responsibility of operating the programme.

Drought Monitoring Within AGROCIA Project

Although this project was first implemented within the country in 1984, but the utilization of the space-based technique particularly in the use of remote sensing techniques for drought monitoring, started in phase II which started in late 1985.

Phase I of AGROCIA have its focus on utilization of cumulative rainfall indices and statistical climate crop yields model to monitor drought, assess the impact on crop production and; to produce and disseminate an operational crop Assessment Early Warning Bulletin. Within the phase II period of the project, which started in 1985, the 'Satellite Crop Monitoring' was designed and conducted to provide an operational satellite imagery and vegetative index analysis.[5] The implementing agencies, DOA and MMS have completed an evaluation of the use of NOAA AVHRR data for monitoring and assessment of growing conditions of major agricultural crops in 1990. In addition, the programme also investigated the possibilities of the NOAA AVHRR data to be used for identification and monitoring of areas affected by cloud.

The Normalised Difference Vegetation Index (NDVI) was used for indicator of biomass in the rice growing field (Lim, 1990). The Normalised Difference Vegetation Index (NDVI) can be represented by:

$$NDVI = (CH2 - CH1)/(CH2 + CH1)$$

Where CH2 is Channel 2
and CH1 is Channel 1

It is reported that from satellite data acquired from 1985 to 1990 were used for computing the NDVI time series, indicate a strong correlation between NDVI and crop calendar of the cropping pattern of the test areas, thus suggested that NOAA AVHRR data can be used to monitor crop conditions. Despite paddy, other major agricultural crops, NDVI, however, was not evaluated.

The biomass indicator then was agreed for adequately serve as 'drought early warning system' tool as to complement the conventional rainfall index method. The use of NDVI for forecasting crop yield was undertaken in the later stage of phase II of AGROCIA project. The correlation of NDVI index to crop yield recorded in the tested areas did not comprehensively represent the real condition, thereby suggesting that further in-depth and exhaustive studies have to be undertaken before it can be used on operational basis.[6] To date, the use of NOAA AVHRR satellite data for the above purpose is still at the experimental stage. The main inherent problems in using this technology is due to the inability to obtain NOAA AVHRR real-time data, as the receiving station at the MMS cannot downgrade the information in the form of Computer Compatible Tape (CCT). The MMS, however, received NOAA AVHRR and GMS data for its operational weather forecasting, but again these data cannot be downgraded to the form of CCT. With the establishment of Malaysia Center for Remote Sensing (MACRES) and its operationalization in January

Appendix I

STATION : FRIM KEPONG

MONTH : JANUARY

Year	Monthly Rainfall (mm)	No	Decreasing Order Rainfall (mm)	EO (mm)	Column For Calculation
1960					
1961	107.19	1	330.45		$R80=\frac{25.+21.59}{2}$ $=23.75$mm EO=118mm $ARI=\frac{R80}{EO}\times 100\%$ =20.01%
1962	69.85	2	258.5		
1963	68.58	3	245.6		
1964	127.51	4	228.6	118	
1965	59.94	5	124.0		
1966	228.6	6	136.65		
1967	245.62	7	127.51		
1968	39.62	8	123.15		
1969	75.95	9	107.19		
1970	330.45	10	89.5		
1971	0	11	88.5		
1972	25.91	12	83.5		
1973	123.19	13	75.95		
1974	21.59	14	69.85		
1975	136.65	15	68.58		
1976	0	16	62.8		
1977	48.5	17	59.94		
1978	258.5	18	48.5		
1979	0	19	39.62		
1980	83.50	20	25.91		
1981	89.50	21	21.59	)	
1982	62.5	22	3.0	)	
1983	3.0	23	0	)Dropped	
1984	88.5	24	0	)	
1985	174.0	25	0	)	

Appendix I (continued)

STATION : FRIM KEPONG

MONTH : MARCH

Year	Monthly Rainfall (mm)	No	Decreasing Order Rainfall (mm)	EO (mm)	Column For Calculation
1960	8.15				
1961	267.72	1	328.5		R80=140.97+126.50
1962	275.59	2	313.0		2
1963	65.79	3	284.99	134	=133.73mm
1964	212.6	4	279.4		EO = 134 mm
1965	156.72	5	275.59		ARI=R80 x 100%
1966	223.77	6	267.75		EO
1967	284.99	7	246.5		
1968	279.4	8	233.0		=99.8%
1969	163.58	9	223.77		
1970	220.47	10	222.0		
1971	-	11	220.47		
1972	40.64	12	212.6		
1973	206.50	13	206.5		
1974	140.97	14	180.59		
1975	180.58	15	163.58		
1976	126.5	16	156.72		
1977	59.5	17	152.5		
1978	141.3	18	148.0		
1979	152.5	19	141.0		
1980	233.0	20	140.97		
1981	148.0	21	126.50	)	
1982	228.5	22	65.79	)	
1983	313.0	23	59.50	)Dropped	
1984	222.0	24	40.64	)	
1985	246.5	25	8.15	)	

Appendix I (continued)

THE CROP ZONING PROCESS

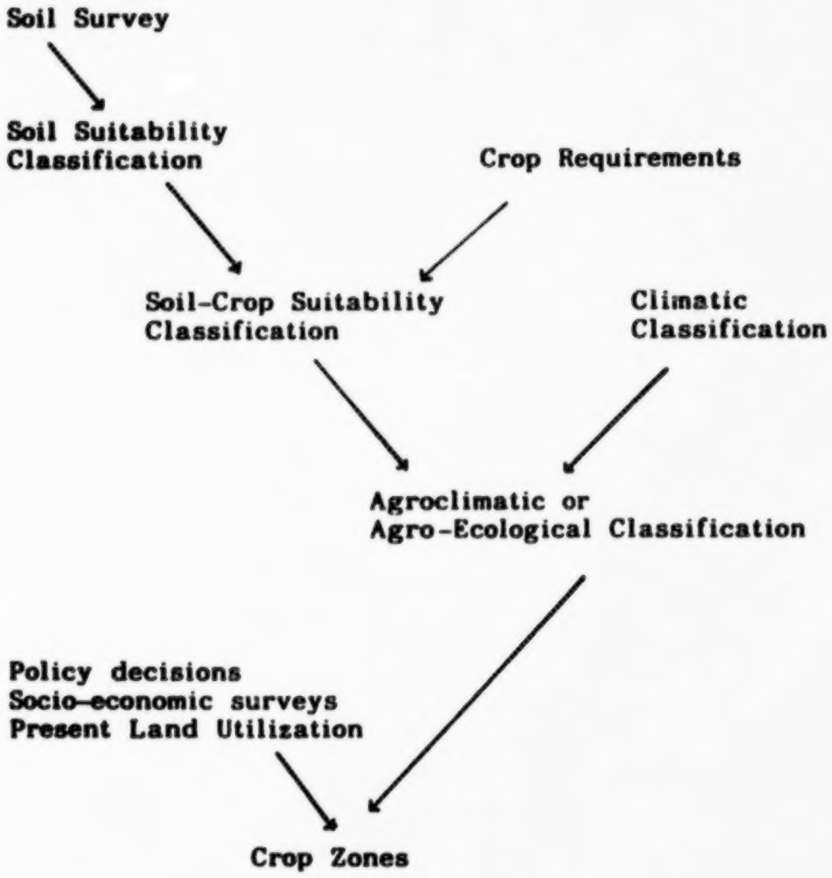
Soil Survey
Soil Suitability Classification
Crop Requirements
Soil-Crop Suitability Classification
Climatic Classification
Agroclimatic or Agro-Ecological Classification
Policy decisions
Socio-economic surveys
Present Land Utilization
Crop Zones

Appendix 2

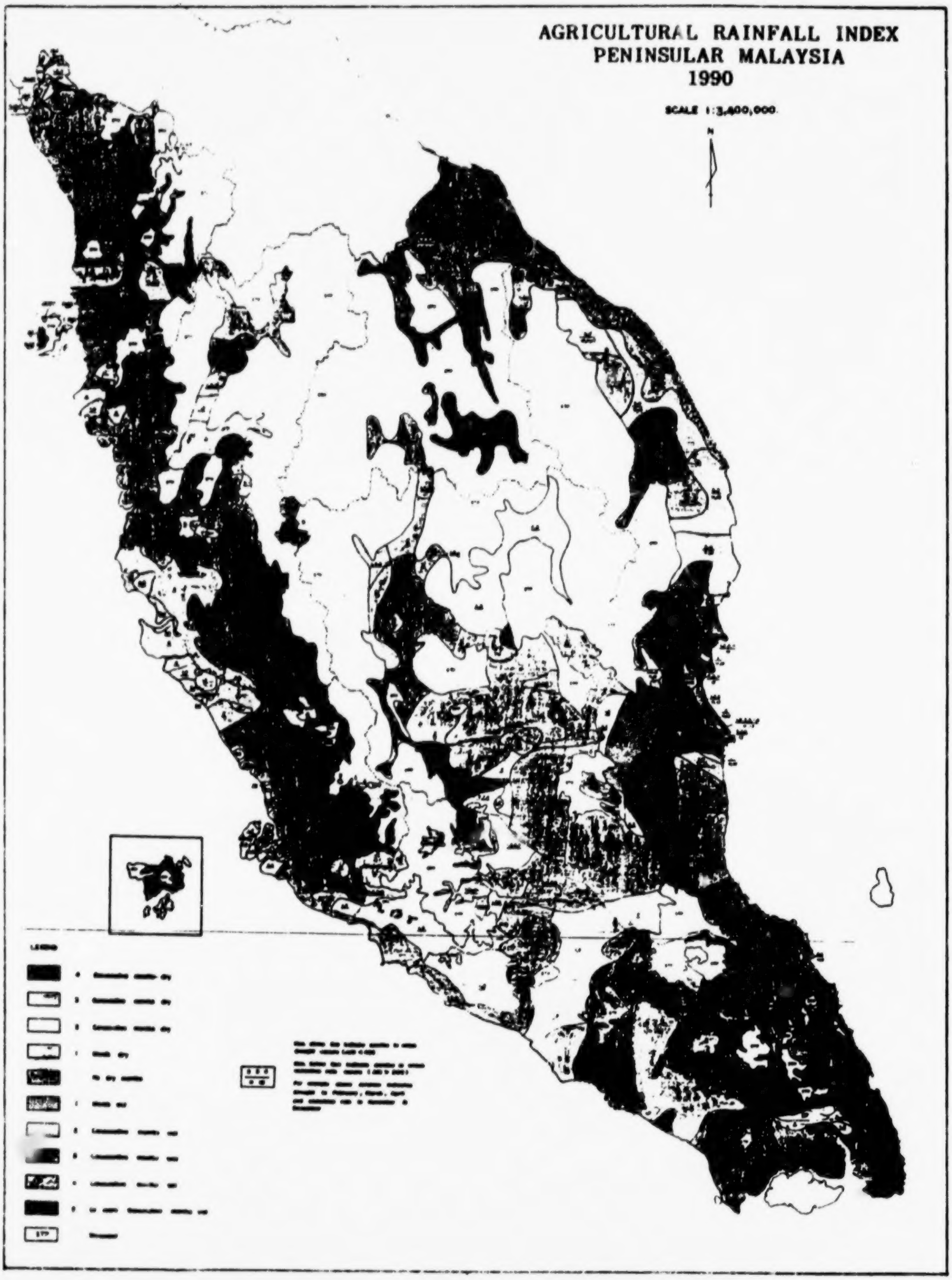

AGRICULTURAL RAINFALL INDEX
PENINSULAR MALAYSIA
1990

SCALE 1:3,400,000
N

1990, all these technical problems have been reviewed. Recently, MACRES arrangement that archiving facilities of HRPLT of NOAA AVHRR data be made; and MACRES will further pursue in the analysis. For this purpose, MACRES with the assistance of European Space Agency (ESA), has, in principle, agreed to sign a cooperative programme on upgrading the MMS receiving and archiving facilities of NOAA AVHRR data. So, with the upgrading of facilities, real time data can be obtained and the use of satellite data to monitor drought can be made operational.

CONCLUSION

Despite the fact that drought is not a major catastrophe in Malaysia, it is still regarded as a formidable problem. There is no national drought management plan as such, but various departments and agencies of the government have come up with a number of measures of drought preparedness. Currently, a number of studies are undertaken by universities and research agencies to locate sources of ground water which are in abundant supply in the north east of the Peninsular. With the upgrading of facilities in Malaysia, particularly with the establishment of MACRES and the upgrading plan for Malaysian Meteorological Services, it is hoped that Malaysia will be able to use the satellite technology not only to map and monitor drought but also for being able to identify other factors that affect agricultural productivity as a whole.

NOTES

1. Ghazali M.Z. and S. Nieuwolt. "The Use of an Agricultural Rainfall Index in Malaysia," Int. J. Biometeor, Vol. 26, (1982) pp. 277-283.

2. Anon (1978). "Report the Agro-ecological zones project, Methodology and Results for Africa." World Soil Resources Report Vol. 1 (FAO, Rome), (1978) pp. 48.

3. Department of Agriculture. "Crops zones for Peninsular Malaysia, A Status Report," (Government of Malaysia, 1985).

4. Department of Agriculture. "Refinement of Agroclimatic Zones of Peninsular Malaysia," (Government of Malaysia, 1989).

5. Department of Agriculture. "Agroclimatic Impact Assessment (AGROCIA)," Programme of Malaysia, (Government of Malaysia, 1985).

6. Lim H.C. "Satellite Monitoring on Rice," (1982) Paper presented at Seminar on Satellite Crop Monitoring, Bangkok, Thailand, 13-16 November 1990.

7. Scarf, F. (1976). Evaporation in Peninsular Malaysia Water Resources Pub. No. 5, Ministry of Agriculture Malaysia.

8. Yong, P.K., N.P. Tung, J. Simon. "Prelimninary Study on the Use of Satellite Data for Predicting Rice Yield in MADA Region," Paper presented at Seminar on Satellite Crop Monitoring, Bangkok, Thailand, 13-16 November 1990.

THE ROLE OF SPACE-BASED OBSERVATIONS IN ASTROPHYSICAL RESEARCH*

J. Grygar
Institute of Physics, Czechoslovak Academy of Sciences
Czechoslovakia

INTRODUCTION

Ground-based observations are essentially possible in a few rather narrow atmospheric windows, namely: (a) optical, that is, visual plus a fraction of the infrared region (wavelengths 0.3 to 20 micrometre (um)); (b) microwave and radio domains (wavelenghts 1 millimetre (mm) to 15 metres (m)); (c) very high-energy gamma rays (energies over 100 giga electron volts (GeV)).

The observations in all windows are hampered by the existence of natural and/or man-made background radiation. Quite often, the signal-to-noise ratio is smaller than one. In the optical region, the angular resolution is severely limited by the inhomogeneities and turbulence in the Earth's atmosphere. The angular resolution of ground-based radio interferometry is naturally limited by the maximum length of the baseline, equal to the Earth's diameter.

From the observational point of view, the universe is a complex source of thermal as well as non-thermal electromagnetic radiation emitted in an extremely wide range of wavelengths (photon energies). Thus, for proper understanding of physical processes in the universe we need good spectral coverage of the whole electromagnetic spectrum, good directional accuracy of the measurements and the best possible angular resolution. This is why space-based observations were an astrophysicist's dream for many decades. Until 1930, the ratio of the longest to the shortest observable wavelength in astronomy was only two to one. The advent of radio astronomy, and particularly the advance of space astronomy, extended this fundamental ratio to the really spectacular value 10^{20}. 1/.

There are several reasons for this impressive improvement:

---

* This paper, which was presented at the United Nations/ European Space Agency Workshop on Basic Space Science for Development, Bangalore, India, 30 April-2 May 1991, does not necessarily reflect the views of the United Nations.

- Astrophysicists realized that heavenly bodies emit a sufficient amount of electromagnetic radiation in all parts of the spectrum, very often due to non-thermal processes (synchrotron radiation, bremsstrahlung, collisions, recombinations, masers, annihilation processes);

- physicists developed sensitive detectors for almost all parts of the electromagnetic spectrum;
- space technology permitted the placement of the detectors beyond the Earth's atmosphere;

- the use of fast computers with large memories completely changed the data acquisition and reduction. Image analysis and reconstruction advanced enormously.

However, this progress is extremely costly. Ground-based astronomy is already an expensive undertaking: per capita expenses in astronomy are considerably larger than in any other branch of natural sciences, high-energy physics included. Table I indicates what is meant by "big science" in ground-based astronomy.

At the time of this writing the whole surface area of primary mirrors of large (diameter greater than 2 m) telescopes equals to about 300 m^2. Within a decade we may expect to get an additional surface area of 1000 m^2, at the cost of $800 million. A similar development is planned in ground-based radio astronomy where big arrays and radio interferometers will become the largest scientific instruments at all 2/.

Switching to space astronomy is, however, much more costly. Every kilogram of payload launched into the Earth's orbit costs about $1,000; the price tag for a single space-shuttle launch is $220 million. Prices of the so-called "Great Observatories," (GRO), Advanced X-ray Astrophysics Facility (AXAF), Space Infrared Telescope Facility (SIRTF) and the Hubble Space Telescope (HST) vary from $500 million to $1.6 billion. Software for control and raw data reduction for HST cost about $70 million. Despite enormous expenses, some 75 astronomical satellites were already put into orbit. The space-astronomy club is naturally rather exclusive now. Its member countries are: United States, European Space Agency (ESA) countries, the Soviet Union (plus some Intercosmos countries), Japan and India. The following paragraphs are devoted to a detailed assessment of the situation in various parts of the electromagnetic spectrum, in regard to space astronomy.

INFRARED ASTRONOMY

The infrared region of of 0.7 um, to 1 mm is for practical astronomical purposes divided into several portions:

(a) The near infrared: 1 to 5 um, which is easily accessible from the ground at least in several spectral windows. Two-dimensional imaging is already possible as well as high-dispersion spectroscopy;

(b) The middle infrared: 5-30 um, which is partly accessible from the ground (high-mountain observatories in very dry climate; Antarctic sites will be very promising) or from high-flying aircraft. Cooled linear arrays are available for low-dispersion spectroscopy, crude imaging is also possible;

(c) The far infrared: 30-300 um, which is accessible from baloons, sounding rockets and space platforms. Radiometric measurements of point or extended sources are possible. Deep cooling of the detectors by liquid helium is a necessity. This cryogenic cooling limits the lifetime of space-borne detectors, but the scientific potential of this region is great;

(d) The submillimetre region: 300-1000 um, which is accessible from space only (except for a small window around 350 um). Sensitive detectors are being developed. Submillimetre astronomy awaits its real start at the end of the present decade.

The infrared spectral region is well suited for studying thermal radiation from rather cool astronomical sources with temperatures 4-4500°K. Until now, most original results were obtained by studying comets, minor planets and interplanetary dust within our solar system and then by investigating early stages of stellar evolution within our galaxy. Infrared observations are indispensable for seeing through dense interstellar clouds consisting of cool gas and dust, particularly in the direction towards the very centre of our galaxy. Moreover, it is now clear that some galaxies emit most of their radiation in the infrared domain (the ratio of infrared to optical luminosity is close to 10^3, for our galaxy it is close to 1). It is generally believed that this excess is due to starburst activity within such systems.

The first all-sky survey in middle and far infrared regions (8.5-120 um) was executed by Infrared Astronomical Satellites (IRAS) in 1983. The primary mirror of the IRAS telescope had an aperture of 0.57 m and in its focal plane 62 cooled semiconductor infrared detectors for survey work, photogrammetry and low-resolution spectroscopy were displaced. During 10 months of active life about 95 per cent of the sky was surveyed at least twice, resulting in an impressive IRAS catalogue of about 2.5×10^5 discrete sources in four bands centred at 12, 25, 60 and 100 um.

The great success of IRAS stimulated the development of a new generation of infrared satellites with imaging capabilities, better angular resolution, higher sensitivity and extended lifetime 3/. Near-infrared imaging in the spectral range 1.2-3.4 um was possible through the the Diffuse Infrared Background Experiment (DIRBE) instrument on the satellite Cosmic Background Explorer (COBE) 4/ and in 1993 an advanced Infrared Space Observatory (ISO) satellite will be launched by ESA. The diameter of the primary mirror is the same as with IRAS, but the spectral coverage is much wider (2-200 um), planned lifetime will be almost doubled and angular resolution and sensitivity will be much better due to advances in detectors and much better cooling of the whole telescope 5/.

The National Aeronautics and Space Administration (NASA) is giving high priority to infrared astronomy, too, by including SIRTF into its "Great Observatories" series. SIRTF will probably be launched around the year 2000 into a circular orbit with a 100,000 km radius. Its nominal lifetime will be at least five years. It should be about 10^6 times more sensitive than IRAS and should provide imaging in the range 2-200 um, spectroscopy in the range 2.5-200 um and photometry to at least 700 um. 6/ Under consideration are also less expensive space-borne instruments, like the Submillimeter Explorer (SMMM) by NASA for submillimetre spectroscopy and FIRST by ESA for far-infrared astronomy. The potential of all these observations is great, indeed. As with the IRAS data, we may expect much original research to be done with archives, based on new space-borne observations in this wide infrared (and submillimetre) spectral region.

ULTRAVIOLET ASTRONOMY

The ultraviolet (UV) spectral region covers the wavelength range 380-10 nm (or energy range of 4-100 eV). For practical purposes we may subdivide it into five sections:

(a) near UV: 380-320 nm (accessible from the ground, but progressively absorbed towards short-wavelength limit, mainly by O_3 molecules);

(b) middle UV: 320-117.5 nm (an extension of optical methods with minor alterations, short wavelength cut-off in reflectivity of magnesium fluoride (MgF_2);

(c) far UV: 117.5-91 nm (Lyman limit);

(d) extreme UV: 91-30 nm (end of optical imaging, it is not quite clear how transparent the interstellar medium is in this spectral domain where the Lyman continuum dominates);

(e) XUV: 30-10 nm (imaging is possible with grazing optics, like in the soft X-ray region).

Ultraviolet radiation is emitted by thermal sources in the temperature range (10-300°) x 10^3 Kelvin. Typical astronomical UV sources are the surfaces of hot stars (blue giants and supergiants, white dwarfs, novae and supernovae) and emission nebulae, illuminated by very hot (early-type) stars. Ultraviolet excesses are often found in active galactic nuclei and/or quasars. Middle and far UV regions represent a gold mine for stellar spectroscopy. Over 300 strong lines can be seen in the UV, in contrast with a mere 60 lines in the visual (optical) domain.

The whole spectral region is accessible from space only; the transparency of the Earth's atmosphere is zero below the ozone limit of 290 nm. Among all spacecraft with UV instruments on board, by far the most successful is the International Ultraviolet Explorer (IUE) - a joint venture by NASA and ESA, launched in 1978. The satellite surpassed all expectations and it may operate until 1995. More than 1500 scientific papers based on IUE observations were published until now and this is the best score for any astronomical instrument to date. 7/ 8/ The only drawback of the never-tiring IUE is the rather small aperture of its primary mirror (0.45 m). In this respect the Soviet ASTRO 1 satellite launched in 1983 with a 0.8 m primary mirror set a new standard for high-resolution UV spectroscopy. Still better was the performance of UV instruments on the ASTRO mission aboard space shuttle Columbia in 1990. Unfortunately, this rather expensive $150 million mission was too short (one week) and there is only a minor chance that the instruments will be given a second opportunity to fly.

The UV capability of the HST is very impressive. Both cameras for direct imaging the Wide Field/Planetary Camera and Faint Object Camera (WF/PC and FOC), both spectrographs, FOS, and the High Resolution Spectograph (HRS), and a high speed photometer (HSP), are designed for UV work until at least the Lyman-alpha line. Although the performance of HST is temporarily limited by spherical aberration of the primary mirror (diameter 2.4 m), it is at the moment by far the best astronomical telescope for the UV spectral region and we may anticipate first important results very soon.

The UV spectroscopy is particularly suitable for detecting the nature and magnitude of mass-loss from stars. Intense stellar wind blowing the matter away from practically all hot early-type stars was discovered in this way. In general, the understanding of violent phenomena in stellar atmospheres is impossible without reliable UV spectroscopy. UV data are also pivotal for studying the interstellar and intergalactic media as well as for the investigations of the physical nature of quasars. The Extreme Ultra Violet (EUV) region is still terra incognita and the first instrument designed for such observations will surely mark beginning of some very interesting astrophysics 9/.

X-RAY ASTRONOMY

By entering the field of high-energy astrophysics, we formally abandon the wavelength terminology and replace it by photon energies: E, expressed in electronvolts. When appropriate, we may use the relation $E = 1.2 \times 10^{-6}/$, where is the wavelength (in metres). Then, the so-called soft X-ray region is defined in the energy range 0.1-6 kilo electron volts (keV). In this region imaging is possible by using the principle of grazing optics, as in XUV band. The so-called hard X-rays extend from 6 to 100 keV (there is no sharp distinction between hard X and soft gamma-ray regions). According to Planck's law, the X-ray region is particularly suitable for observing very hot astronomical objects in the temperature range from 300° KK to 300°. There are, of course, many non-thermal astrophysical processes that exhibit continuum or line radiation in the X-ray domain.

For a long time, the only X-ray astronomical source was the Sun. Its X-ray radiation was discovered by a sounding rocket in 1948 (X-rays in general are absorbed in the Earth's atmosphere above the altitude of 80 km). The first extra-solar point source (Sco X-1) was detected by a fortunate coincidence in a rocket flight in 1962. The first major survey work in the energy range 2-20 keV was done by SAS-1 = Explorer 42 satellite, better known as UHURU, launched at the end of 1970. For almost all the 400 discrete sources found by UHURU, only part were identified. Many of the UHURU sources are in fact close interacting binaries with one compact component (neutron star or black hole). This discovery opened up a very fruitful field of modern stellar astrophysics. During the two decades many successful X-ray satellites have been deployed, among them HEAO 1-3 (1977-1979), EXOSAT (1963-1986), ASTRON (1983-1985), GINGA (1987-1991) and ROSAT (1990-).

NASA plans to launch another Great Observatory called Advanced X-Ray Astrophysics Facility, probably in 1998. It will be by far the largest X-ray facility in orbit and will have a 2 m grazing-incidence telescope with several instruments capable of subarc-second imaging and high-resolution spectroscopy in the 0.1-10 keV band. Because of its expected lifetime of 15 years, it is certain that its impact on astrophysics will be very profound and diverse. 11/

GAMMA-RAY ASTRONOMY

Space-borne gamma-ray astronomy is possible in an extremely wide energy range 1:10^6. The whole domain is usually divided into four bands:

(a) soft gamma: 0.1 to 1 mega electron volts (MeV)
(b) low-energy gamma: 1 to 10 MeV
(c) medium gamma: 10 to 30 MeV
(d) high gamma: 30 to 100 GeV

Above the upper energy limit, the gamma-rays could be detected by ground-based detectors by the Cherenkov techniques or through secondary air-showers. The space-borne instruments must overcome difficult experimental problems; namely, the photon statistics is very poor, the interference level is extremely high (several problems arise from the use of radioisotope sources on utility satellites) and the directional ability is extremely low (several degrees of arc). However, the promise of the field is great, since gamma-rays are frequently produced in the most violent and powerful processes in the universe, including the annihilation of matter/antimatter, such as the 0.51 MeV line.

The first general survey of the gamma-ray sky for energies above 100 MeV was executed by the COS-B (ESA) satellite from 1975 to 1982. During the survey some 10^5 high-energy photons were collected and only 25 discrete gamma-ray sources were found. However, only five of them were identified with known astronomical objects. This may be changed very soon, since in April 1991 another NASA Great Observatory (GRO) was put into orbit - the heaviest astronomical observatory in space (17 tons). It covers the energy range from 20 keV to 30 GeV and its top angular resolution is five arc minutes. One may expect major discoveries in studying neutron stars and active galactic nuclei, perhaps even before this volume will be distributed to the readers. 11/

There appeared one specific problem connected with the discovery of soft (0.3 MeV) gamma-ray bursts (GRB) lasting several seconds by VELA satellites in 1973. 12/ Since then about 100 GRBs have been observed by various satellites and space probes every year. Approximate positions (error boxes) can be retrieved by timing delays if at least four different spacecrafts recorded the same event. To date, some 100 reasonably small error boxes have been identified. With very few exceptions, there has been no recurrence of bursting of the same source within the last two decades. Attempts to identify well-positioned GRBs with known sources in other spectral domains have failed. Some hints of coincidence with archival optical bursts are, however, very interesting. 13/

Extensive photographic sky surveys were conducted by the Harvard College Observatory (1885 to 1953), by Sonneberg Sternwarte (1928-) in Germany, the Odessa Observatory in Russia and Ondrejov Observatory, Czechoslovakia (1953-). The systematic search for archive coincidences with actual GRBs gives interesting limits on the nature of physical processes involved. 14/

It is generally believed that the phenomenon of GRB is closely connected with the sudden release of energy on the surface of old neutron stars. This conjecture has been recently much strengthened by the discovery 15/ made with the aid of the Ginga satellite that a GRB event was preceded by enhanced soft X-ray activity, lasting about 10 s. However, first results from the BATSE experiment at the GRO (Compton) Observatory make the situation more controversial than before.

RADIO ASTRONOMY

Radio observations from the ground are possible in a relatively very wide window from 1 mm to 15 m. However, space platforms are ideally suited for detecting weak signals because of the much lower level of radio interference. This advantage may appear crucial in the near future because of the ever increasing man-made interference. Unfortunately, some navigation satellites produce strong interference in the decimetre region of the radio spectrum that may close vital portion of the radio window before the end of 1992 16/. The extremely good signal to noise ratio in the millimetre domain was recently exploited by the COBE satellite for measuring radio flux with relative accuracy of 10^{-5} (see reference note 5).

Space-based radio telescopes will also greatly improve the angular resolution of very-large-base interferometry (VLBI). Between 1986 and 1987 two ground-based 64 m dishes in Japan and Australia were used simultaneously with a Trafficking Delay Relay Satellite System (TDRSS) with a 4.9 m paraboloid antenna on geosynchronous orbit, at the frequency 2.3 gigahertz (GHz) (wavelength 0.13 m), giving the maximum base-line 2.15 Earth's diameters (2.1×10^8 wavelengths). 17/ The best present angular resolution of the VLBI technique is about 5×10^{-5} arcsec but with the aid of future space interferometers (the international RADIOASTRON project) this almost incredible limit can be improved five fold.

In this way radio astronomy will strengthen its lead in angular resolution which is vital for understanding spectroscopy and is similarly important for studying the distribution and dynamics of cold interstellar (molecular) clouds. Recent examples of the great potential of radio-astronomy are the studies of the nature of the galactic centre and accurate measurements of the minute fluctuations in relic microwave radiation.

OPTICAL ASTRONOMY

Although the range of wavelengths, 0.3-0.7 um is very narrow, it is still the very centre of observational astronomy. While the atmospheric transparency in the optical region is rather good, there are two reasons for placing the telescopes on space platforms, namely the much lower level of background light, and the total absence of the atmospheric turbulence. Thus, in comparison with ground-based telescopes it is possible to obtain much better angular resolution and to detect much fainter sources.

Two vital observatories are now in the orbit: the HIPPARCOS and Hubble Space Telescope. ESA launched the HIPPARCOS in August 1989 and it has been in operation since late November 1989. Although the concept was first suggested in 1967, the actual project did not start until 1984. 18/ Within two and a half years accurate positions of about a million stars will be measured, giving also their distance and proper motions with unprecedented accuracy. Positional accuracy for stars up to 12.4 mag will be better than 0.002 arcsec and photometric accuracy will reach about 0.03 mag. Trigonometric distances of up to 0.5 kiloparsecs (kpc) (present limit is 50 pc) will change many branches of astrophysics, including cosmology.

The Hubble Space Telescope, which was launched by NASA in April 1990, is by far the most expensive astronomical instrument of all time, at a cost $1.6 billion. The history of the project is long and complicated and its performance in orbit has been rather controversial. The low-altitude orbit has a lot of disadvantages but the main problems are thermal jitter of solar panels and the spectacularly wrong shape of the primary 2.4 m mirror. However, both defects could be rectified probably in 1993 while the nominal lifetime of the flagship of the Great Observatories is 15 years. At the time of this writing both imaging and spectroscopic capabilities of HST were proved to be superior to any ground-based telescope and its UV performance is better than that of IUE. 19/ Part of the spherical aberration problem was removed by the ingenious use of computer deconvolution of data.

After the upgrading of HST the angular resolution 0.06 arcsec will be achieved (ground-based record is 0.3 arcsec) and limiting magnitude of 29 mag in direct imaging is expected (ground-based record is about 27 mag in the red). Moreover, infrared imaging and spectroscopy will be added.

The HST probably marks a principal change in the philosophy of modern astronomical observations. 20/ The whole astronomical community is either directly or indirectly involved in the exploitation of this unique instrument, beginning with the process of allocation of observational time and followed by the scheduling of the observations, telemetry (4 terabyte/year!), storage and retreival of the data. Hopefully, HST will soon become a prime example of the benefits of international cooperation among competent scientists.

A journalist asked Dr. Edwin Hubble right before the inauguration of the giant Mount Palomar telescope: "What do you expect to discover with this formidable instrument?" Dr. Hubble responded: "We do expect to discover something totally unexpected. After all, this is the main role of space-based observations in astrophysics."

NOTES

1. Koubsky, P. Kozmos 22, no. 1, (1991) pp. 16.

2. Neugebauer, G., C.A. Beichman, and B.T. Soifer, et al. Science, Vol. 14 (1984) pp. 224.

3. Rieke, G., M.W. Werner, and R.I. Thompson, et. al. Science Vol. 231, (1986). pp. 807.

4. Mather, J.C., et al. Advances in Space Research Vol. 11 (1991) p. 181.

5. Kessler, M.F., Mitt. Astron. Gesellschaft Vol. 68, (1987) pp. 186.

6. Gillett, F.C., J.R. Houck, Physics Today Vol. 44, No. 4, pp. 32 (1991).

7. Kondo, Y., A. Boggess, and S.P. Maran, Annual Review of Astronomy and Astrophysics, Vol. 27, (1989) pp. 397.

8. Wamsteker, W.M. The International Ultraviolet Explorer Project, Proc. United Nations/European Space Agency Workshop on Basic Space Science, Bangalore, India, 30 April-3 May 1991.

9. Linsky, J.L. Comments on Astrophysics Vol. 10, (1985) pp. 247.

10. Canizares, C.R., B.D. Savage, Physics Today, Vol. 44, No. 4, (1991) pp. 60.

11. Klebesadel, R.W., I.B. Strong, and R.A. Olson, Astrophysical Journal Vol. 182, (1973) pp. L 85.

12. Schaefer, B.E., Astrophysical Journal, Vol. 364, (1991) pp. 590.

13. Hudec, R., J. Borovicka, and R. Peresty, et. al. Publications of the Astronomy Institute of the Czechoslovakian Academy of Sciences Vol. 70, pp. 239.

14. Murakami, T., et al., Nature Vol. 350, (1991) pp. 592.

15. Kovalevsky, J. l'Astronomie 102, (1988) pp. 415.

16. Levy G. S., et al., Astrophysical Journal Vol. 336, (1989) pp. 1098.

17. Perryman, M.A.C., Nature Vol. 340, (1989) pp. 87.

18. Burrows, C.J., et al., Astrophysical Journal Vol. 369, (1991), pp. L 21 (see also other papers of Vol. 369, No. 2, part 2).

19. Chaisson, E.J., R. Villard, Space Telescope Science Institute preprint No. 421 (1990).